Explosively-induced ground vibration in civil engineering construction

Barry Michael New

EXPLOSIVELY-INDUCED GROUND VIBRATION IN CIVIL ENGINEERING CONSTRUCTION

by

BARRY MICHAEL NEW MSc

being a thesis submitted in partial fulfilment of the requirements for the degree of Doctor of Philosophy in the University of Durham

February 1984

FRONTISPIECE

THE PENMAENBACH HEADLAND FROM THE NORTH-WEST

EXPLOSIVELY-INDUCED GROUND VIBRATION IN CIVIL ENGINEERING CONSTRUCTION

by BARRY MICHAEL NEW

ABSTRACT

Research has been undertaken to improve techniques used in the prediction of ground vibration caused by civil engineering construction works. In particular, the effects of explosive excavation of rock for subsurface structures is considered. Factors affecting the input and propagation of explosive energy in the rock mass are investigated, and recommendations made on procedures for trial blasting and the most effective data processing and presentation for the derived predictive equations. These developments are supported by blasting trials at two major road construction sites, where vibration measurements were taken during conventional and innovative blasting operations.

A critical review of contemporary dynamic structural damage and intrusion criteria is provided. It is concluded that vibration prediction and control techniques, together with workable damage/intrusion criteria, can be applied which substantially mitigate vibration hazard. The distribution of vibration associated risk between employer and contractor is discussed and contractual options presented.

Techniques to determine the engineering properties of rock masses by analysis of stress waves from explosive and hammer impact sources have been developed and successfully tested. The advantages and limitations of the most promising seismic methods are discussed and field seismic classifications are compared with known rock mass properties and established geotechnical classification systems. The research shows that both rock mass properties and 'site specific' laws of vibration decay may be obtained during the trial blasting sequence of a site investigation programme.

ACKNOWLEDGEMENTS

The work presented in this thesis forms part of the research programme of the Tunnels and Underground Pipes Division of the Transport and Road Research Laboratory and has been carried out in association with the University of Durham. The author expresses his gratitude for the support given by his supervisors, Professor P B Attewell, Engineering Geology Laboratories, University of Durham, and Mr M P O'Reilly, Head of Tunnels and Underground Pipes Division, TRRL.

The Penmaenbach trials were carried out for the Transport and Highways Group of the Welsh Office through Tunnels Engineering Branch of the Department of Transport. The blasting was sub-contracted to Rock Fall Ltd and organised by R Travers Morgan and Partners (Mr O G Teller), Consultants to the Welsh Office for the A55 North Wales Coast Road Scheme.

The Killiecrankie trials were carried out for the Scottish Development Department. The blasting and site preparation works were undertaken by Tarmac Construction (and their sub-contractors Richies Equipment Ltd), by instruction through the scheme consultants, Sir Alexander Gibb and Partners.

The author is grateful for the assistance provided by his Establishment (TRRL) and in particular to Mr D A Barratt and Mr V J Ewan for their help at the sites. Dr G Matheson (TRRL, Scottish Branch) provided advice on the presplit blasting methods.

TABLE OF CONTENTS

LIST OF FIGURES

LIST OF TABLES

LIST OF PLATES

LIST OF APPENDICES

NOTATION

a	acceleration
A	particle displacement
C_p	P- wave propagation velocity
C_s	S- wave propagation velocity
D	side length of block
E_M	elastic modulus
E_D	elastic modulus (dynamic)
f	frequency
g	acceleration due to gravity
G	shear modulus
G_D	shear modulus (dynamic)
$G(f)$	energy spectral density (ESD)
$H(f)$	ESD gain factor
k,K	constants of proportionality
M	weight of explosive
p'	effective stress
PPV	peak particle velocity (abbreviation used in text)
P- wave	compressional wave of dilatation
Q^{-1}	specific dissipation constant
Q_k	phase angle
r	radial distance
R^2	coefficient of determination
S- wave	shear wave of distortion
t	time
T	pulse duration
V	particle velocity
W	weight
$X(f)$	Fourier transform of $x(t)$
$X(k)$, $Y(k)$, $Z(k)$	discrete Fourier transforms
x	linear distance
$x(t)$	inverse Fourier transform of $X(f)$
α,β	empirical exponents (as used in site laws)
α	spatial attenuation parameter
γ	shear strain
ε	compression strain
λ	wavelength (or average number of discontinuities per metre in Section 4.4.1)
μ'_r	effective joint friction coefficient
ν	Poisson's ratio
ν_D	Poisson's ratio (dynamic)
ρ	density
τ	shear stress
τ_s	shear strength

CHAPTER 1

INTRODUCTION

1.1 The research objectives

The research reported in this thesis forms part of a continuing programme concerned with the environmental effects of civil engineering construction in the public sector. In particular, the prediction of ground vibration hazard associated with the explosive excavation of rock is investigated. This method of excavation is widespread in the provision of subsurface services and structures.

The demand for the exploitation of underground space for environmental and energy linked purposes is increasing and seems likely to continue to be of major importance to society in the future. For instance, large civil engineering projects concerned with pumped storage electricity generation and water supply schemes are in progress and feasibility studies on subterranean nuclear waste disposal and petro-chemical storage caverns are being carried out. The exploitation of fossil fuel stocks and mineral resources also demands improved understanding and cost effectiveness of underground construction techniques. The road construction programme includes a number of major schemes which demand the explosive excavation of tunnels and rock cuttings.

The potential impact of such construction schemes often imposes considerable restraint on the viability and execution of the most expedient method of excavation. Explosives inherently give rise to potentially damaging and intrusive vibrations, the prediction and control of which is

vitally important. Although the research presented here is concentrated largely on subsurface construction, the results are equally applicable to most types of civil engineering. The specification of construction techniques is often critically dependent on the possible effects to nearby structures and human tolerance. This is particularly true in urban areas where local conditions may severely inhibit or even preclude the use of blasting techniques.

At the present time pre-construction vibration prediction analyses are often rather hit and miss affairs with little guidance provided by the literature. In many instances they are not carried out at all. This lack of prior knowledge can lead to severe restrictions being placed on the Contractor during the actual works, with consequential increases in costs to the Client.

Most vibration associated problems may be expressed as two separate questions:

(i) what level of vibration will be produced by the proposed construction works? This will depend on the explosive excavation method and the propagation characteristics of the site.

(ii) what is the acceptable level of vibration? This will depend on the type of structures at risk and the sensitivity of the local population to intrusion.

The answers to both these questions are almost always site specific, although some initial appraisal of hazard may be made which is based on experience from other sites.

At present, trial blasts may be detonated as part of the site investigation programme in an attempt to predict the specific vibration characteristics of the site. These trials are often ill-designed and result in contract specifications which create more difficulties than had no such data been available. This thesis seeks to investigate the factors which affect the input of explosive energy, and the propagation of this energy, in the rock mass. The objective is to provide a rational approach to, and a deeper understanding of, trial blasting and the associated prediction of induced vibration from explosive excavation.

The determination of acceptable vibration levels is in many ways more difficult to deal with owing to its subjective nature, particularly with regard to intrusion. A wide variety of contradictory advice on 'safe' vibration levels is available. The increasing influence of the environmental lobby has resulted in some foreign standardising authorities insisting on unreasonably low levels of vibration from blasting. On the other hand explosive manufacturing companies and blasting contractors do occasionally seem rather optimistic on the durability of structures (and people) subject to dynamic loading. The review and discussion given in the thesis seeks to evaluate and reconcile these viewpoints and make balanced recommendations for working damage and intrusion criteria.

A related topic showing potential for progress is the improved and widened application of seismic measurements to the determination of rock mass properties. A pre-knowledge of existing rock conditions is vital to all aspects of underground construction, and seismic techniques can provide useful support to established methods of site investigation. Measurements of seismic parameters provide a method of investigating large volumes of rock without the expense of frequent direct access by boreholes, although

some borehole evidence will be required for calibration purposes. The dynamic response of the rock mass to explosive and other types of energy input is controlled by rock mass properties, such as jointing and elastic characteristics, which are also of great significance in underground construction. This thesis reviews and develops seismic methods which may be used during site investigations. The resulting seismic classifications are compared with other rock mass classification systems and their relative propriety to the known conditions of the test site is discussed.

1.2 Research background and site choice

The research has been guided by the requirements of the construction industry and the need for a deeper understanding of vibration problems has provided generous means of support and motivation to the author. The developments given here are based upon a review of existing knowledge combined with two series of field trials. Certain aspects of the subject have changed little for many years ('site laws' and 'spherical' elastic wave theory), whereas other areas (damage/intrusion criteria and rock classification) have been subject to considerable recent discussion. In the presentation of the review material an attempt has been made to include as much recent information as possible.

The field research has taken place at two proposed road construction sites in the UK. The Penmaenbach site, in North Wales, is for the A55 reconstruction scheme where a considerable amount of drill-and-blast tunnelling is required. The choice of the site was of importance and was influenced by the following factors:

(a) The geology of the Penmaenbach headland is relatively simple

and is well known.

(b) The rock is of interest in an engineering context in that it contains many joints and is of such a strength that drill and blast methods are the only practical means of excavation.

(c) The rock is freely accessible from the surface, and in the area of trials very little of the outcrop was soil-covered.

(d) The headland has been previously penetrated by two tunnels which provide access to rock at depth.

A further important factor was the site investigation programme being carried out for the construction of twin road tunnels, each some 600m in length, through the headland. The promoters of the works (HM Welsh Office) invited the Transport and Road Research Laboratory to advise upon and carry out measurements to establish parameters concerned with the environmental viability of the proposed works. Concern had been expressed as the new tunnels are to be blasted close to the existing unlined rail tunnel which forms the main London-Holyhead route. It was therefore necessary to carry out blasting trials and review work to provide a rational basis for vibration control during tunnel construction and to check that maintaining the integrity of the existing rail tunnel would not unreasonably restrict the contractor. An engineering appraisal regarding the specific blasting site laws and possible damage thresholds has been submitted to the Welsh Office and British Rail (New, 1979).

Thus the trials, with some supplementary seismic explorations, provided both research data and pre-contract design criteria for the new tunnels.

The second site was that for the A9 reconstruction scheme through the

Pass of Killiecrankie in Scotland. Serious problems had come to light late in the design of the scheme, and TRRL were asked by the Scottish Development Department to provide information on the likely effects of the proposed excavation blasting on nearby structures and construction works. The blasting trials carried out were extensive, and unique data were obtained relating to the vibrations produced by a recently developed method of decoupled presplit blasting. The effects of decoupled charges were unknown and the resulting changes in vibration level and character are investigated in detail.

The field of wave propagation in discontinuous media is so complex that it is useful to consider the nature of the geological medium (in particular, its strength) which is of greatest significance in the prediction of construction related blasting vibration. The market share for blasting in a civil engineering construction has been considerably reduced during recent years in favour of mechanised excavation techniques. For instance, the construction of tunnels is now widely carried out by full-face tunnelling or point attack machines, and road cuttings are excavated by ripping equipment whenever possible.

Recent experience on many construction contracts has indicated that contractors specifying mechanical as opposed to explosive methods of excavation were more likely to be successful bidders. These circumstances have arisen for two main reasons:

(i) heavy mechanised equipment capable of efficiently excavating all but the strongest rocks has now been developed, eg Caterpillar D10 ripper, Titan E134 roadheader, Robbins, Jarva tunnelling machines.

(ii) the use of explosives, particularly in urban areas, is often considered undesirable on environmental, security and safety

grounds.

For construction works, particularly in areas where accurate prediction of vibration is considered necessary, blasting is rather unlikely to be used unless the rock strength is high, thereby making other methods untenable. Therefore, at this time, and increasingly in the future, it is the propagation of vibration in strong rocks which will be of dominant interest. The trial sites chosen are representative of the two main classes of strong rock in the United Kingdom. That is, strong igneous rock at Penmaenbach, and a strong detrital (in this case, metamorphosed) material at Killiecrankie. These sites also represent rocks with usefully variable discontinuity characteristics which are described in some detail.

The data obtained from these sites are analysed in both time and frequency domains in an attempt to verify, explain and extend present knowledge from a wide range of sources concerning the prediction of blasting induced vibration during construction works. The conclusions may not be appropriate for application to other types of blasting (eg quarrying) where differing charge weights and site conditions may yield other results.

CHAPTER 2

VIBRATION EFFECTS ASSOCIATED WITH UNDERGROUND CONSTRUCTION

2.1 Introduction

The viability of civil engineering construction techniques will often depend on their effects upon existing structures and their disturbance of the local population. Tunnelling frequently takes place beneath sensitive urban environments and although sub-surface works have many advantages some difficulties may arise. Ground movements of a quasi-static nature have been extensively investigated (Attewell, 1978; O'Reilly and New, 1982), but the effects of vibrations due to tunnelling operations have received considerably less attention.

A major source of environmental problems associated with underground construction is the vibration caused by the detonation of explosives. If damage thresholds or levels of human tolerance are exceeded, construction work may be halted or curtailed with serious consequential losses. Problems due to vibration from blasting are not necessarily confined to urban environments although in some respects they may be most troublesome in residential areas.

In many countries statutory environmental authorities must be satisfied that proposed construction works will conform to acceptable standards; in the UK these powers are vested in Local Authorities through the Control of Pollution Act, 1974. A review paper based on this thesis, combined with other data on full-face tunnelling machines has been published in a

form specific to the tunnelling industry (New, 1982; Appendix A).

Section 2.2 and those following deal with blasting vibration and its damaging effects on structures but it is useful to review briefly other potential problem areas, ie. air overpressure and human intrusion criteria.

2.1.1 Air overpressure

Blasting induced air overpressures may cause problems, usually by breaking windows or dislodging loose plaster, but structures close enough to a blast to suffer such damage will usually be subjected to potentially damaging ground vibration as well. That is, where overpressures in excess of 0.7 kN/m^2 (0.1 psi) occur ground vibrations are likely to exceed 50 mm/s PPV. High overpressures are associated with near surface blasting with low degrees of confinement and therefore are not usually a cause of complaint during underground construction. However, when blasting in portal areas it is clearly advisable to ensure good stemming of the blast holes. Table 2.1 relates sound pressure level to human and structural response. Damage due to air overpressure is most unlikely during careful construction operations but the noise may cause complaints by the local population. Siskind, Stachura *et al* (1980) have reviewed structure response and damage produced by surface mining air overpressures.

2.1.2 Human perception and intrusion criteria

The fears expressed concerning vibration damage are often a result of the extreme sensitivity of the human body to vibration especially in the low frequency range of 1 to 100 Hz. The effect of vibrations on people is to produce physiological effects on the body and psychological

TABLE 2.1

Response to sound pressure level

Sound pressure level			Example source	Response
dB	N/m^2	p.s.i.		
180	20,000	3		Structural damage
170				Most windows break
160	2,000	0.3	Jet aircraft (close to)	
150				Some windows break
140	200	0.03		Damage threshold
130			Large siren at 100 ft	Hearing pain
120	20	3×10^{-3}	Thunder	Hearing discomfort
110			Riveting machine	Windows rattle (blasting complaint threshold)
100	2	3×10^{-4}	Very busy street	
90			Shouting voice	
80	0.2	3×10^{-5}	Pneumatic drill at 20 m	Risk of hearing damage
70			Vacuum cleaner at 2 m	
60	0.02	3×10^{-6}	Normal speech	
50			Office, light road traffic	
40	2×10^{-3}	3×10^{-7}		
30			Whisper	
20	2×10^{-4}	3×10^{-8}	Sound recording studio	
10				
0	2×10^{-5}	3×10^{-9}		Threshold of hearing

reactions, and the extreme sensitivity of the human senses may provoke varied and sometimes irrational behaviour patterns. Human reaction is more likely to be influenced by previous experience and understanding than by the actual level of vibration itself; a person's state of health, temperament and age will all contribute to this reaction. Jackson (1967); Soliman (1968) and Guignard and Guignard (1970) have published useful works on human response to vibration.

The work of Reiher and Meister (1931) has stood the test of time very well and is useful in defining, in quantitative terms, subjective descriptions of human perception of vibration. The ISO Standard 2631 and the BSI DD32: 1974 both provide valuable guidance on acceptable levels of human exposure to vibration.

Apart from helping to define thresholds of perception and annoyance, tolerance scales alone do not provide sufficient information for defining limits for tunnelling generated vibrations as they are generally applicable to situations where vibration is an accepted part of the environment. A different type of criterion has to be considered in areas where vibration does not normally occur or is at a very low level. Vibration may then be considered as intrusive. It is the unpredictability and unusual nature of a souce rather than the level itself which is likely to result in complaints. The effect of intrusion tends to be psychological rather than physiological, and is more of a problem at night when occupants of buildings expect no unusual disturbance from external sources.

A second type of involvement of people with vibrations is in interpreting the effect on buildings or their contents. Not surprisingly, this is particularly true where the person concerned is the owner. Even the

slightest disturbances from an unusual source may excite anxiety and draw attention to minor cracking of plaster or similar effects which were pre-existing or may otherwise have remained unnoticed.

Experience has shown that when vibration levels from an unusual source exceed the human threshold of perception (PPV 0.2 - 0.3 mm/s) complaints may occur. In an urban situation serious complaints are quite probable when PPVs exceed 3 mm/s. Complaints will increase with the duration of the vibration and will be most severe when the 'intrusion' occurs outside normal working hours, particularly at night.

These values apply to vibration of a continuous or semi-continuous nature. Swedish experience (Persson *et al.* 1980) indicates that tolerance levels may be considerably higher during blasting when the vibrations occur as infrequent shocks of brief duration. Tolerance will also be improved provided the origin of the vibration is known in advance and provided no damage is done. Wiss and Parmalee (1974) have shown that levels of perception are considerably higher when the vibration is of a transient rather than continuous nature. They indicate that vibrations at 1.5 mm/sec are 'barely perceptible' and it is not until levels exceed 22 mm/s that they become 'strongly perceptible'. These values relate to their 'mean subject response', their threshold levels being rather lower.

2.2 The effect of vibration on structures

2.2.1 Peak particle velocity (PPV) and associated distortion

Vibration may damage structures in two ways:

(a) by the dynamic forces induced in a structure exceeding its strength, or

(b) by causing compaction of the soil on which the building is founded. The result of this settlement may be to induce quasi-static stresses which result in structural failure. This mode of failure is discussed by New (1978) and is not considered further.

Vibration may be transmitted from the ground into a structure through its foundations; its effect will depend on the natural frequencies, the damping characteristics and the strength of the building as well as upon the magnitude and frequency of the forcing vibrations.

Vibration damage thresholds are generally given in terms of peak particle displacement, velocity or acceleration. It is most usual for peak particle velocity (PPV) to be used as it has been found to be best correlated with case history data of damage and has a theoretical underpinning inasmuch as the strain induced in the ground or structure is proportional to the PPV. The equations relating stress and strain to vibration as described by peak particle velocity are given below.

Consider two particles, within an elastic solid, separated by a distance dx. Let an incident shear wave, of velocity C_s (propagating in the x direction parallel to a line joining the particles) cause a distortion of amplitude dA normal to its direction of propagation.

Then the shear strain, $\gamma = dA/dx$ ... (2.1)

Now the shear stress, $\tau = G\,\gamma$ ... (2.2)

and the shear wave velocity $C_s = (G/\rho)^{\frac{1}{2}}$ ... (2.3)

where G is the shear modulus and ρ the rock density. The wave propagation velocity may also be expressed as the rate of change of distance (x) with respect to time (t)

That is, $C_s = dx/dt$ ... (2.4)

Substituting 2.4 in 2.1

$$\gamma = \frac{dA}{dt} \Big/ C_s \quad \text{... (2.5)}$$

As $\frac{dA}{dt}$ is the particle velocity, V,

$$\gamma = V/C_s \quad \text{... (2.6)}$$

Also,combining 2.2, 2.3 and 2.6

$$\tau = VC_s \rho \quad \text{... (2.7)}$$

Similarly, consider the effects of a compressional wave of velocity C_p which causes a dilatation between the particles of amplitude dA

Then the compressional strain, $\epsilon = dA/dx$ ... (2.8)

Now the stress $\sigma = (\lambda + 2G)\epsilon$ ... (2.9)

and the compressional wave velocity, $C_p = \left[(\lambda + 2G)/\rho\right]^{\frac{1}{2}}$ ... (2.10)

where λ and G are Lames parameters.

Now $C_p = dx/dt$ ... (2.11)

$\therefore \epsilon = V/C_p$ ... (2.12)

and $\sigma = V C_p \rho$ ... (2.13)

Thus for both shear and compressional wave motions the rock strain is proportional to the particle velocity and inversely proportional to to the characteristic wave velocity. In both cases the stress is pro-

portional to the particle velocity, the wave velocity and the density of the rock.

It is vital to recognise that particle velocity is merely a convenient description of the intensity of a vibration and that alone it cannot describe the degree of distortion of the subject rock mass or structure. It is the differential movements within a solid which will result in damage and the 'velocity' of the subject is relatively immaterial. This is analogous with damage to structures by ground subsidence where it is the distortion imposed that causes damage not the overall change in level.

In order to determine the level of strain (or stress) resulting from a nearby blast it is therefore necessary to measure the PPV and to have some information on the type of wave motions (compressional, shear or surface) and their characteristic velocities of propagation.

The dependence of distortion induced in structures on wave propagation velocity has been recognised indirectly by Langefors and Kihlström (1978), who give risk of damage thresholds which are closely proportional to the wave propagation velocity of the rock upon which the structures are founded (*see* Table 2.3). Other velocity criteria discussed in Section 2.2.2 are varied with respect to the frequency of the vibrations; again this effectively reduces the allowable PPV for structures founded on low velocity strata.

It is of significance to note that when vibration damage is discussed and trial blasting results are analysed, little if any allowance is made for the characteristic velocity of the wave motions. For instance, consider a group of vibrations comprising compressional waves followed by shear waves

of slightly lower peak particle velocity. It will be the PPV of the compressional arrivals that will be used to assess the risk of damage despite the fact that the dynamic distortions from the later shear wave arrivals (of slightly lower PPV) may be significantly larger (owing to their lower propagation velocity).

Many instruments used to monitor blast vibrations only show PPV levels and not the full waveform of the vibration wave packet. Where instruments show the wave packet in detail it may sometimes be possible to differentiate between compressional and shear/surface wave arrivals by allowing for their relative times of arrival and discontinuities in the waveforms. With measurements of characteristic wave velocity the strain induced at the point of measurement may be determined.

Although it is essential to recognise that structural damage occurs as a result of distortion, it seems likely that damage criteria associated with vibration will continue to be based on peak particle velocities. There are two main reasons for this:

1. There is very little information available on the damage induced in structures related to dynamic distortion. The limited data that are available on distortions of a quasi-static nature are not readily interpreted in terms of dynamic distortions as the effective strength of a material is often critically dependent on the rate at which the load is applied. For instance, the dynamic tensile strength of rock may easily exceed its static value by an order of magnitude the probable reason being that with the increase in loading rate the weakest link in the material may not necessarily have an opportunity to participate in the fracturing process. Dynamic tensile strength is

not a constant and increases with loading rate (*see* Lama and Vutukuri, 1978, Ch 7).

2. Determination of the characteristic wave velocity of the damaging vibrations is often extremely difficult owing to the complex nature of the wave packet (*see* Section 2.3.1 and Chapter 3).

2.2.2 Construction-induced vibration and damage criteria

A 'state of the art' review of construction induced vibration has recently been published by Wiss (1981) and usefully presents measurements of vibration caused by various construction operations. These data have been converted to metric scales and combined with other information and are presented in Figure 2.1. This graph represents approximate values and provides general guidance only as conditions affecting the input and transmission of vibration will vary considerably from site to site. This form of presentation shows the likely relative intensities from various sources and highlights the fact that even a small charge of dynamite (0.45 kgf, 1 lbf) will produce larger vibrations than those from most 'continuous' types of source. Figure 2.1 shows that the detonation of even small explosive charges will cause transient ground vibration levels considerably in excess of those from construction plant.

The damaging effects of blast-induced vibrations have been explored by numerous authors. For instance, the recent US Bureau of Mines publication by Siskind *et al.* (1980) gives a full discussion of ground vibration and its effects on some fully instrumented test structures. This report is generally concerned with quarry blasting but provides a broad background and bibliography for the whole subject area. Oriard (1979)

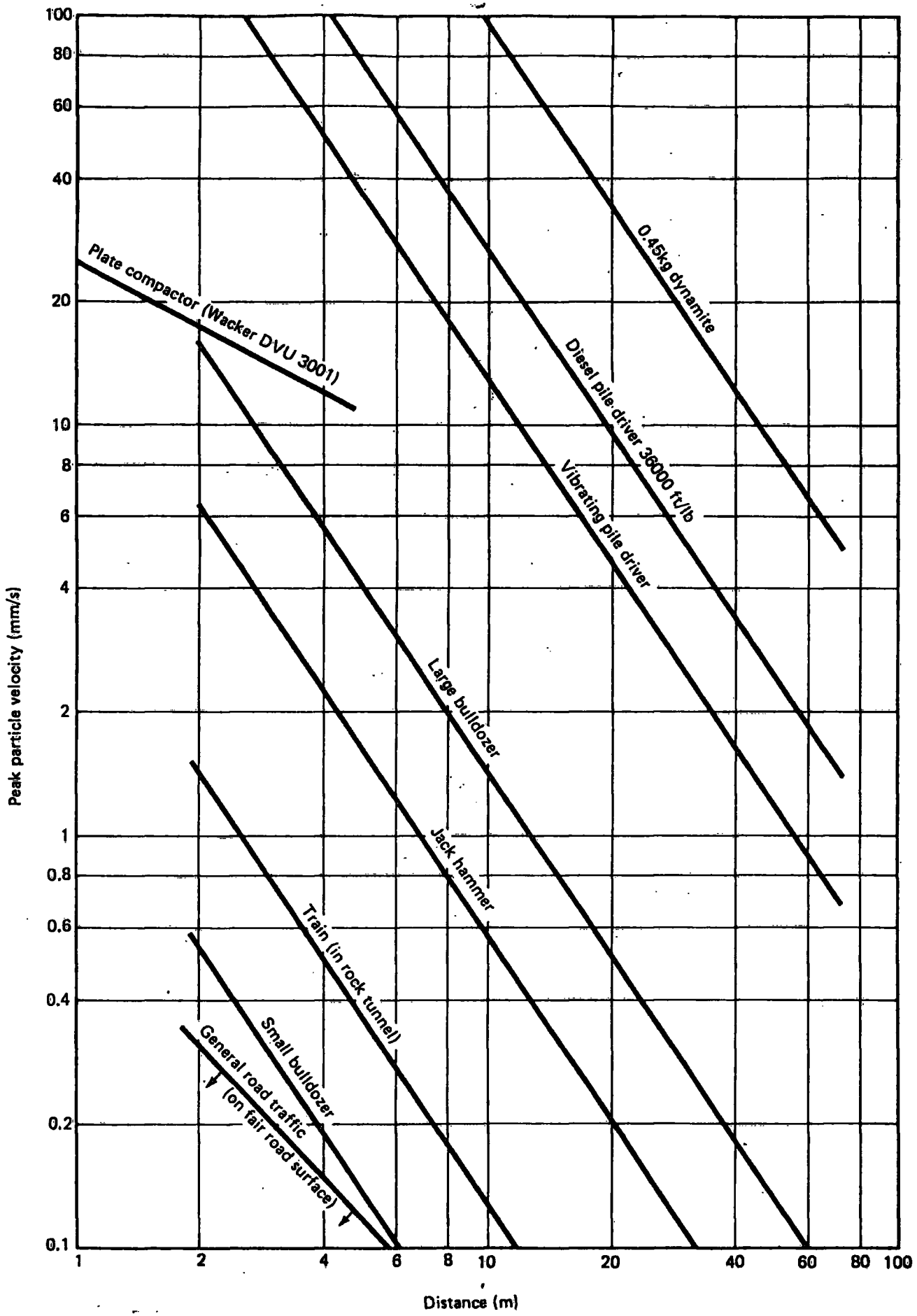

Fig. 2.1 PEAK PARTICLE VELOCITIES FROM VARIOUS SOURCES

gives a most useful and reasoned account of urban blasting practice and philosophy based on many years of experience in the United States. Ambraseys and Hendron (1968) provide an excellent description of the dynamic behaviour of rock masses with special reference to blasting vibrations.

Useful case history records of blasting beneath British conurbations are given by Pakes (1976) and Ashley and Parkes (1976). Both papers described difficulties associated with vibration damage and intrusion in residential areas and discuss ways of minimising disturbance to the local population. More recently, Persson *et al.* (1980) have described blasting techniques used to minimise such problems in Sweden.

Reports of damage to structures have sometimes been associated with unexpectedly low vibration levels, but close reading often reveals that the vibrations had been monitored in only one direction and almost certainly the maximum particle velocity that occurred had not been detected. To determine the maximum particle velocity it is essential to measure the vibrations in three mutually perpendicular directions and to establish the resultant value by vector summation. In the past it has been common practice to monitor construction blast vibrations in one direction only. This practice seems to follow that for measuring the effects of quarry blasting where the direction of the predominant vector component may be predicted with some confidence. However there is often a fundamental difference in the type of wave motion of concern during nearby tunnel blasting compared to that normally associated with quarry workings. Quarrying will usually involve relatively large rounds of explosives at substantial distances from residential structures. It is therefore usual to measure these vibrations at many tens or hundreds of metres from the source. At these distances, and with a near-surface source,

the predominant ground vibrations will be due to surface wave motions with some refracted body wave arrivals. The direction of these motions has become well understood and in practice it has been found satisfactory (and expedient) to measure vertical or vertical and radial motions only. This practice is not acceptable for sub-surface blasting close to structures. In this situation it will often be body wave motions which will predominate. It is rarely possible to predict with any confidence the direction of maximum particle velocity in these circumstances and it is therefore essential to use triaxial transducer arrays.

The establishment of precise or universal criteria which define vibration damage thresholds is not possible and expert judgement based on specific site knowledge and previous case history data will often be necessary. The possibility or degree of damage resulting from vibration will depend on the nature of the source, the transmission characteristics of the intervening geological strata and the inherent strength of the subject structure. The dynamics involved will usually be of a complex nature and many of the variables controlling the resulting structural motions are likely to be unknown. Any suggested damage criteria are, of necessity, a compromise on which engineering judgements may be based; they must not be regarded as hard and fast rules.

Standardising authorities throughout the world have experienced difficulty in defining acceptable standards to be supported by legislative powers. There is no British or International Standard defining vibration thresholds for damage to structures, although such a document is being considered.

Attempts to establish safe levels of vibration have, not unnaturally,

tended to be of a conservative nature and the German Standard DIN4150 is an example which is generally held to be over-cautious and unworkable. The recently published Swiss standards are given in Table 2.2 and again seem rather cautious. They provide a guide to acceptable levels from blasting or traffic/machinery forms of excitation for various types of structure. Langefors and Kihlström (1978) provide a risk assessment for ordinary dwelling houses with varying ground conditions (*see* Table 2.3). Persson *et al.* (1981) report vibration limits enforced in Swedish cities (*see* Table 2.4). In the UK, Ashley and Parkes (1976) have quoted realistic specifications for limiting peak particle velocity, again related to various types of structure (*see* Table 2.5). Other workers (eg. Esteves, 1978; Edwards and Northwood, 1960) have also given 'safe vibration values' and it is of interest to note the overall trend that the more recent the publication the lower the acceptable values have become. This trend does not appear to be supported by much new field evidence of damage at lower particle velocities and indicates a shifting social climate rather than a change in engineering values.

Siskind *et al.* (1980) have produced a comprehensive account on structure response and damage produced by ground vibration from surface mine blasting. This work provides damage probability analyses for various conditions, and Figure 2.2 is, in part, based on their 'alternative safe blasting level criteria' for residential structures. The indicated 'safe' levels fit the case history information well and it is suggested that these levels provide a useful basis for risk assessment. It must be emphasised that there are many recorded instances when particle velocities well in excess of those indicated have not damaged structures. Conversely where a structure is in very poor condition even the slightest vibration may cause inherent weaknesses to become apparent.

TABLE 2.2

Swiss standard for vibration in buildings

(as cited by Wiss, 1981)

Type of structure	Frequency bandwidth Hz	Blasting induced PPV mm/s	Traffic or machine induced PPV mm/s
Steel or reinforced concrete structures such as factories, retaining walls, bridges, steel towers, open channels, underground tunnels and chambers	10-60	30	
	60-90	30-40	
	10-30		12
	30-60		12-18
Buildings with foundation walls and floors in concrete, walls in concrete or masonry, underground chambers and tunnels with masonry linings	10-60	18	
	60-90	18-25	
	10-30		8
	30-60		8-12
Buildings with masonry walls and wooden ceilings	10-60	12	
	60-90	12-18	
	10-30		5
	30-60		5-8
Objects of historic interest or other sensitive structures	10-60	8	
	60-90	8-12	
	10-30		3
	30-60		3-5

TABLE 2.3

Risk of damage in ordinary dwelling houses with varying ground conditions (after Langefors and Kihlström, 1978)

	Sand, shingle, clay under ground water level	Moraine, slate, soft limestone	Hard limestone, quartzy sandstone gneiss, granite, diabase	Type of damage
Wave velocity m/s	300-1500	2000-3000	4500-6000	
Vibration velocity mm/s	4-18	35	70	No noticeable cracks
	6-30	55	110	Insignificant cracking (threshold value)
	8-40	80	160	Cracking
	12-60	115	230	Major cracks

TABLE 2.4

Some typical vibration limits enforced in Sweden when the foundation is on hard rock. Valid for short duration construction blasting (after Persson *et al.* 1981).

Object	Limiting vibration parameter (peak value)		
	Amplitude mm	Velocity mm/s	Acceleration m/s^2
Concrete bunker Steel reinforced		200	
High rise apartment block Modern concrete or steel frame design	0.6	100	
Underground rock cavern roof Hard rock, span 15-18 m		70-100	
Normal block of flats Brick or equivalent walls		70	
Light concrete building		35	
Swedish National Museum Building structure		25	
Sensitive exhibits			5
Computer center Computer supports			2.5
Circuit breaker control room			0.5-2

Note: Lower limit values are enforced for buildings with foundation on piles, without contact with bedrock. Even lower values for foundation on wet clay, sand, or limestone.

TABLE 2.5

Typical specifications for limiting blasting PPV levels (after Ashley and Parkes, 1976)

Type of structure	PPV mm/s
Welded steel gas mains, sound sewers and engineering structures	50
Good residential/commercial and industrial property	25
Housing in poor repair	12
Ancient and historic monuments	7.5

Research is being carried out on response spectra techniques which are intended to improve prediction of vibration damage to structures (Siskind *et al.* 1980; Medearis, 1978; Walker *et al.* 1981). These techniques use measurements of the mass, stiffness and damping characteristics of the subject structures to assess their likely response to vibration. This approach shows promise particularly where specific structures are at risk and the additional investigations are financially acceptable.

In some respects the conventional form of damage criteria already incorporate an important element of response spectra techniques. For instance, the safe level of peak particle velocity, shown in Figure 2.2, reduces considerably at frequencies less than 40 Hz. This coincides with the predominant frequencies (10-30 Hz) associated with the response of residential structures. Further, the variation in safe level shown in Table 2.3 may also be attributed partly to the fact that footing materials characterised by low compressional wave velocities will tend to propagate low frequency wave motions. Here again the recommended safe peak particle velocity is reduced, albeit indirectly, for the lower frequency vibrations. In each of these cases the known response characteristics of residential

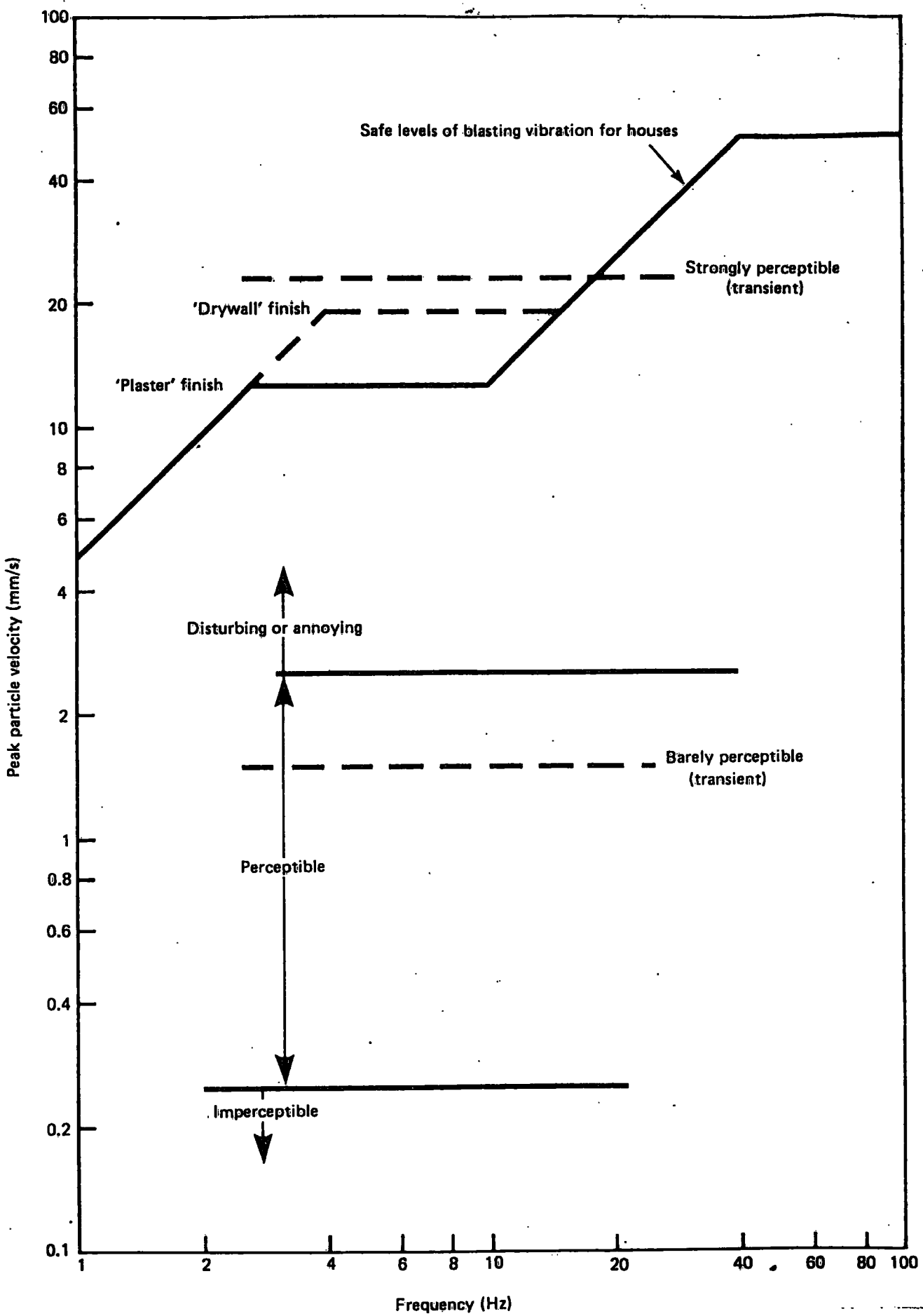

Fig. 2.2. SAFE BLASTING AND HUMAN PERCEPTION VIBRATION THRESHOLDS

structures is matched empirically with an appropriate safe vibration level taking into account the frequency of the forcing motions.

Roberts (1969) has reviewed vibrations caused specifically by civil engineering processes (principally blasting) and a comprehensive review of 'Structural vibration and damage' has been compiled by Steffens (1974) which includes a wide range of case history data on which thresholds of damage may be based.

For nearby construction or excavation blasting where maximum particle velocities occur at frequencies in excess of 40 Hz the review papers cited above indicate that a building in a sound condition is unlikely to be damaged structurally by PPVs below 35 mm/s although 'architectural' damage may occur to weaker structures at PPVs as low as 10 mm/s. However, there seems to be little or no hard evidence of damage to any building by vibrations with PPVs of less than 50 mm/s. This complies with the well established '2 inch/s standard' which has been followed by the explosives industry for a number of years. For frequencies less than 40 Hz a practical safe criteria has been found to be 12 mm/s for older properties with lathe and plaster finish or 19 mm/s for modern homes with plasterboard finish.

2.3 The effect of vibration on subsurface structures

2.3.1 Body and surface wave motions

The majority of published data on blast vibrations relate PPV to range (r) and charge weight (M) where the vibrations are monitored at, or close to the ground surface some tens or hundreds of metres from the blast. These data are not directly relevant to underground constructions as here

we are concerned with vibrations deep into the rock mass and the relevant wave motions may be primarily of the body (compressional and shear) wave types, not surface waves. Body waves radiate in three dimensions whilst surface waves essentially spread only in the dimensions of the guiding surface.

The amplitude of Rayleigh surface wave motion decays rapidly with increased depth below from the surface (*see* Kolsky,1963; Graff, 1975). For example, in a material with a Poissons Ratio of 0.25, the amplitude of the major component (vertical) of particle motion will have decayed to less than 10 per cent of its surface value at a depth of 1.5 wavelengths. In seismology where wavelengths may be very long (low frequency motions) surface wave motions may be significant at depths of several hundred metres. However, in the region close to hard rock blasting operations the frequency of the motions will be relatively high and significant surface wave motions will be confined to within a few tens of metres of the surface. Dowding (1979) states that calculations of surface wave amplitude reduction with depth (when estimating subsurface vibration based on surface seismic measurements) may not be justified. He explains low amplitude reduction of higher frequencies by suggesting that they are shear waves not surface waves and cites the work of Tamura (1976) and Okamoto *et al.* (1963) in support. This does not in any way invalidate the concept of surface wave amplitude reduction with depth but highlights the necessity to establish the type of wave motion present before undertaking attenuation analyses.

The discussion above indicates that when a seismic disturbance comprises mainly surface wave motion, vibration levels at depth will be lower than those at the surface; consequently, predictions of damage at depth, based on surface data, are likely to be somewhat exaggerated. This con-

conclusion is supported by experience from deep mines where it is well-known that subsurface damage due to earthquakes is significantly less than that which occurs at the surface.

When an explosion produces vibrations in a nearby tunnel the wave packet will comprise compressional, shear and possibly some surface wave motions along or around the cavity. A detailed analysis of diffraction effects associated with cavities within solids has been given by Pao and Mow (1971), and Ewing, *et al* (1957) deal with other surface wave effects. The scattering and diffraction of elastic waves with particular reference to cylindrical and spherical cavities is given by Graff (1975) who also provides a useful review of the subject.

For wavelengths that are long compared to the dimension of the discontinuity the particle motions at the discontinuity boundary will be similar to motions in the surrounding solid. The 'small' discontinuity will not affect the general propagation of the wave motion although some scattering will occur. For all situations dealt with in this thesis the wavelength may be considered long (at least 5 times the tunnel diameter) and therefore the position of transducers within the tunnels was not of great importance. As the size of the discontinuity increases (or the wavelength decreases) forward scattering interferes with the incident field to form a shadow zone and the region behind the discontinuity may become relatively undisturbed (eg *see* Graff, 1975). It is therefore generally prudent to locate transducers within a discontinuity, such that they are not within a shadow zone.

2.3.2 Rock Failure mechanisms

There are two principal modes of failure which may occur in an underground opening in rock subjected to vibration (neglecting large differential movements on geological faults and slips in portal areas):

(i) the imposed dynamic forces may exceed the intact strength of the rock or lining

and (ii) structural inhomogeneities (rock jointing, rock/lining interface, etc) which result in weakened shear planes may allow material to be dislodged into the opening. Typically this type of failure will result in 'loosening' of the rock or the fall of blocks from the haunch or roof of an opening.

Given measurements of rock strength the critical PPV for mode (i) failure may be calculated using equations given in Section 2.2.1. Where the opening is lined with concrete a value for the tensile or shear strength of the lining material should also be used. Okazawa *et al.* (1975) have reported that crack initiation in a concrete tunnel lining occured at a PPV of 338 mm/s. This indicates a tensile strength of 4 MN/m^2 for a concrete of 2.4 Mg/m^3 density and a compressional wave velocity of 4500 m/s. 'Slabbing' failure is well-known (*see* Jaeger and Cook, 1976) and commonly results from detonation of explosives. It occurs when compressional waves are incident upon, and reflected at the rock/opening interface. The incident wave is reflected as a tensile wave and, if the resultant tensile stress exceeds the dynamic tensile strength of the rock, fracture occurs and material flies off into the opening with a momentum equal to that in a length of the original pulse corresponding to twice the distance between the free surface and the fracture.

Unlined openings generally only occur in rock with excellent engineering properties (long stand-up time capability) or for short periods during the construction process. Falling blocks of rock (mode ii failure) may occur in these circumstances at low vibration levels. It is obviously not possible to state that rock loosened by normal weathering or otherwise will not be dislodged by even the smallest disturbance.

An attempt at analysis of block stability has been made by Dowding (1977) and later modified (Dowding, 1979). His analysis suggests that blocks in cavern roofs are less stable at high rates of dynamic force reversal where the shear wavelengths are of the same order as the block dimensions. This implies that rock fall is more likely from nearby blasting than for a similar acceleration (with longer wavelengths) due to seismic activity.

Rock fall or slip due to strain waves in a jointed rock mass may occur when the shear stress due to a normally incident shear wave exceeds the shear strength of the joint. As given in Section 2.2.1 the shear stress τ due to a shear wave velocity C_s in a rock of density ρ is given by:

$$\tau = VC_s \rho \qquad \ldots (2.14)$$

Where V is the PPV (normal to the direction of wave propagation). The shear strength τ_s of the rock joint may be defined most simply as the effective stress (ie. total stress minus any porewater pressure) across the joint (p') multiplied by a factor associated with the effective residual friction between the faces of the joint (μ_r'). That is

$$\tau_s = p'\mu_r' \text{ (for cohesionless case)} \qquad \ldots (2.15)$$

Therefore, when $VC_s \rho > p'\mu_r'$ $\qquad \ldots (2.16)$

relative movement of the joint faces may occur.

In practice joint movement does not necessarily result in structural failure and the fall of rock or collapse of an opening will depend con-

siderably on the geometry and nature of the jointing. Note that for this type of dynamic failure the critical vibration parameter is peak particle velocity. A different mode of shear failure must be considered when the wavelength is long compared to the 'block size' and the peak particle acceleration of the rock mass is high. This effect is related to the inertia of the block and the 'rigid body' analysis given in Appendix B may be applied.

The suggested analyses lead to the following conclusions:

(a) PPV is the critical parameter when assessing the possibility of shearing failure due to strain wave deformation in a discontinuous rock mass.

(b) For low frequencies (from distant blasting or earthquakes, say < 10 Hz) accelerations, and hence inertial effects, are likely to be small.

(c) For high frequencies (nearby blasting) accelerations are relatively high and inertial effects may result in significant shear stresses on block faces. This applies to any block size but the effect on large blocks will be more serious as the dislodging force will increase as D^3 (block weight) and the retaining force increases only as D^2 (block face area). D is the face width of the envisaged 'cubic block' (*see* Appendix B).

Although the proposed simple analyses of joint failure may be useful in a qualitative sense it is the writer's view that the direct quantitative application of the derived stability equations is of doubtful practical

significance. The large uncertainties in the values required (that is, the size and distribution of the stress field in the vicinity of the opening, the geometry of the blocks and the joint friction) renders detailed numerical analysis extremely difficult. This conclusion is similar to that made by Ward (1978) concerning the 'static' stability of openings in discontinuous rock masses.

When considering the possibility of rock fall there will be no substitute for detailed individual inspection of doubtful areas by experienced mining engineers. When performing blasting operations in the vicinity of any underground opening it is clearly prudent to maintain close surveillance for rock fall or damage until sufficient confidence has been gained through experience.

2.3.3 Published thresholds of damage

Very little information is available concerning acceptable PPV limits for tunnels or caverns. Langefors and Kihlström (1978) give 300 mm/s as a criterion for the 'fall of rock in unlined tunnels' and a PPV of 600 mm/s is correlated with the formation of new cracks in rock. Hendron (1977) states that these criteria are consistent with his experience for unlined tunnels near nuclear detonations and he asserts that 'unlined tunnels rarely experience visible damage where the free field ground motions are of the order 300 to 600 mm/s unless a loosened piece of rock is detached from the roof by shaking'. This range of values is also verified using the analysis given in Section 2.2.1 and adopting values for rock properties typical of those encountered in unlined rock openings. Persson *et al.* (1980) give 70-100 mm/s as the limit currently enforced in Sweden related to 'hard rock cavern roof,

span 15-18 m'.

Monitoring of vibration and resulting damage to nearby rock faces has been carried out in Canada by Keil *et al.* (1977). Results, including site law analyses (*see* Chapter 3) are given for six sites with various rock types. Their results were mainly derived from benching at heights of 25 to 35 ft and may not be directly applicable to 'tunnel blasting'. The main conclusions of the study were as follows:

> 'The probability of causing damage increases with increasing PPV. However, on the basis of theory, results obtained in this study, and results obtained by others, the risk of causing excessive damage (formation of cracks or openings of discontinuities) to rock can be minimized if PPV's are limited to 24 and 12 in./s (610 and 305 mm/s) at supported and unsupported faces respectively. Although no damage has been observed in certain cases where these velocities have been exceeded, the above criteria are deemed to be appropriately conservative where adverse geotechnical features are absent. More stringent criteria must be used where adverse jointing or discontinuities exist. Careful analyses of potentially unstable wedges or blocks must be made to suit the exact geometry prevailing.'

Sakurai and Kitamura (1977) give an interesting account of vibrations measured in a tunnel as a second tunnel was driven about 30 metres below. As no failures were noted and PPV's induced in the tunnel were quite low (less than 30 mm/s) this work is not useful in assessing damage criteria. However, useful information concerning the direction of propagation of the stress waves from the blasting is given. For instance, the energy from the blast is mainly propagated 'forward' from the tunnel face so it is the 'approach' phase which will be critical with regard to PPV damage. As a consequence measurements taken in the tunnel

under construction (at a distance x behind the face) may seriously underestimate the vibrations induced in an underground opening (distance x) ahead of the face.

An interesting case history of extensive damage to a tunnel caused by a bomb during World War II is reported by Harding (1945). The bomb fell in the Thames during December 1940, close to Tower Pier, and caused extensive damage to the Tower Subway which lay some 10 m below the river bed. The 6 ft 7¾" ID tunnel was lined with cast iron segments and was driven in the London Clay which, at this point, is overlain with Thames ballast. The tunnel was damaged over a length of about 60 m and was completely blocked directly beneath the bomb crater. The lining was cracked over a considerable length and 'closed like a spring over itself' until the point nearest the bomb was reduced to a diameter of 4'2". The bomb was described as a 'near miss' and did not penetrate the tunnel. The bomb weight is unknown but was likely to be in the range 250-1000 kg. It is probable that it was either of 250 or 500 kg which were the most common used at this time by the Luftwaffe. (Personal communications with the Imperial War Museum).

Although several relevant factors are unknown, it is clear that this tunnel was subjected to PPVs well in excess of 2500 mm/s (100 in/s) and its failure was therefore to be expected. However, at distances over 30 m from the impact it seems that little structural damage to the tunnel occurred. The finding agrees with other information given above that lined tunnels are very resistant to blast damage. This case history suggests that further useful data on blast damage to underground structures might be obtained from historical records of the 1939-45 period.

2.4 The effect of earthquakes on underground openings

The lack of case history data concerning the effect of blasting on underground openings makes it desirable to consider the information available on the effect of shaking by earthquakes. The difference in the character of the vibrations generated by blasting (high frequencies) and earthquakes (low frequencies) is discussed earlier in this Chapter and because of these differences any conclusions drawn by analogy must be considered with caution.

Damage to underground storage facilities is of current interest, particularly in the fields of nuclear waste disposal and rock storage caverns, and has stimulated recent review work. Rozen (1976) has published the most comprehensive review on damage to shallow underground openings and correlates damage (if any) with earthquake intensity and and epicentral proximity for 71 tunnels. Dowding and Rozen (1978) and Dowding (1977 and 1979) have analysed the data and arrived at the following conclusions.

1. Collapse of the tunnels from shaking occurs only under extreme conditions. It was found that there was no damage in both lined and unlined tunnels at surface accelerations up to 0.19 g. In addition, very few cases of minor damage due to shaking were observed at surface accelerations up to 0.25 g. There were a few cases of minor damage, such as falling of loose stones, and cracking of brick or concrete linings for surface accelerations above 0.25 g and below 0.4 g. Most of the cases of similar damage appeared above 0.4 g. Up to surface acceleration levels of 0.5 g, no collapse (damage) was observed due to shaking alone.

2. Tunnels are much safer than above ground structures for given intensity of shaking. While only minor damage to tunnels was observed in MM-VIII to IX levels, the damage in above ground structures at the same intensities is considerable. Furthermore, it should be noted that the effect of the damage is a function of the use of the tunnel and building.

3. More severe but localized damage may be expected when the tunnel is crossed by a fault that displaces during an earthquake. The degree of damage is dependent on the fault displacement and on the conditions of both the lining and the rock.

4. Tunnels in poor soil or rock, which suffer from stability problems during excavation, are more susceptible to damage during earthquakes, especially where wooden lagging is not grouted after construction of the final liner.

5. Lined and fully grouted tunnels will only crack when subjected to peak ground motions associated with rock drops in unlined tunnels.

6. Tunnels deep in rock are safer than shallow tunnels.

7. Total collapse of a tunnel was found associated only with movement of an intersecting fault.

The significance of the data is well shown in Figure 2.3 (*after* Dowding 1979). Observed damage thresholds are shown related to peak surface acceleration, Modified-Mercalli (Neumann, 1954) intensity and Richter (Gutenberg and Richter, 1956) magnitude. These scales are defined by Pratt *et al.* (1978). A Figure is also given (by Dowding) indicating a minor damage bandwidth of between 200 and 920 mm/sec PPV. This suggests a frequency of about 1 Hz when associated with his equivalent acceleration threshold. Dowding (1979) also considers the problem concerning the

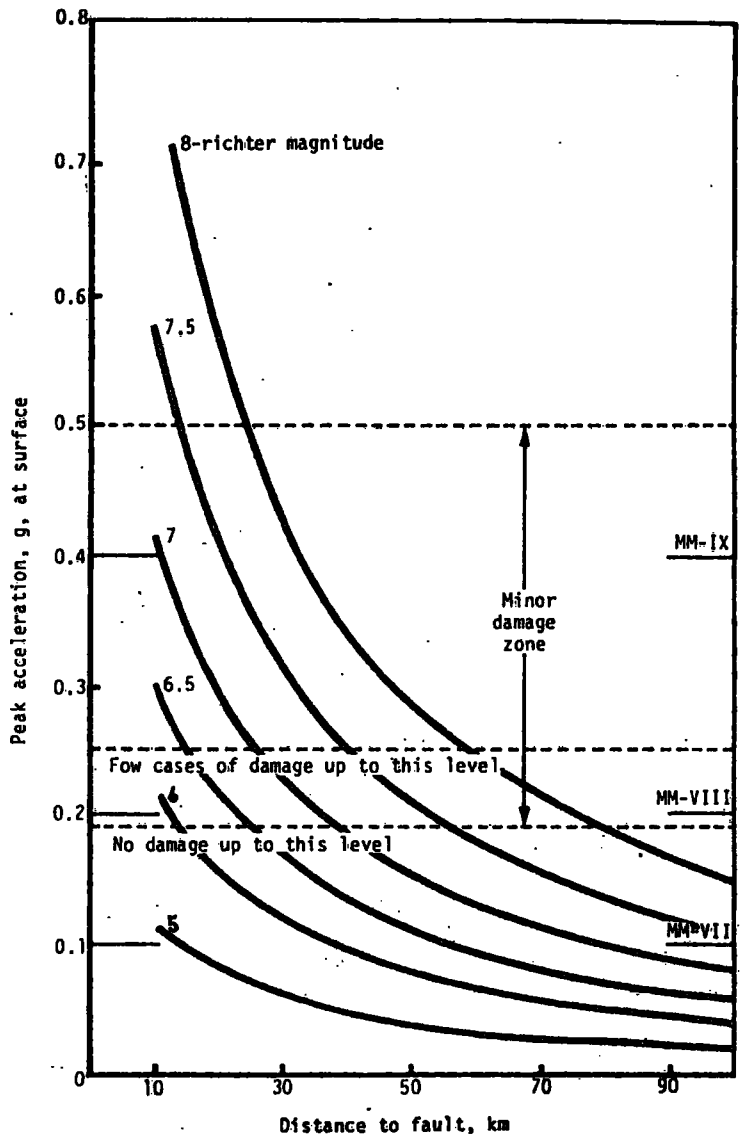

Fig. 2.3 EARTHQUAKE DAMAGE TO TUNNELS (after DOWDING, 1979)

effect of epicentral distance and amplitude reduction with depth (*see* also 2.3.4).

Pratt *et al.*(1978) have also undertaken a review on 'Earthquake damage to underground facilities' which is specifically aimed at seismic risk for underground nuclear storage in the USA. Their conclusions are very similar to those of Dowding and Rozen (1978) which probably follows from their heavy reliance on Rozen's original data base. They do however include data related to damage to oil wells during the 1964 earthquake in Alaska. They confirm that, as for tunnels, vertical structures such as wells and shafts are less susceptible to damage than are surface facilities.

Application of the information given in Figure 2.3 is not possible without some guidance on likely levels of seismic activity in the area of a particular structure. Burton (1978) has published an 'Assessment of seismic hazard in the UK' which may provide guidance for design of underground structures. His main conclusions are as follows:

(a) damaging earthquakes (presumably to surface structures) do occur in the UK and it is likely that accelerations reach, and may exceed, 0.1 g.

(b) this analysis indicates that accelerations of at least 0.1 g may be considered for particular design purposes within the UK.

It appears that seismic events of Richter magnitude of greater than 6 are very rare in the UK and that for the Inverness area (one of the most seismically active UK sites) the statistical '100 year event' has a magnitude of just over 5. Inspection of Figure 2.3 would therefore

indicate that even minor damage to a soundly constructed tunnel or cavern is extremely unlikely in the UK, and generally little consideration need be given to seismic hazard for most purposes. However, Burton's review indicates that where the opening is to be sited within 10 km of a known seismically active fault, larger accelerations than 0.1 g must be considered as a possibility.

2.5 Slope stability under dynamic loading

Blasting vibrations may impose dynamic loadings on slopes in the vicinity of underground construction work which may result in rock fall or total slope failure. The problems will generally be greatest in the portal areas where slopes are often at their steepest and the blasting close to the surface. Humphries (1937) has reported a slip of some 3000 tons of rock at a tunnel portal during blasting. Plate 2.1 shows the steeply-dipping joint failure (or flow banding) immediately above the portal stonework.

Dowding (1979) has shown that damage to tunnels caused by earthquake shaking is at its greatest in portal areas and he attributes a proportion of this to 'landslides of masses through which the tunnels passed'.

Static analyses of slope stability are dealt with fully by Hoek and Bray (1977) and Attewell and Farmer (1976), but neither seriously consider the effect of dynamic loadings. Seed and Goodman (1964), Sarma (1975) and Sarma (1981) have provided analyses concerned with the earthquake stability of a soil slope subject to shaking, and they give methods of calculating the additional loading imposed by vibration, which may be applied to more complex analytical methods.

PLATE 2.1 ROCK SLOPE FAILURE ABOVE ROAD TUNNEL PORTAL (1932) AT PENMAENBACH

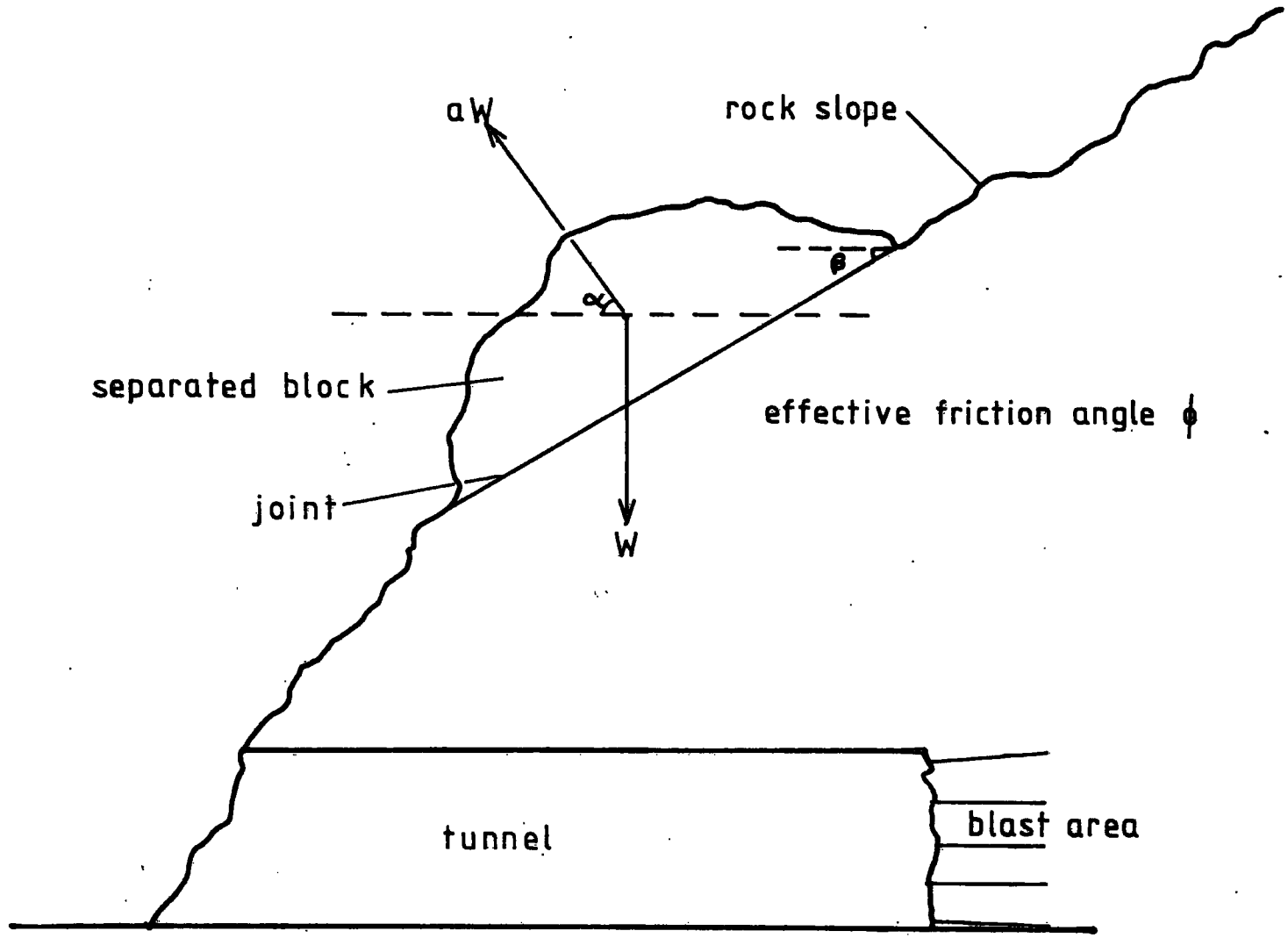

Fig. 2.4 ROCK SLOPE STABILITY WITH DYNAMIC LOADING

Consider the rock slope shown in Figure 2.4 where the 'daylighting' joint separates a section of rock, weight W, from the rock mass. For clarity this analysis considers only gravitational, frictional and inertial forces and deliberately neglects other factors, principally hydrostatic, which may also affect stability. The analysis is independent of the type of wave motion and considers the destabilising inertial forces contributing to the slope failure. Similar forces opposite in direction will also occur during the passage of the wave train; these will tend to increase the stability of the slope.

Consider the destabilising phase of the incident wave motion:-

Let α = angle of peak particle acceleration to the horizontal

β = joint inclination angle (dip)

a = effective acceleration due to vibration expressed as a factor of g (the gravitational acceleration)

ϕ' = effective friction angle of joint (joint friction plus roughness coefficient, *see* Attewell and Farmer, 1976)

The force downjoint inducing sliding

$$= W\sin\beta + aW\cos(\alpha + \beta) \qquad \ldots (2.17)$$

The force resisting sliding (no cohesion)

$$= [W\cos\beta - aW\sin(\alpha + \beta)] \tan\phi' \qquad \ldots (2.18)$$

At the threshold of stability (Factor of Safety = 1)

eq 2.17 is equal to eq 2.18. At 'failure' acceleration, a_F,

$$\sin\beta + a_F\cos(\alpha + \beta) = [\cos\beta - a_F\sin(\alpha + \beta)] \tan\phi' \qquad \ldots (2.19)$$

$$\therefore\ a_F[\cos(\alpha + \beta) + \tan\phi'\sin(\alpha + \beta)] = \tan\phi'\cos\beta - \sin\beta \qquad (2.20)$$

$$\therefore \quad a_F = (\tan \phi' \cos\beta - \sin\beta) / [\cos(\alpha + \beta) + \tan \phi' \sin(\alpha + \beta)] \quad \ldots (2.21)$$

$$\therefore \quad a_F = \sin(\phi' - \beta) / \cos(\phi' - \alpha - \beta) \quad \ldots (2.22)$$

The acceleration angle (α_c) at which a_F is a minimum will occur when the denominator of eq 2.22 is a maximum

that is $\cos(\phi' - \alpha - \beta) = 1$ ... (2.23)

$$\therefore \quad \phi' - \alpha - \beta = 0 \quad \ldots (2.24)$$

$$\therefore \quad \alpha_c = \phi' - \beta \quad \ldots (2.25)$$

From 2.22 and 2.23

$$\underline{a_{F(min)} = \sin(\phi' - \beta)} \quad \ldots (2.26)$$

That is, the minimum acceleration for failure is a function of the dip of the failure surface and the effective friction angle of the surface.

Practical application of these stability equations is subject to similar difficulties as those described earlier for block stability in tunnels. However, one factor, the estimation of stress across the joint, will be more easily assessed as it may depend more upon the rock weight than the highly modified stress field associated with subsurface excavations.

The estimation of effective friction angle ϕ' may be extremely difficult as the interlocking effects of asperities on the joint surface may considerably increase the effective friction (joint shear strength) beyond that expected for surface-to-surface contact of flat rock samples. It should be noted that the acceleration factor, a, is applied to the loosened rock as a whole. In practice consideration must be given to the relative dimensions of the 'loose' rock section and the wavelength of the incident

vibration. It might be that peak particle accelerations are different at various parts of the unstable block due to temporal phase variation and an 'effective' value for a may need to be estimated.

By considering the character of these dynamic forces some insight may be gained as to why slopes do not fail as readily as this type of calculation often indicates. Considering a stress wave, of say, 100 Hz, the direction of the dynamic forces alternates every 0.005 seconds. This implies that some 0.005 after the maximum destabilising motion an equal and opposite motion actually improving the 'static' stability may occur. Further, the amplitude of the high particle motion at frequencies likely to arise from nearby blasting will be in the order of 0.1 mm. This is considerably less than the likely persistence of the 'interlocking' asperities contributing to the friction along the joint.

2.6 In-tunnel train-induced vibration

When considering the likely effects of blasting-induced vibration on subsurface structures it is clearly useful to have knowledge of 'ambient' levels to which the structure has been subjected. The brief review given below was undertaken to assess the likely level of vibration induced by trains at the site of the Penmaenbach trials and in the Pass of Killiecrankie. Subsequently, train induced vibrations were measured and the results are given in Sections 6.7 and 7.4.5.

Steffens (1974) has reviewed many sources giving details of vibration levels from rail traffic. Most of the reviewed work relates to vibrations in man-made structures and the frequencies measured were all less than 100 Hz. These data reflect the natural frequencies of the structures

rather than the frequencies actually excited in the ground mass by the trains. These data show that vibrations of between 0.1 and 2 mm/s (at between 5 Hz and 70 Hz) may be expected to occur in structures within 100 m of a railway. Steffens does not give any data, and none has been found elsewhere, concerning vibrations in unlined rock tunnels or on bedrock close to a railway track.

Much existing information seems to relate to steam-hauled trains and it is assumed that most data were obtained on a conventionally-jointed track. It is well-known that the level of vibration from wheeled traffic is heavily dependent on running surface irregularities (*see* Whiffin and Leonard, 1971). New (1974) gives details of bridge vibrations from rail traffic where (neglecting quasi-static deflections due to train weight) almost all the vibration is clearly attributable to the impact of each axle (wheel pair) with a rail joint.

The conditions in the rail tunnels at Penmaenbach and Killiecrankie were materially different from those cited above in two ways:

(i) the track throughout the tunnel was long-welded, ie. there were no rail joints at all in the vicinity of the measurements;

(ii) the vibrations generated by the trains pass through the track ballast directly into the rock mass upon which the transducers were mounted.

2.7 Demolition-induced tunnel vibration

Sections 2.3 and 2.4 have discussed and reviewed vibration hazard to sub-surface structures resulting from various man-made and naturally-occurring sources. It became apparent during this review that one potentially damaging source of vibration has not been considered in the literature; that is, damage risk to tunnels due to explosive demolition of a large building.

Urban clearances of high rise blocks have increased dramatically during recent years as a result of socially unacceptable living conditions and structural failures. Piecemeal demolition of such structures is dangerous, lengthy and causes great environmental distress to the surroundings. Explosive demolition has been shown to be quicker, more economical and therefore generally more acceptable.

The urban areas where these demolitions are becoming necessary are often underlain by sub-surface structures and in particular railways in tunnels. The demolition of Oak and Eldon Gardens at Birkenhead in 1979 caused considerable concern to British Railways who owned an old brick-lined tunnel which passed closely beneath the demolition site. Although some vibration measurements were taken at this site, none was ever published (personal communication with British Rail).

In November 1981 the opportunity arose to carry out vibration measurements in a tunnel closely beneath two tower blocks as they were demolished. London Transport asked the author to advise on the likely effects to the Central Line running tunnels which passed closely beneath the blocks to be demolished.

The following brief case history is presented here because of its direct relevance to the subject of this thesis and because it is not possible to refer to other published work of this kind.

Owing to structural faults the two highrise blocks, owned by the London Borough of Newham, were demolished by the Contractors (Ogdens) on the 22 November 1981 (Dadson, 1981). The rather spectacular nature of the event stimulated many reports in the national press of the following day.

The position of New Town and Stratford Points relative to the Underground tunnels and access shaft are shown in Figure 2.5. The buildings were previously weakened and the explosives detonated during a number of ½ second delays to soften up the structure at various floor levels immediately before collapse was caused. This process served to reduce the vibration levels that would have resulted if only the base of the building had been blown out and the upper levels of the structure had hit the ground as a rigid mass. The skill of the Contractor in collapsing the buildings almost within their own plan area also contributed significantly to minimising vibration problems. This is because the rubble pile progressively formed by the lower floors tends to cushion the high energy impacts from the upper floors.

The demolition of New Town Point, which at its closest was less than 30 m from the tunnels, gave the greatest cause for concern, and although calculations based on vibration transmission data, energy to be dissipated and subsurface damage criteria had indicated that damage to the tunnels was unlikely it was considered prudent to close the railway during the actual demolition.

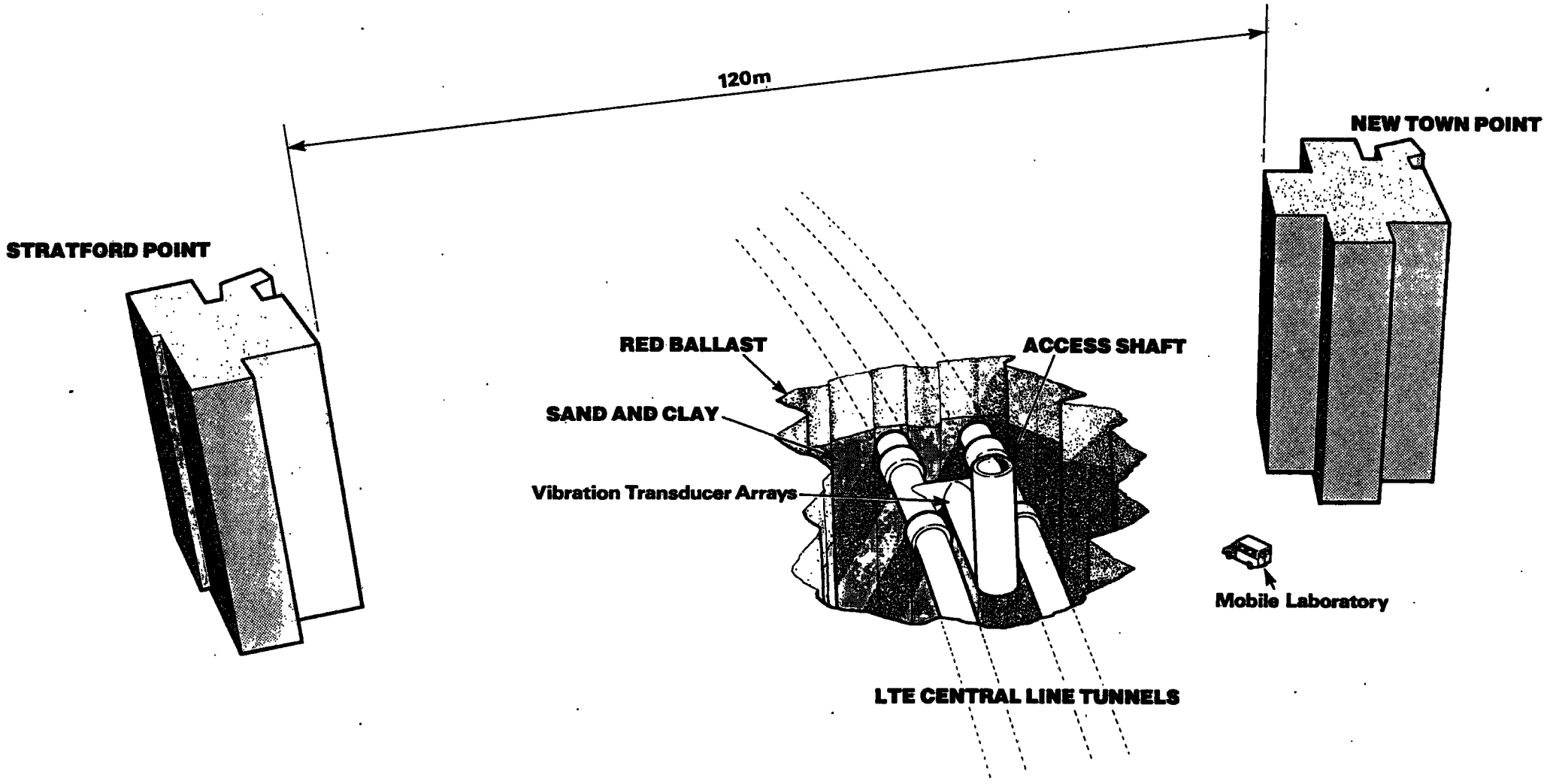

Fig. 2.5. NEWHAM DEMOLITION SITE LAYOUT

The tunnels were constructed during the late 1930's, through sandy clays overlain by red ballast, using a compressed air technique. They are of normal Underground construction with cast iron segmental linings 12 feet in diameter and have a cover of about 7 m. The shaft was of similar construction and has a diameter of 15 feet. The subsurface structures were thoroughly inspected before the demolitions and found to be in good condition with no significant evidence of water ingress despite being below the water table.

Triaxial vibration transducer arrays were bolted to the tunnel lining and in the access shaft. Other similar transducer arrays were placed just below the ground surface at the shaft top and on the road surface at a point approximately equidistant between the blocks. The signals from the transducers were amplified and recorded by a multi-channel ultra-violet oscillograph. The peak particle velocities (PPV) in the vertical, radial and horizontal directions were measured from the oscillograph traces and the 'real time' resultant PPV was calculated as described in Section 6.1. The 'radial' direction is defined as the direction from the transducer array toward the vibration source in a horizontal plane, and the 'horizontal' direction is perpendicular to the 'radial'.

The PPV's recorded are given in Table 2.6. The maximum subsurface resultant particle velocities recorded were 7.4 mm/s and 4.1 mm/s for New Town and Stratford Points, respectively. During the New Town Point collapse the surface ground motions close to the shaft reached 12 mm/s: for Stratford Point this value was 3.3 mm/s. These values were closely as predicted and were well below the threshold of damage for this type of structure. The transducer arrays in the tunnel and shaft all showed

in-phase motions of very similar amplitude. This was a consequence of the low frequency (long wave length) of the major motions which was approximately 7 Hz. The major ground motions occurred between 3-6 seconds after the initial detonation and resulted from the impact of the buildings; the motions due directly to the explosions being very small. The principal vector components of the subsurface motions were always vertical and at least three times greater than the radial motions. The horizontal motions in the tunnel were very small although in the shaft and at the surface positions they were significant. Strains in the tunnel lining were very small as the induced particle displacements were less than 0.2 mm and the wavelengths involved greater than 20 m.

It was of considerable interest to note that transducers mounted either on or close to the surface showed significant vibrations due to the actual explosions whilst those at depth in the tunnel showed no vibration from this cause. It is suggested that air overpressure was responsible for this observation. When interpreting the results from surface transducers (due to virtually unconfined demolition charges) great care must be taken if damage is to be correctly attributed to either ground vibration or air shock effects.

The vibration caused by the demolition was about an order of magnitude greater than that caused by the passing of trains which generally produced PPV's between 0.4 mm/s and 0.8 mm/s in the access shaft and tunnel.

The series of photographs in Plate 2.2 show the demolition of New Town Point at approximately one second intervals subsequent to the shot-firing instant at A. B shows the early delay charges softening up the

TABLE 2.6

Peak particle velocities during building collapses

Transducer array position/ orientation	NEW TOWN POINT			STRATFORD POINT		
	Distance from ℄ of building (m)	Peak particle velocity mm/s	Resultant peak particle velocity mm/s	Distance from ℄ of building (m)	Peak particle velocity mm/s	Resultant peak particle velocity mm/s
Tunnel springing/	48		7.0	95		4.1
Vertical		6.8			3.9	
Radial		2.3			1.1	
Horizontal		0.1			0.5	
Tunnel haunch/	44			99		3.9
Vertical		7.3	7.4		3.8	
Radial		2.3			1.1	
Horizontal		0.2			0.7	
Half way up shaft	42		7.0	100		3.2
Vertical		6.5			3.1	
Radial		1.8			0.7	
Horizontal		1.4			0.8	
Buried ½m below surface by shaft	45		12.0	106		3.3
Vertical		10.9			3.1	
Radial		5.0			1.8	
Horizontal		3.7			2.0	
Mounted on road surface (St Pauls Drive)	97		1.9	112		1.5
Vertical		1.3			1.2	
Radial		1.7			1.4	
Horizontal		0.7			0.9	

upper floors of the building and it is not until about 2 seconds after initiation that the building first starts to drop. The state of collapse at the instant of maximum PPV in the tunnels is shown in E with the scene after the dust cloud has cleared (several minutes later) in Plate F. These photographs form part of a high speed (20 frames/sec) stills record of the event which was also recorded at 150 frames/sec on 16 mm cine film.

Stratford Point was demolished some 5 minutes after New Town Point and the tunnels were then thoroughly inspected. No evidence of damage or disturbance was found and the railway was opened for normal traffic.

PLATE 2.2 THE DEMOLITION OF NEW TOWN POINT


ORDEN


B


D


F

CHAPTER 3

EXPLOSIVELY-INDUCED GROUND VIBRATION AND DYNAMIC ROCK PROPERTIES

3.1 Correlations of vibration (PPV) with charge weight and distance

When an explosive charge is detonated in a rock mass the rock close to the charge is subjected to violent anelastic deformations which may result in vapourisation, heating, shattering, and elastic and plastic deformations. The remainder of the energy from the explosion is discharged into the surrounding rock mass in the form of stress waves. The factors influencing the initiation and propagation of these wave motions, and in particular their magnitude and attenuation with distance, are of great importance as they are used to predict the likelihood and extent of damage to nearby structures.

Broadly, the ground motions resulting from a blast will depend upon the weight of explosive fired, the distance between the explosion and the observation point and the rock mass characteristics. The effect of each of these factors is very complex (*see* Section 3.3), and at present a satisfactory theoretical approach for calculating the form of these motions has not been developed. Therefore, scaling of field measurements is used almost exclusively to predict the magnitude and character of the vibrations from explosions.

A wide range of field data is available and several similar empirical approaches are in common use. The principal variables are usually related by an equation of the form:

$$PPV = K M^{\alpha} r^{-\beta} \quad \ldots (3.1)$$

where PPV is the peak particle velocity, M is the charge weight and r is the distance from the explosion. The constants K, α and β, are dependent on conditions imposed by the site geology and the type of explosion. Two special cases of this formulation are most commonly used:

$$PPV = K(r/\sqrt{M})^{-n} \quad \text{(square root scaling)} \quad \ldots (3.2)$$

and $$PPV = K(r/\sqrt[3]{M})^{-n} \quad \text{(cube root scaling)} \quad \ldots (3.3)$$

where again n is an empirical constant.

In the absence of specific field data peak particle velocities may be predicted by substituting values for the constants, suggested by numerous authors (*see* Hoek and Brown, 1980, for list), into equations 3.1, 3.2 and 3.3. In practice, where vibration damage is thought to be possible, it is desirable for trial blasts to be carried out. This allows the determination of specific 'site laws' which may be used in conjunction with structural damage criteria to determine the maximum charge weight which may be safely detonated at a particular site.

The 'square root' and 'cube root' scaling methods both allow simple graphical presentation of the derived site laws. These laws are graphically shown (Figure 3.1) as a straight line (on a log-log plot) with a slope of -n and an intercept of K at unit scaled distance.

Fig. 3.1. SCALED DISTANCE SITE LAW FORMAT.

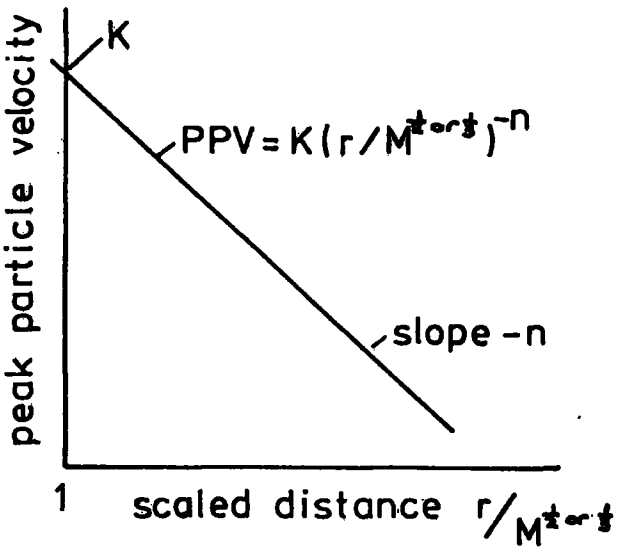

Because of the difference in the forced scaling of r to M these two methods lead to different predictions of peak particle velocity based on the same field measurements. Where extrapolation beyond the bounds of the field data is not required the predictions will be similar whichever method is used. However, where prediction is required beyond the scaled distance range of the trial blasts, significant differences may result from the two methods. This situation is clearly unsatisfactory, as is the somewhat arbitary scaling of r to M inherent in both methods. It has been argued that these empirical laws should be 'shaped' by dimensional analysis (Ambraseys and Hendron, 1968; Newmark, 1968). The dependent variables considered in their analyses are the particle displacement, velocity, acceleration and the frequency of the ground motions which result from an explosion. The independent variables considered most significant in influencing ground motions are the weight of the explosive, M, the range, r, the rock density, ρ, the compressional wave velocity, C_p and the time, t. Historically the character M has been used in the literature although Q or W may also be found to represent charge weight.

The dimensional analysis results in 'cuberoot' scaling laws for explosions of different sizes in the same medium. This approach has led to equation 3.3 being used extensively (Sauer *et al.* 1964; Newmark and Haltiwanger, 1962). the $r/\sqrt[3]{M}$ scaling of the 'horizontal axis' may be expressed in metric or imperial units and care must be taken that 'scaled distances' are clearly specified in terms of $m/kgf^{\frac{1}{3}}$ or $ft/lbf^{\frac{1}{3}}$ ($1m/kgf^{\frac{1}{3}}$ = $2.52\ ft/lbf^{\frac{1}{3}}$). Note that the size of the charge, M, is given in terms of explosive weight rather than energy, this being valid as energy is directly proportional to charge weight. If, however, data are scaled from various types of explosive the relative strengths of the explosives (Dick, 1968; Hoek and Bray, 1977) should be taken into account.

The alternative 'square root' scaling method ($r/\sqrt{M}$, $1m/kgf^{\frac{1}{2}} = 2.21ft/lbf^{\frac{1}{2}}$), is used by the US Bureau of Mines and is frequently preferred by workers such as Oriard (1971) who shows the 'limits of experience' for peak particle velocities from blasting (Figure 3.2). The scatter of about an order of magnitude is typical of the variations which may be found at various sites. Oriard also indicates the expected levels of peak particle velocity likely to result from confined blasting. This may be particularly relevant in a tunnelling context, as the initial charge of a tunnelling round may be heavily confined by the rock.

It has been argued (Ambraseys and Hendron, 1968) that square root scaling has 'no basis in dimensional analysis' and that cube root scaling should be used if estimates of motions are required which necessitate extrapolations beyond the limits of existing data. However, experimental evidence (Devine, 1966: Snodgrass and Siskind, 1974; Devine and Duvall, 1963) indicates that in certain situations 'square root' scaling does normalise the data very well. That is, the correlation coefficients were

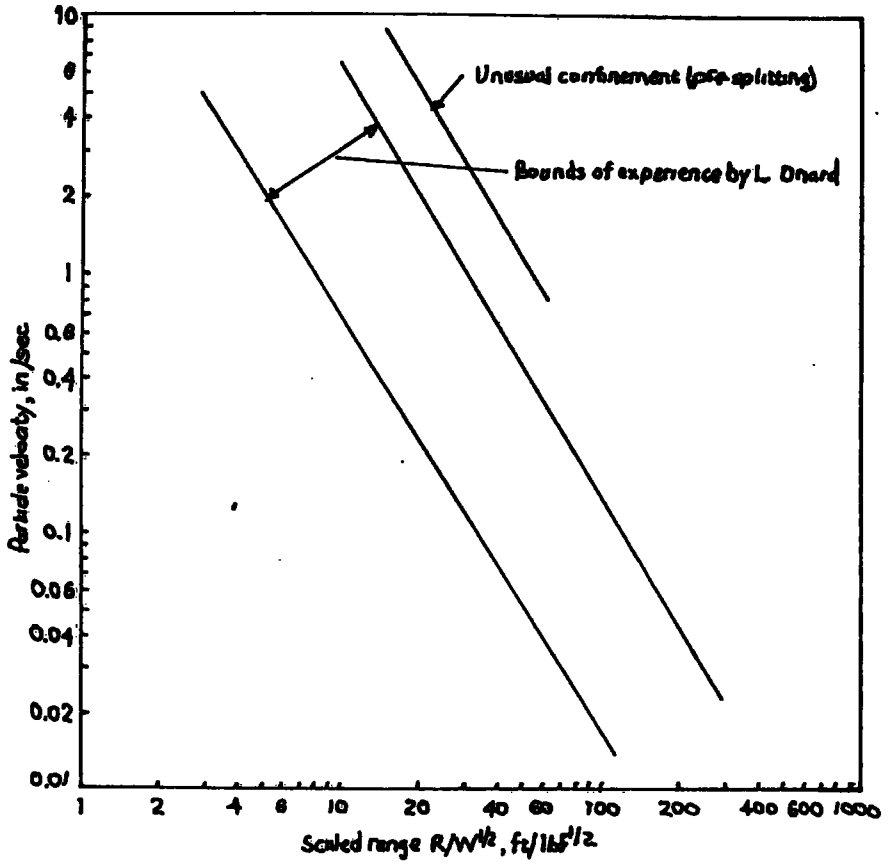

Fig.3.2 MAXIMUM PARTICLE VELOCITY v SCALED RANGE, SQUARE ROOT SCALING (after ORIARD,1971 AS CITED BY HENDRON,1977)

higher using $r/\sqrt{M}$ scaling than for $r/\sqrt[3]{M}$ scaling.

It will be shown (*see* Section 3.3) that neither scaling method can be generally appropriate and that the best estimate of relative scaling between r and M is site-specific and is best obtained by the analysis of trial blast data using the method shown in Section 3.2.

Several authors have recognised these problems and have derived site specific values for the constants K, α and β rather than just K and n. For instance, Holmberg and Persson (1979) give values for Swedish bedrock of 700, 0.7 and 1.5 (PPV in mm/s, M in kgf and r in metres) for K, α and β respectively, Also, Vorob'ev *et al.* (1972) have developed equations related to Rayleigh surface waves and found values of K = 707, α = 0.68 and β = 1.56.

Nicholls *et al.* (1971) have used two-variable regression analyses to determine values for α and β individually. These data have then been presented graphically in terms of peak particle velocity against distance with various lines representing different charge weights. Subsequently the data have been presented in scaled distance 'square root' format with standard deviations of the regression lines indicated.

It is usual to present blast vibration data in scaled distance graphical format with a 'best fit' straight line obtained by linear regression analysis (*see* Appendix C). A great volume of data in this form is available in the literature and almost without exception the peak particle velocity is well represented by a power law decay with scaled travel distance. That is, the measured PPV decay can be well represented by a straight line with negative slope on a log-log plot, although the

actual slope and intercept values may vary considerably from site to site and with different blasting conditions.

3.2 Determining the site constants (K, α, β) by multiple linear regression analysis

Having obtained field data relating peak particle velocity to explosive charge weight and range, it is clearly important to process and present the information in the best and most useful manner. The arbitary forced scaling of r to M implicit in equations 3.2 and 3.3 is unsatisfactory, (*see* Section 3.3) but does allow simple graphical presentation of the data in an easily usable format. However, the exploitation of equation 3.1 allows site specific scaling of r to M which will enable predictions to be made using equations better correlated with field data. The improved correlation is the direct consequence of the more versatile equation with three variables (PPV, M and r) rather than two (PPV and $r/\sqrt{M}$).

The constants K, α and β in equation 3.1 may be determined by transforming the equation and applying a three-variable multiple linear regression analysis to the data as follows:

from eq 3.1 $(PPV = K\, M^{\alpha}\, r^{-\beta})$

$$\log PPV = \log K + \alpha \log M - \beta \log r \qquad \ldots (3.4)$$

In this form 'best' values for K, α and β may be calculated based on the usual regression criteria that the sums of the squares of the deviations shall be minimised. For simple regression (two variables) these deviations are taken as deviations from a straight line whereas for this three

variable analysis they are represented by deviations from the plane, KABC, shown in Figure 3.3.

The application of this form of analysis is given in Chapters 6 and 7 and the resulting equations may be used to give a 'best' prediction of PPV. In this form, however, simple graphical presentation is not possible and some authors (eg Nicholls *et al.*) have resorted to plotting PPV against range for numerous values of charge weight. It is possible, however, to plot the data, using the constants and exponents calculated by the multiple regression, in the convenient PPV v 'scaled distance' format.

Transforming equation 3.1

$$PPV = K(r/M^{\alpha/\beta})^{-\beta} \qquad \ldots (3.5)$$

where the term $r/M^{\alpha/\beta}$ is the 'scaled distance'. Thus the data may be presented in the same convenient format as for square or cube root scaling (*see* Figure 3.1) but without the forced scaling relationship.

The coefficient of determination (R^2) for the three variable regression will always be greater than that obtained using the two-variable analysis for square or cube root scaling. (Except where, by chance, α/β is equal to $\frac{1}{2}$ or $\frac{1}{3}$ when the correlation will, of course, be numerically the same.) The higher the value for R^2 the better the data is fitted to the representative equation. Routine statistical tests of the significance of the correlations may be carried out and confidence limits calculated for the predictive equation if required. Generally, however, statistical analysis of the results will not be found any more useful than a straight-forward visual appraisal of the data plotted in scaled distance form.

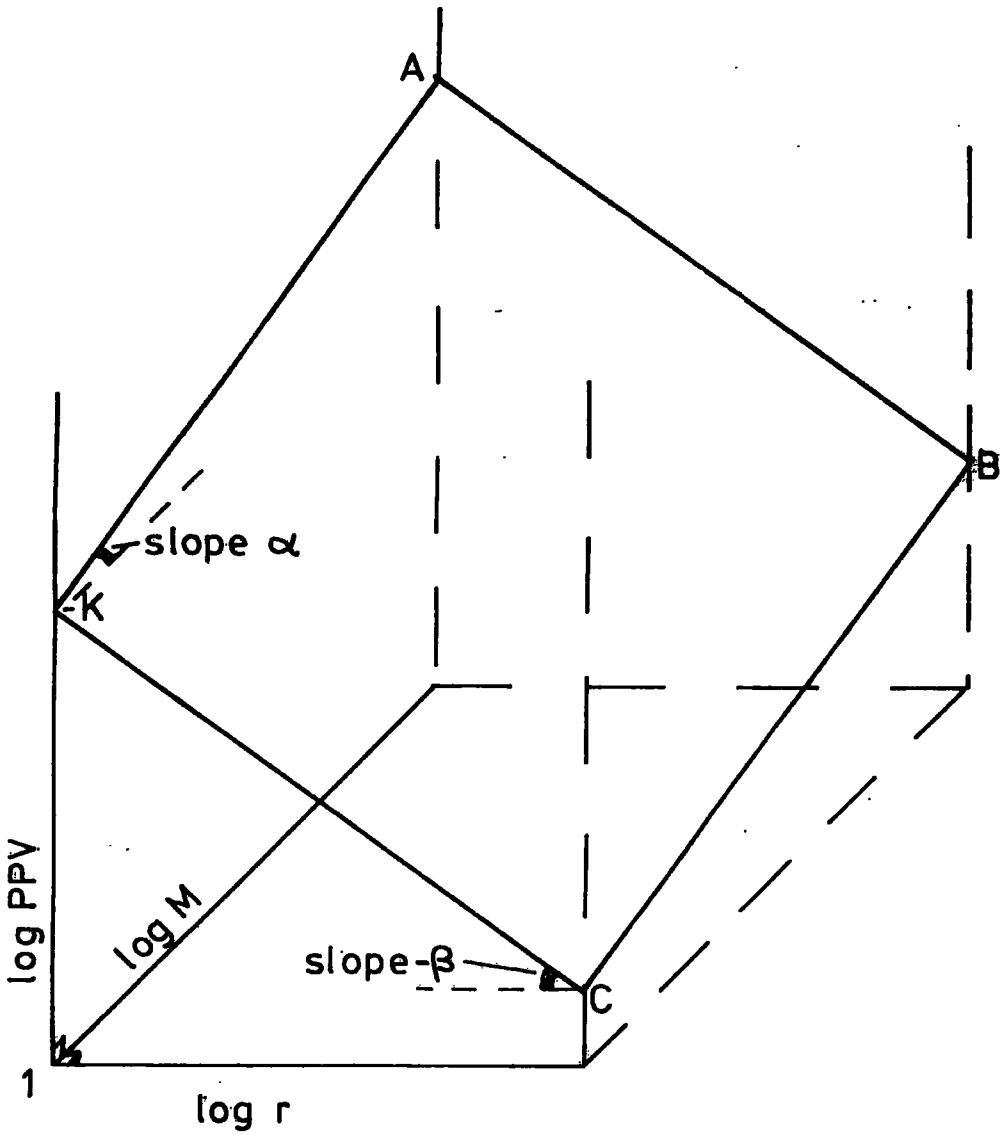

plane KABC is defined by :-

$$\log PPV = \log K + \alpha \log M - \beta \log r$$

Fig. 3.3. 3-D SITE LAW FORMAT

Although the projection shown in Figure 3.3 is most useful in visualising the multivariate regression equations 3.1 or 3.5, it is not appropriate for routine graphical presentation of data. Isometric or hypometric graph pads are not available with logarithmic scaling, and even where the plane is clearly defined the position of individual points in three dimensions is most confusing. Further, this form of presentation of field data does not materially improve upon that shown in Figure 3.1 and equations 3.1 or 3.5.

3.3 The factors which influence the 'peak' particle velocity

3.3.1 Introduction

Although it is accepted that the empirical equations given in Sections 3.1 and 3.2 do describe the peak particle velocity induced by a blast, little discussion of the form and constituents of the equations has taken place. A fuller understanding of the effects of varying charge weight and range may be expected to lead to better design of blasting trials and the reduction of vibration due to improved blasting techniques.

Theoretical analyses have centred around solutions for the disturbances produced by some arbitary pressure function acting on the internal surface of a spherical cavity in a homogeneous elastic solid. This type of analysis leads to an equation of the form.

$$PPV = K\, M^{\frac{1}{3}}/r$$

where K is dependent on the magnitude of the pulse pressure and the elastic characteristics of the rock mass. This equation leads to inaccurate prediction of blast vibrations, tending to underestimate the

effect of charge weight and to an even greater degree the attenuation with distance (*see* empirical equations given above for comparison).

Several more complex physical-mathematical models have been investigated in an attempt to describe the behaviour of waves in massive rock. These models are reviewed by Clark (1966) but none yields useful formulations for the prediction of vibrations under field conditions. This point has been forcefully made by Duvall *et al.* (1966) in the following Chapter of the conference proceedings where they propose that empirical methods should be used. The problems associated with these theoretical approaches and their conflict and inability to comply with field conditions and practice are dealt with below during discussion of the main factors influencing the empirical constants, K, α and β.

3.3.2 The nature of an explosion and the intercept constant K

The intercept constant K is the value of the peak particle velocity at unit scaled distance; that is where $(r/M^{\alpha/\beta}) = 1$. It may be considered as describing the initial magnitude of the blast-induced vibration (for unit charge weight) whose decay with distance will subsequently be described by the term $r^{-\beta}$. The exponent α describes the increase of peak velocity due to increasing charge weight.

Theoretical solutions define the initial disturbing force as some pressure function on the wall of a cavity. Solutions are available for step pulses, pulses with exponential decay and with both exponential rise and decay. Sharpe (1942) has suggested that this latter assumption 'probably corresponds quite closely to that which exists in practice'. All these solutions predict that the induced peak particle velocity will

be proportional to the assumed peak applied pressure.

In practice it is impossible to predict the form or magnitude of an explosive induced pressure pulse in a rock mass and the complex factors affecting the initial pulse are discussed below.

It is useful to consider the particular field conditions applied to blasting for construction works. The object is to excavate the material as efficiently as possible whilst causing a minimum of damage or disturbance to the surroundings. An idealised picture of the fracturing caused by an explosion in a borehole near to a free face is given in Figure 3.4. In the immediate vicinity of the charge the rock may be vapourised or melted and beyond this will be pulverised and shattered rock. Radial cracking will occur with some preferential growth in the direction of the major principal stress. These cracks will be opened by the gaseous products of the explosion and may interact with existing discontinuities within the rock mass to provide broken rock. Where the explosion is close to a free face further tensile breakage of rock by 'slabbing' may occur and gas expansion fractures may break out the remaining volume of rock creating a crater. Outside the volume of damaged rock the stress waves induced by the explosion will propagate into the rock mass. For convenience the zone of damaged rock will be referred to as the 'anelastic zone' and the rock beyond as the 'elastic zone'. It is the propagation of the vibrations within the 'elastic zone' which are dealt with here and the actual comminution process is considered only where it affects the induced vibrations.

The actual value of the constant K will depend on the conditions imposed by the rock mass, the type of explosive and its method of

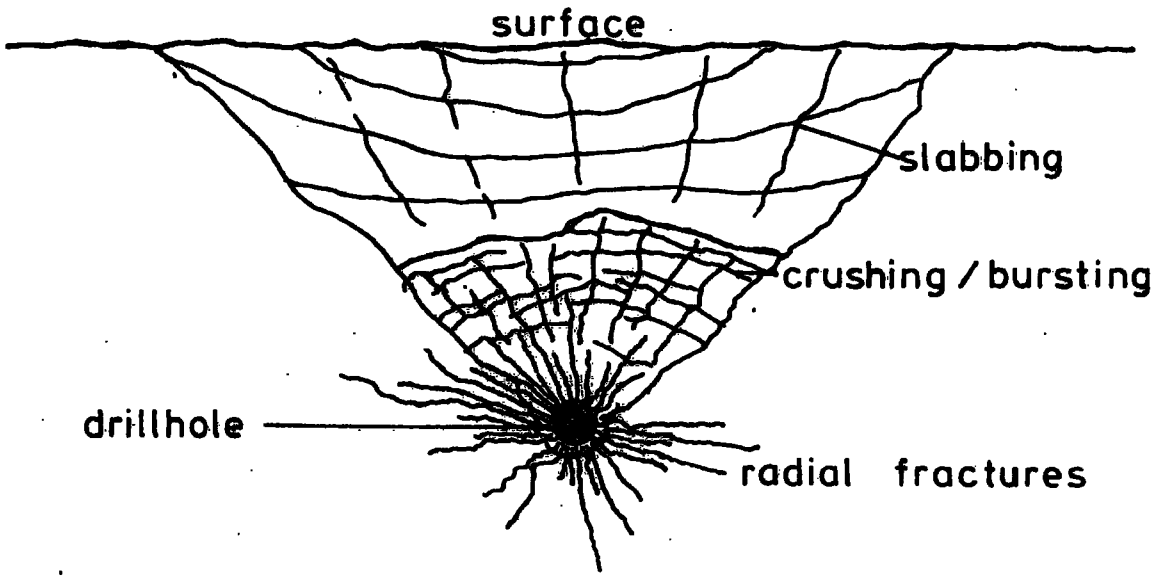

Fig.3.4 IDEALISED EXCAVATION CRATER

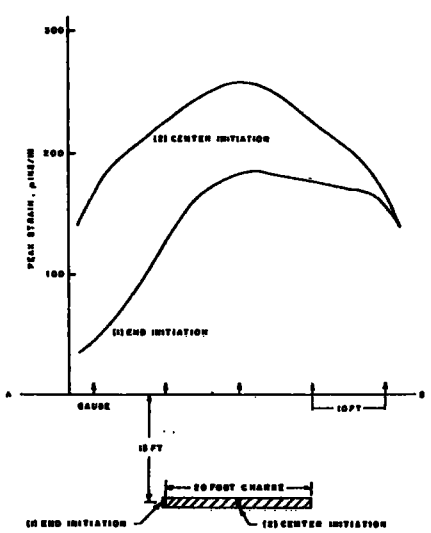

A comparison between end and center initiation for a 20-ft charge.

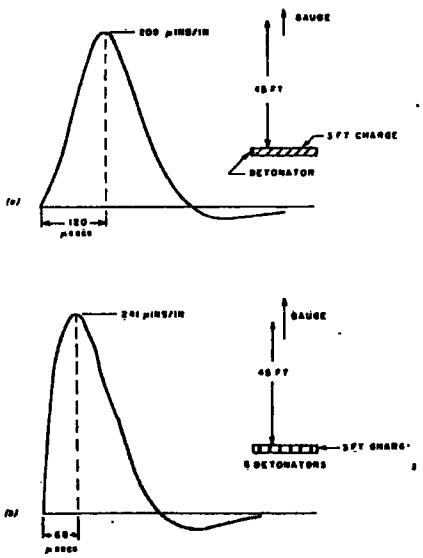

A comparison of the strain waves generated by a 3-ft charge when (a) it is initiated at one end only; (b) it is initiated at six points along its axis.

Fig.3.5 EXPLOSIVE STRAIN PULSE VARIATION WITH SINGLE OR MULTIPLE INITIATION POINTS (after STARFIELD, 1966)

detonation.

3.3.2.1 The explosive and its initiation

The energy of an explosive is usually described in terms of 'weight strength' or 'bulk strength' normalised to the energy yield of 100 per cent strength blasting gelatine. Explosives may vary considerably in terms of energy yield and as the 'energy' term in the empirical equations is referred to explosive weight (rather than energy content) the constant K will reflect the power of the particular explosive used.

The detonation of a given explosive charge will yield, in a very brief period, an amount of energy which, in the elastic zone, will initially radiate outward in the form of a large compressional pulse. The amplitude or peak particle velocity of this pulse will depend upon the time taken for the explosive to release its energy. The quicker the release of the energy the greater the induced particle velocity and the briefer the pulse. The time taken will depend on the confinement of the explosion by the rock mass as the speed of the reaction in the explosive is pressure-dependent. Where the charge is fired in a deep borehole packed tightly with explosive well tamped and stemmed, the pressure due to the initial stages of the explosion builds up rapidly and causes an acceleration of the explosive process. It is worth noting that for dynamite the degree of packing with a tamping pole is between 1.0 and 1.25 kg/dm^3 whereas with a pneumatic cartridge loaders up to 1.70 kg/dm^3 may be achieved.

Where the explosion is poorly-confined such a rapid pressure build-up will not occur and the duration of the compressional pulse will be

will be longer with consequent reduction of peak particle velocity. Poor confinement will occur where charges are close to a free surface, in a weak or broken rock and where small diameter charges are used in large drill holes.

The speed with which the explosion occurs is also dependent on the characteristic velocity of detonation (VOD) and the method of initiation of the charge. The VOD is defined as the velocity of detonation in an unconfined column of explosive 32 mm in diameter initiated by a standard No. 6 detonator. Some explosives (such as submarine or plaster gelatines) have very high (7500 m/s) VODs whereas others (such as special gelatine) have unconfined VODs of about 2500 m/s. When detonated using strong primers the VOD of special gelatines increases by at least a factor of two.

The energy from a cylindrical charge may also be released more quickly by initiating from a central point (rather than from one end) or using several simultaneous detonation points on the same charge (*see* Figure 3.5).

3.3.2.2 The conditions imposed by the rock mass

The degree of confinement will also greatly affect the proportion of the explosive energy transmitted as vibration. For instance, a charge fired at considerable depth in a strong rock will use little of its energy in breaking the rock and much will be transmitted in the form of vibration. The effect of the confinement is to increase the effective strength of the rock in the vicinity of the borehole. A charge close to the surface will expend a much greater proportion of its energy in creating new fracture surfaces and other anelastic losses.

The effect of charge confinement is one of the most important factors influencing vibrations from blasting. Figure 3.2 shows that the value of K may be an order of magnitude greater for a 'pre-split' or 'unusually confined' charge than for a similar charge weight fired with a small burden.

The strength of the rock will also affect the peak particle velocity at the beginning of the elastic zone; a weak rock can support a lower level of particle velocity than can a strong rock.

Figure 3.6 shows the approximate amount of explosive and the number of drillholes required for various types of rock and tunnel face areas. Note that the metamorphic rocks, mica schists and granite gneisses, are often the most resistant to blasting. They tend to absorb the shock imparted by the blasting rather than shatter. Igneous rocks such as granite or diorite, usually shatter readily but may be costly to drill due to their high silica content.

Thus rock strength and 'breakability' will determine the proportion of explosive energy transmitted into the elastic zone in the form of vibration. Further, it can be shown (Blake, 1952; Sharpe, 1942) that the duration of the compressional pulse (hence magnitude) is dependent on the elastic constants of the rock mass; rocks with lower moduli values propagate pulses of greater duration.

3.3.2.3 The effect of decoupling

A decoupled blast comprises the detonation of a relatively small diameter explosive charge in a larger diameter drillhole. The degree of

Relationship of explosives consumption to face area

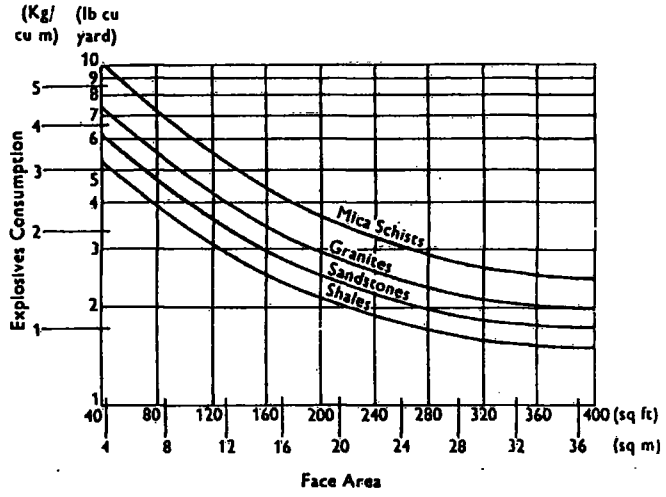

Relationship of number of shotholes to face area

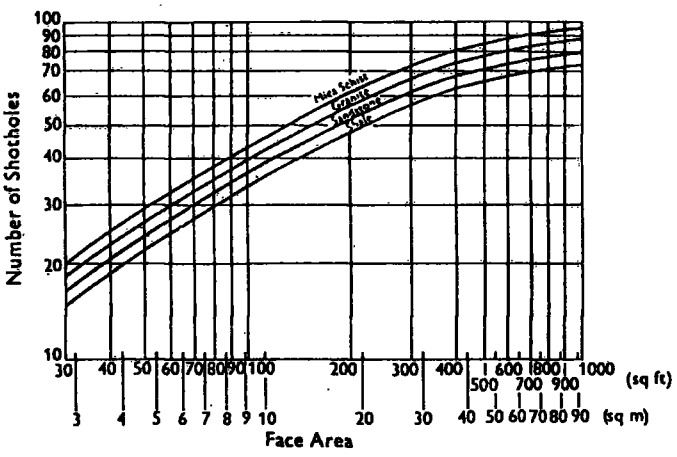

This graph has been constructed assuming that 35 mm ($1\frac{3}{8}$") diameter holes are drilled, using 28 mm ($1\frac{1}{8}$") diameter explosive cartridges. If 44 mm ($1\frac{3}{4}$") diameter holes were drilled, accommodating 37 mm ($1\frac{7}{16}$") diameter cartridges, larger burdens could be used and the number of holes required would be less. This is particularly so with the wedge cut rounds where fewer cut holes would be required.

Fig. 3.6 EXPLOSIVE CONSUMPTION AND NUMBER OF SHOTHOLES FOR TUNNELLING (after ICI LITERATURE)

decoupling may be defined as the hole/charge diameter ratio (or alternatively, the square of this ratio).

The space around the charge may be filled with normal stemming material but may in certain circumstances be left empty. Clearly the presence of the void or the greater porosity of the stemming material (compared to that of the rock) will tend to reduce the peak gas pressure created in the borehole and thus reduce the PPV transmitted to the rock mass. Voids around the charge may also affect the duration of the pulse transmitted to the rock.

In laboratory tests on stemmed decoupled explosives Fogelson *et al.* (1965) have shown that the amplitude of the displacement pulse was significantly reduced by decoupling. The duration of the pulse was also slightly reduced by increased decoupling, but changes in stemming materials had little or no influence. The significant reduction in strain pulse amplitude caused by decoupling in stemmed holes had previously been reported by Atchison *et al.* (1964).

The use of <u>unstemmed</u> decoupled charges is now being recommended for presplitting in rock excavation for civil engineering contracts (*see* Chapter 7). Although it is to be expected that peak particle velocities from this type of charge will be less than those from conventional bulk blasts, no relevant research or field data was available to verify or quantify the reduction in vibration levels. Research to determine these effects has been carried out and is described in Chapter 7.

3.3.2.4 The effect of explosive/rock impedance match

The ability of a strain wave to propagate across the boundary from one medium to another would be expected to be dependent on the characteristic impedances of the media concerned. (*see* Jaeger and Cook, Ch 13; 1976). Atchison and Pugliese (1964) proposed that the pressure, or stress, transferred from an explosive to the surrounding rock will, to some extent, be dependent on the explosive/rock impedance ratio (where characteristic impedance is the product of density and detonation, or propagation, velocity). They found that explosives with impedances more nearly matching the impedance of the rock produced higher peak strains and transferred more of their energy to the rock. The results from their tests provided a simple empirical method for predicting the relative effectiveness of different explosives for breaking granite from a knowledge of the impedances and detonation pressures of the explosives.

Further trials reported by Nicholls and Hooker (1965) also show that as the explosive/rock impedance ratio approaches unity, more rock is crushed and a larger percentage of the explosive energy is transferred to the rock as seismic energy. They showed that the effect of changes in impedance ratio was considerably greater than that predicted by acoustic theory.

Although the effects noted by Nicholls and Hooker (1965) were substantial, their variation in impedance ratio of from 0.165 (permissible ammon-dynamite < 5% to 0.522 (high pressure gelatine, 80%) was much higher than would occur in most field situations. That is, for construction blasting, the choice of explosive will be dictated principally by commercial objectives (cost, availability, packaging, safety, etc)

rather than with reference to any advantage that may be gained by selection of an explosive with a particular impedance. It is, however, important to note the general principle that the intercept constant K will increase with increasing explosive characteristic impedance. That is, explosives with high densities and detonation velocities will give higher vibration levels than those with low densities and detonation velocities.

3.3.3 The effect of charge weight and the exponent α

The assumption of a single spherical charge made by most theoretical models is rarely, if ever, true for field excavation processes. This assumption leads to the generation of a pulse the duration of which is proportional to the diameter of the charge with a peak particle velocity proportional to the cube root of the energy released by the charge (Ziolkowski and Lerwill, 1979). That is, when expressed in terms of charge weight,

$$PPV \propto M^{\frac{1}{3}}$$

A considerable complication of the theoretical approach occurs when the assumption of spherical symmetry is not acceptable (*see* Graff, 1975). In particular, these complications involve the generation of shear wave motions superimposed upon the compressional waves which alone were considered for the case of spherical symmetry. For a cylindrical charge of constant radius it has been suggested that $PPV \propto M^{\frac{1}{2}}$ (Snodgrass and Siskind, 1974; Jaeger and Cook, 1976).

The actual shape of excavation charges is cylindrical. Generally a number of individual cylindrical charges will be fired simultaneously (a 'delay') and it will be the complex collective effects of all the

charges in one delay which will produce the vibrations. As with the constant K so the exponent α is critically dependent on the effective time taken for the explosive to release its energy and the proportion of the energy which is ultimately transmitted as vibration. The exponent α reflects the variation of PPV with change in charge weight and distribution for a given set of conditions. The constant K reflects the variation of PPV with a change in field conditions for a constant charge weight and distribution.

Figure 3.7 (Nobel Explosives Company) shows a typical drilling pattern for the excavation of a small or medium sized tunnel. The type of cut illustrated is the 'burn cut' which uses parallel drill holes with a larger relieving hole around which the initial millisecond delay charges are fired. The later charges then fire using the cavity created to provide the necessary relief.

Note that in this case the initial millisecond delay detonators fire individually (except for No. 8) and may therefore be considered as single cylindrical charges. However, the later parts of the round fire a number of holes nominally simultaneously. In fact, because of small variations in the period of delay in the detonators and the spatial distribution of the charges, even the firing of a single delay is by no means instantaneous.

Close to the explosive the duration of the initial compressional pulse is typically about 1 ms (*see* Chapters 6 and 7). An indication of the accuracy of the time delay detonators is expressed in terms of standard deviation and is as follows (personal communications, Nobel Explosives Company)

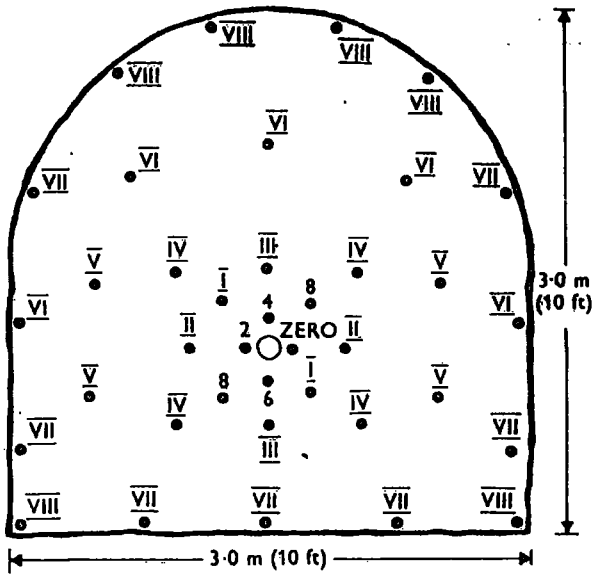

Arabic Numerals —Short Delay Periods

Roman Numerals —Half Second Periods

Type of rock	Granite
Face area	8·8 m² (95 sq ft)
No. of holes drilled	38 (plus one 76 mm (3") in diameter)
Rock broken	20·2 m³ (26·4 cu yd)
Rock drilled	4·6 m/m³ (11·6 ft/cu yd)
Depth of pull	2·3 m (7' 6")
Type of explosive	High strength gelatine
	28 mm × 200 mm (1⅛" × 8")
Quantity of explosive	43·8 kg (96·5 lb)
Rock: Explosive	0·46 m³/kg (0·274 cu yd/lb)
Explosive: Rock	2·15 kg/m³ (3·65 lb/cu yd)

Tunnel round using burn cut and incorporating 76 mm (3") diameter relieving hole

Fig. 3.7 TYPICAL DRILLING PATTERN FOR 'BURN CUT' TUNNEL ROUND (after ICI LITERATURE)

Delay period(s)	Std Dev(s)
5	0.08
½	0.04
0.485	0.007
0.03	0.003

Therefore even with millisecond delay detonators the firing of nominally simultaneous explosions will in fact produce distinct and separate compressional pulses. The spread (in time) of the energy input for a given delay will be a function of the number of separate detonations involved and the accuracy of the particular batch of detonators used. Where detonating cord is used the time spread will depend upon the equality of cord length to each charge of the delay from the initiating point.

The 'effective' firing instant will also depend upon the physical separation of the charged drillholes as the compressional wave propagation velocity of the rock may not be considered as infinite for most tunnel rounds and rock conditions. For instance the charge holes for delay VIII in Figure 3.7 are separated by as much as 3½ metres. Therefore, for a rock with a characteristic velocity of say 3500 m/s the time taken for the pulse to travel from one drillhole to the other may be similar to the duration of the individual pulses. Thus, where the point of vibration measurement is in line with these holes the pulses may be observed as two separate arrivals.

From the discussion above it is clearly impossible to describe the complexity of the source with sufficient accuracy for theoretical solutions to provide reliable results. The exponent α is therefore best obtained by empiricism.

3.3.4 The effect of range and the exponent β

When vibrations from an explosion propagate into a rock mass they are subjected to two fundamental mechanisms of attenuation. The first involves geometrical factors which spread the available energy in space, and the second comprises losses due to the imperfect elasticity of the rock. Geometrical factors result in a spatial redistribution of the vibrational energy whereas imperfections in elasticity result in permanent loss of vibrational energy, ultimately in heating the rock mass.

Theoretical solutions (Sharpe, 1942; Blake, 1952) neglect absorption losses and consider the case of spherical symmetry with body waves diverging in an elastic continuum or the two dimensional spreading of surface waves. These solutions yield:

$$PPV \propto \frac{1}{r} \text{ for spherical propagation}$$

$$\text{or} \quad PPV \propto \frac{1}{r^{\frac{1}{2}}} \text{ for surface propagation}$$

These formulations grossly underestimate the losses observed in the field which indicate that $PPV \propto 1/r^{(1.5 \rightarrow 2)}$. The fact that particle velocities attenuate far more rapidly than these equations predict has been attributed to 'dissipation' by Jaeger and Cook (1976) and 'to inelastic deformation in the rock mass' by Ambraseys and Hendron, (1968). The discussion given below will indicate that the higher attenuation of peak particle velocity may be more reasonably explained by geometrical factors than to inelastic loss mechanisms.

Consider the resultant peak particle velocity induced by an actual explosion under field conditions. In the 'elastic' region a large com-

pressional pulse with some complex shear wave vibrations will propagate outward. Close to the source the arrivals of all wave motions will be closely simultaneous, and the initially received pulse is large and dominant with a short 'tail' (*see* Holmberg and Persson, 1979). As the disturbances propagate into the discontinuous (finite boundaries, joints, faults, bedding, lithological changes, etc) rock mass the wave packet will tend to spread owing to the different velocities of the constituent wave motions.

Even if only compressional waves are initially excited extensive mode conversion to slower wave motions will occur at rock mass discontinuities where reflection and refraction of the wave energy will take place. There will be steadily less and less superposition of wave types. Thus the resultant peak particle velocity will inevitably be reduced by the spreading of the energy into a longer wave packet. Eventually, in the far field, the wave packet will separate into compressional wave and shear and surface wave motions as observed at distance from earthquakes.

The general spreading of the wave packet is also accompanied by an increase in duration of the initial compressional pulse, which, close to the source will produce the maximum particle velocity. This has been noted by Newmark and Haltiwanger (1962) who suggest that the duration of the initial pulse is approximately half the source to observation point travel time. That is, pulse duration increases linearly with range (*see* Figure 3.8). Clark (1966) has also noted that 'another parameter which exhibits a notable difference from elastic behaviour is the pulse duration, which increases (*see* Figure 3.9) as the first power of scaled travel distance'. The measurements reported in Chapters 6 and 7 also indicate that an approximately linear increase of pulse duration occurs with

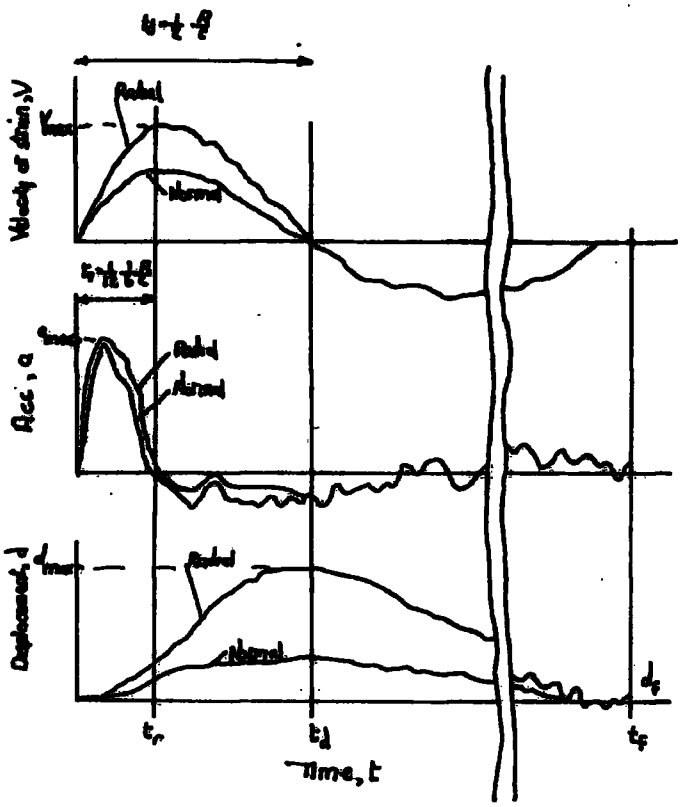

Fig. 3.8 TYPICAL WAVE FORMS FOR DIRECT-TRANSMITTED GROUND SHOCK (after NEWMARK & HALTIWANGER, 1962)

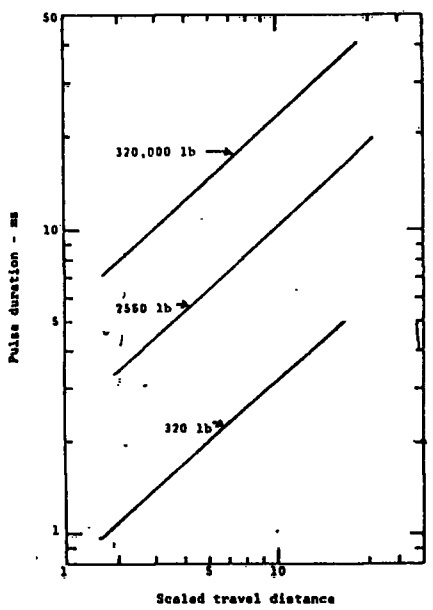

Fig. 3.9 PULSE DURATION vs SCALED TRAVEL DISTANCE IN SANDSTONE (after CLARK, 1966)

increasing travel distance. This spreading of the initial pulse or the wave packet cannot be reasonably explained in terms of the dispersive consequences of frictional losses (Knopoff, 1956) as it is well-known that the characteristic velocity of body waves in rock is practically independent of frequency. Farr (1978) discusses this and the concept of 'no dispersion attenuation' which theoreticians face when considering field rock masses.

Goldsmith (1966) discusses possible mechanisms of dispersion and concludes that 'the observed dispersive features may also be produced by factors other than anelastic behaviour of the medium (rock). The presence of any type of physical discontinuities, such as faults, will produce reflective effects resulting in changes of wave form'. Geometrical dispersion has been illustrated by studies of explosive pulses in bounded elastic media by Goldsmith and Allen (1955). Goldsmith has also pointed out that 'anisotropy plays a significant role in pulse observations and, in consequence, will lead to dispersion even when dissipative mechanisms are absent'.

It is difficult to evaluate the likely magnitude of absorption losses in the field as most measurements have been obtained on laboratory samples rather than over ranges up to 200 m in rock masses. Jaeger and Cook (1976) have stated that dissipative attenuation does not assume significance until the propagation distance is a few orders of magnitude greater than the wavelength of the motion. For the case of construction-induced vibrations this will represent several hundreds of metres. Other authors (Ambraseys and Hendron, 1968; Attewell and Ramana, 1966) have attributed a value of about $\frac{1}{210}$ to the specific dissipation constant, Q^{-1}.

Now as $\frac{1}{Q} = C_p\alpha/\pi f$, (Clark, 1966)

then $\alpha = \pi f/C_p Q = \pi/Q\lambda = 0.015/\lambda$ Neper/m,

and $\alpha = 0.13/\lambda$ db/m.

Where C_p is the compressional wave velocity, α the spatial attenuation coefficient, λ is wavelength and f is the frequency. Farr (1978) has concluded that: 'In all field studies amplitude differences attributable to absorption correspond only to the very lowest rock attenuation (0.1 to 0.2 db/m) determined from the laboratory measurements'.

For ranges of interest in tunnel blasting operations (say < 200 m) and wavelengths typically generated by blasting (say > 10 m) the field absorption will result in, at most, only a few db's of attenuation. This may be regarded as insignificant when compared to measured field or theoretical geometrical losses at these ranges.

Further, if field absorption were significant it might be expected to produce a non-linear decay (when plotted log-log format as in Figure 3.1) of the form PPV $\propto \exp(-\alpha r)$. Such a non-linearity is not present in field data for these ranges. An examination of laboratory data covering the attenuation of pulses in diorite indicates that the decay is more closely expressed as a power law than by an exponential relation (Goldsmith, 1966). If this observation holds true for field data then absorption losses, whether small or otherwise, will be assimilated into and be described by, the exponent β.

Recently theoretical investigations of seismic wave propagation have been undertaken by a number of authors (Brennan and Smylie, 1981;

Kjartansson, 1979) and McKenzie *et al.* (1982) provide a useful bibliography and discussion of the most recent work in this field. They cast considerable doubts, from both theoretical and experimental viewpoints, on the widely cited work of Ricker (1953). These analyses make the assumption that the specific dissipation factor (Q^{-1}) is a constant which may be justified for the small strains ($<10^{-6}$) associated with exploration seismology. However, it has been shown that where strains in excess of 10^{-6} are present, Q^{-1}, will not be constant (Winkler, *et al.* 1979). It can be shown (by substitution of appropriate values in equations 2.6 and 2.12) that where potentially damaging construction-induced vibrations are considered, the strains involved are between 10^{-6} and 10^{-1} and therefore the assumption that geologic materials may be treated as linearly elastic is not acceptable in these circumstances. Larson (1982) has arrived at the same conclusion in his studies of PPV attenuation rates in various rocks.

It is of interest to note that it is now a widely accepted experimental observation (Ricker, 1977; Gladwin and Stacey, 1974) that the duration of a compression pulse will increase with increasing propagation time (even for Q = constant). This increase has been described by an equation of the form

$$T = T_0 + kt \qquad \text{(Gladwin and Stacey, 1974)}$$

where T_0 and T are the pulse durations at the source and after time elapsed (t), respectively. The constant k is associated with the transmitting medium.

The available theoretical analyses often involve considerable simplifying assumptions and yet result in complex descriptions of seismic

pulse propagation. Future theoretical research of use when considering construction blast-induced wave packets must allow for a strain-dependent specific dissipation factor and, even more importantly, for the separation of wave types with propagation distance. A suitable analysis of this kind is not yet available owing to the complexity of the theory involved and the difficulties involved in defining input parameters and when analysing the field data. Examples of field data are given later in this thesis and show how, close to the blast, the initial compressional wave motions dominate the observed PPV whilst with progressively greater distances later wave arrivals give rise to the maximum PPV.

From the discussion above it seems likely that, for civil engineering construction purposes, the majority of the attenuation of PPV may be attributed to geometrical rather than absorption factors. Further, the wide range of field blasting data available shows clearly that the attenuation of PPV with range may be well represented by an equation of the form

$$PPV \propto r^{-\beta}$$

where β is a site specific constant which may range typically between 1.5 and 2.

3.4 The design of trial blasts

Trial blasts should be carried out where initial desk studies show that nearby structures could be at risk. The trials should be designed with a clear concern for the factors which will influence the induced PPV during the excavation works, as indicated in the previous section. Wherever possible the materials and techniques used during the trials must simulate those expected for the full-scale excavations. This will include:

(i) the type of explosive,

(ii) the drillhole diameter and depth,

(iii) the coupling of the explosive to the rock (tamping, stemming, water in-hole, hole/explosive diameter ratio),

(iv) the confinement imposed by the rock mass on the explosion. It will be desirable to simulate both 'confined' and 'partially confined' blasts for tunnelling works,

(v) multiple hole shots with appropriate hole spacing and detonating accessories,

(vi) similar shot point/structure ranges and paths,

(vii) wherever possible full-scale charge weights,

(viii) the ranges at which PPV is measured should be as broad as possible, not only centred on those of specific interest.

Changes in site conditions between the time of the trials and the works must also be considered. For instance, are there any new sensitive structures to be introduced or will seasonal changes in the water table have any effects?

It is recommended that plenty of data points be obtained. The cost of firing additional charges, or obtaining measurements at additional ranges, will be small compared to the mobilisation costs involved and will probably provide valuable information, or at least greater confidence in the derived predictive equations. The results of trial blasts should be analysed using the three variable correlation analysis discussed in Section 3.2 and demonstrated in Chapters 6 and 7. It is field practice to predict limiting charge weights based on an 'upper bound' line drawn parallel to the regression line such that all data points lie beneath it (*see* Section 6.5).

Costs and inconvenience will generally be minimised if the trials are carried out as part of the normal site investigation programme for the works. This will also ensure that the information gained will be of assistance in the preparation of tender documents and bids for the contract.

To reduce the peak particle velocities induced by tunnel blasting it is necessary to spread the round over a number of 'delays'. This reduces the effective charge weight fired at any instant, thus lowering the particle velocities. The type of cut chosen may also influence induced vibration levels with cuts which impose the least confinement being preferred where low vibration thresholds must be observed. For example, 'fan cuts' impose lower confinement on the initial delays than that imposed during the early parts of a parallel holed 'burn cut' (Langefors and Kihlström, 1978). However, the type of cut employed will often be determined by economic factors and with the increasing use of multiple boom drilling jumbos it is becoming more and more desirable to employ parallel hole cuts. It is usually found more convenient to drill a series of holes all parallel to the tunnel axis rather than a complex array of holes at various angles into the face. Multi-boom drilling jumbos may also drill several parallel holes simultaneously, but this becomes less easy where angled holes are required. The provision of 'relief' by drilling uncharged holes close to the initial delays will aid fragmentation and reduce vibration levels.

Occasionally the rock breaking mechanism demands the firing of many holes simultaneously. This may be the case when presplitting is being carried out as, due to the interaction required between the holes, it is essential to fire and presplit over certain optimum sized slabs. This type of problem is unlikely to occur when tunnelling but may be encountered

during construction of rock caverns or cuttings using presplit techniques.

Tests have been carried out (Devine *et al.* 1965) to determine if, and to what extent, a vertical presplit fracture plane placed between a blast point and a detection point will reduce vibration levels. The results of numerous field blasts indicated that the presence of a presplit fracture plane did not significantly reduce vibration levels. Further, it was shown that the vibration levels from the blast used to form the presplit can be higher than any of the breakage blasts.

As discussed in Section 2.2.1, damage is a deformation-related phenomena and although PPV is, in part, a measure of material strain, a knowledge of characteristic wave velocity is required to determine the induced level of strain. It is therefore suggested that where damage observations are related to vibration measurements the dynamic strain is also considered. This will require the identification of the type of wave present and an assessment of its characteristic velocity during the trial blasting. As discussed in Chapter 2, the relation between dynamic strain and structural damage is not established and further research and well-documented case histories are required.

3.5 The determination of *in situ* rock properties from seismic data

3.5.1 Introduction

The establishment of blasting site laws requires the detonation of a number of relatively small explosive charges which enable the attenuative effects of the rock mass to be evaluated. These explosions may also be considered as geophysical sources in a broader sense and

analysis of the wave forms received at distance will yield useful information concerning the engineering properties of the rock mass.

The deployment of vibration transducers at various known distances from the explosive source (to establish site laws) may allow the measurement of compressional and shear wave velocities and frequencies. These measurements will provide a basis for the calculation of rock mass classification (3.5.4) and the dynamic elastic moduli of the rock mass. Static moduli may be estimated from empirical correlations. Knowledge of rock mass classification and moduli are of considerable interest at the design stage of underground openings and where trial blasting is carried out it is clearly sensible to make the greatest use of the data obtained in this context. Geophysical investigations of this kind can provide valuable supplementary data to conventional site investigations, based largely on borehole data, by providing access to the rock mass as a whole. At present site investigations of this kind are rarely carried out because of the difficulties and ambiguities which are often encountered during the interpretation and evaluation stages.

This section discusses and develops applications of trial blast data in establishing rock mass properties associated with tunnel stability and support requirements. The applications of the analyses developed here are given in Chapter 6.

The delineation of rock head by seismic refraction methods and seismic borehole logging are both carried out on a fairly routine basis and are not discussed here. Lama and Vutukuri (1978, Ch 7) discuss dynamic measurement of rock sample and mass properties in detail and provide an extensive bibliography on the subject. They also list

details of dynamic measurements on many rock types. Similar, but less recent work, is reported in Chapters 7-9 of the Handbook of Physical Constants edited by Clark (1966).

3.5.2 The 'velocity ratio' approach

The velocity of seismic wave propagation in a rock depends on its rigidity, compressibility and density which are affected by the degree of weathering, fracturing and the state of stress in the rock. The measurement of seismic velocity provides a means of assessing rock quality that does not require full access to the region of interest.

Onodera (1963) proposed that the ratio of the dynamic elastic modulus of an *in situ* rock mass to that of an intact specimen could be used as an index of rock soundness, the dynamic moduli being derived from compressional wave (P-wave) velocities measured in the field and laboratory. Deere *et al.*(1966) correlated other experimental velocity ratios with Rock Quality Designation (RQD). RQD is the percentage of solid borehole core recovered greater than 0.1 m in length.

The determination of the velocity ratio requires the measurement of the *in situ* P-wave velocity of the rock, using surface or borehole geophysical techniques, followed by measurement of the P-wave velocity of an intact core specimen taken from a borehole. The intact specimen should preferably be tested under an axial load equivalent to that estimated from its former depth in the field. The velocity ratio is the *in situ* velocity divided by the intact velocity; it is close to one for fresh rocks with few joints and less than one for sheared, altered or weathered rock or rock containing many joints.

Subsequently Deere (1968a) suggested that the square of the velocity ratio may be used interchangeably with the RQD for engineering purposes. This seismic method has obvious potential for the site investigations carried out before tunnelling in rock (Scott *et al.* 1974) and has also been proposed by Deere (1968b) as a method for determining the rock quality ahead of a tunnelling machine.

There are, however, a number of problems that arise in the interpretation and use of seismic velocity data. These relate to the type and state of the joints in the rock mass. The freshness, filling, alteration and in particular the normal stress across a joint may lead to a seriously inaccurate assessment of the rock quality. This type of problem has previously been noted by Cratchley *et al.* (1972) in their report of geophysical measurements on a tunnel for the Foyers Hydroelectric Scheme driven beneath cover ranging up to 100 m, where they found no correlation between wave velocity and fracture spacing. Further they observed 'that when logged in the Glen Lia pilot tunnel all joints appeared so tight that it was not surprising that the tunnel velocities showed virtually no change from laboratory values'.

The writer has reported (New and West, 1980) laboratory and field studies together with a discussion concerned with the difficulties that may be encountered with the velocity ratio approach. Relevant abstracts from the conclusions of this work are given below:

> 'From the tests on rock with open joints it was found that P-waves passed through the shortest available path in the intact rock because an open joint so attenuated the signal that the receiver was unable to respond. For closed and relatively unaltered jointing, laboratory tests showed that the direct

stress imposed by even shallow overburden may render such jointing acoustically transmitting. This indicates that measurements of P-wave velocity (used to calculate the velocity ratio or otherwise) may be insensitive to the frequency of joints in a rock mass and should therefore be used with caution for engineering purposes.

For underground excavations in rock the interpretation of seismic velocity data, in an engineering context, may be improved considerably by allowing for effects resulting in the acoustic closure of the joints. For example, the circumstances which limit the applicability of the velocity ratio approach discussed in the Introduction can now be defined. If the velocity ratio is low, for both deep and shallow sites, it shows that the rock quality is probably poor. If the velocity ratio is high for shallow sites it shows the rock quality is good. However, if the velocity ratio is high for deep sites it cannot necessarily be taken to show that the rock quality is good because of the possibility of acoustic closure of joints.'

Sjogren *et al.* (1979) have correlated RQD with P-wave velocity in a number of igneous and metamorphic rocks with unweathered and unaltered jointing. They give the following relationship

Velocity m/s	3000	3500	4000	45000	5000	5500
Cracks/m	19	13.5	9.5	6.5	4	3.5
RQD	25	45	63	78	88	94

Further, they compare P-wave velocity with tunnel support requirements as developed in Sweden since 1956. This classification was as follows:

'Velocities below 4000 m/s were found to be related to faults, contact zones, etc with highly fractured rock, where in general

a higher degree of reinforcement was necessary when tunnelling. In contrast, velocities above 5000 m/s were considered to indicate competent rock masses with in general little need of reinforcement. The transition values between 4100 m/s and 4900 m/s were divided into two groups. Rock sections with velocities from 4100 m/s to around 4400 m/s generally proved to need more extensive support measures, while in the velocity range between 4500 m/s and 4900 m/s a continuous improvement of rock quality could be observed. Extremely low velocities - below 3000 m/s - were considered to indicate cavities in the bedrock filled with soil, or completely crushed and fragmented rock material. It ought to be noted that this classification of the longitudinal velocities was related to hard crystalline rock masses; in less consolidated rocks the same pattern was observed, but at lower velocity limits. If we compare these velocity limits with the corresponding fracture frequencies we can note that the velocity 4000 m/s corresponds to an average of about 10 cracks/m and velocities $\geqslant$5000 m/s to less than 5 cracks per meter. The extremely low velocities (below 3000 m/s) are obtained in rock material with pieces smaller than 5 cm.'

The information given by Sjogren *et al.* seems to apply to rock with an 'intact' P-wave velocity of between 5500 and 6000 m/s. Their attempts (and those of Cecil, 1971) to correct for variations of 'intact' velocity values at different sites by applying 'multiplication factors' would be better replaced by a velocity ratio approach which effectively normalises the data for each site.

Figure 3.10 (after Sjogren *et al.*) shows the relation between actual tunnel support measures and P-wave velocities in a number of tunnels. It must be emphasised that these correlations will only apply to rocks of the types specified earlier.

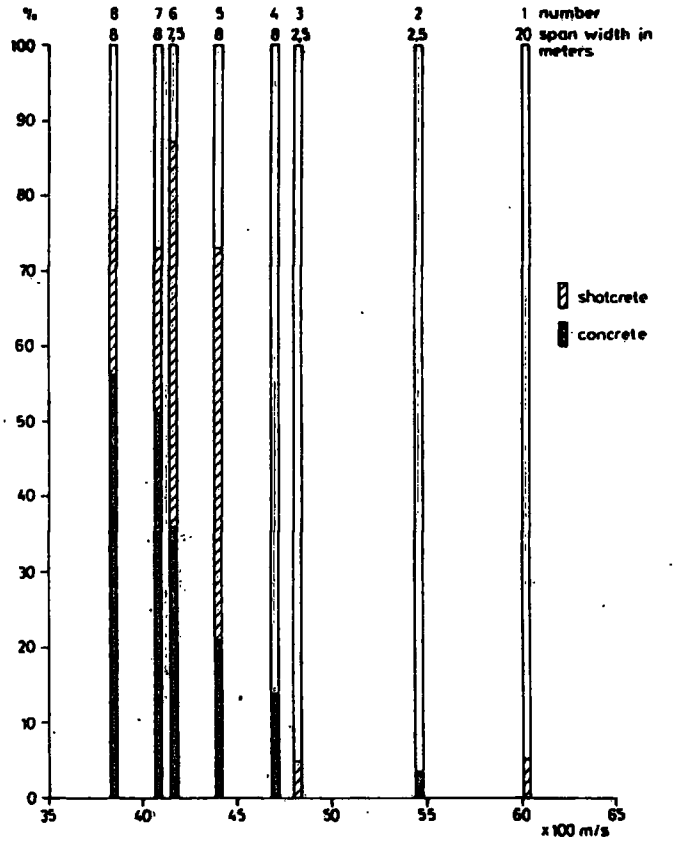

Relation between mean longitudinal velocities, median Md, and percentage tunnel support measures, shotcrete, and concrete lining. Number (1): Mongstad, (2) Torp, (3): Hamang, (4-8): Rendalen.

Fig. 3.10 P-WAVE VELOCITY v TUNNEL SUPPORT (after SJOGREN et al, 1979)

3.5.3 *In situ* dynamic and static moduli

When measurements of P and S-wave velocities are available, values of dynamic moduli (and Poisson's ratio) for the rock may be calculated. The formulae required for these calculations are given in Section 6.6.2 and derivations may be found in Jaeger and Cook (1976). Application of these equations is obviously dependent on whether the precise moment when shear wave arrivals (often superimposed on decaying P-wave motion) commence is discernible on the vibration records.

Dynamic moduli for the Penmaenbach rhyolite *in situ* are given in Section 6.6.2 of this thesis. Strictly, however (for reasons given below), it is not correct to apply the formulae in this way to discontinuous materials where the apparent (measured) velocities of P and S waves are affected differently by the discontinuities. This matter appears to have been generally overlooked by the literature and is discussed further below.

Figure 3.11 gives empirical correlations (Coon, 1968) between field dynamic modulus of elasticity and field static moduli. Note the large spread of data resulting in poor correlation coefficients. This may, in part, reflect the difficulties and inaccuracies associated with jacking and pressure chamber tests (field assessment of static modulus) but it is suggested that another reason for the poor correlation is the different effect of joints on the transmission of P and S-waves.

Consider P and S wavefronts, from a common source, normally incident upon a tight, fresh, unaltered joint with a small stress across it. P-waves (particle motion normal to joint plane) will be transmitted

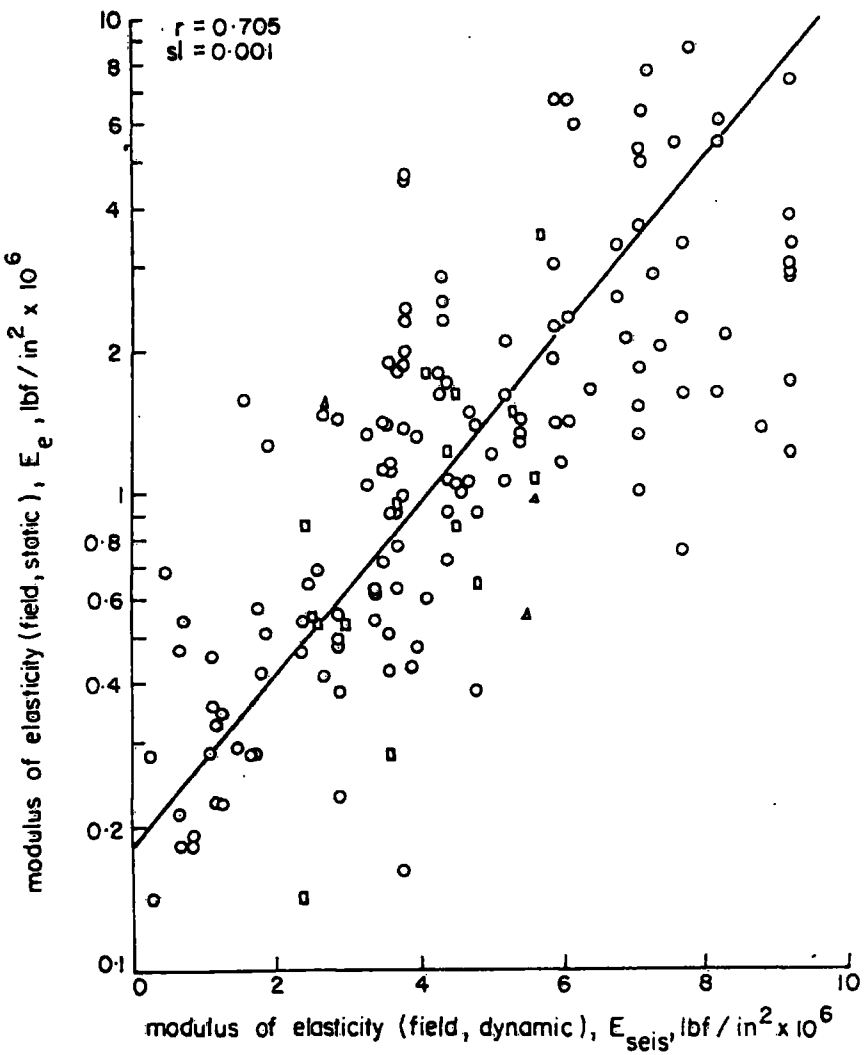

Comparison of in situ static modulus of elasticity and dynamic modulus of elasticity (after Coon, 1968).

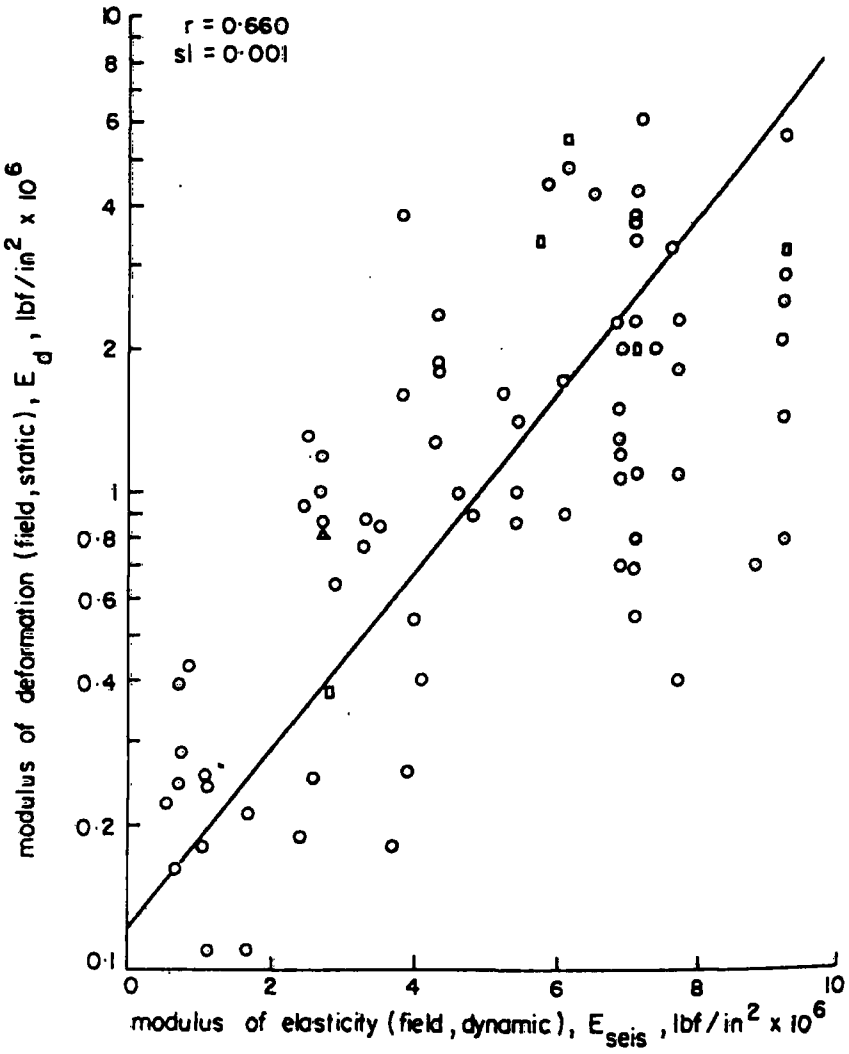

Comparison of in situ static modulus of deformation and dynamic modulus of elasticity (after Coon, 1968).

Fig 3.11 CORRELATION OF STATIC AND DYNAMIC MODULI (as cited by LAMA and VUTUKURI, 1978)

directly across the joint whereas S-waves may have to seek a route 'around' the joint due to the very low shear strength of the joint. Similarly an open water filled joint will transmit P-waves but not S-waves. The concept that a material with these joint characteristics may effectively appear as a continuum to a P-wave but discontinuous to S-waves is of considerable importance.

It follows that the ratio of P and S wave velocities (which determines the dynamic elastic moduli) may be critically dependent on the geometry (persistance, frequency, orientation) and nature of the jointing (aperture, filling, etc). This suggests that measurement and careful study of P-wave *and* S-wave characteristics (frequency, velocity and attenuation) may provide a powerful seismic method for investigating the discontinuous properties of rock masses. The following Section 3.5.4 deals with S-wave frequency in this context but further research into S-wave velocity variation in discontinuous rock seems highly desirable.

Where joints are not tight, fresh and unaltered P-waves may also be forced to seek an 'intact' path and calculations based on relative P and S wave velocities may reflect more accurately the true elastic properties of the rock mass. This also applies to 'continuous' materials such as intact samples tested in the laboratory (*see* Section 4.3.3).

Despite their severe limitations the relations in Figure 3.11 may be used to estimate static rock mass moduli (from dynamic measurements) without undertaking often-expensive jacking tests. A book on the determination of *in situ* modulus has been published by ASTM (1970) and contains useful contributions by well-known workers in the field.

The writer appreciates that pre-knowledge of deformation and elastic moduli may be useful to a tunnel designer. However, it is emphasised that their use in the design of tunnel linings and support will often be of limited and dubious value, particularly when applied to 'relative stiffness' solutions in hard rock (Einstein and Schwartz, 1979). This is due to the fact that it is the inelastic dilation of the rock surrounding an opening (caused by stress relief and weathering effects) that will dominate support loads and deflections. The elastic deformations will usually be only a small part of the actual displacements of concern and will have taken place partly ahead of, and immediately behind the working face (Egger, 1980). Although 'temporary support' measures may be applied almost immediately after blasting they will not significantly resist elastic deformations but will inhibit weather-induced dilation and subsequent rock fall. The time-dependence of tunnel distortions has been usefully discussed in a recent paper by Fairhurst and Daemen (1980).

There are, however, some occasions when information on moduli may be of importance. For example, in the design of a tunnel which is later to be subjected to surcharge pressures or where a tunnel passes close to another opening. In both these cases knowledge of the rock mass moduli will be important and may allow calculation of lining load and deformations due to the revised stress fields imposed.

3.5.4 The correlation of S-wave frequency with static rock mass properties

Schneider (1967) has given an empirical correlation between the received S-wave frequency and the static *in situ* deformation modulus of rock masses. Bieniawski (1978) has presented this correlation with

further field data which tends to confirm its accuracy (*see* Figure 3.12). Roussel (1968) has published a theoretical justification of this correlation using viscoelastic rheological models. Simplistically, the concept is not hard to envisage, that is, the 'stiffer' the 'spring' the higher its natural frequency. *In situ* moduli and S-wave frequency are therefore likely to be correlated and apparently provide a most satisfactory link between seismic and static modulus measurements.

It should be noted that the source used during determination of S-wave frequency was a sledge hammer falling from a height of 1 m at a 'distance' may be of considerable importance particularly in the light of the wave spreading effects described in Chapter 3. This technique is often referred to as the 'petite seismique' method. Bieniawski (1978) also reports (Figure 3.13) good correlation between *in-situ* static modulus of deformation and the Geomechanics rock mass rating (RMR, *see* Section 4.4.2). The equation associated with his 'best fit' regression line is

$$E_M = 1.76\ (RMR) - 84.3 \qquad \ldots (3.6)$$

This is simplified to $E_M = 2\ (RMR) - 100$ in Figure 3.13

$$\ldots (3.7)$$

Combining this equation with that linking S-wave frequency and static modulus of deformation:-

$$E_M = 0.054f - 9.2 \text{ (from Figure 3.12)} \qquad \ldots (3.8)$$

$$\therefore\ 0.054f - 9.2 = 1.76\ RMR - 84.3$$

$$\underline{RMR = 0.0307f + 42.7} \qquad \ldots (3.9)$$

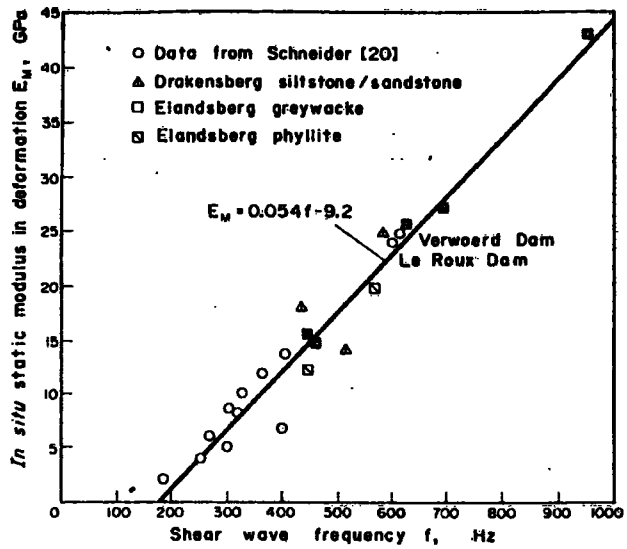

Correlation between static modulus of deformation E_M and shear wave frequency f from 'petite sismique'.

Fig. 3.12 after BIENIAWSKI (1978)

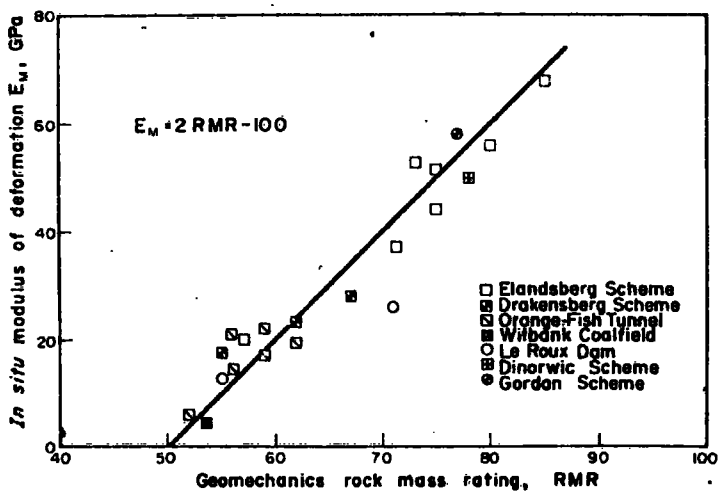

Relationship between *in-situ* modulus and rock mass rating.

Fig. 3.13 after BIENIAWSKI (1978)

This equation provides for a direct calculation of RMR based on S-wave frequency.

3.5.5 Tunnel support design based on seismic data

The seismic and rock mass property correlations given and discussed above provide a basis for the design of tunnel support, using seismic field data. They are presented schematically in Figure 3.14 which also indicates their linking sources. As with other techniques this approach should not be used in isolation but in combination with, and in support of, other established methods.

These seismic methods have some attractive features:

(a) the cost of obtaining the data is likely to be relatively low,

(b) measurements will generally fit easily into the normal site investigation or trial blast programme,

(c) seismic measurements inherently investigate large volumes of material,

(d) seismic measurements are critically affected by the joint frequency, filling, alteration, stress, etc. which are often the dominant parameters controlling support requirements.

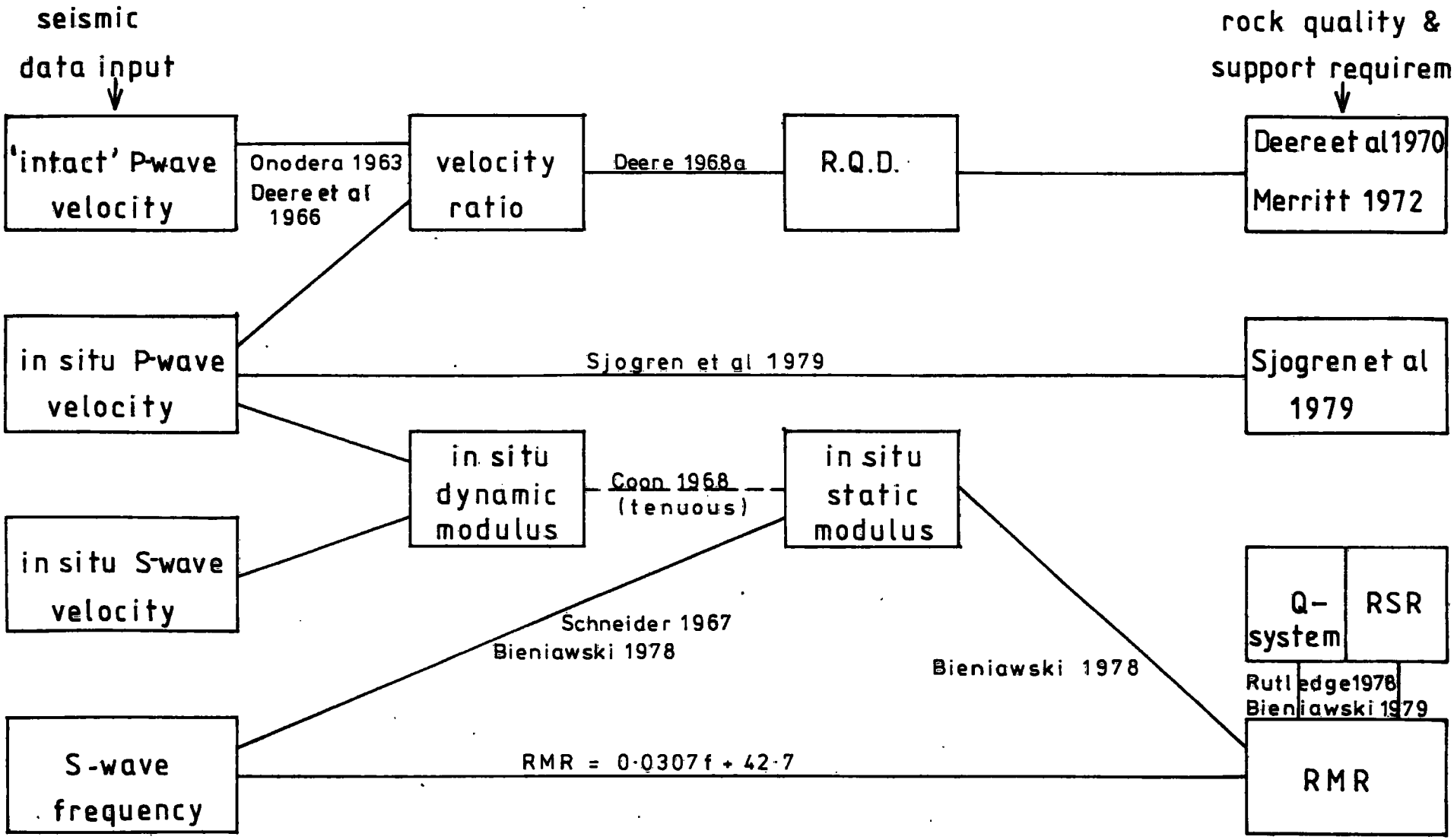

Fig. 3.14 SEISMIC EVALUATION OF ROCK QUALITY AND SUPPORT REQUIREMENTS

CHAPTER 4

THE SITE OF THE TRIALS AT PENMAENBACH

4.1 The North Wales coastal route

Communications to the west of the River Conway in North Wales have always been hampered by the mountainous nature of the terrain. The coastal route, shown in Figure 4.1, between the River Conway and Anglesey is obstructed by two water crossings, the River Conway itself and the Menai Strait, and two mountainous headlands at Penmaenbach and Pen-y-clip. To the south of the narrow coastal plain the mountains of Snowdonia present serious engineering difficulties for both roads and railways.

As a vital part of its plan to improve the congested road system in this area HM Welsh Office are implementing a substantial improvement scheme for the A55 coast road. This road, together with the railway, forms a main artery of communication within the area and onward through the port of Holyhead to Ireland.

A new road crossing of the Menai Strait was completed on 11 July 1980 when the road deck above the reconstructed Britannia railway bridge at Bangor was opened to traffic. The original bridge, completed by Stephenson in 1850, was destroyed by fire and new steel arch spans, replacing the original twin tubes, were built on the existing towers. These new spans were designed with capacity to accept a second level deck of sufficient width for the new four lane highway. This road link effectively replaces the Telford suspension bridge (built 1826), about

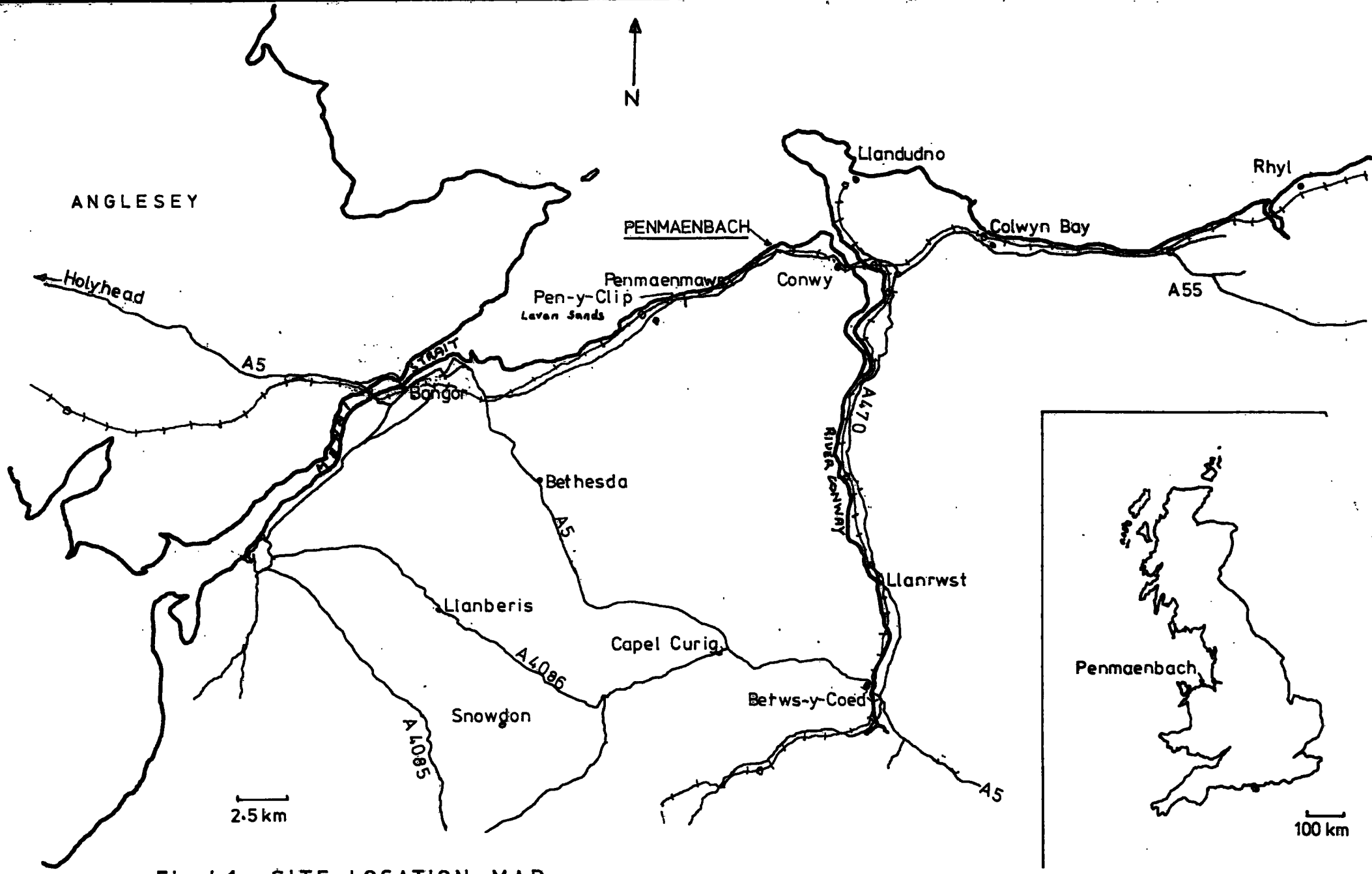

Fig. 4.1 SITE LOCATION MAP

1 mile to the east, which is still open to local traffic. Plans for the other water crossing at Conway have yet to be finalised but it is expected to be by immersed tube tunnel in the estuary rather than by the originally proposed bridge. A final decision has also to be reached on whether to tunnel through or go around the Pen-y-clip headland by marine viaduct.

It has been decided that a new section of the A55 road will pass through the Penmaenbach headland in tunnel. The western side of the headland is shown in the frontispiece. The present A55 passes through the tunnel (left centre),and to the left of the portal the 'shelf' for the old Telford road may be seen. The railway passes into a tunnel behind the wall to the rear of the beach (centre right). The proposed tunnel route (*see* Figure 4.2) is immediately south of, and generally parallel to, the main line rail tunnel which, in places, is less than 30 m away. The location and proposed construction of these new tunnels in relation to the existing tunnel provided an excellent site to test and develop the concepts outlined in Chapter 3.

Trial blasting was required to determine the site laws prior to the contract tender stage in order to satisfy the clients and their consultants that maintaining the integrity of the existing tunnel would not unduly restrict the contractor during construction. It was also necessary to provide British Rail with a form of engineering appraisal regarding both the site laws and damage thresholds indicated by the literature (*see* Chapter 2). The acceptance, by British Rail, of realistic vibration levels was clearly of great importance as the arbitrary imposition of low vibration limits could render the construction of the new tunnels uneconomic.

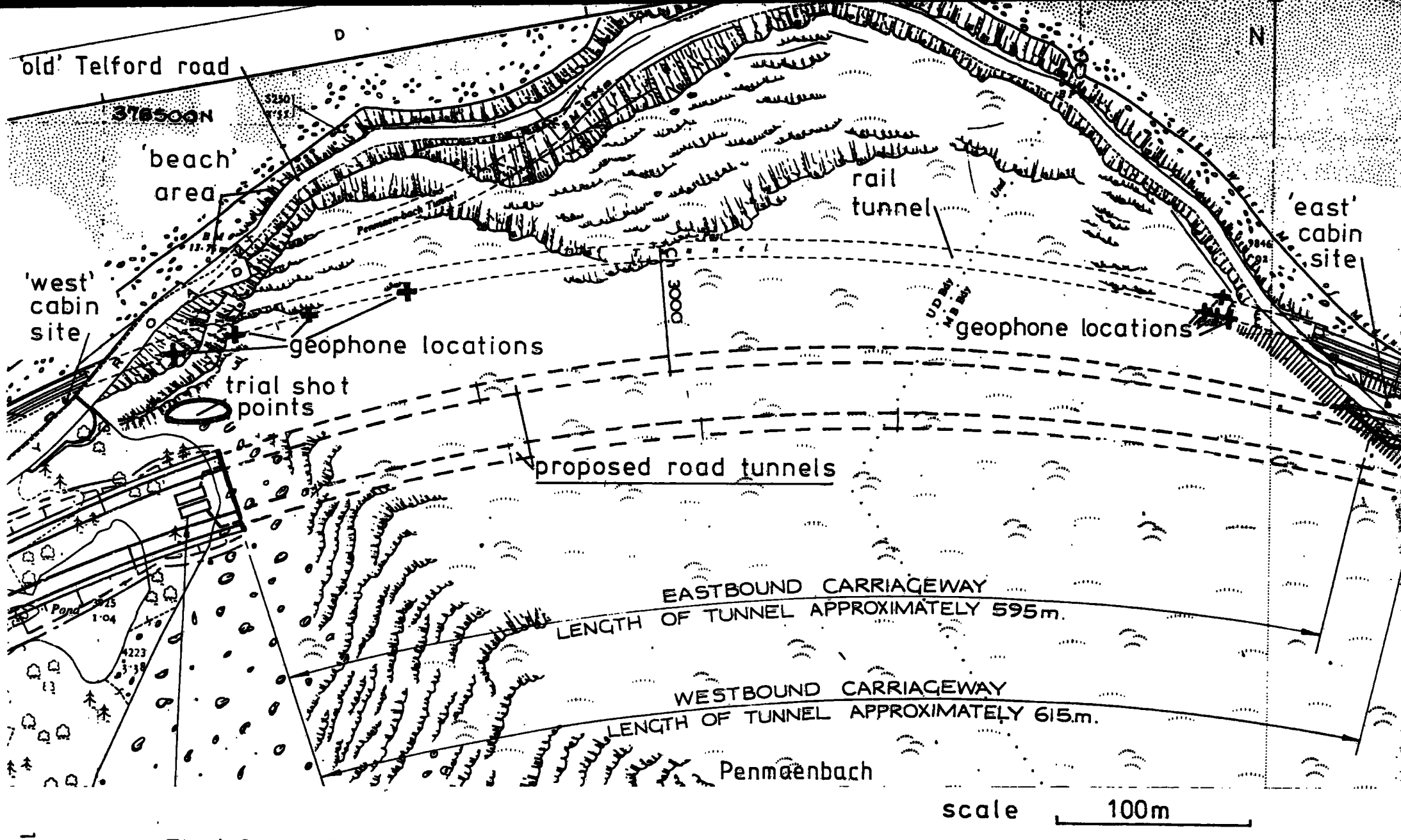

Fig.4.2 SITE MAP

It is of interest to consider briefly the history of land communications along this part of the coast. The Act of Union with Ireland in 1800 increased the number of important travellers from Holyhead and Irish MPs became 'vociferous in loud complaint' at the appalling journey from Holyhead to Westminster. Although roads to the south from Betws-y-coed to Bangor via Bethesda (the present A5) had been improved by Telford by 1819, the coming of the railway age and the Telford coast road improvements were to materially change the pattern of travel in the area.

Before 1826 the mountainous Penmaenbach headland was either passed over the sands at low tide or by way of the difficult inland route over the Sychnant Pass between Conway and Penmaenmawr. In 1826 Telford built a road by blasting a shelf around the cliffs and this formed the trunk road until 1932. Despite the road improvements it still took the mail coaches from London nearly 27 hours to reach the packet ships at Holyhead and the administration of a troubled Ireland urgently required faster communications. The climate of political will therefore existed to promote early railway schemes from the greatest engineers of the times. After many difficulties and much competition between companies the Chester and Holyhead Railway Act of 1844 was given the Royal Assent.

By May 1845 contracts had been let for many of the railway sections of which contract 7, 'the Penmaenbach Tunnel and its approaches', was awarded to John Harding and John Cropper for the sum of £59,611. This tunnel, then reported as 632 yards in length through basalt, was driven from adits to the beach. These adits are still visible and appear to act as drainage and ventilation ducts (*see* Plate 4.1). Despite many financial and engineering difficulties the tunnel was completed on 16 November 1846 with much celebration in Conway and the vicinity (Herepaths

PLATE 4.1 ROCK EXPOSURE AT ADIT ENTRANCE

Journal and Railway Magazine). The line, through the tunnel, between Chester and Bangor was opened to passenger traffic on 1 May 1848 and onward to Holyhead by May 1851. A history of the Chester and Holyhead Railway has been written by Baughan (1972) but contains little detail of the tunnel construction. Any records that did exist were apparently lost during a fire, some years ago, at Llandudno Junction motive power depot.

The last major civil engineering works at Penmaenbach were to improve Telford's road by widening and the provision of a cut-off tunnel avoiding the most precarious section of the old road. The works began in 1930 and the short tunnel was opened to traffic in December 1932. A good account of the works was given by Humphries (1937) but this does not include detail of the blasting techniques used.

4.2 The geology of the site

The geology of the area is given fully by Smith and Neville George (1961) and is also described in a site investigation report carried out for the Welsh Office by Soil Mechanics Ltd in 1974. Figure 4.3, based on the ¼ inch to the mile Geological Survey Solid mapping, shows the principal geological boundaries in the area and Figure 4.2 maps the site on a scale of 1 to 2500.

The underlying rocks in the vicinity of Penmaenbach are of Ordovician age. Penmaenbach itself is thought to be the vent of a pene-contemporaneous volcano and, although rhyolitic in composition, has been described as intrusive (rhyolite is usually regarded as extrusive). The headland may be the result of more than one intrusive event, and if multiple phase intrusions have occurred, the rock at depth may be subject

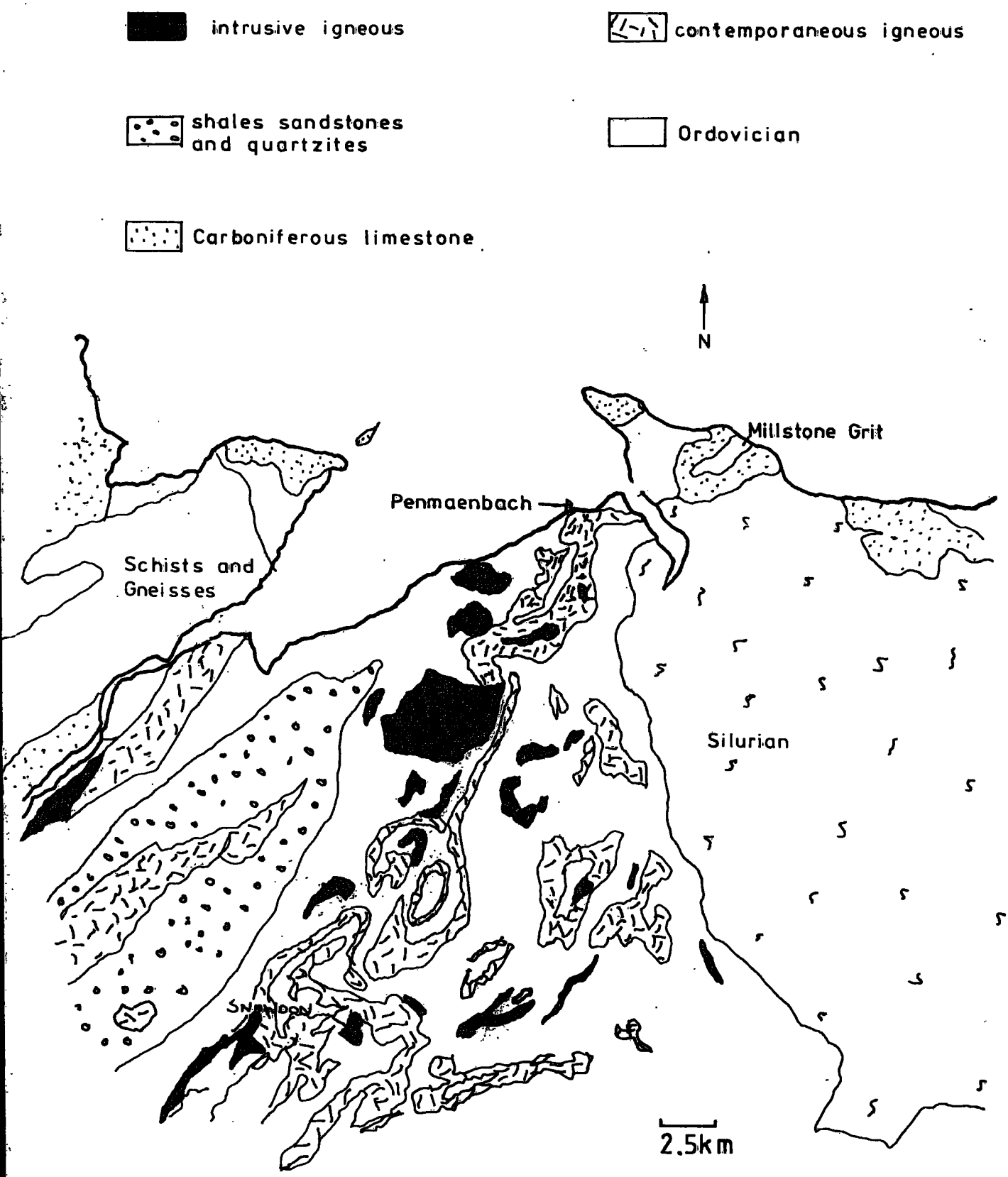

Fig.4.3 PRINCIPAL GEOLOGICAL BOUNDARIES

to 'contact zones' where a fresh intrusion impinges an existing igneous material.

The shape of the headland appears to be largely determined by the discontinuity orientation, with slopes varying from shallow to almost vertical. To the west the rhyolite is thought to underlie the coastal plain at depth. Penmaenbach is thought to be the origin of the lavas and pyroclastic deposits of Conway Mountain which lies to the east.

The rhyolite is petrographically described as fine-grained holocrystalline consisting generally of subhedral quartz dominant over alkali feldspar and ferromagnesium minerals. Occasional subhedral phenocrysts of alkali feldspar are present and secondary carbonate is present throughout. In the proposed portal areas flow banding occurs in the groundmass around the phenocrysts and sericite is seen to replace feldspar in places. Generally rhyolites may have a silica content of about 70 per cent with between 20 per cent and 40 per cent quartz (Hatch *et al.* 1972). Plate 4.2 shows a piece of heavily weathered material recovered from the upper slopes and indicates the contorted nature of the flow banding. Relatively fresh material is shown on the left of the sample where fracture has occurred along a flow banding plane. The fresh rhyolite is a grey/green colour and very strong. Weathering produces a grey/cream surface which tends to highlight any flow banding present.

The eastern portal area is overlain by drift deposits of sand and clay with angular gravels and boulders. At the western portal there is considerable depth of coarse angular scree.

PLATE 4.2 FLOW BANDED RHYOLITE SAMPLE

4.3 Intact rock properties

This section gives details of rock properties required in later Chapters of the thesis. Full details of the site investigations are given by Soil Mechanics (1974) and these have been supplemented by further boreholes in the vicinity of the proposed tunnel portals (Soil Mechanics, 1979). The results given below were (except where stated) obtained by the writer and generally relate to the rock in the vicinity of the trial blast and tunnel western portal areas.

4.3.1 Rock strength

The Soil Mechanics (1974) report gives full details of unconfined compression tests, indirect tensile (Brazilian disc) and point load strength tests carried out on borehole samples of the rhyolite. Their results are summarised in Table 4.1 which is reproduced from the Soil Mechanics Engineering Interpretation and Discussion Report of September 1974.

Further UCS tests on cores recovered from the Western portal area during 1979 have indicated that the rock in this region has an average strength around 250 MN/m^2 with a recorded maximum of 305 MN/m^2 (Personal communications with R. Travers Morgan and Partners).

To supplement these results Schmidt hammer tests were carried out at five locations in this area. In each case sound, reasonably fresh exposures were selected and care was taken to avoid loosely-jointed areas of rock. These precautions were only partially successful and it was noted in the field that the weathering and loosening of the

TABLE 4.1

Summary of rock testing results (After Soil Mechanics, 1974)

	Mean Value $\bar{x}$ MN/m^2	Standard deviation(s) MN/m^2	Relative error $S = s/\bar{x}$	Number of Results
Unconfined compressive strength	204			2
Brazilian disc	13.5			3
Point load* Diametral	11.2	3.2	0.29	27
Point load* Axial	19.1	3.6	0.19	16

*Point load strength test results combine a number of mean values and therefore represent a much greater number of individual test results.

surface rock might materially affect the rebound number. Puffs of dust from surrounding joints and a dull rather than solid sound were common indications of loosened rock.

Ten rebound number readings were taken at each location with the mean and standard deviation calculated from the six highest values. The four lower values were discarded to remove any anomalously low values due to loosened rock. The mean Schmidt numbers were as follows:

Position A	55.5	2.9 (Std Dev)
Position B	59.7	1.4 (Std Dev)
Position C	54.7	1.2 (Std Dev)
Position D	58.2	1.6 (Std Dev)
Position E	58.5	3.3 (Std Dev)

Grand mean 57.3

These values were rather lower than had been expected for this extremely

hard rock and further tests were carried out on a large sample of fresh rock available in the laboratory (*see* Section 4.3.3). This sample gave consistent Schmidt hammer readings of 67 ± 1 and 'sounded' far more reliable than any measurements taken on the weathered rock in the field.

The treatment of Schmidt hammer data and its comparisons with unconfined compression tests is dealt with by Carter and Sneddon (1977). Their empirical relationship is given in Figure 4.4. Note that a Schmidt number of 67 corresponds to a value of about 300 MN/m^2 unconfined compressive strength. Thus the value for the UCS of a fresh intact sample obtained using Carter and Sneddon's empirical relationship agrees extremely well with the recent values obtained by the conventional strength testing of cores.

The lower value (57.3) obtained in the field corresponds to a value of about 150 MN/m^2 which may be appropriate for the weathered surface rock. However the effects of the weathering, in particular the loosening of the joints render these measurements unreliable.

4.3.2 Elastic modulus and Poisson's ratio

Elastic modulus and Poisson's ratio tests on one 54 mm diameter borehole sample were carried out by Soil Mechanics. Four electrical resistance strain gauges (two horizontal and two vertical) were mounted diametrially opposite about mid-height of the specimen. Loads were applied at an approximately constant rate of strain on a standard test frame. Three load cycles were applied over the ranges 2.0, 4.0 and 10.0 MN/m^2 (unloading to 0.1 MN/m^2). The deformation modulus was calculated for the best straight line relationship over the test range

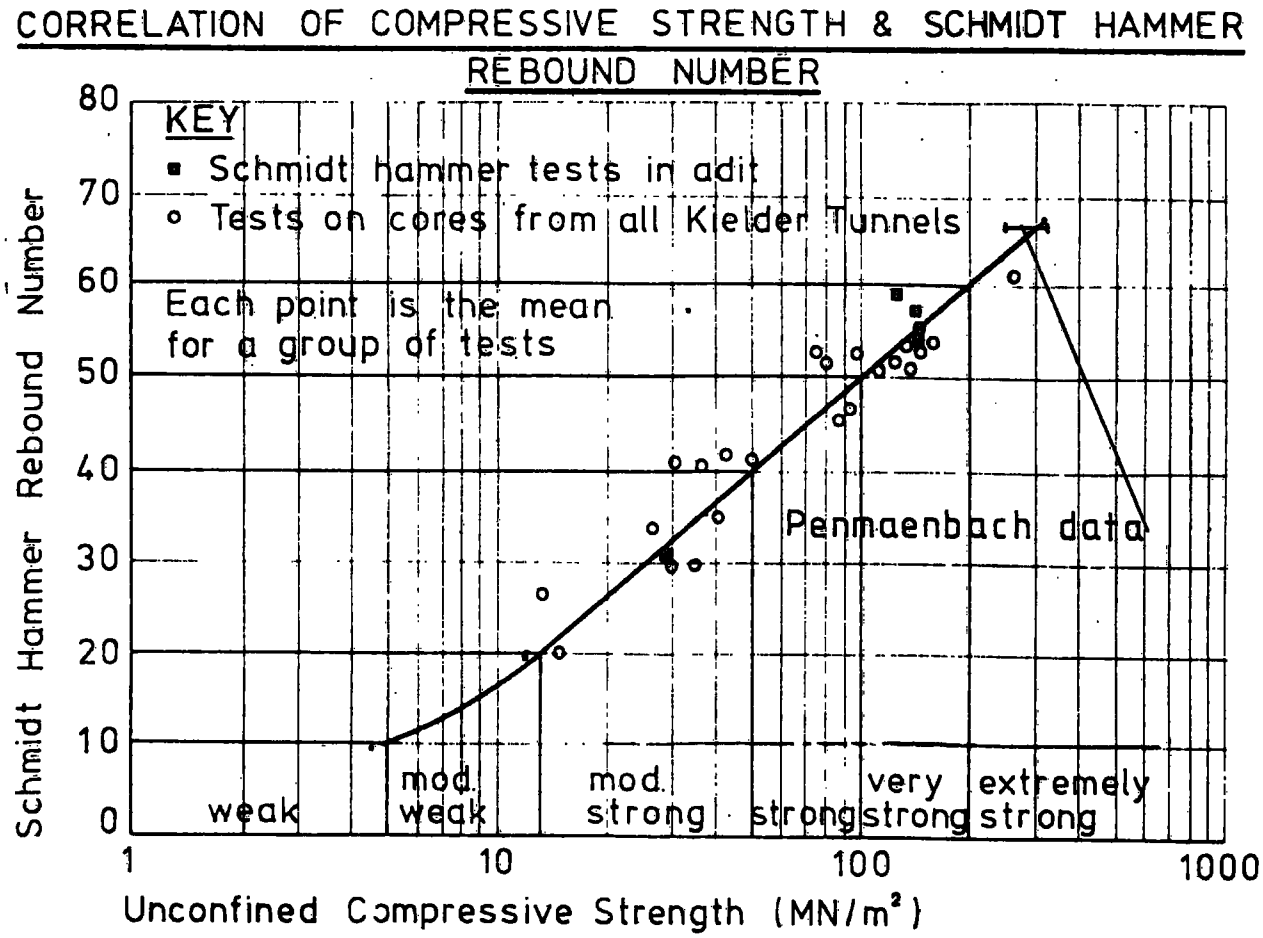

Fig. 4.4 COMPRESSIVE STRENGTH — SCHMIDT HAMMER CORRELATION (after CARTER & SNEDDON ,1977)

(0-10 MN/m^2) and was closely of linear elastic form. The modulus was found to be 56000 MN/m^2 and the ratio of horizontal to vertical strain, Poisson's ratio, was 0.15.

4.3.3 'Intact' seismic velocity

The determination of 'intact' wave velocity is necessary in order to calculate intact dynamic moduli and rock mass velocity ratio which is demonstrated and described in Section 6.6.

A large sample, weighing about 40 kgf, was recovered from the site and sawn into a roughly cubic shape. Opposite faces (designated A-B, C-D, E-F) were diamond sawn flat but were not exactly parallel. This sample was totally free of visible fractures and was considered as a truly intact specimen.

The characteristic compressional wave velocity (at 54 kHz) was measured using an ultrasonic tester known commercially as the PUNDIT (made by CNS Instruments, *see* Elvery and Vale, 1973) and the process is shown in Plate 4.3. New (1976) gives a description of the PUNDIT and its use on intact and jointed rock samples. This instrument comprises two piezo-electric ceramic probes one of which inputs a pulse whilst the other detects the wave arrivals through the specimen. The pulse transit time is measured and digitally displayed. The timer detects the first wave arrival and therefore it is the compressional (P-wave) velocity which is calculated from the measured pathlength through the sample and the transit time [Velocity = Distance/Time]. In this case the shape of the waveform, as displayed on an oscilloscope, did not permit the measurement of shear wave velocity although this is sometimes

PLATE 4.3 'INTACT' ULTRASONIC VELOCITY MEASUREMENT


PUNDIT
CASTROL LIMITED LONDON

possible with the PUNDIT.

TABLE 4.2
'Intact' Compressional Wave Velocity

Between faces	Transit time μs	Distance mm	Velocity (Cp) m/s
A-B	37.6	206	5479
C-D	32.8	176	5366
E-F	35.0	187	5343

The transit times were repeatable to 0.2μs and the 'distance' was measured by vernier caliper to an estimated accuracy of 1 mm.

The mean value for compressional wave velocity was 5396 m/s and there was no indication of significant anisotropy within the sample. This value was confirmed at several points *in situ* where it was possible to make 'indirect' PUNDIT measurements on fresh intact exposures. A value for shear wave velocity was not obtained but, assuming a value for Poisson's ratio, the elastic modulus may be calculated (*see* Section 6.6.2). In this case taking Poisson's ratio as 0.15 the dynamic elastic modulus was 72,250 MN/m^2 (10.5×10^6 lbf/in^2).

Coon (1968) has given an empirical correlation between static and dynamic moduli for 'intact' rock (*see* Figure 4.5). It is of interest to note that the static modulus for the rhyolite (56,000 MN/m^2, 8.12×10^6 lbf/in^2) would indicate a dynamic modulus of about 11×10^6 lbf/in^2 from Coon's 'best fit' regression line for non-foliated rocks. The measured value of 10.5×10^6 lbf/in^2 therefore agrees extremely well with Coon's correlation.

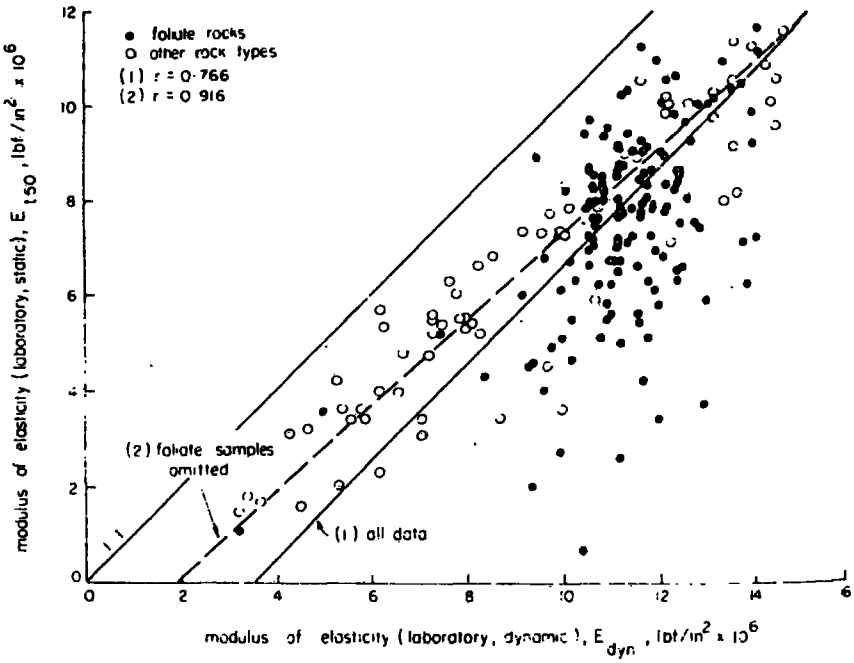

Comparison of laboratory static and dynamic moduli (after COON, 1968).

Fig. 4.5 as cited by LAMA and VUTUKURI, 1978

4.4 Rock jointing and classification

4.4.1 Observations of jointing

The rock of the headland is exposed in many places and is fractured by many discontinuities. Discontinuity observations reveal no generally-preferred orientation although in localised areas significant joint sets are readily identifiable. In the western portal area, for example, there is a major set dipping steeply to the north which tends to dominate the form of the north-facing exposures. The majority of the joints appear tight, unaltered and in many cases welded. Apparently 'loose' pieces of rock cannot easily be removed even with the use of hand tools. Weathering of the joints does tend to open them near the surface and in areas not subject to severe erosion this gives rise to the appearance of a more frequent joint occurrence. Beach exposures (subject to rapid erosion by the sea) appear to have a mean joint spacing of almost double that measured 'inland' in the area of the trial blasting. Also measurements in the rail tunnel suggest lower joint frequencies than those obtained from weathered areas of rock. It should also be noted that the rock in the rail tunnel has been subjected to blasting and about 130 years of weathering.

These effects may tend to exaggerate the engineering significance of the jointing. Plate 4.1 illustrates the jointing typical on the north western face of the headland. The photograph shows the most westerly construction adit between beach and rail tunnel and reveals three joint sets (two dominant) plus random jointing.

Measurements given in Table 4.3 on three mutually perpendicular

scanlines (Nos 1, 2 and 3) were taken in the vicinity of the trial blast holes. Scanlines 4 and 5 were taken on the cliff to the beach close to the area shown in Plate 4.1. Observations on the almost vertical scanline 5 presented some operational difficulties (*see* Plate 4.4).

TABLE 4.3
Scanline measurements of joint spacing

Scanline	Scanline length (m)	No. of joints	Mean spacing (m)	RQD Deere (1964)	RQD*
1	10	103	0.10	64	72
2	8.35	38	0.22	89	92
3	5	64	0.08	61	63
1 + 2 + 3	23.35	205	0.11	72	78
4	10	50	0.20	91	91
5	6.3	32	0.20	88	91

The joint spacing data for each scanline has been analysed in the manner originated by Priest and Hudson (1976). This method assumes that the joint spacing takes a negative exponential distribution and on this basis the RQD* may be calculated from the equation

$$RQD^* = 100e^{-0.1\lambda}(0.1\lambda + 1)$$

where λ is the average number of discontinuities per metre. The significance of this formulation is that RQD (rock quality designation, Deere, 1964) may be calculated using only the number of joints in a given distance.

The joint spacing distribution for the combined scanlines 1, 2 and

PLATE 4.4 OBSERVATION OF NEAR VERTICAL SCANLINE

3 is given in Figure 4.6 and is reasonably represented by the negative exponential curve,

$$f(x) = \lambda e^{-\lambda x}$$

where f(x) is the frequency of a discontinuity spacing, x.

The distribution histograms did not all appear to be of good negative exponential form and in most cases a heavily-skewed normal distribution (log-normal) may have been more appropriate. The apparent absence of very close joint spacing (below 2 cm for this rock) has been noted and discussed by Hudson and Priest (1979, p 355). The modification of this theory to account for multiple parameter distributions would detract greatly from the concept and does not seem useful when the assumption of a negative exponential distribution does give a satisfactory correlation.

The differences between RQD and RQD* are a little greater than might have been expected ('within 5 per cent') from the field results of Priest and Hudson (1976) and more recently by Wallis and King (1980). These differences may be explained, in part, by the limited lengths of the scanlines, although some of the error could be due to the joint distribution not being of a closely negative exponential form (*see* above). It is recommended by Priest and Hudson that the scanline length should be at least 50 times the mean discontinuity spacing and that at least 200 values are required to complete a satisfactory histogram.

Scanlines were not taken in the rail tunnel but it was noted that in most areas toward the Western postal the joint spacing was between

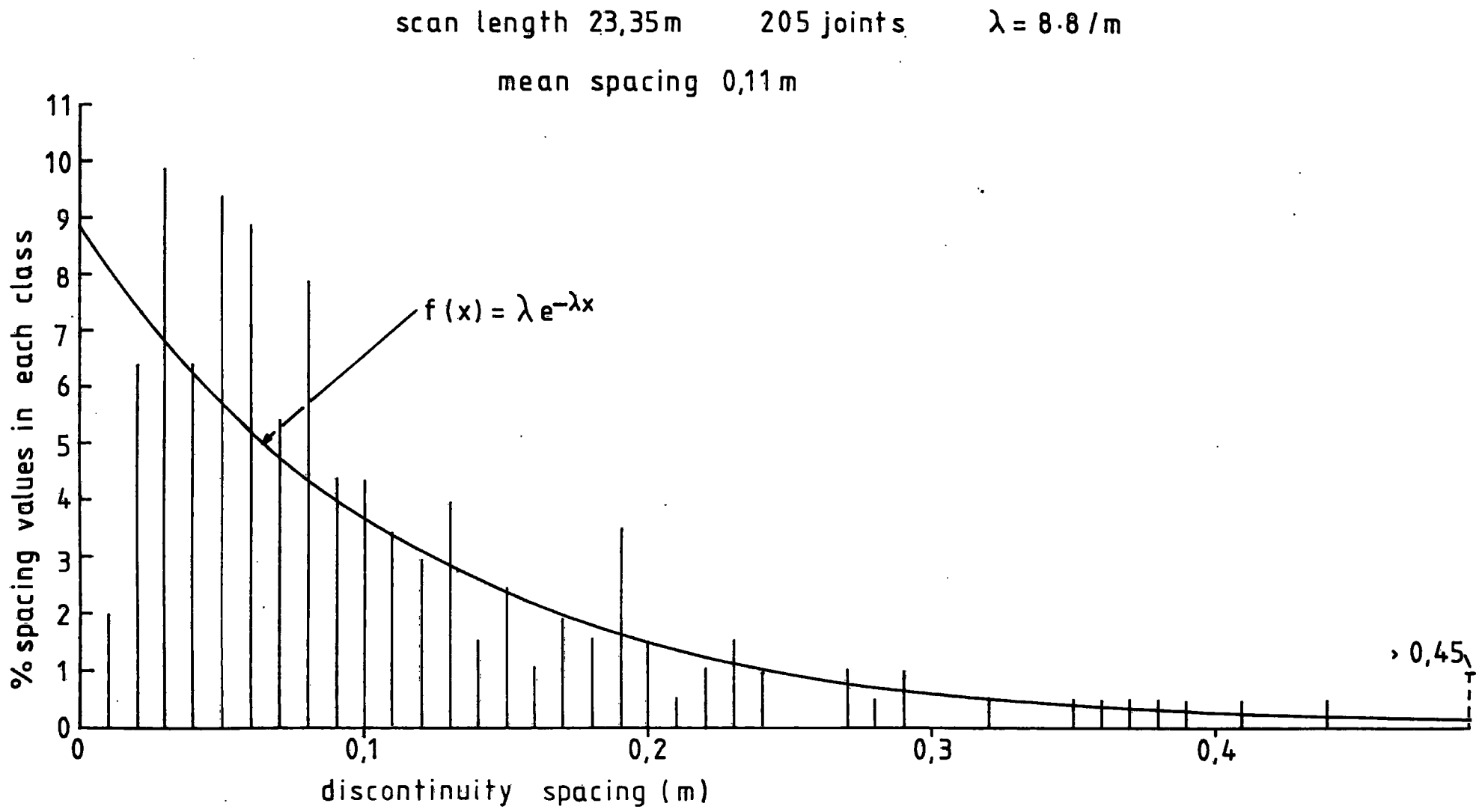

Fig. 4.6 DISCONTINUITY SPACING DISTRIBUTION. (SCANS 1, 2 & 3 COMBINED)

0.10 and 1 m. There were generally 3 sets (two dominant) plus random joints visible.

The rhyolite material itself is essentially impermeable and all water flow is ducted through the major discontinuities. Isolated seepage was observed from joints above the present A55 and the old Telford road. Small water inflows and drippers were noted in the portal areas within the rail tunnel but the quantity was negligible. Results from standpipes obtained and interpreted by Soil Mechanics indicate, as expected, that the headland is of low rock mass permeability.

4.4.2 Rock classification

The 'rock quality' may be assessed employing currently-available empirical methods using data from the observations of rock exposures and other tests. There are many methods of classifying rock masses and in his comprehensive report 'Tunnel design by rock mass classifications' Bieniawski (1979) deals fully with the six most commonly referred to systems. They are:

(a) Terzaghi's rock load classification
(b) Lauffer's classification
(c) Rock quality designation (RQD) (Deere, 1964)
(d) RSR concept (Wickham, Tiedemann and Skinner, 1974)
(e) RMR geomechanics classification (Bieniawski, 1974)
(f) Q-System (Barton, Lien and Lunde, 1974)

The application of, and relative merits of, these systems are fully discussed by Bieniawski (1979) and this recent report forms a most

useful reference text.

Of these classifications the most recently developed, c, d, e and f, are those most widely considered in the prediction of ground stand-up time and support requirements. The direct application of RQD values to rock support design (Deere, 1968b; Merritt, 1972) is considered to have severe practical limitations in that it neglects many vital rock mass properties. Its main attraction is that it provides a quick and inexpensive index which may be utilised in other more complete classification systems. Used alone it does not provide an adequate description of a rock mass. Appendix D gives Deere's (1968b) general description of RQD application to support requirements and Merritt's (1972) correlation of RQD with tunnel support and span.

The RSR concept was developed primarily in relation to tunnel support by steel ribs and is not generally recommended for use where rockbolts, mesh and shotcrete are to be used.

The Geomechanics and Q-System have rather similar constituative parameters although the classifications are calculated in a very different manner. These systems have been numerically correlated through case history data (Bieniawski, 1976). The relationship, with data points, is given in Figure 4.7 and takes the form

$$RMR = 9 \ln Q + 44$$

Other recent correlations given by Rutledge (1978) are:

$$RMR = 13.5 \log Q + 43 \qquad \text{(S.D. 9.4)}$$

$$RSR = 0.77\ RMR + 12.4 \qquad \text{(S.D. 8.9)}$$

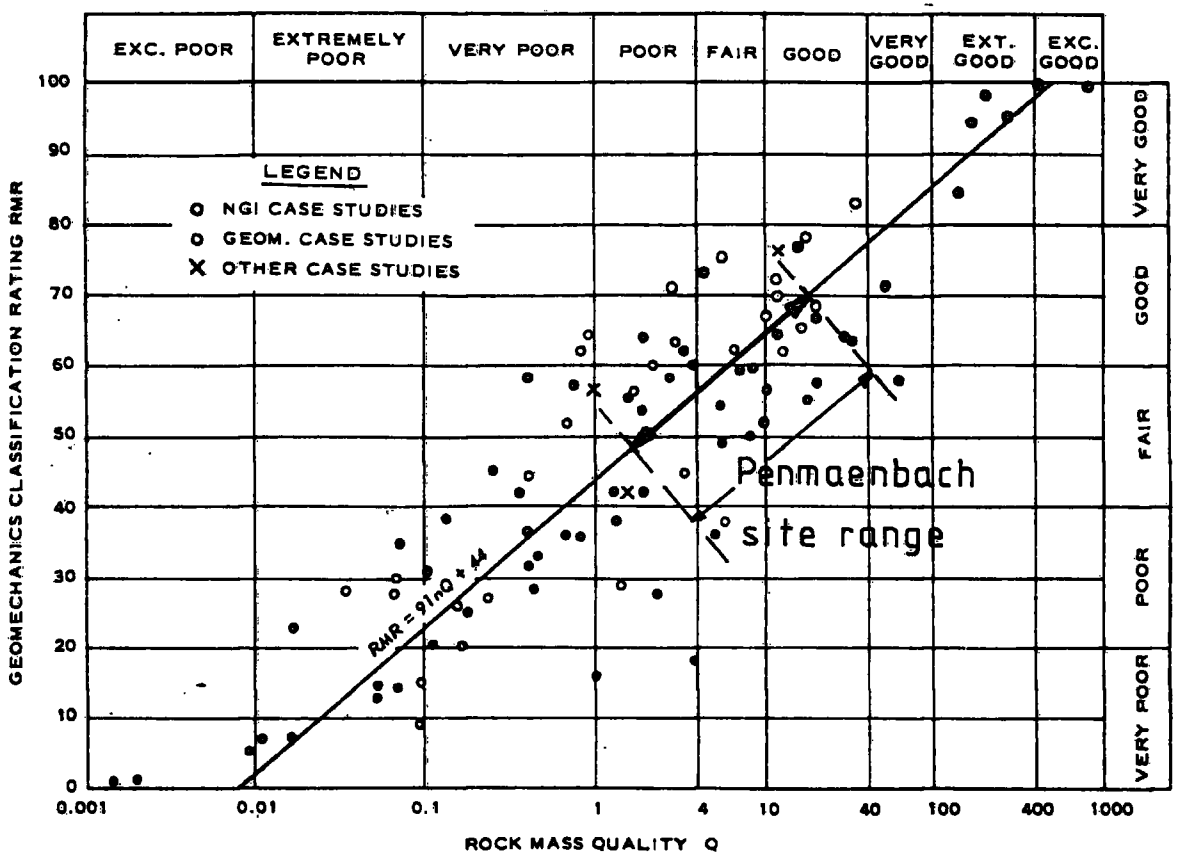

Fig 4.7 GEOMECHANICS (RMR) — Q-SYSTEM CORRELATION (after BIENIAWSKI, 1976)

and RSR = 13.3 log Q + 46.5 (S.D. 7.0)

It should be noted that the Q-System does not include a factor directly associated with rock strength and tends to indicate a longer stand-up time for a given span, than does the Geomechanics Classification. The latter classification is therefore more conservative than the Q-System which reflects a difference in tunnelling practice in Scandinavia based on the depth of experience of underground construction in almost uniformly good rock of metamorphic and igneous origin.

The Geomechanics Classification, RMR, has been adopted here to assess the rock mass condition by an 'established' method. The correlation with the Q-System is good, particularly in sound rock (although support recommendations may be rather different) but RMR has an advantage here as it has been specifically correlated with *in situ* deformation modulus, a parameter linked to wave propagation velocity in rocks.

The Geomechanics Classification details are given by Bieniawski (1979). This system was used to determine the range of RMR values calculated from observations given in this Chapter. These observations are intended to relate particularly to the relatively unweathered rock mass within 150 m of the rail tunnel western portal.

TABLE 4.4

Geomechanics classification (uncorrected for joint direction)

Parameter		RMR Value	
		Best case	Worst case
1	Strength of intact rock	15	12
2	RQD	19	14
3	Joint spacing	17	10
4	Joint condition	22	18
5	Ground water	9	6
	Total	82	60

As the joint direction was variable and there is often a steeply-dipping set sub-parallel to the proposed tunnel direction a rating adjustment value of -12 (very unfavourable)is applied to both RMR case values, giving

RMR = 48 to 70

This range spans classes II and III ('good rock', 'fair rock') for which average stand-up times of 6 months (4 m span) and 1 week (3 m span) are predicted.

It is revealing to note that the rail tunnel (span 7½ m), which for most of its length is unsupported, has remained structurally sound for 130 years. In this case therefore, the Geomechanics Classification would appear to be very conservative.

The above analysis does not allow for any areas of serious faulting and geological information from the few sections of the rail tunnel where brick arches have been built and would be useful.

There are several further indications of rock behaviour which are worthy of note:

(a) During annual 'drumming and scaling' of the rail tunnel, very little loose rock is apparent. The tunnel seems to be in excellent condition despite its age and method of construction, although in places some of the brickwork may require attention in due course. Plate 6.1 shows the British Rail tunnel inspection train with high level work platforms.

(b) During construction of the short road tunnel in 1931 two incidents of note occurred:

(i) blasting for the western portal shook some 3000 tons of rock down onto the main road (*see* Plate 2.1). The road remained closed until the drives from East and West had met and no further falls or movements occurred;

(ii) a minor fall of rock in the railway tunnel was noted after a blast in June 1931.

(c) Mortar tell-tales dated April 1922 are visible in major joints associated with overhanging rock on the old Telford road. Although many of these steeply-dipping joints daylight, no movement appears to have taken place. Historical records reveal that travellers were as likely to be injured by falling sheep as rock on this stretch of road.

CHAPTER 5

THE TRIAL BLASTING PROCEDURE

5.1 Organisation

When blasting operations are to be carried out on, or close to, areas with public access a considerable effort is often necessary to obtain permission from the appropriate authorities and to take the required safety precautions. For the blasting at Penmaenbach this task was carried out by the Consultants (RTM) for the Scheme as an extension to the site investigation programme which was in progress at that time. This procedure was agreed by the Employer and removed any problems associated with the letting of a new contract. The blasting work was therefore let as a sub-contract by the contractor for the site investigation works, Soil Mechanics Limited.

The proposed procedure for the trial had been agreed, in outline, by the writer with RTM ,HH and British Rail at a meeting some weeks previously. At this meeting BR stated their safety requirements and suggested possible periods during which the trials might take place. It was subsequently agreed that the blasting would take place between 06.00 and 10.00 hours on Sunday 17 May 1979. A full 'track possession' of the London-Holyhead main line between Llandudno Junction and Penmaenmawr was arranged for the period between 02.30 and 11.30 on that day. This period allowed for the re-positioning and checking of transducers and, after the trial, removal of equipment located in the rail tunnel.

Agreement was also obtained for similar track possessions on two previous Sundays. These periods were used to install equipment in various parts of the tunnel for other purposes (*see* Section 6.7).

It was considered prudent to close a few hundred metres of the A55 (which passes close by the trial site), during the actual blasting. This was to protect traffic from unexpected rock falls and to prevent distraction to drivers. This resulted in the road closure for five periods of about 10 minutes each. The local police and Gwynedd County Council gave their approval for this action and Soil Mechanics Limited implemented the road traffic control. Lookouts were positioned on the Penmaenbach headland to warn and prevent any members of the public straying into the area of blasting.

Special arrangements were also made for transport and on-site positioning (by mobile crane from the A55) of the TRRL instrumentation cabin. It is of interest to note that insurance cover for losses to a value of £1M was considered necessary for the trial.

5.2 The explosive charges and their location

Rock Fall Limited of Glasgow were awarded the sub-contract to 'drill, charge and fire trial blasts specified and agreed with the Engineer'.

5.2.1 Drilling and charging

Drilling the 19 holes required was carried out during the week preceding the blasting using a hand-held air-powered and flushed

percussion drill. The near-vertical holes were all driven to a depth of 3.5 m and after drilling were plugged to prevent ingress of dirt or water. The hole depth was chosen to eliminate rock fracture or crack opening at the surface. This condition was specified by the Engineer to minimise rock damage which might hinder the subsequent construction of the new road tunnel approaches in this vicinity. For the same reason a maximum charge of 1 kgf of explosive per hole was specified. Thus, where blasts of more than 1 kgf were required, several charges were to be simultaneously fired. Thus a condition of 'confined blasting' was imposed upon the trials although it transpired that some charges did disturb the rock surface and may be treated as 'unconfined' or 'partially confined' blasts. The explosive was specified as '80 per cent strength gelatine or equivalent' the contractor choosing ICI 80 per cent Special Gelatine. This explosive is a waterproof gelatine commonly used for controlled underground excavation and is specified as follows:-

weight strength	85 per cent BG (blasting gelatine)
bulk strength	79 per cent BG
density	1.4 g/ml
detonation velocity	3.5 km/s (unconfined)

The explosive was supplied in 200 mm sticks, 30 mm in diameter and in this form weighed 0.85 kgf/m. After the insertion of the detonator the explosive was tamped and stemmed with quarry waste in the usual manner. The shot firer was positioned by the south wall of the A55 in direct oral and visual contact with the writer who gave the instructions to 'fire' the charges at the appropriate moment.

5.2.2 Charge to transducer distances

The positions of the shot holes and the vibration transducers mounted in the rail tunnel were surveyed by RTM staff, referring the individual transducer and shot hole locations to bench marks set up in the tunnel and on the hillside. These positions were mapped and are shown in Figure 5.1. A table of direct distances is given in Table 5.1. Where more than one shot hole was charged for a single delay (for charges over 1 kgf) adjacent holes were chosen and their average distance from the transducers is given at the foot of the Table.

5.2.3 The compliance with the vibration limit

It has been agreed with British Rail that the trial blasting would be controlled such that a resultant PPV of 25 mm/s should not be exceeded in the rail tunnel. Information, referred to in Chapter 2, indicated that it was extremely unlikely that any damage to the tunnel would occur below this level. Analysis and calculations based on previous case history data (principally after Oriard, 1971, Figure 3.2) suggested than an initial single shot of 1 kgf would allow the equipment to be set to suitable gain and calibration values without the possibility of exceeding the agreed limit.

5.3 The vibration transducers

It was decided at an early stage in the project that all vibration measurements would be expressed in terms of particle velocity. Thresholds of damage are known to correlate with particle velocity. This is reasonable as the dynamic stresses within a structure are proportional

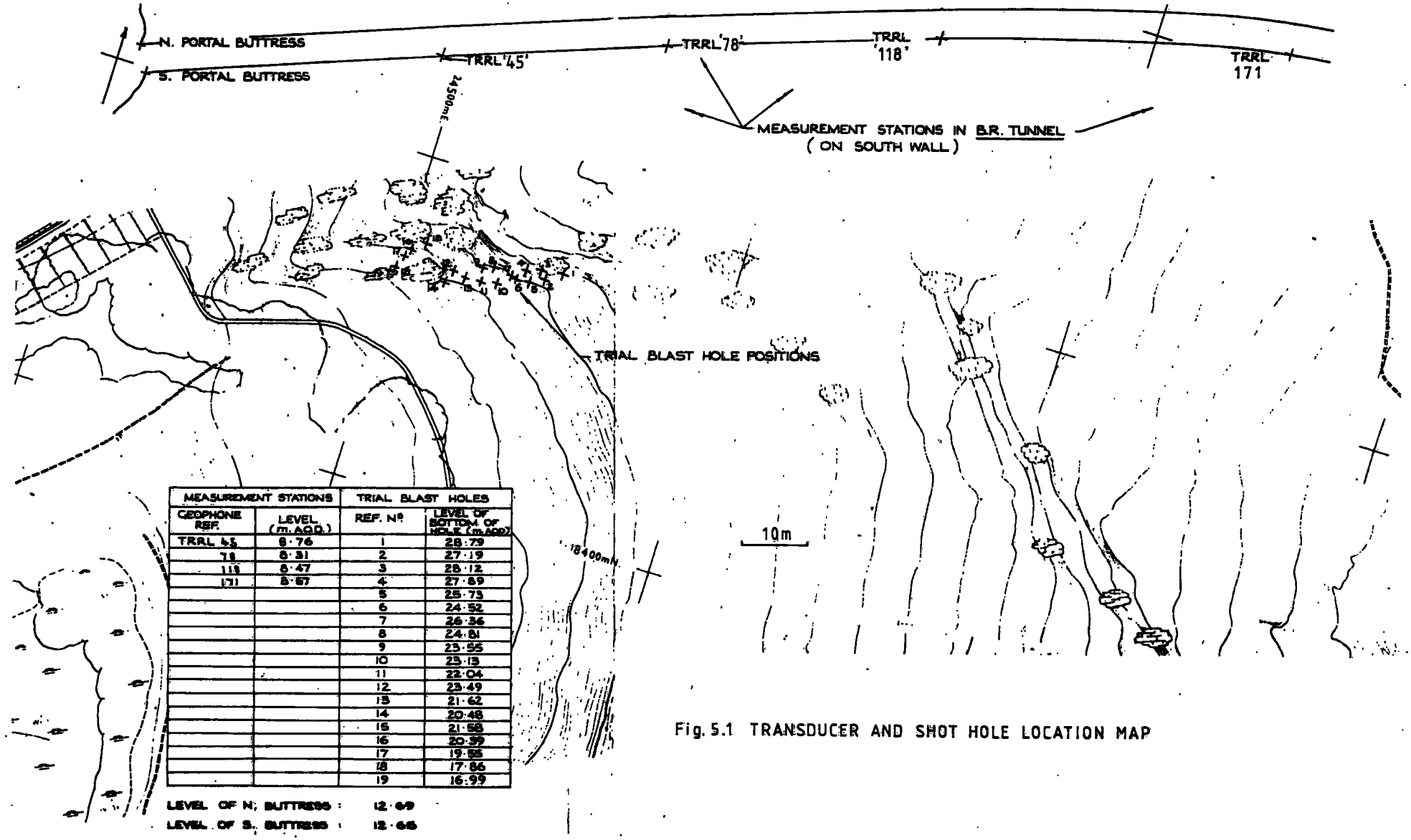

MEASUREMENT STATIONS		TRIAL BLAST HOLES	
GEOPHONE REF.	LEVEL (m.AOD.)	REF. Nº	LEVEL OF BOTTOM OF HOLE (m.AOD)
TRRL 45	8·76	1	28·79
78	8·31	2	27·19
118	8·47	3	28·12
171	8·67	4	27·89
		5	25·73
		6	24·52
		7	26·36
		8	24·81
		9	23·55
		10	25·13
		11	22·04
		12	23·49
		13	21·62
		14	20·48
		15	21·58
		16	20·39
		17	19·55
		18	17·86
		19	16·99

LEVEL OF N. BUTTRESS : 12·69

LEVEL OF S. BUTTRESS : 12·65

Fig. 5.1 TRANSDUCER AND SHOT HOLE LOCATION MAP

TABLE 5.1

DIRECT DISTANCES BETWEEN SHOT HOLES AND TRANSDUCERS (m)

SHOT HOLE REF NO	TRANSDUCER REFERENCE POSITION			
	45	78	118	171
1	41.9	43.1	70.9	117.5
2	50.7	43.8	72.7	119.7
3	39.8	43.6	72.9	120.3
4	39.0	44.4	74.7	122.3
5	39.5	44.5	74.5	121.9
6	38.1	44.8	75.8	123.6
7	38.3	45.6	76.7	124.5
8	35.8	45.5	78.0	126.5
9	35.1	46.2	79.3	128.0
10	37.4	46.5	78.4	126.5
11	36.3	47.4	80.3	128.7
12	35.1	49.3	83.4	132.3
13	35.3	48.2	81.9	130.7
14	35.6	50.6	84.9	133.9
15	30.7	48.9	85.2	135.2
16	31.3	50.8	87.4	137.4
17	32.1	51.9	88.5	138.5
18	33.4	53.7	90.2	140.1
19	34.1	54.7	91.3	141.1
2, 3 & 5	40.0	44.0	73.4	120.6
9, 11 & 13	35.6	47.3	80.5	129.1
15, 16	31.0	49.8	86.3	136.3

to particle velocity (*see* Section 2.2.1).

5.3.1 Selection and calibration

The choice of transducer type was essentially between various geophones and piezoelectric accelerometers. It was expected that most of the vibration energy at Penmaenbach would lie in the bandwidth 20-500 Hz, and although accelerometers have some advantages of specification (wider frequency response) a high-quality geophone-type transducer was selected. Geophones are self-generating transducers producing an electrical signal capable of transmission through hundreds of metres of cable, whereas accelerometers require a stable power supply and charge amplifiers close to their site positions. In tunnel environments this may be impracticable and inconvenient. From previous experience with both types of transducer the geophone has been found the more robust and reliable in operation. They are also less expensive. Further, the geophone provides an analogue voltage proportional to particle velocity whereas it is necessary to integrate the accelerometer output to give particle velocity. In use piezoelectric accelerometers are often subject to temperature drift and electrical noise problems not found with geophones.

The geophones selected were made by Sensor Nederland BV and supplied by Fenning Environmental Products of Luton. Their specification is given in Figure 5.2. As shown in the Figure these geophones have a low (4.5 Hz) natural frequency and are sensibly responsive to frequencies down to a few hertz.

Each geophone was tested on the rig shown in Plate 5.1 by comparison with an accelerometer of known calibration. For practical

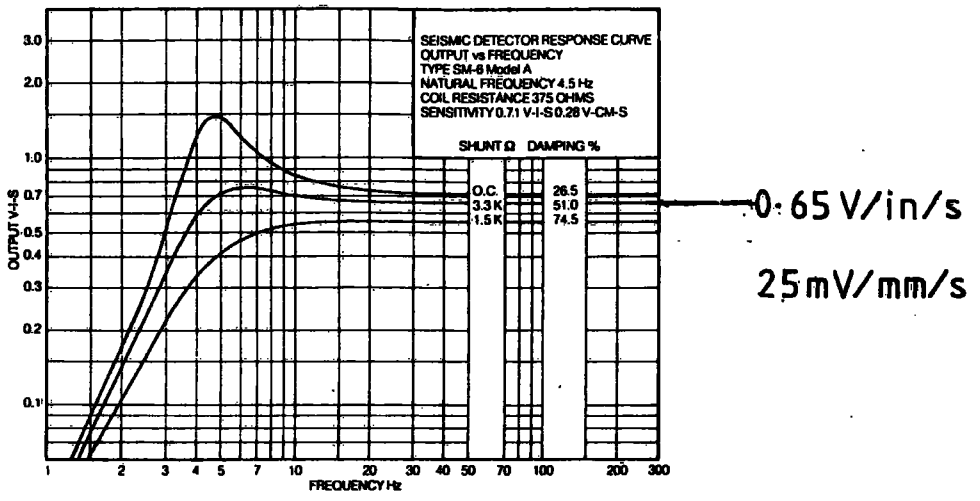

Fig. 5.2 GEOPHONE RESPONSE CURVES

(after SENSOR TRADE LITERATURE)

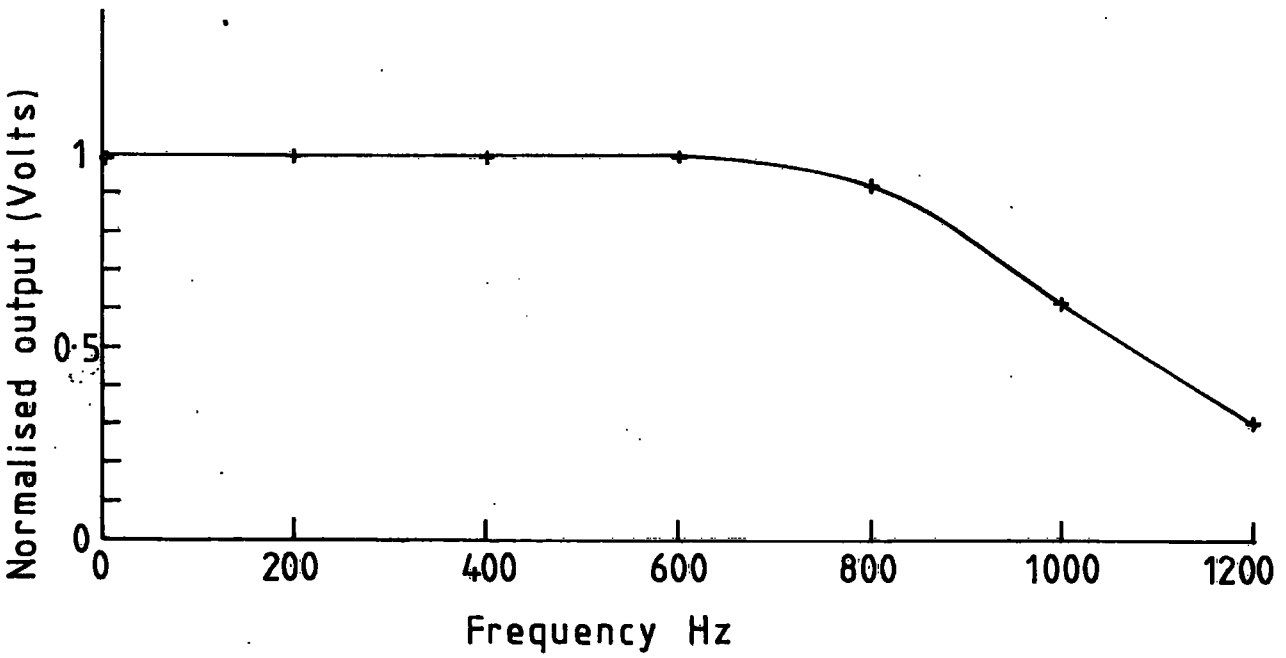

Fig. 5.3 CASSETTE RECORDER FREQUENCY RESPONSE

purposes all the geophones were found to be similar in performance. Their sensitivity remained constant to 1 kHz then increasing slightly before falling rapidly. At 2 kHz their sensitivity was reduced by over 95 per cent. The vibrating table shown in the Plate 5.1 may be rotated through 90^{0} allowing both 'horizontal' and 'vertical' type geophones to be calibrated. This facility also allowed confirmation that the geophones could be used satisfactorily when inclined at up to 20^{0} from their nominal orientation (vertical or horizontal). Sample geophones were tested with both long and short transmission cables to confirm that cable length did not influence output. Each geophone was marked and tested when connected to the recording system by the cable with which it was to be used on-site, confirming that all connections were sound. It was important that all the equipment installed within the tunnel during a 'track possession' period worked immediately and reliably as access for repairs was not possible until the next 'possession', one week later.

5.3.2 In-tunnel location and mounting

For the trial blast at the western portal area all the geophones were mounted on the south wall of the tunnel about 1 m from the tunnel floor. The geophone arrays are identified by their distance from the tunnel portal as follows:

Distance from Portal (m)	Geophone array type
45	3 mutually perpendicular
78	- do -
118	single
171	single

PLATE 5.1 GEOPHONE TEST AND CALIBRATION RIG

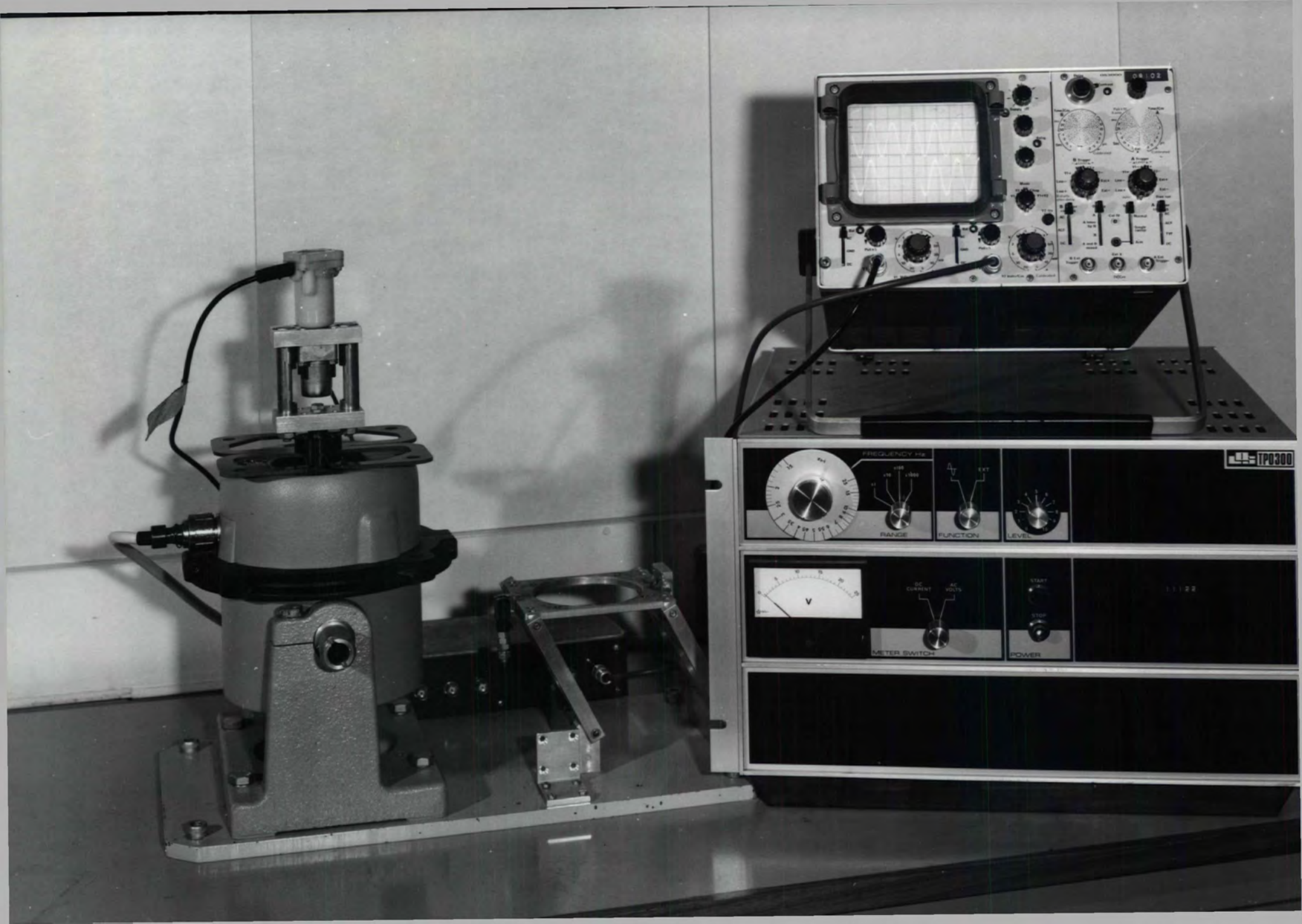
FREQUENCY Hz
RANGE
FUNCTION
EXT
LEVEL
TPO300
DC CURRENT
AC VOLTS
METER SWITCH
START
STOP
POWER

At positions 45 and 78 the arrays were oriented such that one geophone had its axis of sensitivity 'pointed' directly toward the shot holes. The geophone package was then rotated about this axis ensuring that no transducer was more the 20^{o} from its 'nominal' orientation. Thus one transducer monitored radial motions, and the other two, horizontal and vertical (approximately) motions respectively. The single transducers at 118 and 171 were 'pointed' directly at the shot holes, again recording radial particle motions. The geophones were mounted rigidly on an aluminium cube which in turn was bolted to a steel bracket fixed to the tunnel wall. The cube could be rotated before clamping on the bracket, to allow correct orientation. Plate 5.2 shows a three-dimensional geophone array being mounted on the tunnel wall.

At each desired distance into the tunnel suitable mounting areas were 'drummed' with a hammer to assess their rigidity within the rock mass. Most of the large 'faces' tested rang true although occasionally a dull note clearly indicated an unsuitable 'loose' block.

After fixing the brackets the geophone packages were bolted on and covered by polythene bags to protect them from dust and water. The transducer cables were then laid in the tunnel cess and secured to the rock where necessary. A portable 2 kW generator mounted on a light rail truck was used to provide both lighting and power for the drilling. The drilling and bracket fixing in both portal areas was completed during the track possession on Sunday 3 June.

5.4 Signal conditioning and recording

The cabling from the transducers was run into the instrumentation

PLATE 5.2 GEOPHONE ARRAY ON TUNNEL WALL

cabin located at the trackside a few metres from the tunnel portal (Plate 5.3). The cabin was provided with a 240 V mains supply from a distribution box situated above the cabin on the A55. This facility was laid on by the local Council and gave a reliable, relatively noise-free source of ample power which is highly desirable when using this type of electronic equipment.

The signals were conditioned to appropriate levels by instrumentation type amplifiers housed within an ultraviolet (UV) recorder. Plate 5.4 shows the chart recorder (and other equipment) being reloaded with UV sensitive photographic paper. The performance of the recorder with various input waveforms was tested in the laboratory and found to be satisfactory in the bandwidth 0-1 kHz. At higher frequencies the spot displacement decreased rapidly due principally to the galvanometer specification. The galvanometers were specified by their manufacturer as having a natural frequency of 1600 Hz and a 'flat' sensitivity curve to 1 kHz.

The eight data channels were recorded in parallel (*see* Figure 6.2) and the paper speed was usually the maximum possible (1 m/s) for this recorder.

Up to four data channels could be recorded on an FM cassette tape recorder. The recorder's specification suggested lack of linearity at frequencies in excess of 625 Hz. However, the tests shown in Figure 5.3 indicate that its performance was closely linear up to 800 Hz and still usefully sensitive to 1 kHz. An oscilloscope was available to monitor the progress of the signal through the system; this allowed the gain settings to operate at full dynamic range without the risk of 'clipping'

PLATE 5.3 THE INSTRUMENTATION CABIN AT THE WESTERN PORTAL

PLATE 5.4 RECORDING EQUIPMENT IN CABIN

or other forms of waveform distortion occurring. A schematic of the equipment is given in Figure 5.4.

5.5 The blasting sequence

On the Friday before the trial blasting a meeting, attended by TRRL, RTM, HH and Rock Fall Ltd, was held to finalise blasting procedure. It was agreed that:

(a) Five minutes before each blast a warning would be sounded.

(b) A whistle was to be blown to announce the shot firer's readiness to detonate.

(c) The writer counted down '5, 4, 3, 2, 1 Fire'. This permitted the instrumentation to be run at precisely the right moment. This was vital as the chart recorder was producing paper at a rate of 1 m/s.

(d) The first blast was to be 1 kgf and was to be used to establish the correct gain settings for the signal conditioning equipment.

(e) The second blast would be of 1 kgf, $\frac{2}{3}$ kgf and $\frac{1}{3}$ kgf with $\frac{1}{2}$s delays.

(f) Subsequent blasts depended on the initial results, bearing in mind the PPV limit of 25 mm/s.

The actual blasting sequence followed is given in Table 5.2

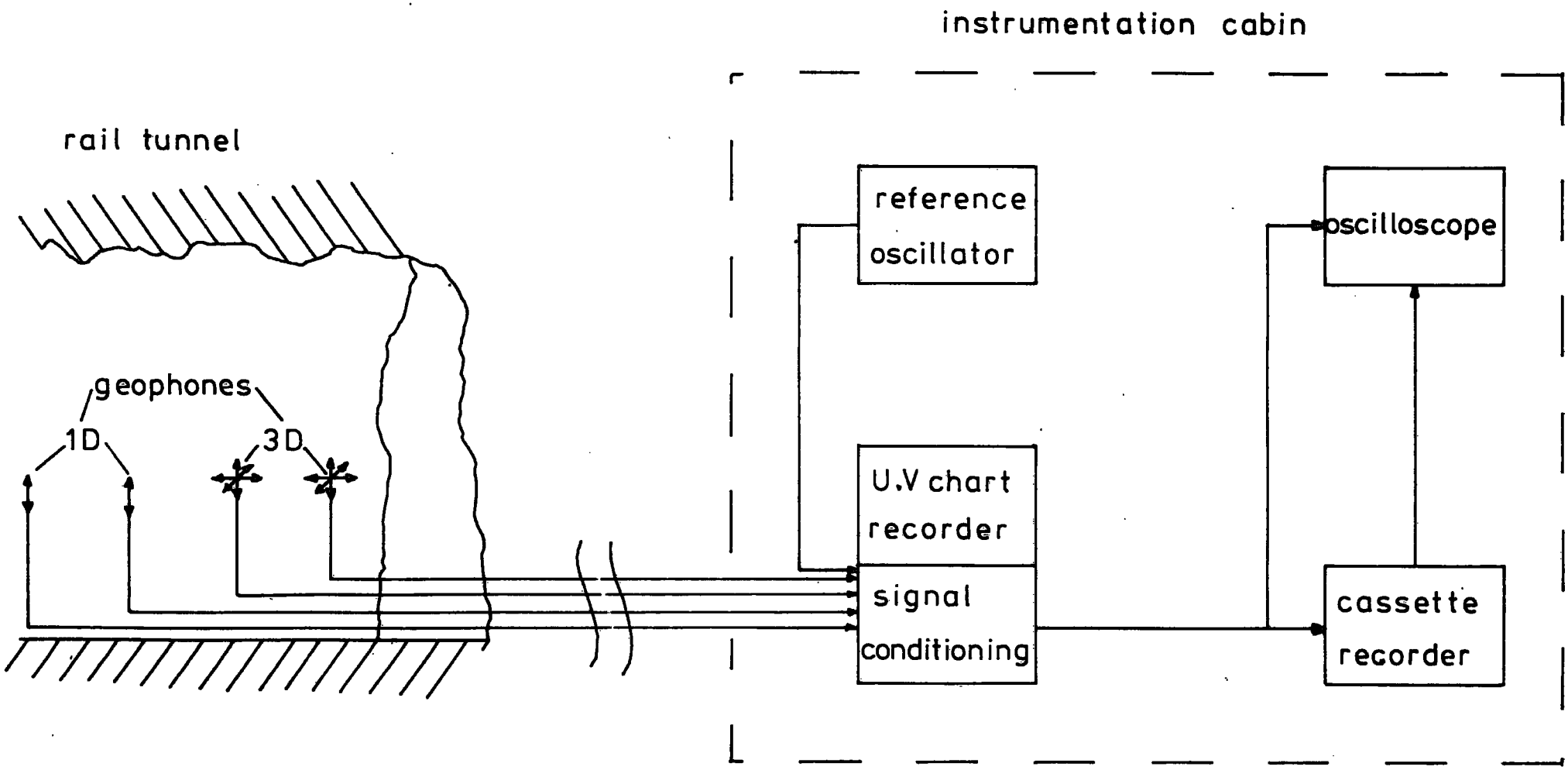

Fig.5.4 SCHEMATIC OF VIBRATION MEASURING EQUIPMENT

TABLE 5.2

The blasting sequence

Blast No.	Charge weight (kgf)	Delay between charges (s)	Shot hole ref.	Remarks
201	1	-	1	'Setting up' blast. No surface disturbance
202a	1	½	19	-do-
b	$\frac{2}{3}$	½	18	-do-
c	$\frac{1}{3}$		17	-do-
203a	2	1	16, 15	-do-
b	1		12	Considerable surface loosening and opening of joints in blast hole.
204	3	-	9, 11, 13	Some opening of joints and rock loosening.
205a	3		2, 3, 5	Some spoiling of surface rubble and cobble sized fragments.
b	1		10	

There was some concern that, where multiple holes were charged to give a single delay (for charges > 1 kgf), the detonation of each was simultaneous (*see* Section 6.3). Close inspection of the records indicated that the detonations were closely simultaneous except in the case of blast 4. This record indicates that one of the 3-1 kgf charges actually fired about 100 ms after the simultaneous detonation of the other two.

The delay period for multiple blasts was extended from ½s to 1s after blast 2 as some motions had not quite died away before the wave

packet from the next delay arrived.

At the completion of the blasting an inspection of all areas where rock fall or damage might have occurred was carried out. No such falls were noted; the only damage occurred within a few metres of the shot holes.

5.6 Supplementary seismic measurements

In addition to the trial blasting it was necessary to carry out hammer-seismic measurements to acquire data necessary for the assessment of rock quality as discussed in Section 3.5 In particular, measurement of the frequency of S-wave motions induced by a sledge-hammer blow (Section 3.5.4) was required to enable rock quality correlations to be tested (Section 3.5.5). These tests also provided additional data on P-wave velocities which are used together with 'blasting' P-wave velocities for the determination of'velocity ratio' in Section 6.6. These measurements were carried out in the area of the proposed western tunnel portals close to the location of the trial blast holes.

The motions produced by a hammer blow were monitored by three, three-dimensional, transducer arrays rigidly mounted at various measured distances from the source. The instrumentation used was the same as that described in Sections 5.3 and 5.4 except that a more versatile UV recorder was employed. This Bell and Howell recorder has double the chart width and up to four times the paper speed available from the recorder used during the blasting trials. This enabled significantly-improved records to be collected and provided more accurate measurements of seismic velocities and frequencies. The

original recorder was ideal when mainly amplitude data (for 'site laws') was required but the low chart speed (1 m/s) made velocity measurements difficult. The equipment was mounted in a Range Rover which was parked at the foot of the hillside. Plate 5.5 shows the equipment in use.

PLATE 5.5 SEISMIC RECORDING EQUIPMENT AND RANGE ROVER

CHAPTER 6

THE FIELD RESULTS AND THEIR ANALYSIS

6.1 Initial data processing

A seismic record sheet was completed for each blast and a typical sheet is shown in Figure 6.1. These sheets were completed during blasting and noted the instrumentation configurations and amplifier gain settings. Associated with each sheet was the UV chart record of the blast vibrations (*see* Figure 6.2). The maximum peak particle velocities occurring during the blasting were measured from the chart records given in Tables 6.1 - 6.5.

The resultant peak particle velocities given in the Tables were calculated in two ways:

(a) The resultant was first calculated by the vector summation of the three contributory components irrespective of their time of incidence. That is, the three maximum PPVs were summed whether or not they occurred simultaneously. This is sometimes referred to as the pseudo-resultant.

The resultant peak particle velocity was calculated as follows:

$$V_{Resultant} = \left[V^2_{'Radial'} + V^2_{'Horizontal'} + V^2_{'Vertical'} \right]^{\frac{1}{2}}$$

(b) The 'real time' resultant over the period of a recording was calculated in a similar manner except that the vector

SEISMIC RECORD SHEET No 86

SITE Penmaenbach tunnel west portal area DATE 17/6/79 TIME 07 58

SOURCE BLAST 3(203) Hole No 16 15 1 sec delay 12

Charge 2kg 1kg

U.V. CHANNEL	GEOPHONE /CABLE IDENT.	GEOPHONE LOCATION/ ORIENTATION	AMP GAIN X	U.V. mV/cm	SENS. mm/s/cm	TIMING MARK INTERVAL (s)	CASSETTE CODE/ CHANNEL	CASSETTE START/ FINISH	P.P.V mm/s	REMARKS
2	S5/D1	171 r	10	10	0·4	0.01	—			2kg blast confined
3	S6/C1	118 r	10	20	0·8	↓	—			1kg blast considerable
4	P1/A1	45 V	1	200	8		R1	123-125		surface breakage of
5	S2/A3	45 H	1	200	8		R2	123-125		rock. Almost
6	S1/A2	45 r	1	200	8		R3	123-125		unconfined)
7	P2/B1	78 V	1	100	4		B4	123-125		
8	S3/B2	78 H	1	100	4					
9	S4/B3	78 r	1	100	4					

Fig 6.1 RECORD SHEET

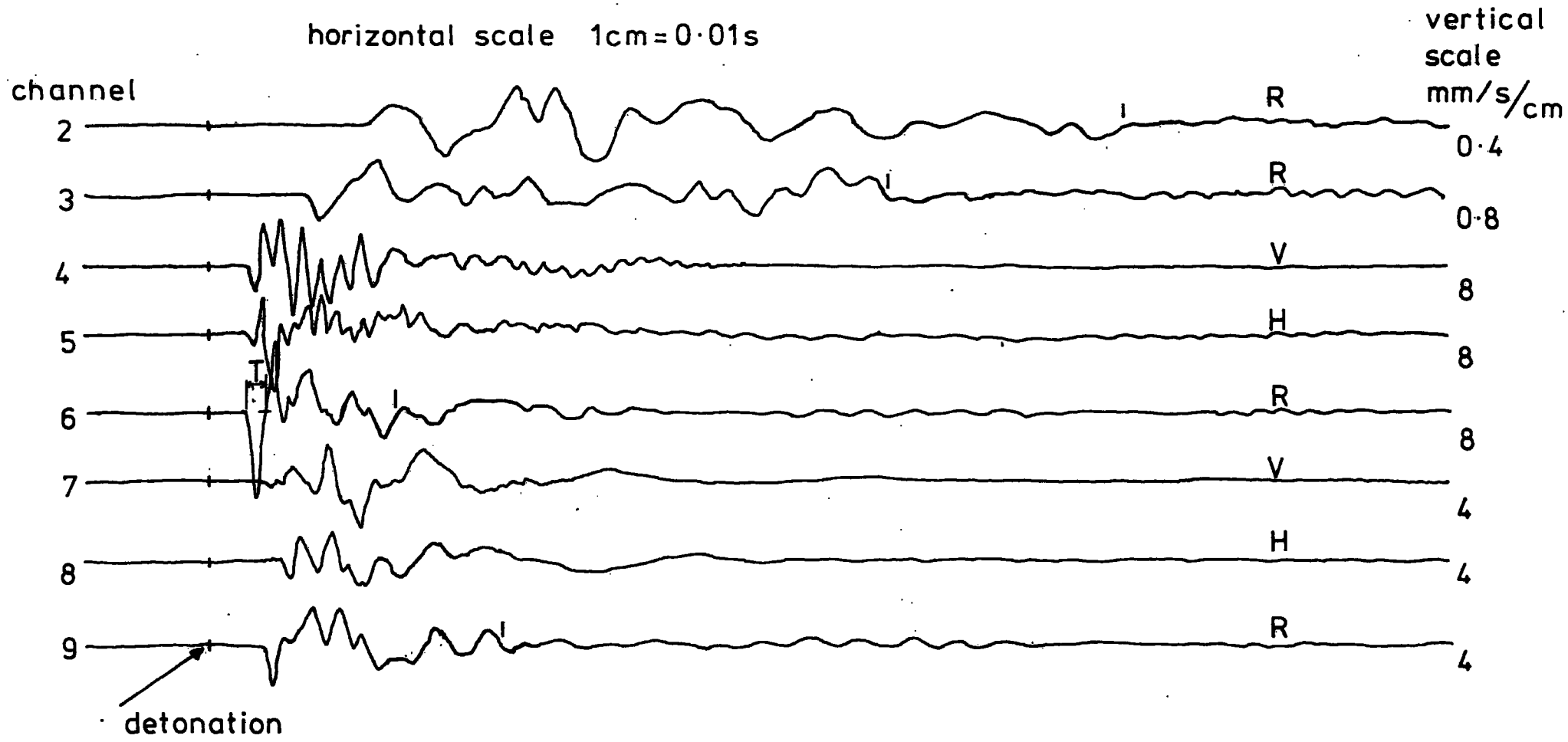

Fig.6.2 VIBRATIONS FROM 2kgf DETONATION — BLAST 3

Table 6.1

Results from blast 1

Geophone reference	Shot distance (m)	$R/\sqrt{M}$	$R/\sqrt[3]{M}$	Peak particle velocity (PPV, mm/s)	Resultant PPV (max.) (mm/s)	Resultant PPV (real time) (mm/s)	Compressional pulse length (ms)	Remarks
171r	117.5	117.5	117.5	± 0.2			6.0	Single 1kg detonation
118r	70.9	70.9	70.9	± 0.6			4.0	in shot hole 1, to set
45v	41.9	41.9	41.9	± 1.2				up instrumentation
45h	41.9	41.9	41.9	± 1.0				Poor low amplitude
45r	41.9	41.9	41.9	± 1.2			2.6	data except at 78M
78v	43.1	43.1	43.1	± 1.0				
78h	43.1	43.1	43.1	± 1.24	2.95	2.8		
78r	43.1	43.1	43.1	+ 2.48			3.2	
				- 1.84				

Table 6.2

Results from blast 2

Geophone reference	Shot distance (m)	$R/\sqrt{M}$	$R/\sqrt[3]{M}$	Peak particle velocity	Resultant PPV (max.)	Resultant PPV (real time)	Compressional pulse length	Remarks
171r	141.1	141.1	141.1	+ 0.15 - 0.24			7.2	Poor data at position 45 (wrong gain setting)
118r	91.3	91.3	91.3	+ 0.34 - 0.38			5.4	
45v	34.1	34.1	34.1	- - 3.2	6.54	-		
45h	34.1	34.1	34.1	- - 3.15				
45r	34.1	34.1	34.1	+ 4.75 - 2.5			-	
78v	54.7	54.7	54.7	+ 1.32 - 1.2	2.42	1.95		
78h	54.7	54.7	54.7	+ 1.2 - 0.92				
78r	54.7	54.7	54.7	+ 1.64 - 1.24			3.1	

171r	140.1	171.6	160.4	+ 0.10 - 0.16			-	2/3kgf hole 18
118r	90.2	110.5	103.3	± 0.18			5.0	Poor data at position
45v	33.4	40.9	38.2	± 1.5				45 (wrong gain setting)
45h	33.4	40.9	38.2	+ 2.5 - 2.8	4.04	3.3		
45r	33.4	40.9	38.2	+ 2.2 - 2.5			3.0	
78v	53.7	65.8	61.5	+ 1.0 - 1.08				
28h	53.7	65.8	61.5	+ 0.68 - 0.88	1.74	1.3		
78r	53.7	65.8	61.5	+ 1.04 - 0.8			2.2	
171r	138.5	240.0	199.7	+ 0.07 - 0.10			-	1/3kgf in hole 17
118r	88.5	153.4	127.6	+ 0.11 - 0.14			-	
45v	32.1	55.6	46.3	+ 1.22 - 0.97				
45h	32.1	55.6	46.3	+ 1.8 - 2.0	2.81			
45r	32.1	55.6	46.3	+ 1.5 - 1.7			3.2	
78v	51.9	89.9	74.8	± 0.8				
78h	51.9	89.9	74.8	± 0.6	1.17			
78r	51.9	89.9	74.8	± 0.6			2.1	

Table 6.2 (cont)

Table 6.3

Results from blast 3

Geophone reference	Shot distance (m)	$R/\sqrt{M}$	$R/\sqrt[3]{M}$	Peak particle velocity	Resultant PPV (max.)	Resultant PPV (real time)	Compressional pulse length	Remarks
171r	136.3	96.4	108.2	+ 0.24 - 0.32			8.4	2kg in holes 15 and 16
118r	86.3	61.0	68.5	+ 0.40 - 0.56			6.5	
45v	31.0	21.9	24.6	+ 7.2 - 6.4				
45h	31.0	21.9	24.6	+ 7.76 - 5.44	16.0	12.3		
45r	31.0	21.9	24.6	+ 12.00 - 9.28			3.3	
78v	49.8	35.2	39.5	+ 3.4 - 2.6				
78h	49.8	35.2	39.5	+ 2.0 - 1.84	4.84	3.9		
78r	49.8	35.2	39.5	+ 2.8 - 2.72			3.5	

171r	132.3	132.3	132.3	+ 0.14 - 0.08			6.5	1kg in hole 12
118r	83.4	83.4	83.4	+ 0.32 - 0.28			4.0	Considerable surface loosening and opening of joints.
45v	35.1	35.1	35.1	1.28	2.42			Not a confined blast.
45h	35.1	35.1	35.1	+ 1.6 - 0.8				
45r	35.1	35.1	35.1	± 1.28			2.3	
78v	49.3	49.3	49.3	± 0.48	1.15			
78h	49.3	49.3	49.3	± 0.56				
78r	49.3	49.3	49.3	+ 0.88 - 0.56			3.0	

Table 6.3 (cont)

Table 6.4

Results from blast 4

Geophone reference	Shot distance (m)	$R/\sqrt{M}$	$R/\sqrt[3]{M}$	Peak particle velocity	Resultant PPV (max.)	Resultant PPV (real time)	Compressional pulse length	Remarks
171r	129.1	91.3	102.5	+ 0.36 - 0.24			8.2	'2kgf' initial shock. This should have been a single 3kgf detonation
118r	80.5	56.9	63.9	+ 0.64 - 0.72			5.5	
45v	35.6	25.2	28.3	+ 1.6 - 3.2				The records indicate a faulty detonation possibly of 2kgf then 1/10s later 1kgf. The data has been processed on this assumption but must be regarded with suspicion Some opening of joints and rock loosening.
45h	35.6	25.2	28.3	± 2.08	4.51	3.80		
45r	35.6	25.2	28.3	± 2.4			3.9	
78v	47.3	33.5	37.5	± 1.6				
78h	47.3	33.5	37.5	± 1.44	4.54	4.10		
78r	47.3	33.5	37.5	+ 4.0 - 2.8			4.1	
171r	129.1	129.1	129.1	+ 0.20 - 0.16				'1kgf' second shock
118r	80.5	80.5	80.5	± 0.32				
45v	35.6	35.6	35.6	± 1.28				
45h	35.6	35.6	35.6	± 1.92	2.81			
45r	35.6	35.6	35.6	± 1.6				
78v	47.3	47.3	47.3	± 0.8				
78h	47.3	47.3	47.3	± 1.2	2.15			
78r	47.3	47.3	47.3	+ 1.6 - 0.8				

171r	126.5	126.5	126.5	+ 0.14 - 0.09			6.2	1kg charge in hole 10.
118r	78.4	78.4	78.4	+ 0.27 - 0.32			4.0	low amplitude data
45v	37.4	37.4	37.4	± 1.28	1.91			
45h	37.4	37.4	37.4	± 1.04				
45r	37.4	37.4	37.4	± 0.96			3.2	
78v	46.5	46.5	46.5	± 0.64	1.77			
78h	46.5	46.5	46.5	± 0.80				
78r	46.5	46.5	46.5	+ 1.44 - 0.80			3.0	

Table 6.4 (cont)

Table 6.5

Results from blast 5

Geophone reference	Shot distance (m)	$R/\sqrt{M}$	$R/\sqrt[3]{M}$	Peak particle velocity	Resultant PPV (max.)	Resultant PPV (real time)	Compressional pulse length	Remarks
171r	120.6	69.6	83.6	+ 0.36 - 0.38			8.0	3kgf charge in holes 2, 3 and 5
118r	73.4	42.4	50.9	+ 0.96 - 1.16			6.3	Some spoiling of surface rubble and cobble sized fragments
45v	40.0	23.1	27.7	+ 1.92 - 2.4	4.78	3.6		
45h	40.0	23.1	27.7	+ 3.36 - 1.76				
45r	40.0	23.1	27.7	+ 2.4 - 1.6			4.1	
78v	44.0	25.4	30.5	± 2.4	7.69	7.6		
78h	44.0	25.4	30.5	+ 2.4 - 3.04				
78r	44.0	25.4	30.5	+ 6.64 - 4.96			4.2	

components were summed at simultaneous times. This involved the digitisation of the data and the computation of the 'real time' resultant for each blast vibration record. Figure 6.3 shows the real time 'resultant' peak particle velocities for blast 3 and is typical of those obtained from the other blasts.

It should be noted that the 'real time' resultant is the actual peak particle velocity recorded and will generally be less than that calculated as in (a) above. However, since it is possible that all three 'maximum' vector components may occur simultaneously during subsequent construction, it is arguable that method (a) should be used to establish the site laws. To illustrate this problem the chart records with their computed 'real time' results are given in Figures 6.4 and 6.5 for the 3 kgf charge of blast 5. It is interesting to note the difference in these records which are derived from the same shock at similar distances from the blast; the differences being due to the different properties of the intervening rock mass.

Figure 6.4 shows that the maximum vector component, at position 78 m, for the radial, vertical and horizontal (r, v and h) directions is due to the initial compressional pulse. These maxima therefore occur simultaneously and the 'real time' resultant is almost identical to that of the more conservative resultant calculated by the method (a) above (7.6 mm/s and 7.69 mm/s respectively). However, Figure 6.5 shows that at position 45 m the maximum individual components do not occur at the same time. For the radial direction the maximum is due to the initial compressional pulse whereas for the vertical and horizontal the maximum follows later in the shear wave arrivals. In this case the resultant values computed by methods (a) and (b) are 4.78 mm/s and 3.6 mm/s,

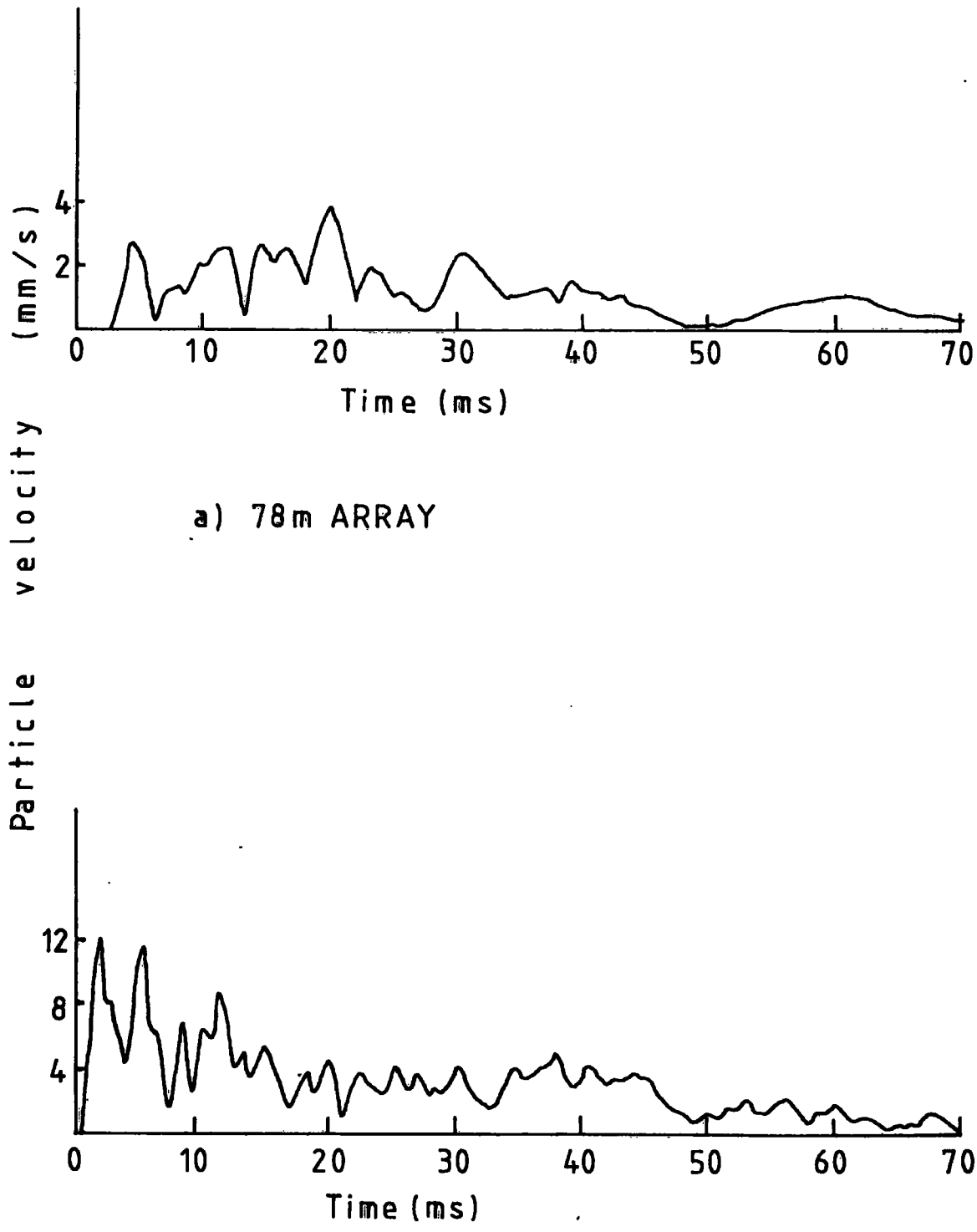

a) 78m ARRAY

b) 45m ARRAY

Fig. 6.3 REAL TIME RESULTANT (BLAST 3, 2 kgf)

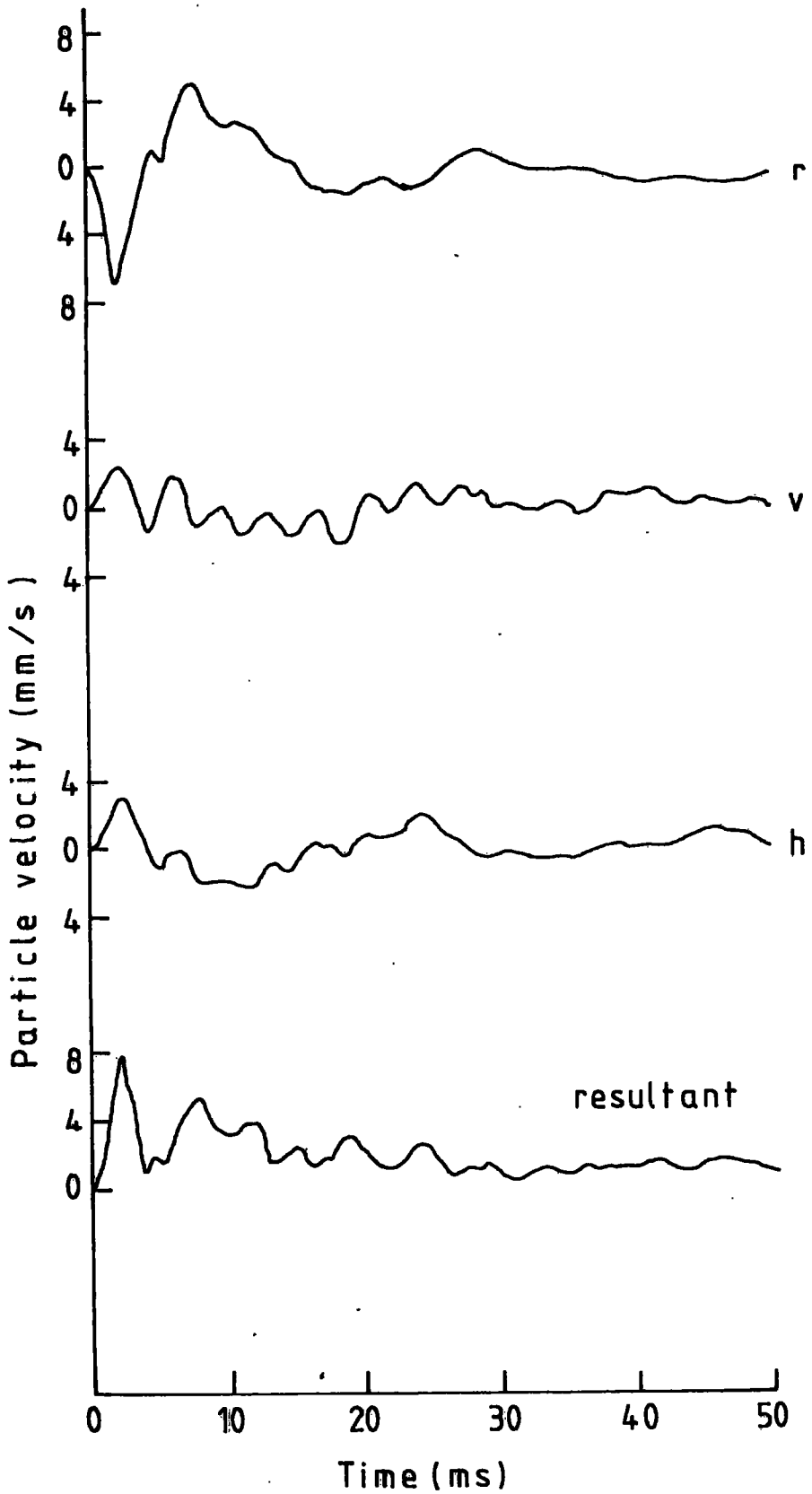

Fig.6.4 RESULTANT AND VECTOR COMPONENT PARTICLE VELOCITIES AT 78m ARRAY (BLAST 5, 3 kgf)

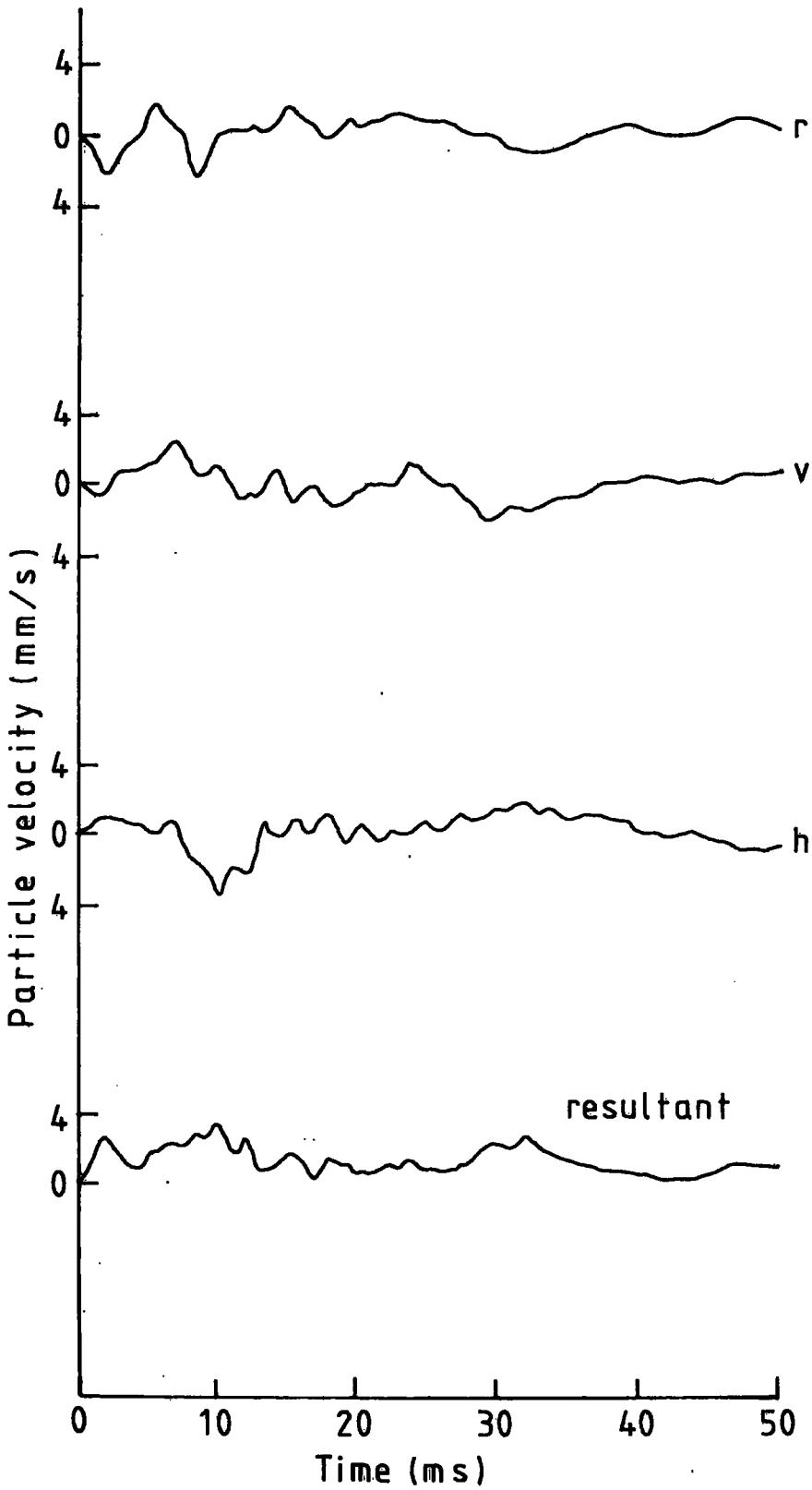

Fig. 6.5 RESULTANT AND VECTOR COMPONENT PARTICLE VELOCITIES AT 45m ARRAY (BLAST 5, 3kgf)

respectively. It is interesting to note that although position 78 m is 4 metres further from the blast than position 45 m, the recorded PPV was rather higher. This may be attributable to variations in the attenuative properties of the rock mass or some form of wave guidance due to jointing characteristics.

6.2 The site laws; square and cube root scaling methods

The data in Tables 6.1 - 6.5 have been abstracted and grouped to provide graphical presentations of the site laws. Table 6.6 defines the axes of each log-log graph together with the Figure reference. Appendices E, F and G list the data groupings.

TABLE 6.6
Site law presentation format

Figure	Vertical axis Peak particle velocity mm/s	Horizontal axis Scaled distance m/kgf$^{\frac{1}{2}}$ or $\frac{1}{3}$
6.6a	Resultant (max)	$R/\sqrt{M}$
6.6b	" "	$R/\sqrt[3]{M}$
6.7a	Resultant (real time)	$R/\sqrt{M}$
6.7b	" "	$R/\sqrt[3]{M}$
6.8	Radial	$R/\sqrt{M}$
6.9	"	$R/\sqrt[3]{M}$

The least squares 'best fit' lines together with their power law equations and correlation coefficients (*see* Section 3.1) are given for each group of data both in the Appendices and in the Figures.

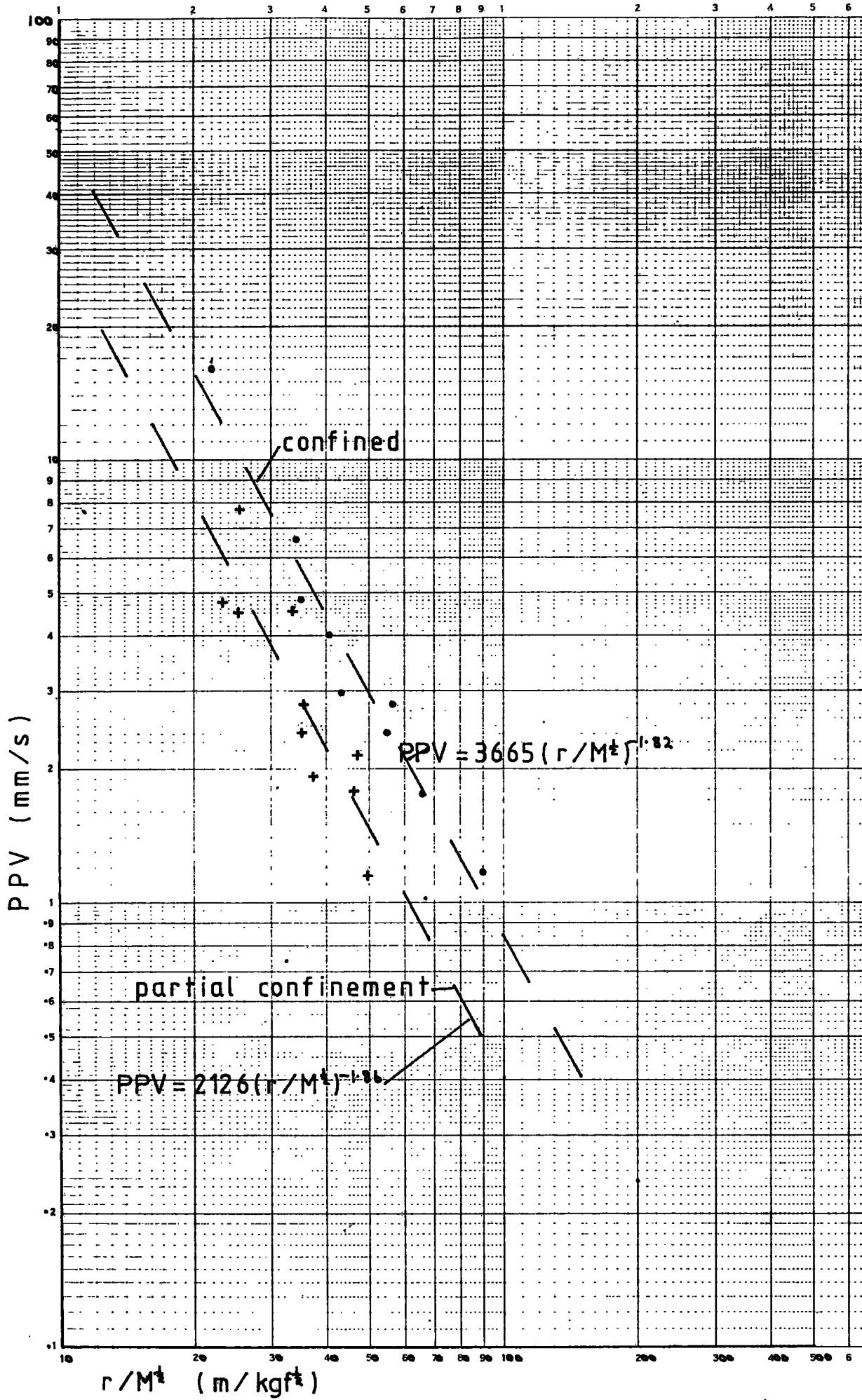

Fig. 6.6a. RESULTANT 'max' PPV v SCALED DISTANCE, $r/M^{\frac{1}{2}}$

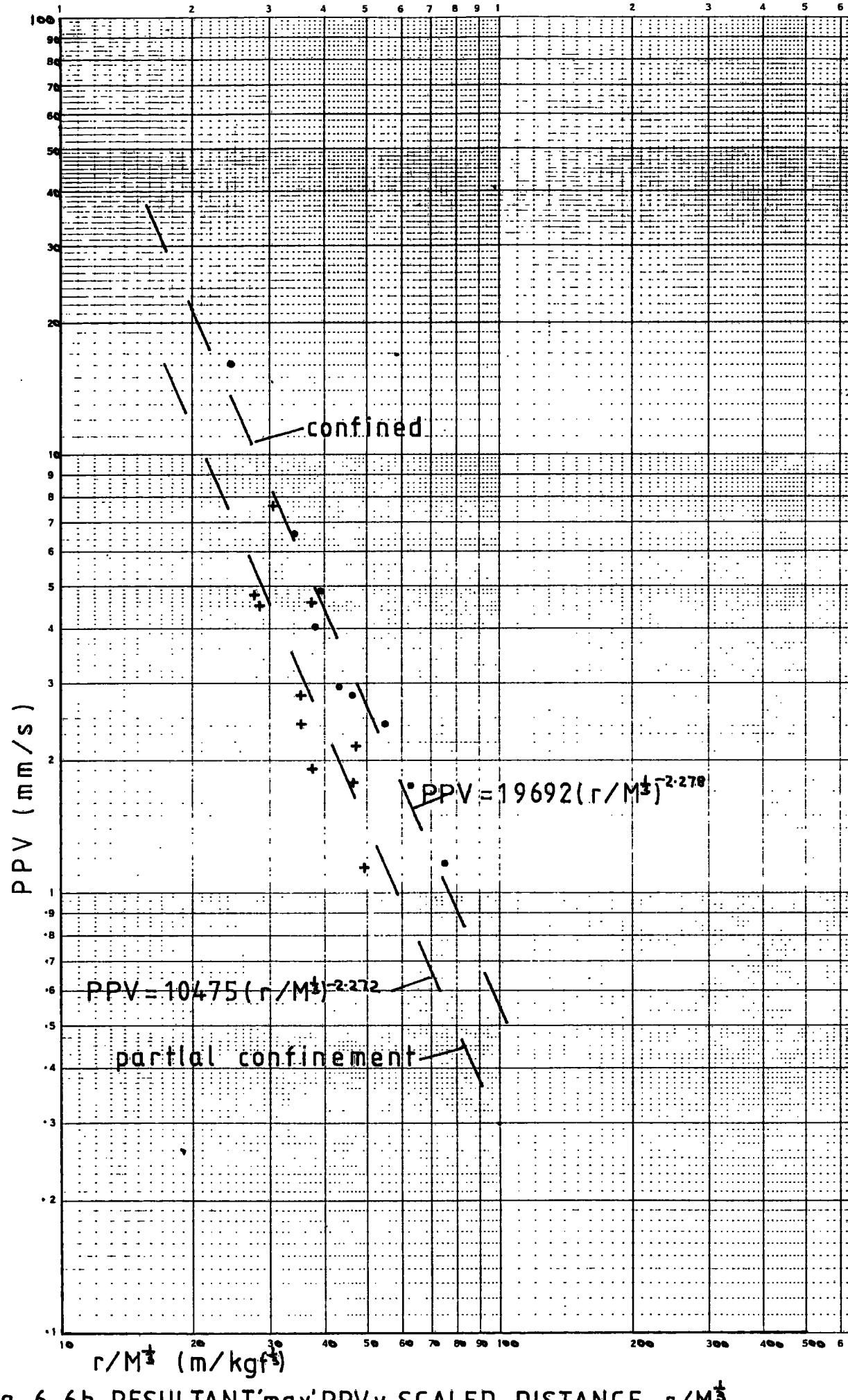

Fig. 6.6b. RESULTANT 'max' PPV v SCALED DISTANCE, $r/M^{\frac{1}{3}}$

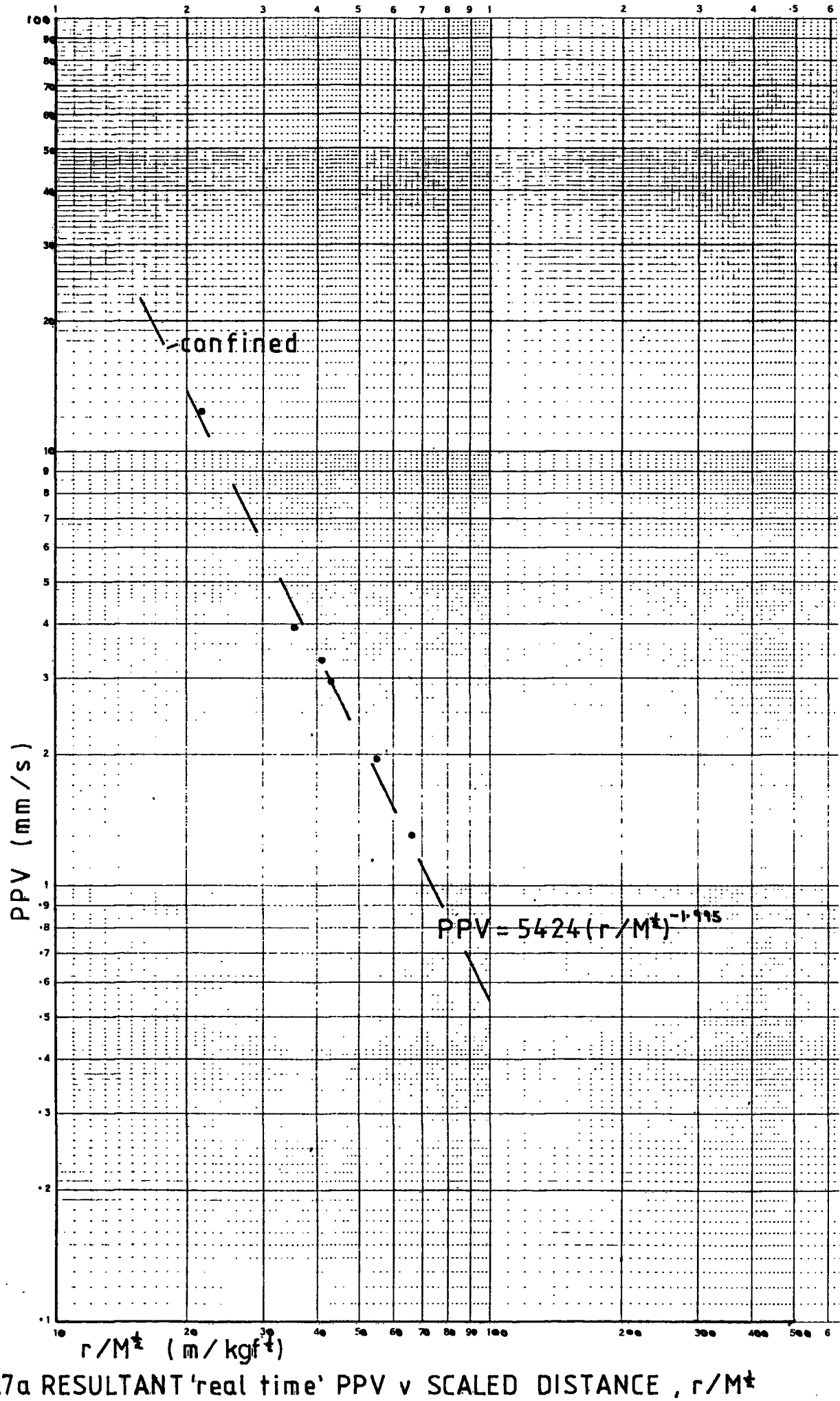

Fig. 6.7a RESULTANT 'real time' PPV v SCALED DISTANCE, $r/M^{\frac{1}{2}}$

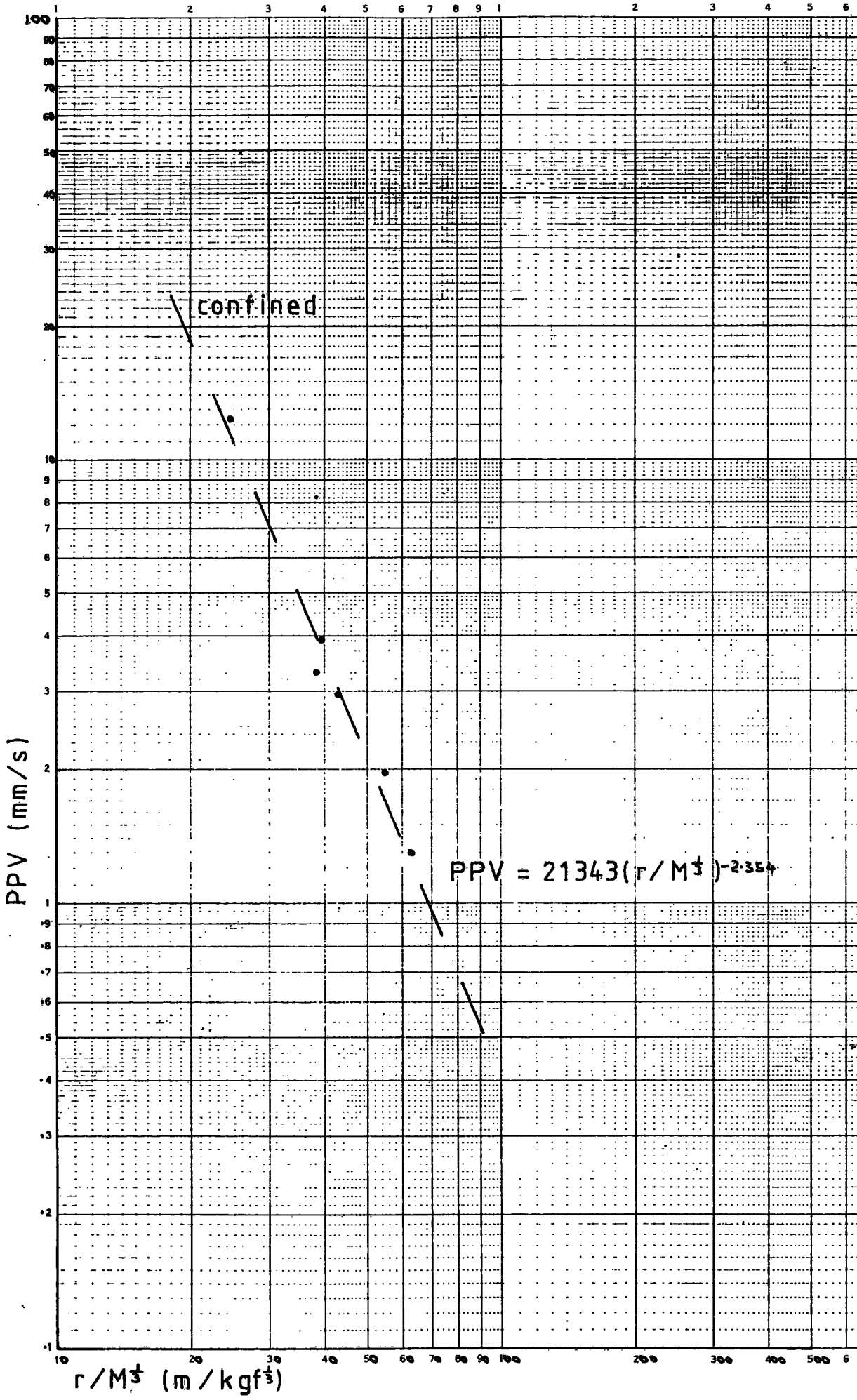

Fig.6.7b RESULTANT 'real time' PPV v SCALED DISTANCE, $r/M^{\frac{1}{3}}$

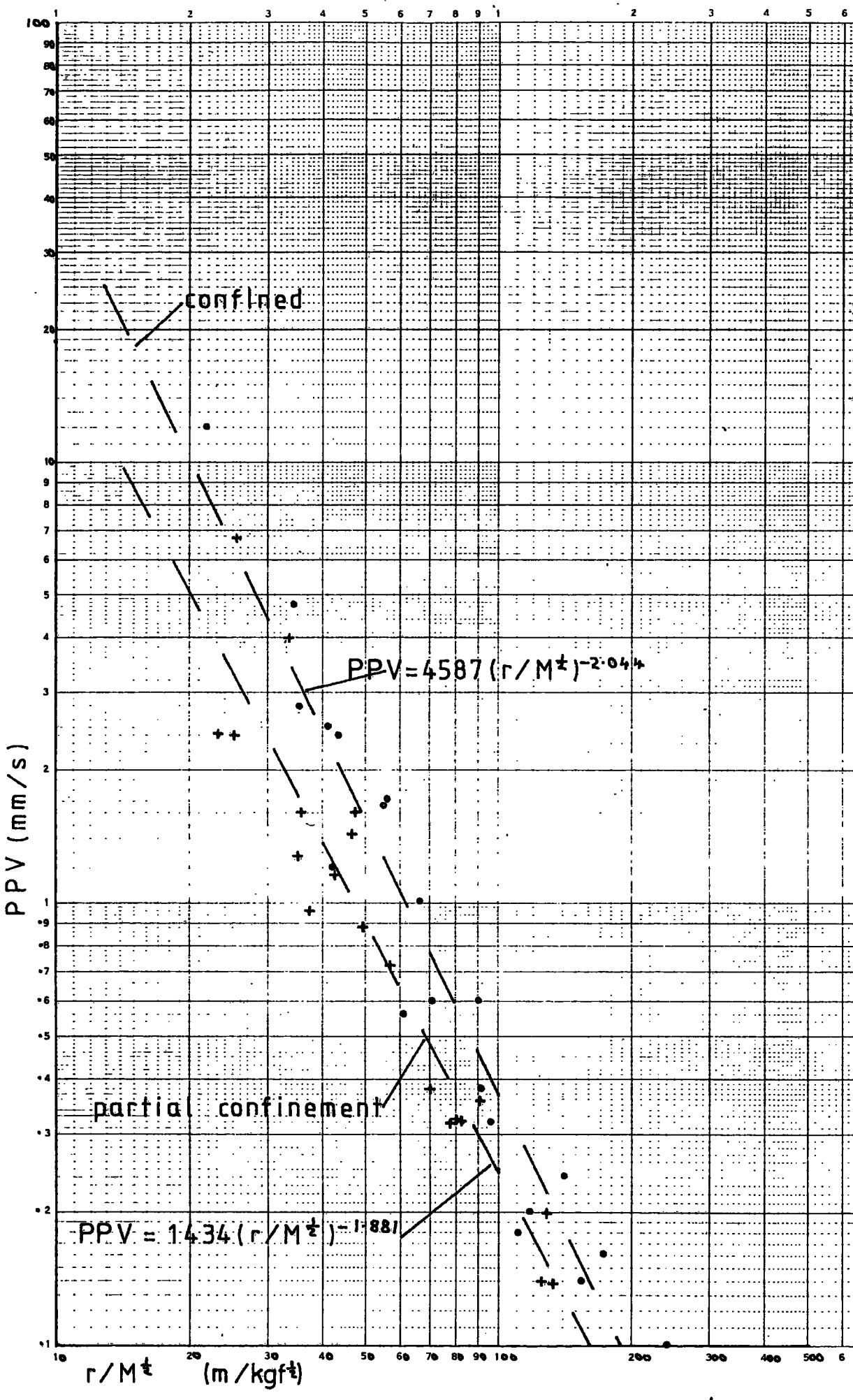

Fig.6.8 RADIAL PPV v SCALED DISTANCE, $r/M^{\frac{1}{2}}$

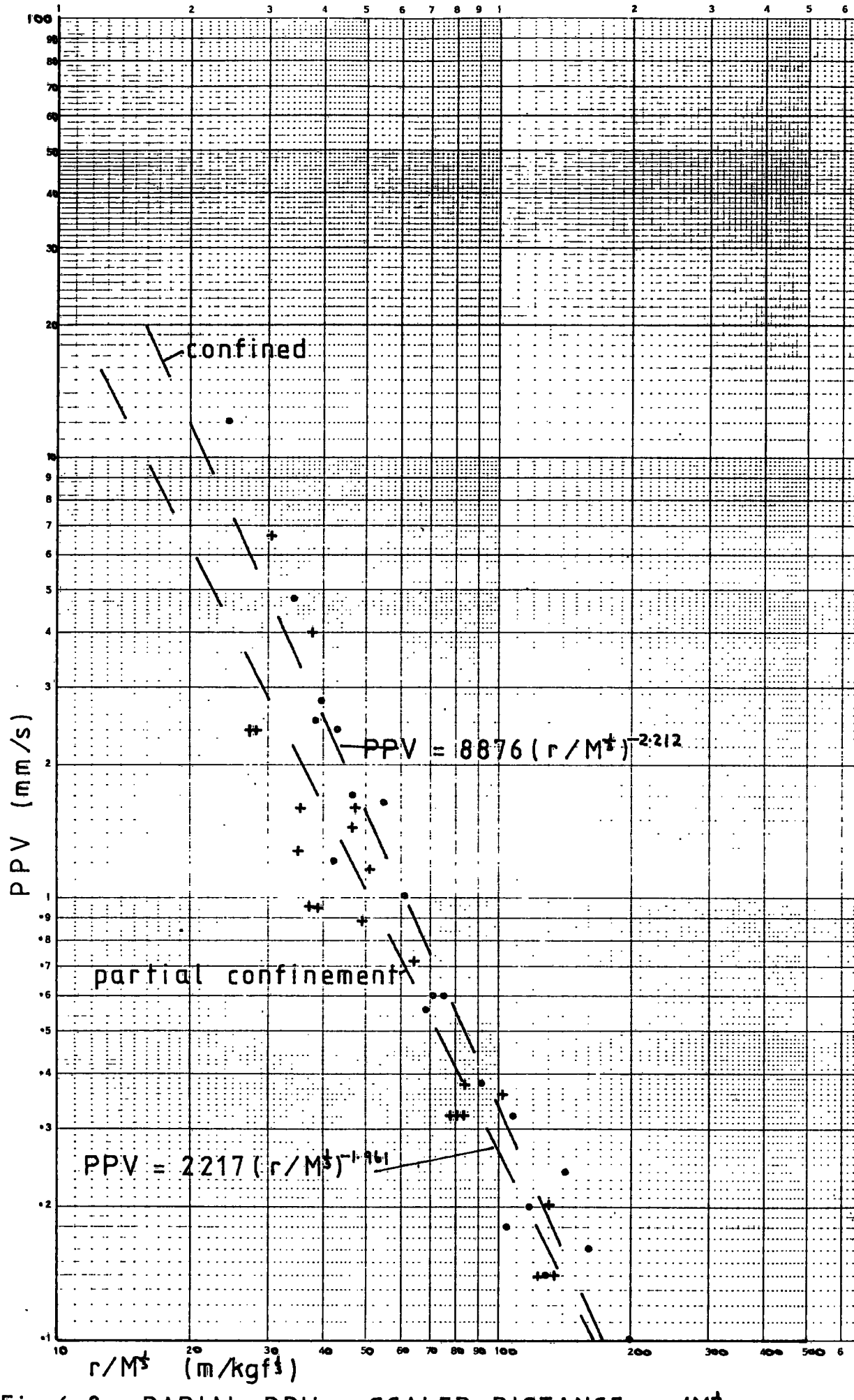

Fig.6.9 . RADIAL PPV v SCALED DISTANCE , $r/M^{\frac{1}{3}}$

The equations relating peak particle velocity (PPV in mm/s) to scaled distance ($r/\sqrt{M}$) or $r/\sqrt[3]{M}$ are as follows:

Resultant (max, confined)		$PPV = 3665(r/\sqrt{M})^{-1.820}$	$R^2 = 0.961$
	or	$PPV = 19692\ (r/\sqrt[3]{M})^{-2.278}$	$R^2 = 0.965$
Resultant (max, partial confinement)		$PPV = 2125\ (r/\sqrt{M})^{-1.860}$	$R^2 = 0.783$
	or	$PPV = 10475\ (r/\sqrt[3]{M})^{-2.272}$	$R^2 = 0.676$
Resultant (real time, confined)		$PPV = 5424\ (r/\sqrt{M})^{-1.995}$	$R^2 = 0.991$
	or	$PPV = 21343\ (r/\sqrt[3]{M})^{-2.354}$	$R^2 = 0.978$
Radial (confined)		$PPV = 4587\ (r/\sqrt{M})^{-2.044}$	$R^2 = 0.935$
	or	$PPV = 8876\ (r/\sqrt[3]{M})^{-2.212}$	$R^2 = 0.945$
Radial (partial confinement)		$PPV = 1434\ (r/\sqrt{M})^{-1.881}$	$R^2 = 0.899$
	or	$PPV = 2217\ (r/\sqrt[3]{M})^{-1.961}$	$R^2 = 0.874$

where R^2 is the coefficient of determination as defined in Appendix C.

6.3 The site laws; site specific scaling method

Figures 6.10, 6.11 and 6.12 present, in graphical format, the 'site specific' laws calculated by multiple regression analysis as described in Section 3.2. The data was taken from Tables 6.1 - 6.5 and grouped as shown in Appendices E, F and G.

The equations relating peak particle velocity to the 'site specific' scaled distance ($r/M^{\alpha/\beta}$) are as follows:

Resultant (max, confined)	$PPV = 10{,}000(r/M^{0.399})^{-2.093}$	$R^2 = 0.972$
Resultant (max, partial confinement)	$PPV = 67.45(r/M^{1.132})^{-0.947}$	$R^2 = 0.846$
Resultant (real time, confined)	$PPV = 8138(r/M^{0.451})^{-2.102}$	$R^2 = 0.993$
Radial (confined)	$PPV = 7727(r/M^{0.373})^{-2.177}$	$R^2 = 0.947$
Radial (partial confinement)	$PPV = 1197(r/M^{0.552})^{-1.845}$	$R^2 = 0.900$

Note that, as expected, the correlation coefficients for these data are better than those for either square or cube root scaling methods given in the previous Section.

It is of interest that the data for confined blasts are better correlated with the predictor equations than those described as partially confined. This reflects the field conditions which allow a well-confined blast to be accurately described whereas the actual *degree* of confinement imposed when significant rock breakage occurs may be varied and difficult to ascertain.

By substitution of a relevant value of range, r, the PPV may be expressed as a function of charge weight, M.

Figure 6.13 shows the predicted values for PPV, at a range of 30 m, for values of charge weight. Note that, in this case, the predicted 'site specific' PPV lies about midway between the predictions based on square and cube root scaling methods. This results from the specific scaling exponent (α/β) being 0.399 which lies between one-half and one-third, the square and cube root scaling exponents. The value

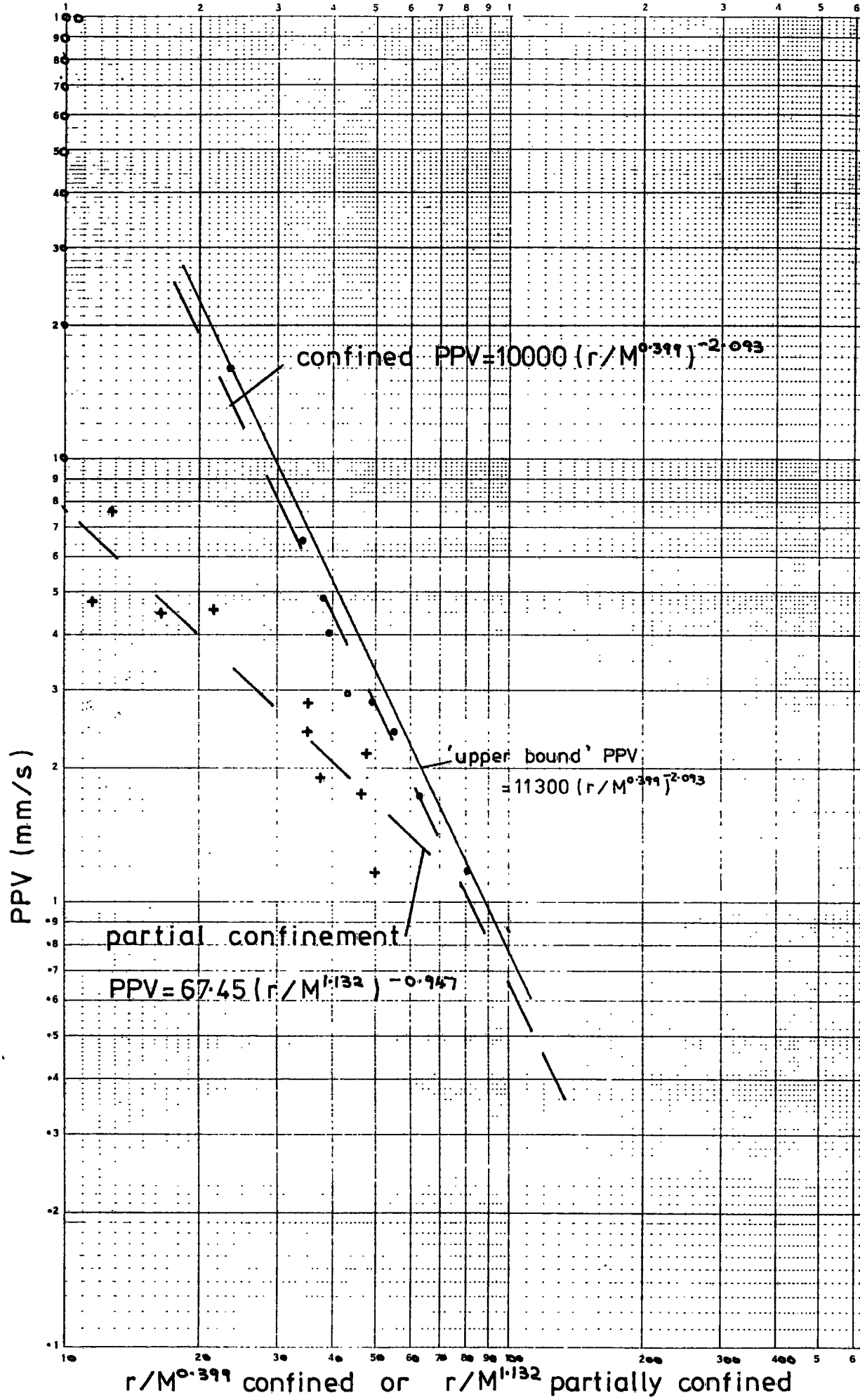

Fig 6.10 RESULTANT 'max' PPV v SITE SPECIFIC SCALING

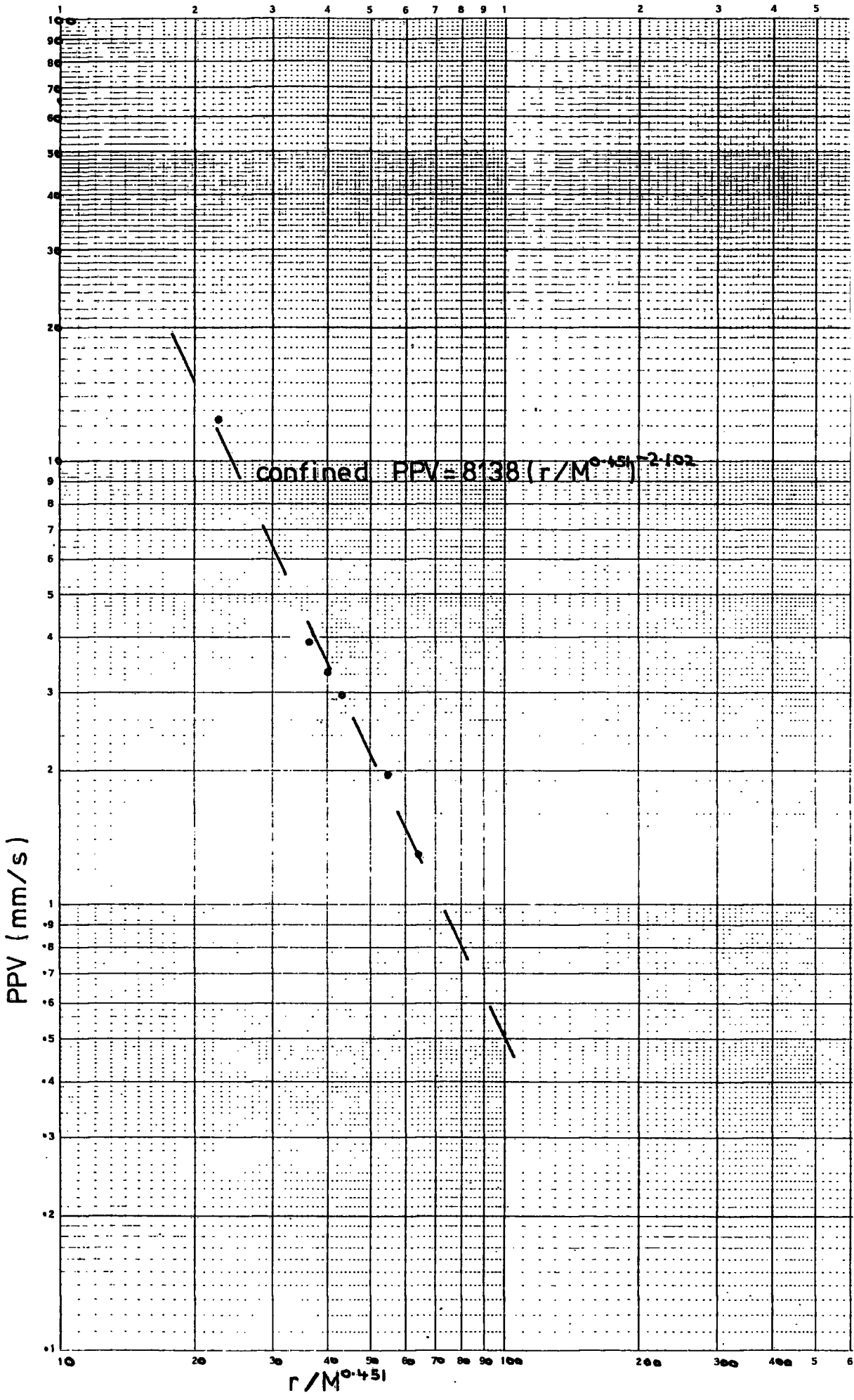

Fig. 6.11 RESULTANT 'real time' PPV v SITE SPECIFIC SCALING

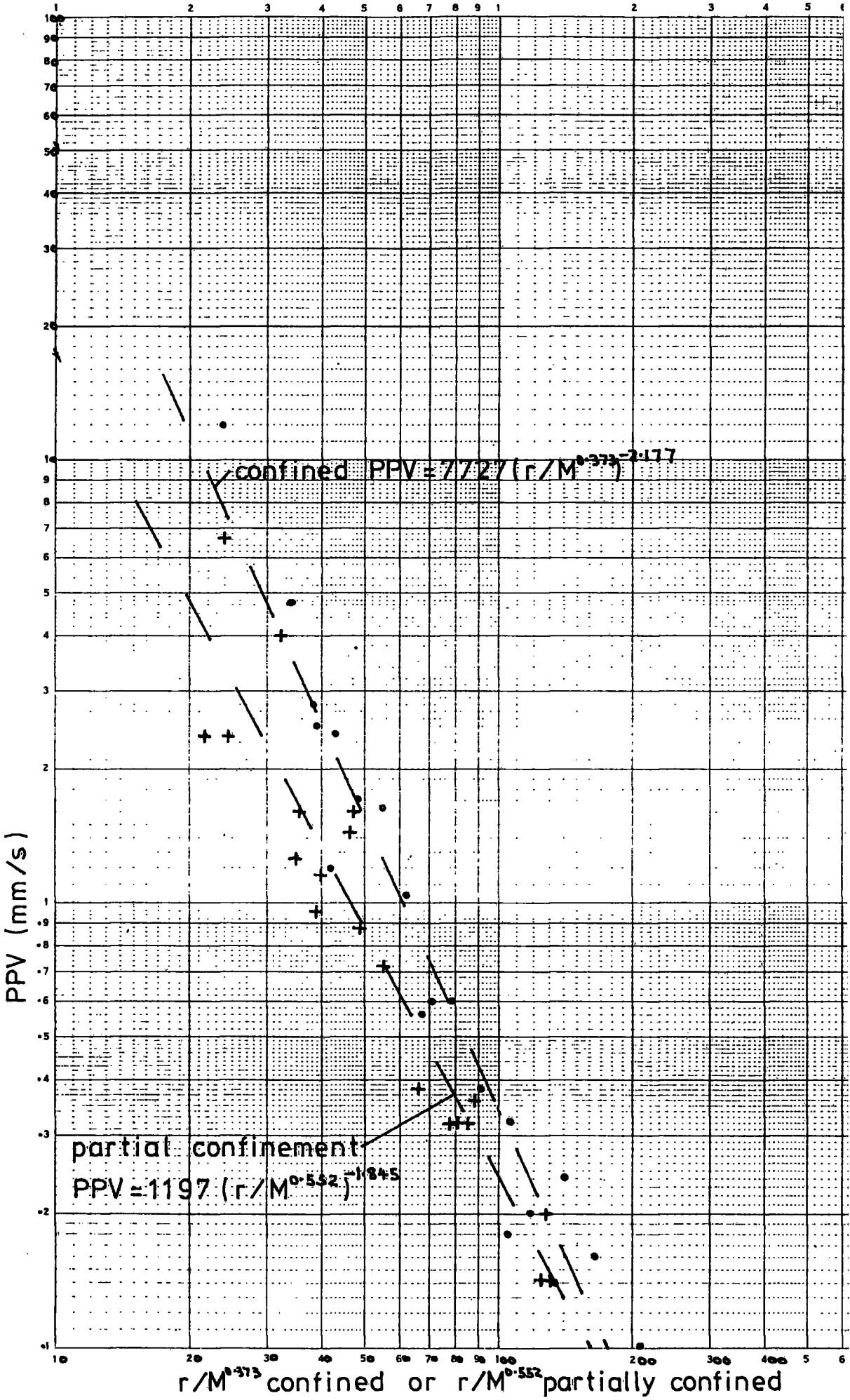

Fig 6.12 RADIAL PPV v SITE SPECIFIC SCALING

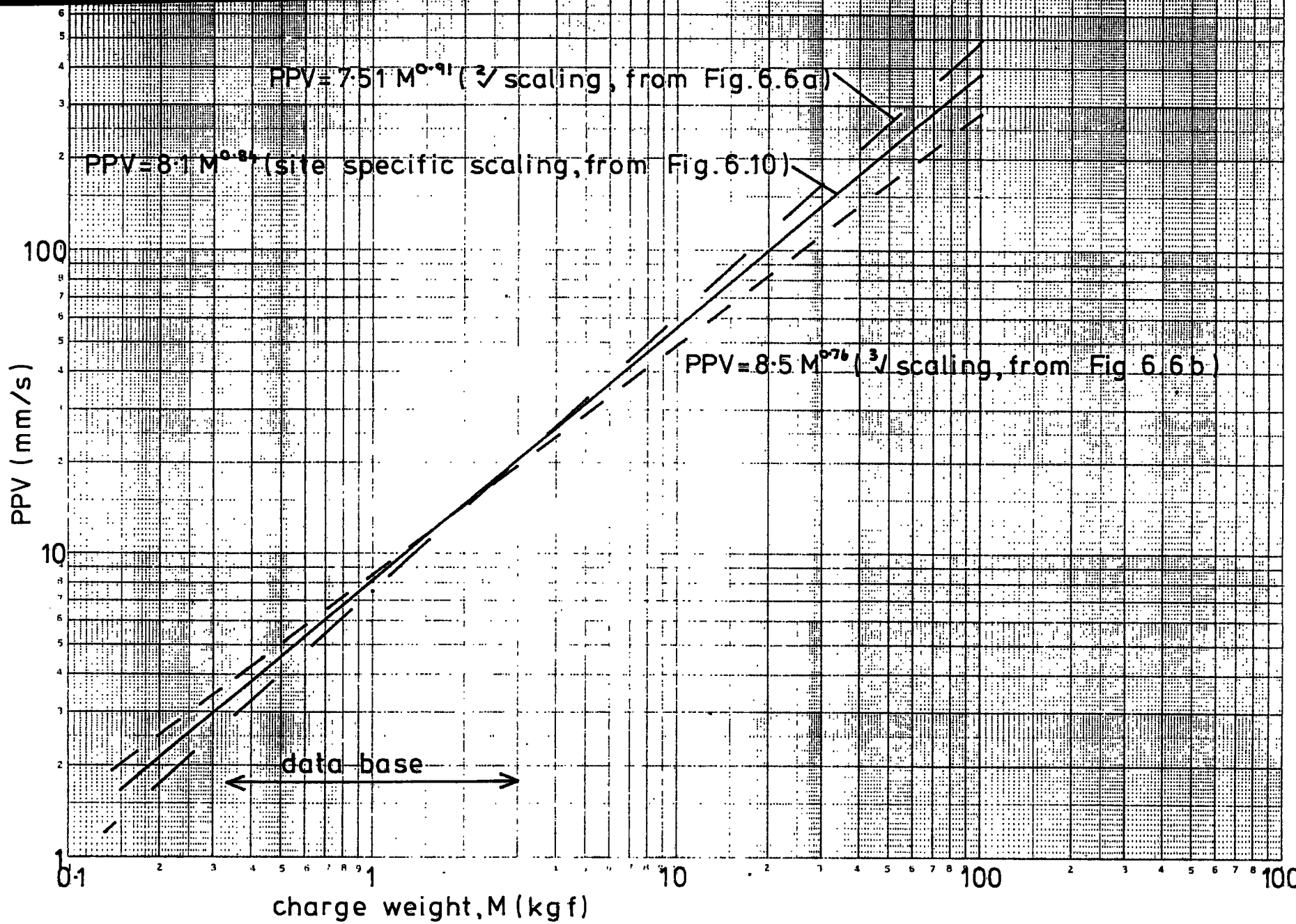

Fig.6·13 PREDICTED RESULTANT PPV v CONFINED CHARGE WEIGHT (range r = 30m)

of 30 m was chosen as the closest the new tunnels were to approach the existing rail tunnel at any stage of the design. The 'confined' resultant equation was used as this represents the potentially most hazardous condition.

6.4 The duration of the vibrations

6.4.1 Wave packet duration

As discussed in Section 3.3.4, it is to be expected that the wave packet spreading away from the source will increase in duration with propagation distance. This spreading may be largely explained by the differing characteristic velocities of the compressional, shear and surface waves which are created at the explosive source and by mode conversion during propagation.

For simplicity the duration of the radial wave packet is measured although in practice the vertical and horizontal packet durations appear similar and could probably be used if necessary.

Wave packet duration is arbitarily defined as the period between the first observed arrival until a point when the PPV never again exceeds 25 per cent of its peak value. This period will include the majority of the vibration energy in the wave packet and removes the difficulty of deciding when the low level vibrations in the tail merge into the noise level of the system. Figure 6.14 shows the increase in the duration of the wave packet with distance from the source. The spread of the data at larger ranges is considerable but the trend is unmistakable.

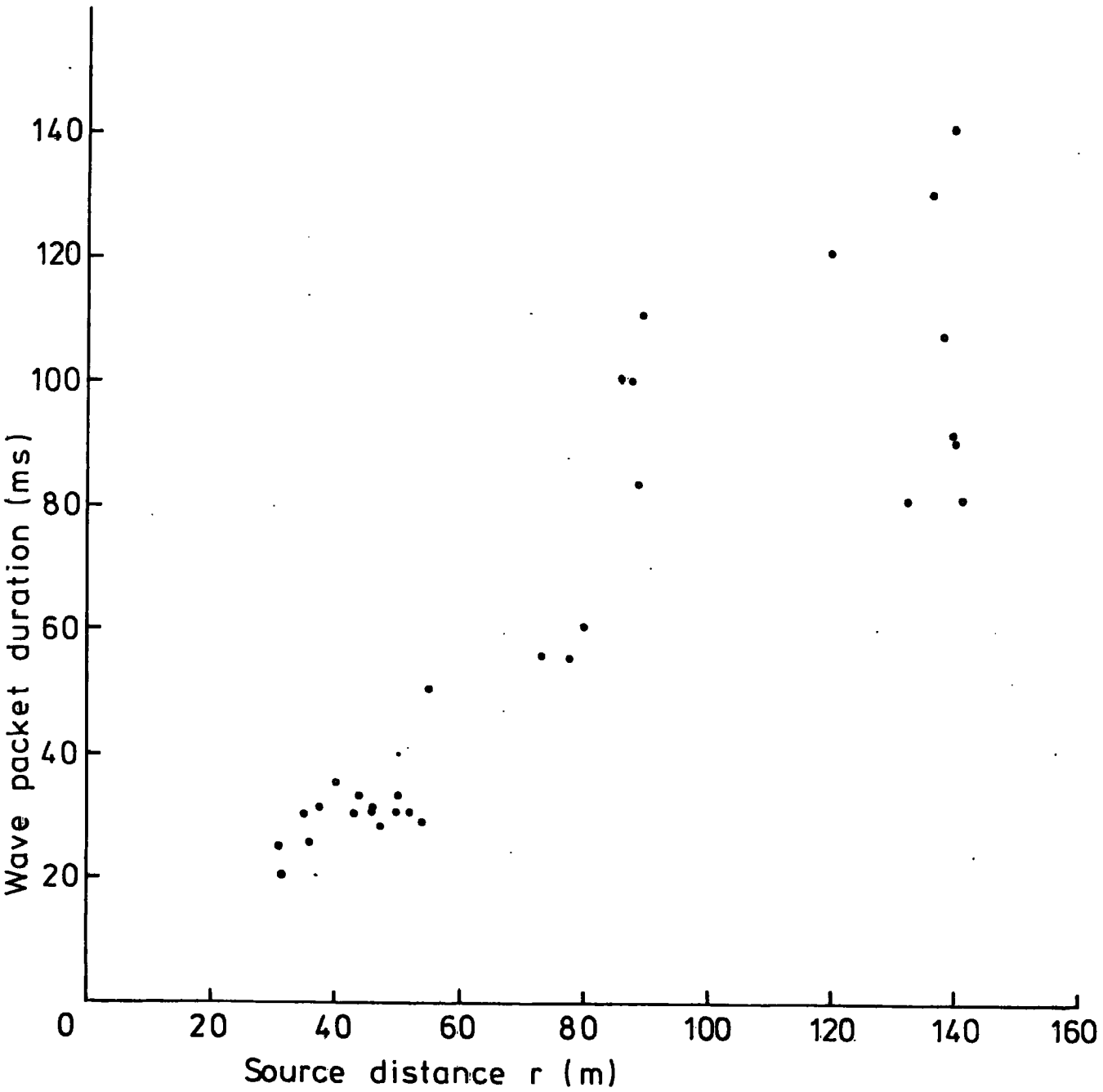

Fig. 6.14 WAVE PACKET DURATION v SOURCE DISTANCE

The pattern of the data is well represented by the example given in Figure 6.2.

Note the differences in the duration and character of the wave packet with increasing distance from the source:

(a) Channel 6 is 31 m from the source, is dominated by the initial compressional wave pulse and has a duration of 25 ms.

(b) Channel 9 is 50 m from the source and comprises a clearly defined compressional pulse followed by slower (probably shear) wave motions of similar size. The wave packet duration is about 40 ms.

(c) At 86 m (Channel 2) and 136 m (Channel 1) the wave packet duration have increased to 100 ms and 130 ms respectively.

Further measurements of the increase in wave packet duration, including data obtained within a few metres of the source, are given in Chapter 7.

6.4.2 Initial pulse duration

The duration of the initial pulse, (T), is defined as the duration (in milliseconds) of the initial half wave motion of the first wave arrival at the transducer array (eg *see* Figure 6.2). In the radial direction and for distances of less than 60 m this first arrival gave rise to the maximum PPV recorded during each blast. At greater distances however, the maximum radial PPV sometimes coincided with the first arrival, but on many occasions occurred later in the wave packet. This was due to the build up of slower shear wave

motions and possibly surface wave effects along the tunnel sidewalls.

Figure 6.15 shows the increase in the duration of the initial pulse for the three charge weights fired. Note that the increase of pulse duration with radial distance is similar for all charge weights but that the pulse duration intercept constant increases with charge size. This increase in initial pulse duration is due mainly to the geometrical factors and to the variations within detonators (*see* Section 3.3.2).

6.5 Application of the site laws

Having established site specific scaling laws relating PPV to charge weight and distance, the maximum charge weight per delay to be fired may be determined. This information is usefully considered by the Engineer prior to the issue of tender documents as it may be that low charge weights will make the drill and blast method uneconomic.

For the Penmaenbach tunnels it was initially agreed by British Rail that 100 mm/s should be regarded as an acceptable value for maximum PPV, although it seemed likely that a rather lower value may be used in practice. The value of 100 mm/s was largely based on the review and discussion given in Chapter 2 of this thesis.

Given the value for maximum PPV and the minimum distance between the blasting and the rail tunnel (30 m), the maximum charge weight may be calculated using the equations given in Section 6.3.

Consider the equation for the resultant PPV (max, confined)

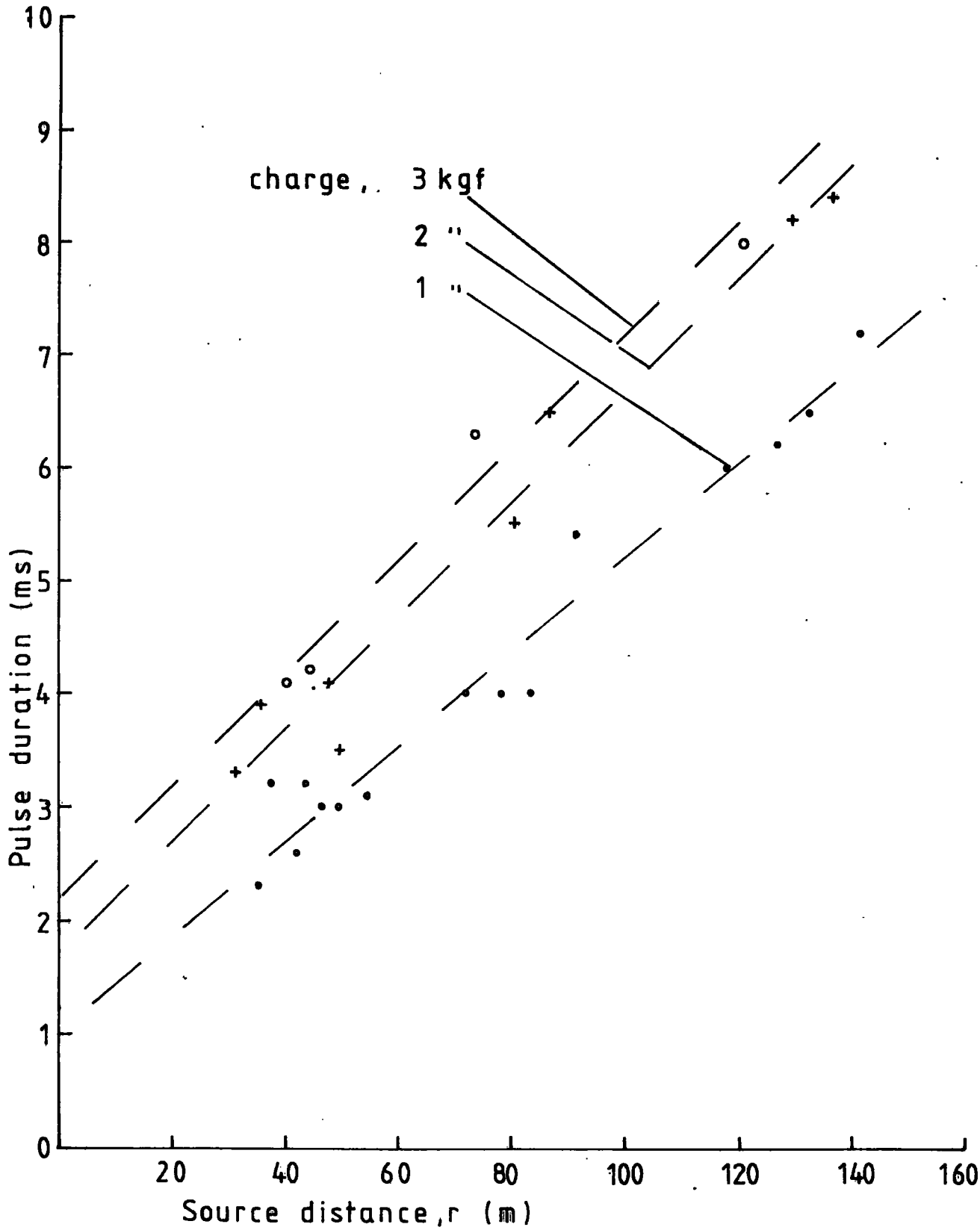

Fig. 6.15 PULSE DURATION v SOURCE DISTANCE

$$PPV = 10{,}000\ M^{0.835}\ r^{-2.093} \quad \text{(from Appendix E)}$$

$$M = \left[\frac{PPV\ r^{2.093}}{10{,}000}\right]^{\frac{1}{0.835}}$$

Substituting PPV = 100 mm/s and r = 30 m

M = 20.3 kgf

It must be remembered that this value for maximum charge weight is based on the regression equation for the best fit straight line through the data. To ensure that the limiting PPV was not exceeded a similar calculation based on the equation an 'upper bound' line as shown in Figure 6.10 (such that all data points were beneath the line) should be carried out.

That is $PPV = 11300\ M^{0.835}\ r^{-2.093}$

$$M = \left[\frac{PPV\ r^{2.093}}{11300}\right]^{\frac{1}{0.835}}$$

M = 17.5 kgf

Proprietary tunnel blasting rounds such as that shown in Figure 3.7 indicate that restricting the contractor to a maximum charge weight per delay of 17.5 kgf would not unreasonably inhibit the construction method.

Having established the maximum charge weight per delay and the maximum PPV it is possible to consider the stresses and strains to be imposed in the adjacent rail tunnel. Close to the blast (say less than 50 m) compressional wave motions dominate all others (*see* Section 6.4)

and calculations should be based on the compressional wave velocity (C_p). Measurements of characteristic rock mass wave velocity are given in Section 6.6 and the average value of C_p is 4672 m/s. The density of the rock was 2.62 Mg/m^3.

From equation 2.12 the maximum compressional strain is given by

$$\varepsilon = V/C_p$$

where V is equivalent to the maximum allowable PPV of 100 mm/s

$$\varepsilon = 0.1/4672$$
$$= 21 \text{ microstrain}$$

The maximum compressional stress is given by substitution in equation 2.13.

That is, $\sigma = VC_p\rho$

$$\sigma = 0.1 \times 4672 \times 2.62$$
$$= 1224 \text{ kN/}_m2$$

These values of strain and stress are more than an order of magnitude lower than those which the intact rock may be expected to sustain. This does not, of course, guarantee that the *in situ* rock will not be subjected to distress and the acceptability or otherwise of these deformations will be based on an overall assessment of the tunnel stability as discussed elsewhere in this thesis.

For partially confined charges, as used for later delays in the tunnel round, greater charge weights per delay will be acceptable and

and similar calculations may be performed using the appropriate site law equation. Deformation calculations for the far field (further than about 50 m) should be based on shear/surface wave velocities because, as described in Section 6.4, at these distances these wave types predominate.

6.6 Rock quality and dynamic properties

6.6.1 Velocity ratio and rock quality designation (RQD)

In order to calculate the velocity ratio and hence RQD (*see* Section 3.5.2) it is necessary to measure the intact P-wave velocity (taken as 5396 m/s, *see* Section 4.3.3) and the *in situ* P-wave velocity. The trial blasts provided numerous measurements from which the *in situ* P-wave velocity was calculated. This was simply accomplished by differencing the distances of two transducers and dividing by the difference in the arrival times of the first wave motion at each array. These velocities are given in Table 6.7. In some circumstances a clear discontinuity of arrival waveform made it possible to determine S-wave velocity as well, although the use of these measurements in the calculation of dynamic moduli is questionable (*see* Section 3.3.3). Note that the velocities apply to rock at distances between transducer arrays as shown in Figure 5.1 and not to rock close to the blasting. Details of the wave velocity in the 'near' blast area could not be calculated from the blast data as the 'instant' the blast was initiated was not recorded. It is assumed that the time taken by the compressional wavefront to travel to the nearest array (position '45') was the same as the time taken to travel a similar distance toward the other transducers at positions 118 and 171. The time differences between arrivals at positions 45 and 78 were not great enough to allow reasonably-accurate velocity calculations

to be made. The wave velocities given in Table 6.7 therefore relate to largely undisturbed rock subjected to substantial overburden stresses.

TABLE 6.7
Trial blast; body wave velocities

Blast/Delay	P-wave velocity m/s			S-wave velocity m/s		
	'Path'			'Path'		
	45/171	45/118	118/171	45/171	45/118	118/171
2/a	4836	4780	4902			
2/b	4850	4733	4990			
2/c	4756	4974	4527	2756		2137
3/a	4897	4987	4545	2793		2136
3/b	4628	4600	4657	2722		
4/a	4675	4726	4629	2577	2814	2260
5/a	4357	4338	4370			
5/b	4455	4556	4372	2414		
Mean	4682	4712	4624	2652	2814	2178
Std D	194	216	226			

Grand mean 4672 (Std D.206) 2512 (Std D. 281)

Based on the grand mean P-wave velocity, the Velocity Ratio (VR) and RQD are calculated below (as described in Section 3.5.2).

VR = P-wave velocity (*in situ*)/P-wave velocity (intact)

= 4672/5396 = 0.866 (Std dev 0.038)

and RQD = $(VR)^2$ = 0.75 (Std dev 0.067)

= 75% (Std dev 6.7%)

This mean value for RQD determined by seismic methods agrees very closely with the mean value obtained by the measurements on rock exposures detailed in Section 4.4.1 (*see* Table 4.3).

Further measurements of P-wave velocity, obtained by the hammer seismic method (Section 5.6), are given in Table 6.8. The initial part of a typical UV record of a hammer impact is shown in Figure 6.16 and the method of processing is indicated. A 1 kHz reference (not shown) was used as the time base and corrections were made where necessary for individual galvanometer offsets. The full details of the amplifier gains, disposition of transducers and other relevant information were recorded on log sheets as for the trial blasting (Figure 6.1).

The results gave a mean value of 4646 m/s which is only 0.6 per cent lower than that given by the blast method above. This indicates that the rock 'at depth' has similar characteristics to those of the near-surface material traversed by the hammer induced vibrations. This confirms other site observations that the surface weathering of the rock is of a superficial nature and that immediately below the surface the joints are generally tight and unaltered.

The extreme values for P-wave velocity measured by both seismic methods were 4314 m/s and 4987 m/s, which corresponds to an RQD range (via Velocity ratio) of 64 per cent to 85 per cent. Thus both the average and extreme values of RQD assessed by the seismic methods agree very well with those obtained by scanline surveys of rock exposures (Table 4.3).

A limited hammer/seismic survey was also carried out along the southern wall of the rail tunnel. These measurements were taken between the western portal and a point some 150 m to the east. Transducer-hammer impact separations varied between 14 m and 27 m and the mean of six P-wave velocity measurements was 4164 m/s. The velocities varied

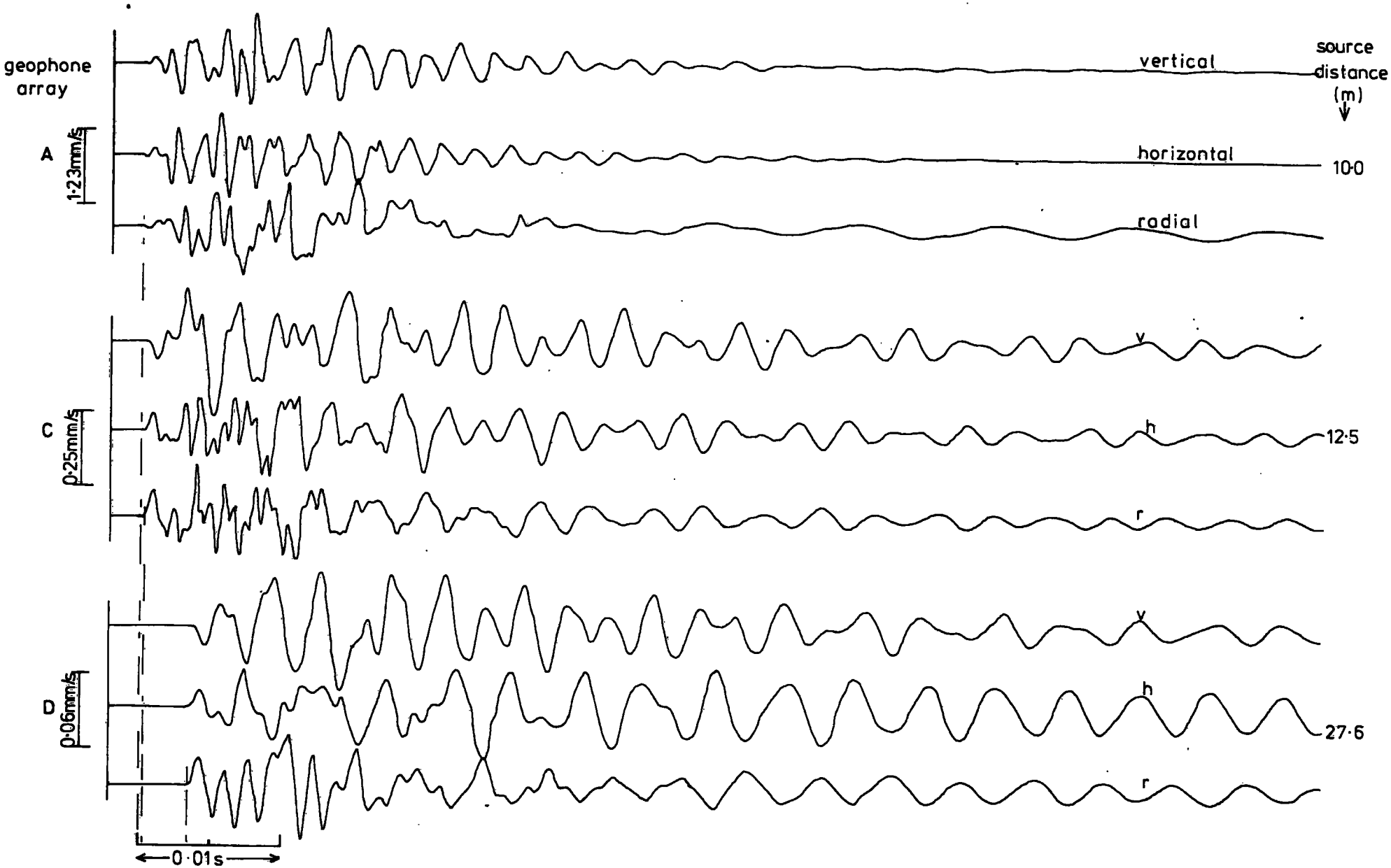

Fig. 6.16 HAMMER GENERATED VIBRATIONS (PPV v time)

TABLE 6.8
Hammer induced vibration velocity and S-wave frequency

UV record ref	Source distance to transducer A	C (m)	D	Path reference	Path difference (m)	Transit times(s)	S-wave frequency at A	C (Hz)	D	P-wave velocity m/s
102	4.5	27.0	42.1	A-C	22.5	.0047	1250	950	600	4787
				A-D	37.6	.0082				4585
				C-P	15.1	.0035				4314
104	"	"	"	A-C	22.5	.0049	1200	850		4592
				A-D	37.6	.0084				4476
				C-D	15.1	.0035				4314
107	"	"	"	A-C	22.5	.0046	1300	940	700	4891
				A-D	37.6	.0078				4820
				C-D	15.1	.0032				4719
108	"	"	"	A-C	22.5	.0048	1400	860	700	4688
				A-D	37.6	.0079				4759
				C-D	15.1	.0031				4871
111	43.3	20.8	5.7	C-A	22.5	.0049				4592
				D-A	37.6	.0083				4530
				D-C	15.1	.0034				4441
114	"	"	"	C-A	22.5			620	1000	
				D-A	37.6					
				D-C	15.1	.0035				4314
123	28.6	6.1	9.0	C-A	22.5	.0049	850	1300	1000	4592
125	"	"	"	"	"	.0052		1250		4327
127	4.5	27.0	42.1	A-C	22.5	.0047				4787
				A-D	37.6	.0079				4759
				C-D	15.1	.0037				4719
128	"	"	"	A-C	22.5	.0047	1500			4787
				A-D	37.6	.0079				4759
				C-D	15.1	.0032				4719
130	10.0	12.5	27.6	A-C	2.5	-	1100	1000		
				A-D	17.6	.0033				4631
				C-D	15.1	.0032				4719
133	"	"	"	A-C	2.5		950	1150	800	
				A-D	17.6	.0036				4889
				C-D	15.1	.0032				4719
								Mean		4646
								Std D		178

from 4575 m/s to a minimum of 3333 m/s in a section of the tunnel supported for some metres by a brick arch. These results suggest that the rock surrounding the tunnel has been noticeably changed by the tunnel construction process (black powder blasting) or other subsequent weathering and stress relief processes. It is of particular interest that the section requiring special support gave by far the lowest seismic velocity readings obtained on the site.

The range of RQD values obtained by the seismic method is similar to that obtained by direct observations and classifies the rock in the range 'fair' to 'good'. (For Deere's classification *see* Section 4.4.2.) The predicted support requirements (*after* Deere, 1968b; Merritt, 1972) would involve random rock bolting in the 'good' areas to pattern bolting at 1 m to 2 m centres in the 'fair' areas. Where locally-disturbed areas are found, such as that 'identified' in the rail tunnel, meshing and shotcrete or lagged steel sets may be required.

6.6.2 Field dynamic moduli

The severe limitations and inaccuracies inherent in the calculation of dynamic moduli from seismic velocity data have been discussed in Section 3.5.3 but these properties are calculated below for completeness (*see* Jaeger and Cook, 1976 for relevant equations).

A value for dynamic shear modulus (G_D) based on apparent S-wave velocity (C_S) may be obtained from the following equation:

$$G_D = \rho C_S^2$$

where ρ is the density of the rock.

$$\therefore \quad G_D = 2.62 \times 10^3 \times 2512^2 = 1.6533 \times 10^{10} \text{ N/m}^2$$

$$= 16533 \text{ MN/}_{\text{m}}{}^2$$

Poisson's ratio (ν_D) is given by

$$\nu_D = \frac{\frac{1}{2}(C_P/C_S)^2 - 1}{(C_P/C_S)^2 - 1}$$

where C_P is P-wave velocity

$$\nu_D = \frac{\frac{1}{2}(4672/2512)^2 - 1}{(4672/25=2)^2 - 1} = 0.297$$

Now the dynamic modulus of elasticity E_D is given by

$$E_D = 2G_D(1 + \nu_D) = 42887 \text{ MN/m}^2$$

The anomalously high value of dynamic Poisson's Ratio is the direct consequence of the low measured value for S-wave velocity resulting from a longer effective pathlength for S-wave motions. It is well-known that at very small strains in jointed rock the dynamic Poisson's ratio is less than the static Poisson's ratio and will often tend to zero (Jaeger and Cook, 1976, Ch 6). That is, small strains are taken up by discontinuity closure and do not induce strains normal to the applied stresses.

Now the dynamic modulus of elasticity may also be found from:

$$C_P = \left[\frac{E_D}{\rho} \frac{(1 - \nu)}{(1 + \nu)(1 - 2\nu)} \right]^{\frac{1}{2}}$$

and as $\nu \to 0$, $C_p \to (E_D/\rho)^{\frac{1}{2}}$

(this simplification implies that $C_p \rightarrow \sqrt{2}\, C_s$)

$$E_D = \rho\, C_p^2$$

$$= 2.62 \times 10^3 \times 4672^2$$

$$= 57{,}188 \text{ MN/m}^2$$

This value is close to that obtained from laboratory static tests described in Section 4.3.2 and indicates that the rock mass has similar dynamic and static elastic properties at small strains. The dynamic modulus is not sensitive to Poisson's ratio when the ratio is small. For instance, an increase from 0 to 0.15 (the static value) only gives an 11 per cent increase in dynamic elastic modulus. It should be noted that dynamic tests carried out at ultrasonic frequencies (Section 4.3.3) on a fresh intact sample resulted in a dynamic modulus of elasticity of 76286 MN/m^2 for C_p = 5396 and ν = 0.

6.6.3 S-wave frequency and Rock Mass Rating (RMR)

Table 6.8 gives the frequency of the S-wave arrivals derived from the UV chart recordings of hammer induced vibrations for various distances. Following the 'petite seismique' technique described in Section 3.5.4 the *in situ* static modulus of deformation may be calculated. More significantly, using equation 3.9, developed in Section 3.5.4, the RMR may be estimated directly from the S-wave frequency.

The mean value of S-wave frequencies measured at ranges between 5 and 30 m from the hammer impact was 975 Hz. Below 5 m the waveform was complex due to the almost simultaneous arrival of both body wave types. Beyond 30 m surface wave motions were apparently well developed and their arrivals made the measurement of S-wave frequencies very diffi-

cult. At ranges between 5 m and 30 m it was usually possible to discriminate between the initial P-wave motions and the larger S-wave vibrations which followed a few milliseconds later.

From equation 3.9

$$\underline{RMR = 0.0307f + 42.7 = 72.6, \text{ for } f = 975 \text{ Hz}}$$

This value classifies the rock as class II 'good rock' and suggests a 'standup time' of several months according to the Geomechanics Classification (RMR). The value is essentially the same as that obtained using 'uncorrected' RMR from field measurements (Table 4.4) but is higher (implying lower support requirement) than the RMR corrected for the worst possible discontinuity orientation (Section 4.4.2).

For class II 'good rock' the Geomechanics Classification (RMR = 72.6) suggests excavation of the full face with 3-5 ft advance and complete support within 60 ft of the face. The support recommended involves roof bolts 10 ft long spaced 8 ft with occasional wire mesh and 2 in of shotcrete in roof as required.

6.6.4 Hammer pulse and wave packet duration

Many of the vibrations induced by hammer impacts gave a clear P-wave pulse at the start of the wave chain (*see* Figure 6.16). The duration of this initial compressional pulse was measured, and, as with the blast data, was observed to increase with increased source/transducer separation. These data have been treated as described in Section 6.4 and a graph plotted showing the characteristic (*see* Figure 6.17). A linear regression analysis of the 36 data points gives:

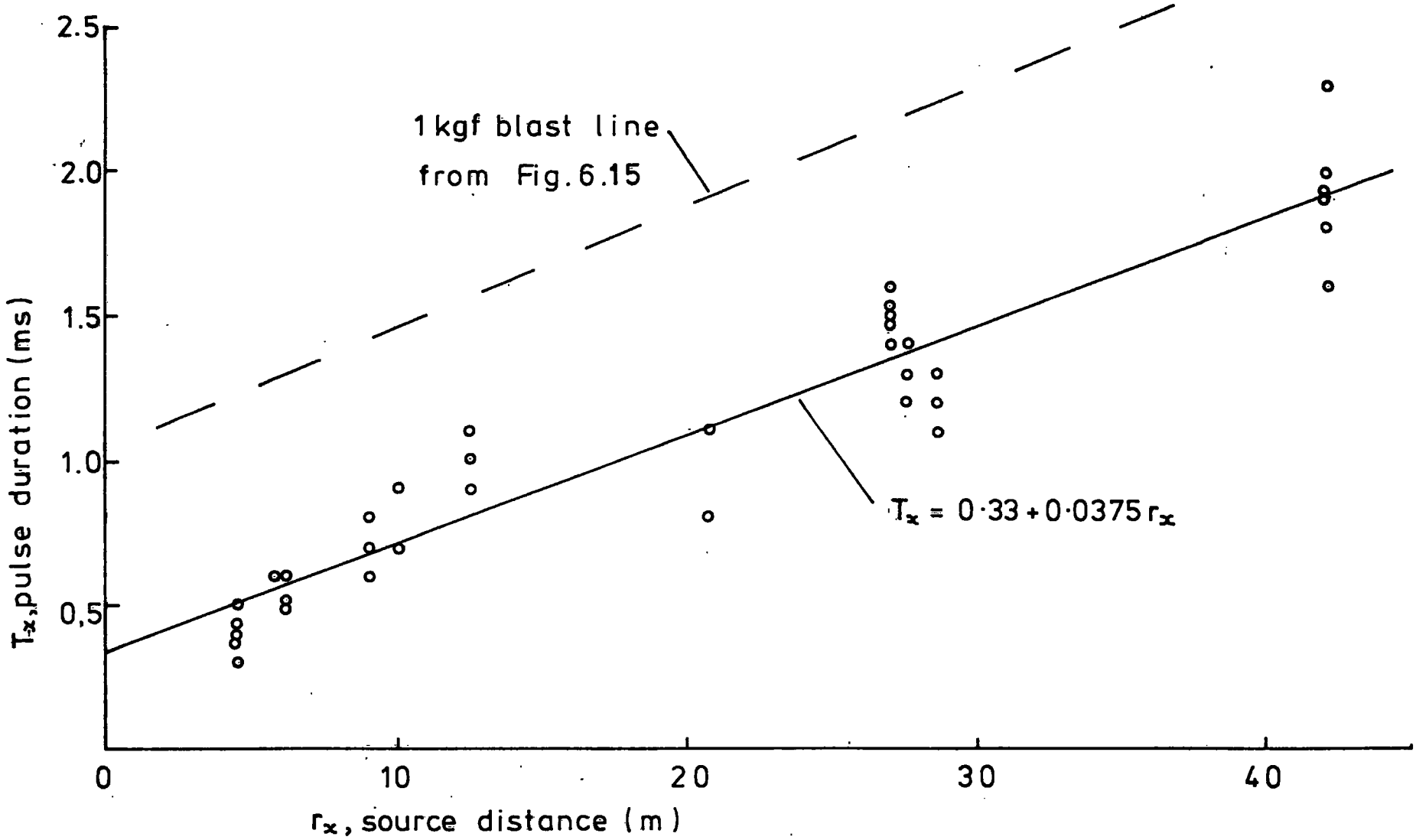

Fig.6.17 PULSE DURATION v HAMMER IMPACT DISTANCE

$$T_x = 0.33 + .0375\ r_x \qquad R^2 = 0.90$$

where T_x is the pulse duration in milliseconds and r_x is the source/transducer separation in metres.

Note that the hammer-induced pulse duration increases with range at a very similar rate to that observed for the blast pulse. That is, the slopes of the regression lines are similar. The offset constant, representing the pulse duration at the source is about one-third of that associated with the 1 kgf blast pulses. This confirms the trend observed from the blasting data. Direct comparison of offset constants due to blasting and hammer impact energies is not appropriate due to the completely different input transfer function of the two energy sources. The former produces heat and considerable mechanical damage whereas the great majority of the hammer impact energy is transmitted into the rock mass as strain waves.

It should be noted that the initial pulse duration will vary with rock type for both hammer and blast-induced vibrations. In general, the weaker and more jointed the rock the longer the initial pulse will be. For instance, reanalysis of the hammer seismic tests carried out in weak Lower Chalk at Chinnor (Hudson *et al.* 1980) shows an initial pulse duration of 3 ms at 10 m source distance. This is almost five times as long as that measured at Penmaenbach.

6.7 Train-induced vibration

The equipment used was the same as that described in Chapter 5. Geophone locations are shown on the site plan (Figure 4.2) and Tables 6.9 and 6.10 give details of transducer orientation and positioning.

Note that train-induced vibrations were monitored at the eastern portal as well as at the western end of the tunnel.

The 'horizontal' geophones were mounted with the axis of sensitivity normal to the tunnel centre line. For the triaxial arrays this implies that the other horizontal geophone in the array is sensitive to vibration parallel to the tunnel centre line.

TABLE 6.9

Geophone locations for train vibration measurement (eastern portal area)

Geophone configuration	Distance from portal (m)	Position in tunnel	Instrumentation channel
Single vert	50.5	1m above cess N wall	2
" "	41.4	" " " S "	3
3D ARRAYS			
Vertical	53.5	" " " " "	4
Normal to tunnel axis			5
Parallel to tunnel axis			6
Vertical	43.4	5m " " " "	7
Parallel to tunnel axis			8
Normal to tunnel axis			9

TABLE 6.10

Geophone locations for train vibration measurement (western portal area)

Geophone configuration	Distance from portal (m)	Position in tunnel	Instrumentation channel
Single horizontal	171	1m above cess.S wall	2
" "	118	" " " " "	3
3D ARRAY	78	" " " " "	4 5 6 7
3D ARRAY	45	" " " " "	8 9

Plate 6.1 shows the eastern portal of the rail tunnel with the train used for the annual inspection and 'drumming and scaling' about to enter.

Vibration records were obtained from a total of 83 trains and a typical data sheet (Figure 6.18) was prepared for each. Figure 6.19 shows a brief extract from the UV chart record obtained during the passing of the train cited on the data sheet, Figure 6.18.

During the week commencing 3 June measurements were taken with the instrumentation cabin located at the eastern portal and the abstracted results are given in Table 6.11. On 10 June, during the second rail possession, the cabin was moved to the western portal and further data gathered during the following week; these results are given in Table 6.12.

PLATE 6.1 EASTERN RAIL TUNNEL PORTAL WITH INSPECTION TRAIN

SEISMIC RECORD SHEET No 15

SITE Penmaenbach rail tunnel (east portal) DATE 6/6/79 TIME 11 48

SOURCE loco 25292 with 11 various freight wagons

Down

U.V. CHANNEL	GEOPHONE /CABLE IDENT.	GEOPHONE LOCATION/ ORIENTATION	AMP GAIN	U.V. mV/cm	SENS. mm/s/cm	TIMING MARK INTERVAL (s)	CASSETTE CODE/ CHANNEL	CASSETTE START/ FINISH	P.P.V mm/s	REMARKS
2	P3/C	N wall / vert	x10 ↓	10 ↓	0·4 ↓	0·1	—	—	0·10	
3	P4/D	S wall / vert						—	0·44	
4	P1/A1	vert					Q/1	110-116 ↓	0·26	
5	S1/A2	30 ⊥					Q/2		0·14	0·36 (resultant)
6	S2/A3	〃					Q/3		0·20	
7	P2/B1	vert					Q/4		0·36	
8	S3/B2	30 ⊥					—		0·30	0·51 (resultant)
9	S4/B3	〃					—		0·20	

Fig.6.18 TYPICAL DATA SHEET

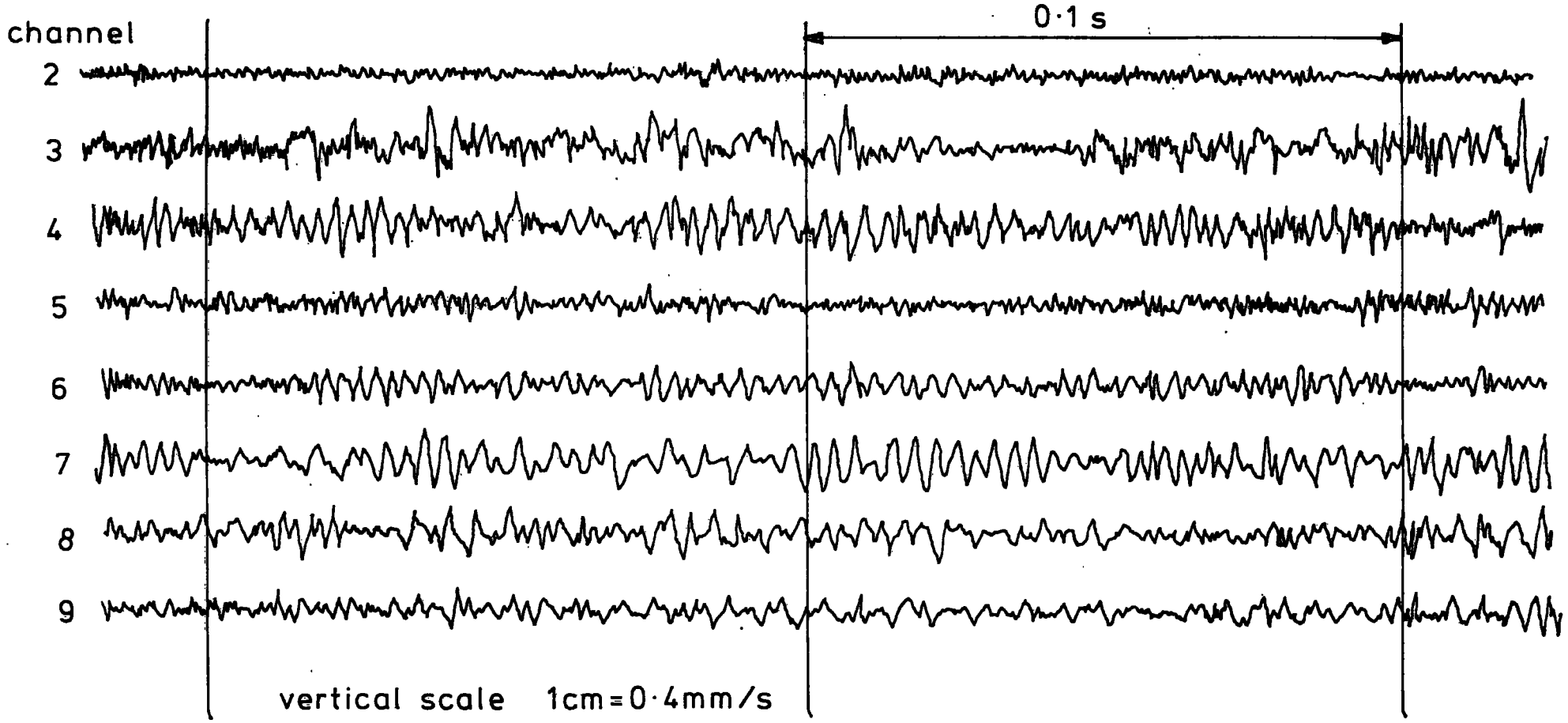

Fig 6.19 EXTRACT FROM U.V. CHART RECORD OF TRAIN INDUCED VIBRATIONS

TABLE 6.11 EAST PORTAL AREA VIBRATION

DIESEL MULTIPLE UNITS

'DOWN' Peak particle velocity (mm/sec)						'UP' Peak particle velocity (mm/sec)					
Record No	Ch.2	Ch.3	RESULTANT Ch.4,5,6	RESULTANT Ch.7,8,9	Description	Record No	Ch.2	Ch.3	RESULTANT Ch.4,5,6	RESULTANT Ch.7,8,9	Description
3	0.10	0.34	0.37	0.49	2 CARS						
7	0.10	0.30	0.36	0.33	?	32	0.14	0.12	0.21	0.27	4 CARS
8	0.10	0.64	0.46	0.45	2 CARS						
13	0.32	0.36	0.35	0.53	4 CARS						
18	0.10	0.34	0.34	0.35	2 CARS						
26	0.10	0.32	0.44	0.43	4 CARS						
30	0.12	0.38	0.33	0.45	?						
38	0.06	0.16	0.24	0.31	4 CARS						
MAX	0.32	0.64	0.46	0.53							
MIN	0.06	0.16	0.24	0.31							
MEAN	0.13	0.36	0.36	0.42							
PASSENGER (INTER-CITY)											
2	0.08	0.34	0.41	0.46	7 CARS	11	0.18	0.18	0.28	0.30	10 CARS
4	0.10	0.42	0.37	0.44	7 CARS	17	0.16	0.14	0.30	0.33	7 CARS
5	0.16	0.40	0.43	0.49	11 CARS	24	0.20	0.18	0.31	0.36	10 CARS
9	0.12	0.32	0.40	0.50	11 CARS	28	0.18	0.16	0.32	0.44	6 CARS
12	0.12	0.36	0.39	0.42	7 CARS	36	0.22	0.20	0.30	0.36	11 CARS
20	0.12	0.42	0.40	0.53	10 CARS	40	0.16	0.16	0.27	0.31	8 CARS
22	0.08	0.40	0.55	0.53	6 CARS						
25	0.10	0.42	0.38	0.47	8 CARS						
34	0.08	0.26	0.16	0.36	7 CARS						
37	0.04	0.08	0.15	0.20	8 CARS						
MAX	0.16	0.42	0.55	0.53		MAX	0.22	0.20	0.32	0.44	
MIN	0.04	0.08	0.15	0.20		MIN	0.16	0.14	0.27	0.30	
MEAN	0.10	0.34	0.36	0.44		MEAN	0.18	0.17	0.30	0.35	
FREIGHT + MISC											
1	0.08	0.24	0.32	0.35	6 BULK + GUARDS VAN	6	0.14	0.12	0.24	0.31	4 FLAT WAGONS
10	0.10	0.40	0.44	0.50	16 BULK	21	0.16	0.20	0.34	0.47	7 FULL BALLAST WAGONS
14	0.10	0.40	0.35	0.44	10 FLATS (FORD) + 4 EMPTY	33	0.20	0.16	0.34	0.46	3 WAGONS + GUARDS VAN
15	0.10	0.44	0.36	0.51	11 MIXED	39	0.12	0.12	0.22	0.33	FREIGHT LINER
23	0.08	0.36	0.29	0.34	TRACK INSPECTION						
27	0.08	0.34	0.37	0.43	4 BOGIES + GUARD						
29	-	0.16	0.17	0.15	TRACK RECORDING UNIT						
31	0.16	0.32	0.49	0.63	APPROX 30 EMPTY COAL WAGONS						
35	0.04	0.20	0.22	0.34	21 MIXED + GUARD						
MAX	0.16	0.44	0.49	0.63		MAX	0.20	0.20	0.34	0.47	
MIN	0.04	0.16	0.17	0.15		MIN	0.12	0.12	0.22	0.31	
MEAN	0.09	0.32	0.33	0.41		MEAN	0.16	0.15	0.29	0.39	

TABLE 6.12 WEST PORTAL AREA VIBRATION

DIESEL MULTIPLE UNITS

'DOWN' Peak particle velocity (mm/sec)						'UP' Peak particle velocity (mm/sec)					
Record No	Ch.2	Ch.3	RESULTANT Ch.4,5,6	RESULTANT Ch.7,8,9	Description	Record No	Ch.2	Ch.3	RESULTANT Ch.4,5,6	RESULTANT Ch.7,8,9	Description
50	0.16	0.16	0.81	0.38	?	56	-	0.08	0.38	0.88	4 CARS
54	-	0.32	0.81	0.31	2 CARS	57	-	0.08	0.27	1.19	2 CARS
61	-	0.08	0.85	0.44	2 CARS	62	-	-	0.39	0.50	2 CARS
70	0.20	0.40	0.95	0.44	4 CARS	80	-	-	0.31	0.38	4 CARS
79	-	-	0.95	0.39	2 CARS	81	-	-	0.28	0.33	2 CARS
82	-	0.20	1.00	0.38	?						
MAX	0.20	0.40	1.00	0.44		MAX	-		0.39	1.19	
MIN	0.16	0.08	0.81	0.31		MIN	-		0.27	0.33	
MEAN	0.18	0.23	0.90	0.39		MEAN	-		0.33	0.66	
PASSENGER (INTER-CITY)											
44	0.18	0.24	0.95	0.53	7 CARS	41	0.08	0.08	0.27	0.27	8 CARS
49	0.48	0.20	1.05	0.43	7 CARS	47	0.10	0.12	0.36	0.27	11 CARS
59	0.44	0.24	1.07	0.43	11 CARS	52	0.06	0.10	0.48	0.43	7 CARS
63	0.28	0.24	0.98	0.46	11 CARS	60	-	0.08	0.48	0.26	7 CARS
66	0.24	0.24	1.00	0.55	7 CARS	67	0.12	0.12	0.45	0.39	10 CARS
68	0.44	0.28	1.07	0.46	7 CARS	73	-	-	0.45	0.31	10 CARS
72	0.36	0.16	0.99	0.34	7 CARS	76	0.08	0.08	0.30	0.29	7 CARS
74	0.32	0.32	0.95	0.53	7 CARS						
83	0.40	0.20	1.16	0.47	10 CARS						
MAX	0.48	0.32	1.16	0.55		MAX	0.12	0.12	0.48	0.43	
MIN	0.18	0.16	0.95	0.34		MIN	0.06	0.08	0.27	0.26	
MEAN	0.35	0.24	1.02	0.47		MEAN	0.09	0.10	0.40	0.32	
FREIGHT + MISC											
46	-	0.08	0.99	0.43	5 BULK LIQUID + GUARD	42	-	-	0.19	0.17	1 FLAT + 1 GUARD
65	-	0.22	0.87	0.50	2 CARS + OBSERVATION CAR	43	-	-	0.31	0.23	6 BULK LIQUID + GUARD
71	0.16	0.12	0.91	0.43	15 LIQUID + GUARD	45	-	-	0.21	0.13	BALLAST PLACER
75	0.16	0.16	1.06	0.66	11 BALLAST WAGONS	48	0.10	0.08	0.38	0.36	23 FLATS + GUARD
77	0.12	0.12	0.42	0.73	8 BALLAST WAGONS	51	0.12	0.10	0.44	0.24	14 BALLAST WAGONS
						53	0.24	0.12	0.75	0.56	21 FREIGHT LINERS
						55	0.08	0.08	0.33	0.21	10 BALLAST WAGONS
						58	-	0.08	0.38	0.82	LIQUID CARRIERS
						64	0.08	0.10	0.45	0.36	8 LIQUID, 2 COAL + GUARD
						69	0.16	0.08	0.68	1.17	14 WAGONS
						78	-	-	0.23	0.27	LOCOMOTIVE ONLY
MAX	0.16	0.22	1.06	0.73		MAX	0.24	0.12	0.75	1.17	
MIN	0.12	0.08	0.42	0.43		MIN	0.08	0.08	0.19	0.13	
MEAN	0.15	0.14	0.85	0.55		MEAN	0.13	0.09	0.40	0.41	

At the eastern portal a maximum resultant peak particle velocity of 0.64 mm/s was recorded. Although there was considerable variation within each group of trains, due mainly to speed variation, the mean value of peak particle velocity for multiple units, diesel hauled passenger and freight trains was about the same.

A similar pattern was found at the western portal but the vibration levels were higher with a maximum resultant peak particle velocity of 1.17 mm/s.

The resultant peak particle velocities were calculated as described in Section 6.1(a) which as previously stated, provides an inherent safety factor since it is unlikely that the maximum velocities recorded individually from the three dimensional transducer arrays will occur simultaneously. Analysis of all the records showed that the frequency of the vibrations, in the rock of the tunnel wall, was principally in the bandwidth 200-800 Hz. These unexpectedly high frequencies may result from the complexity and close proximity of the source and the very high stiffness of the propagating medium (rhyolite).

There were indications that the tunnel vibrations were excited not only through the wheel/track interface, but were also transmitted by sound. There was a high level of noise in the closed environment of the tunnel and vibrations at 900 Hz were clearly attributable to the locomotive horn that was often sounded as the train entered the tunnel. The high frequencies measured are consistent with the sound produced by the trains. It was later confirmed, by measurements of train vibrations taken in the area of the trial shot holes, that these high frequencies were induced in the rock (not just in the transducers). High frequencies were again recorded although the sound level, at the

transducers, from the train was negligible.

It is concluded that, under present circumstances, if two trains passed in the tunnel their cumulative effect may result in a peak particle velocity of about 2 mm/s in the rock. It should be noted that in the past considerably higher levels of vibration might have occurred when poorly-sprung steam locomotives crossed rail joints (the present track is long-welded).

These results indicate that vibrations from the drill and blast construction of the adjacent road tunnels were likely to be many times higher than the ambient level due to the passage of trains.

CHAPTER 7

BLASTING TRIALS AT THE PASS OF KILLIECRANKIE

7.1 Introduction

Subsequent to the trials at Penmaenbach the opportunity arose to carry out an extensive trial blasting programme at the Pass of Killiecrankie in the Tayside Region of Scotland. This allowed the trial blasting techniques developed for, and at, Penmaenbach to be further refined and extended.

As at Penmaenbach, the research was carried out in parallel with the attainment of specific objectives concerned with the development of the British trunk road network. In response to a request from the Scottish Development Department the author carried out a series of vibration measurements to assist with the design specification for the A9 improvement works.

These measurements comprised the determination of vibration levels produced by a series of trial blasts and by road and rail traffic.

The objectives of the measurements were:-

(a) To determine the seismic wave propagation characteristics of the rock (parallel and normal to schistosity); in particular the attenuation of peak particle velocity (PPV) with distance.

(b) To determine the effect of various charge weights.

(c) To determine the effect of charge confinement by the rock.

(d) To determine the effect of decoupling the charge as inherent in the proposed presplit technique.

(e) To measure the induced PPV at selected points on local structures.

(f) To determine ambient vibration levels from trains and road traffic.

The objectives listed above were critical to the viability of construction methods for the major rock cuttings which were required for the new A9 which is to be cut along the steeply-sided Pass. The trials also provided the opportunity for testing and refining blasting techniques, and in particular providing new information on vibration induced by recently-developed presplitting methods.

A major consideration in the design of rock cuts for roads (and rock caverns) is the projected cost of maintenance of the excavated faces. In the past careless use of bulk blasting techniques has sometimes resulted in highly unstable rock faces which either collapse or require expensive scaling and support works. The use of presplitting or smooth blasting techniques (Langefors and Kihlström, 1978) greatly reduces the blast damage to the final rock exposures. In Scotland, where extensive rock cuttings are required, a particularly successful technique of presplitting using decoupled charges has been developed (*see* Figure 7.1). Plate 7.1 shows a successfully presplit rock face on the A9 at Aviemore, some 50 kilometres to the north of the

PLATE 7.1 PRESPLIT ROCK FACE AT AVIEMORE

Killiecrankie site. The objective of presplitting is to create a major discontinuity in the plane of the final rock exposure prior to the removal of the bulk of the rock. The presence of this discontinuity plane and the careful design of the following bulk blast, protects the remaining rock from blast damage, thus reducing maintenance costs.

The use of presplitting may also allow for more steeply-sided rock slopes to form part of a road design. This may significantly reduce the volume of rock to be excavated and therefore lessen the cost of the scheme.

For caverns in rock an undamaged final rock profile will considerably enhance the short and long term stability of the opening. Where the cavern is to be used for the storage of liquids an undamaged surface is also clearly an advantage.

A feature of the presplit method currently under development is that it typically requires a number of parallel blast holes (100 mm diameter) to be charged with 25 mm diameter explosives and fired simultaneously (*see* Figure 7.1). Experience has shown that a minimum presplit panel size must be created by simultaneous explosions and therefore the quantity of explosive cannot be reduced below certain limits prescribed by the method. Where blast-induced vibration is a problem this presplit technique may not be viable as levels cannot be reduced by increasing the number of delays in the round (thereby reducing individual charge weights).

The use of presplitting at the Pass of Killiecrankie was considered potentially hazardous as several valuable existing structures and certain

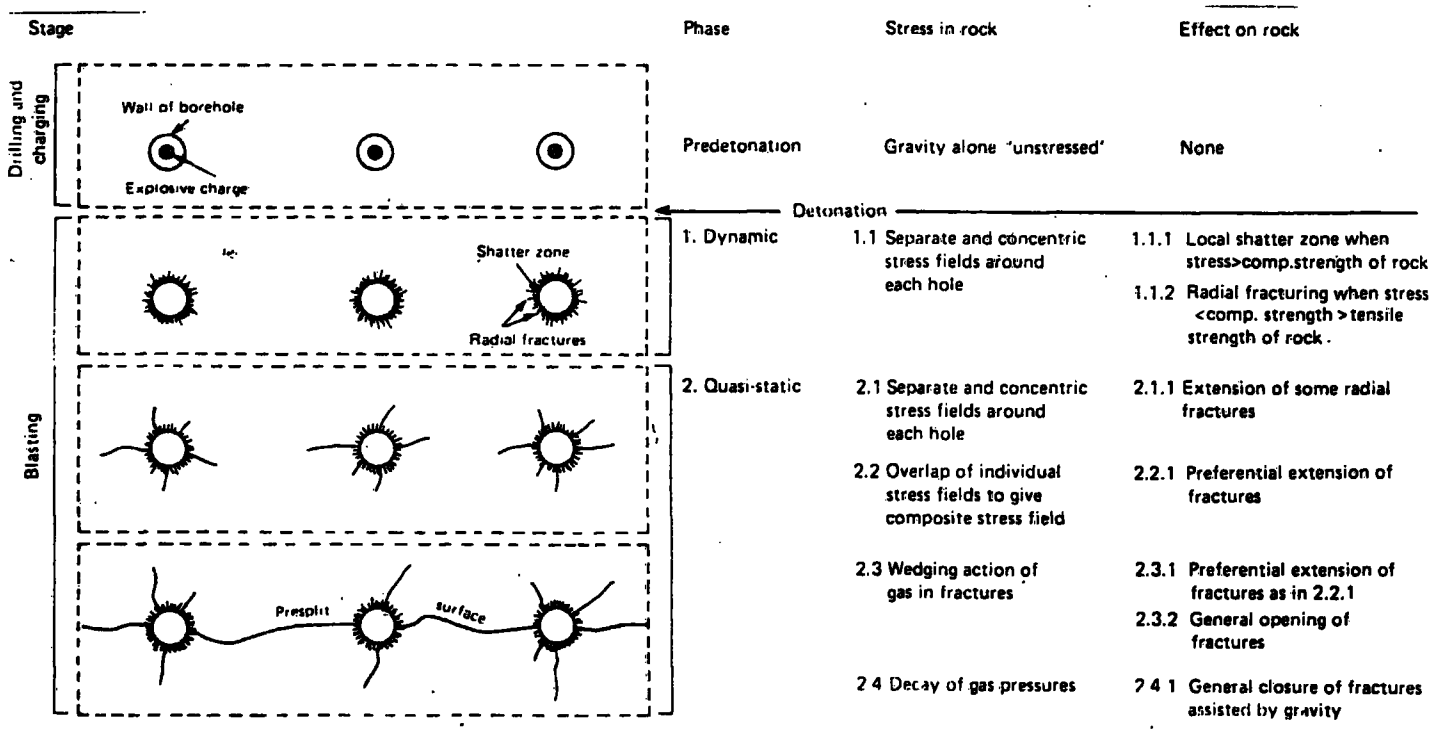

Fig. 7.1 BASIC MECHANISM OF PRESPLIT BLASTING (from TRRL LF 854)

elements of the new road construction were thought to be at severe risk. This conclusion had been based largely on the fact that previous measurements of vibration from presplit blasting had shown very high vibration levels. This is shown clearly in Figure 3.2 (*after* Oriard). These results, however, had been obtained from well coupled charges (explosive tight in drill-hole and well stemmed), and it was thought that the proposed method, using heavily-decoupled charges, would produce considerably less vibration. No vibration measurements from this type of explosion were available and it was therefore decided to conduct an examination of the effects of decoupling during a programme of trial blasting at the site.

The discussion given in Chapter 3 of this thesis clearly indicates that leaving an annular gap around the explosive would substantially reduce the initial blast pressure and create a significant mismatch in the effective rock/explosive impedences. Both these factors were known to reduce the vibrations transmitted to the rock mass, and experimental evidence was required to determine the scale of the effect.

Although subsurface construction was not required at Killiecrankie, the trial blasting objectives with regard to the establishment of site laws and considerations of vibration effects on local structures is common to all such construction sites. The use of the blasts as seismic sources in order to determine subsurface rock quality was not required. Also the highly variable nature of the rock (*see* below) makes application of the techniques used at Penmaenbach largely impracticable for the verification of an experimental method.

Local rock exposures and borehole and trial pit excavations have

provided adequate knowledge of the rock and drift deposits to be removed. There was little information of rock quality at depth and therefore no basis of comparison with geophysical predictions such as those described in Chapter 3 and carried out at Penmaenbach.

7.2 The Killiecrankie Site

7.2.1 The Pass of Killiecrankie and the A9 improvement

The Pass of Killiecrankie forms a natural route for communication between Pitlochry and Blair Atholl. As such it carries the major road (A9) between the Scottish lowland region and the north of Scotland via Inverness (*see* Figures 7.2 and 7.3). The river Garry flows through the Pass with the road and the main Perth-Inverness railway line on the slopes above its eastern bank.

In recent years the A9 has increased in importance as a result of the opening up of the North Sea oilfields and consequently it carries a considerable volume of commercial traffic. The development of Aviemore as a tourist centre and major skiing area has also given rise to considerably increased road traffic. Owing to the mountainous nature of the route the old A9 was often narrow and tortuous, and the journey from Perth to Inverness was rather slow and unsuitable for heavy commercial traffic. The Scottish Development Department has therefore placed considerable emphasis on improving the road, and many major schemes along the route have been completed.

At present the A9 through the Pass of Killiecrankie is a narrow, often bendy, single carriageway and this is to be replaced by a twin-

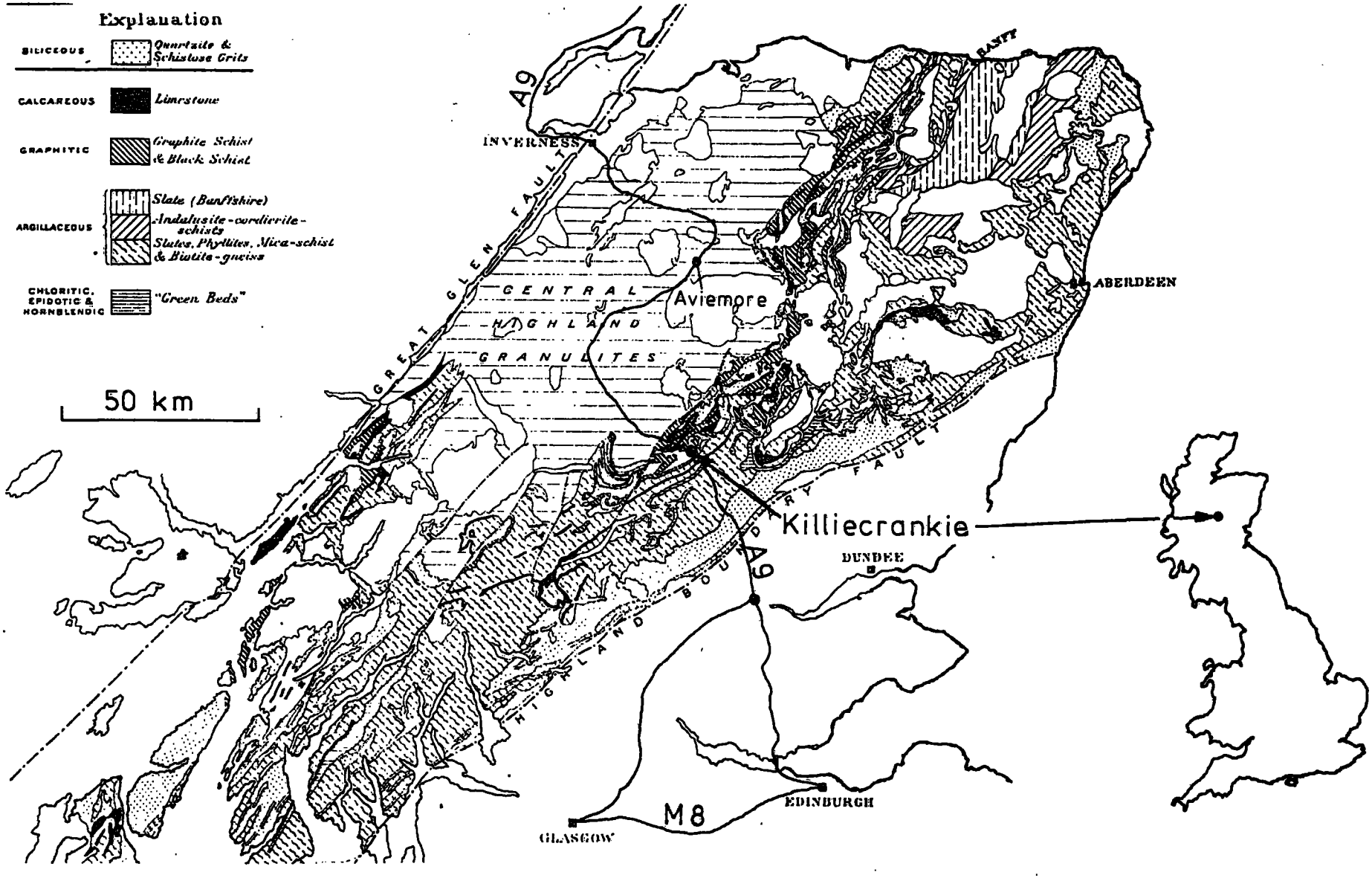

Fig. 7.2 SITE LOCATION AND AREA GEOLOGY

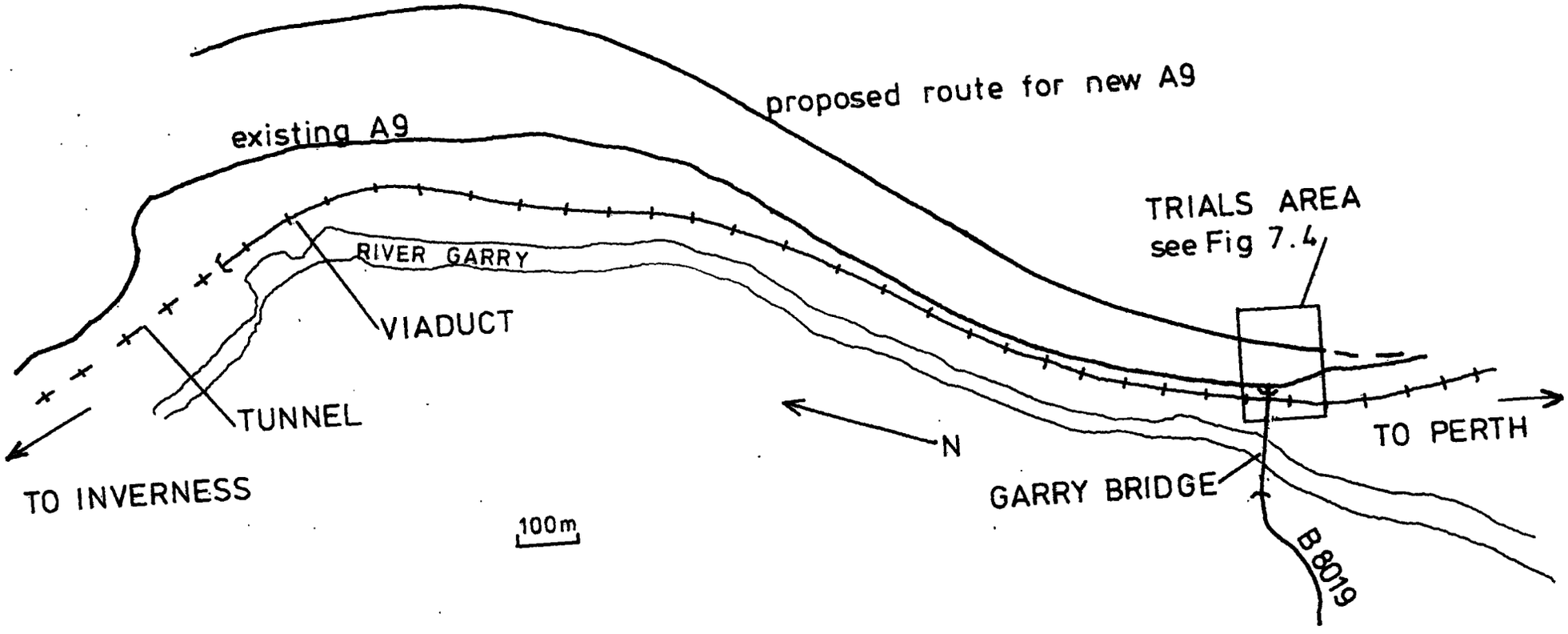

Fig.7.3 THE PASS OF KILLIECRANKIE

lane dual carriageway situated on a shelf excavated higher up the steeply sided slope to the east. The site investigations for the works are now complete and the design is currently being finalised. It is hoped that work will commence in 1983.

The Pass runs in a North-South direction and its sides are of a very steep wooded nature. Much of the Pass is owned by the National Trust and is designated as being of great landscape value.

7.2.2 The geology of the site

The Pass of Killiecrankie lies within a mountainous area known generally as the Grampian Highlands. The Highlands are bounded by the Great Glen Fault to the north, and the Highland Boundary fault to the south. These faults cut across country in a south-west to north-east direction and contribute greatly to the variety in the geology of Scotland. The majority of the rocks are in excess of 500M years old and are distributed in two assemblages, named 'Moinian' and 'Dalradian', which are approximately arranged towards the Great Glen and the Highland Boundary, respectively.

A full description of the geology of the Highland Schists may be found in the British Regional Geology of the Grampian Highlands (Read, 1948). Figure 7.2 shows the lithological divisions of the Dalradian and (with some additions) is taken from the Regional Geology.

The rocks of the Pass comprise the 'Killiecrankie Schists' which are a massive, competent quartzitic sub-group of the Dalradian. These rocks represent former sandstones and mudstones of sedimentary origin

which have been penetrated by intrusion of basic igneous rocks and metamorphosed to quartzite and quartz-schist (from sandstone), mica schist (from mudstone) and hornblende-schist (from igneous). In the fresh state they are generally strong, reasonably hard and impervious. The original sedimentary rocks were probably laid down as continental shelf deposits which, after consolidation were intruded by basic sills. The metamorphosis took place during the Caledonian Orogeny and the rock structure is extremely complex as there have been three major folding episodes during the Caledonian earth movements. In addition to this folding the rocks were later subjected to wrench faulting associated with the Loch Tay Fault system.

The topography of the Pass is dominated by the down-cutting action of the river Garry, and the general condition of the bedrock suggests that much of the broken and weathered rock has been stripped off by glacial action. Subsequently, superficial glacial deposits have covered much of the Pass although in the area of the blasting trials the rock outcropped freely with little covering.

Examples of most of the Killiecrankie Schists could be found in the vicinity of the trial blasting area although the rock outcrop comprised mainly a medium-grained, strong quartzite and closely-foliated quartz and mica schists.

The differences in these metamorphic rock types can be slight, with no transition zone from one to the other. Where the original material was 'pure' sandstone the metamorphosis has resulted in quartzite as mica was not present in sufficient amounts for schistosity to develop.

The rock colour ranges from almost white to dark grey sometimes with brownish shades. The 'whiteness' of the rock is mainly dependent on the percentage of quartz present and sometimes the quartzites have a pinkish hue. Occasionally outcrops of a very dark grey-green hornblende schist were observed. Weathering was generally slight although a few narrow bands of very micaceous material could be readily broken down with a hammer. These bands were identified by heavy, often coloured, staining of the mica crystals which are particularly lacking in strength. The schistosity, which runs in an east-west direction, also tends to permit water penetration into the rock which accelerates the weathering process.

7.2.3 Rock properties

As discussed above the rock structure of the Pass is complex with frequent changes of rock type over distances of just a few metres. However, the great majority of the rocks present lay in the range moderately strong to very strong (12.5 - 200 MN/m^2) and the description 'strong' (50 - 100 MN/m^2) covers the bulk of the rock in the trial blasting area.

Laboratory tests on six different samples gave saturated bulk densities from 2.69 to 2.79 Mg/m^3 with moisture contents varying between 0.15% and 0.84%. Unconfined compressive strength varied between 49.1 MN/m^2 and 114 MN/m^2 and elastic moduli between 32000 MN/m^2 and 76500 MN/m^2 when stressed up to 1 MN/m^2. A test to 3 MN/m^2 resulted in a modulus of 100000 MN/m^2.

The frequency of the jointing is conveniently described in terms of RQD which was almost always better than 60% and usually in the range

70% - 90%. The joints recorded on borehole logs were mainly associated with foliation and were often smooth and brown stained. Other rather poorly-defined joint sets and random jointing, not associated with foliation, were apparent at rock outcrops throughout the site. A sample of rock considered typical of that in the blasting area was sawn into an approximately cubic shape and its characteristic seismic velocity measured as described in Section 4.3.3. The sample was mainly quartzite with some thin foliated inclusions. The compressional wave velocity was 4900 m/s, 4750 M/s and 4700 m/s in three mutually perpendicular directions. The slight difference (3%) in velocity between parallel and normal to the foliation is not significant. Two other samples from elsewhere in the Pass had average (of similar triaxial measurements) compressional velocities of 4040 m/s and 4510 m/s. *In situ* seismic velocities based on results obtained during the trial blasting indicated velocities between 3800 m/s and 5500 m/s.

A full site investigation report in two volumes (fieldwork and laboratory tests) has been prepared (Soil Mechanics Ltd, 1973) and an interpretive geotechnical report considers the effect of the geology on the design of the new road (Sir Alexander Gibb and Partners, 1981).

The information on the local geology given above provides background information which was of assistance in designing the the trial blast programme and interpreting the results. In particular, significant variations in rock structure and properties which may affect wave propagation characteristics, must be known at the time the trial blasts are planned. For instance, at the Pass of Killiecrankie the presence of the schistosity in a well-defined direction suggested that the vibration propagation characteristics of the rock mass may vary with the direction

of propagation relative to the direction of the schistosity. It was therefore decided to take measurements of vibrations from the blasts in two directions; one parallel to and the other normal to the direction of the schistosity. If significant variations were found it would then be possible to give 'site laws' appropriate to the particular direction of the travelling waves.

7.3 The trial blasting

7.3.1 Organisation

The Killiecrankie to North of Calvine section of the A9 Perth - Inverness trunk road improvement scheme comprises two stages. The first runs from the northern end of the Pass of Killiecrankie and extends to by-pass Calvine some 12 km to the west. This stage was under construction in 1982. The second stage, at present still under design (early 1982), requires the construction of about 2½ km of dual carriageway and runs at high level on the eastern side of the Pass of Killiecrankie between the Garry bridge and Killiecrankie village. The schemes are promoted by the Scottish Development Department and Sir Alexander Gibb and Partners are retained as Engineers. The author was asked to prepare a specification for a series of trial blasts to resolve difficulties discussed in Section 7.1. A trial blast programme was drawn up in collaboration with Dr G Matheson of TRRL Scottish Branch, who supplied details of the proposed presplit blasting techniques. TRRL was responsible for the supervision of all aspects of the blasting and vibration measurement and analysis.

Tarmac Construction, who were already on site nearby working on Stage 1, were contracted to carry out various site works including:

(i) the construction of an access roadway to the trial blast area,

(ii) the installation of a pipe beneath the A9 to carry cables,

(iii) site clearance and the removal of topsoil,

(iv) the drilling and charging of the shot holes to the author's instructions (this work was sub-contracted to Richies Equipment Ltd).

(v) provision of personnel to arrange and supervise the necessary road and rail closures.

The trials were carried out after discussions with the Authorities responsible for the various structures in the vicinity, that is, Tayside Regional Council (the Garry Bridge) and British Rail (culverts and retaining walls), together with their consultants, James Williamson and Partners. Rail possessions and road closures were arranged for two successive Sundays, and similar control and safety precautions were made to those used at Penmaenbach (*see* Section 5.1).

Measurements of ambient vibration levels from road and rail traffic were made at the blasting site and, in response to a request from British Rail, further measurements of train-induced vibration were made on the railway (in a tunnel and on a viaduct) at the northern end of the Pass.

7.3.2 The trial blast area

A site plan of the blast area and surroundings is given in Figure 7.4. The trials were located at this part of the site for the following reasons:

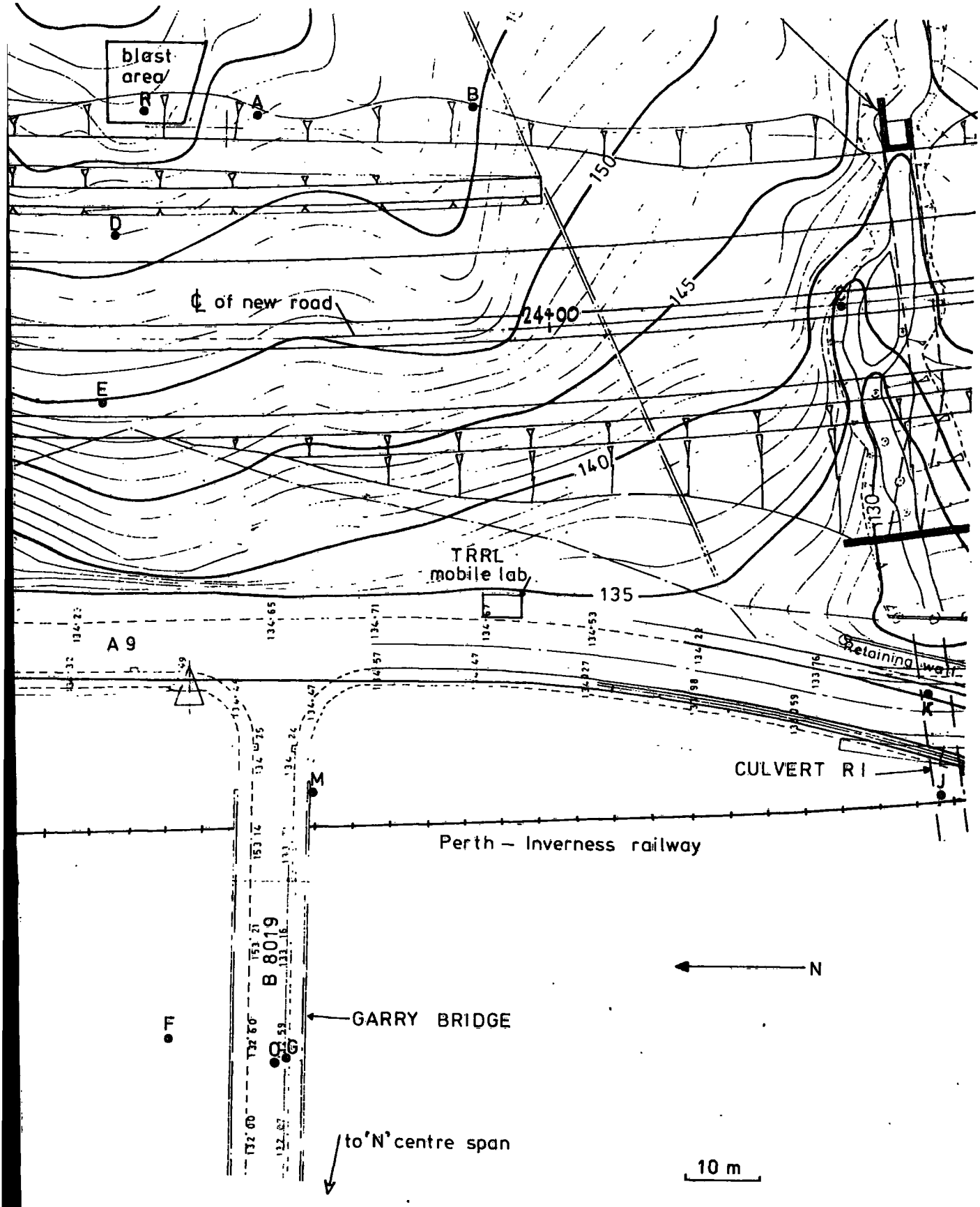

●—transducer array location

Fig.74 KILLIECRANKIE BLAST AREA SITE PLAN

(a) the majority of the blasting for this section of the new road was to take place at this end of the site,

(b) the major structures at risk and closest to the proposed blasting (the Garry Bridge, culvert R1, the railway and the existing A9) were in this area,

(c) the rock was easily accessible, and after removal of top-soil, the fixing of the vibration transducers and drilling and firing the trial charges was fairly straightforward,

(d) a convenient parking area for the mobile laboratory and a mains power supply were made available,

(e) the rock was thought to be typical of that which was to be excavated throughout the Pass,

(f) adequate sight lines were available for communications during road closures.

Plate 7.2 is taken from the western abutment area of the Garry road bridge. The steel box girder spans are supported on two concrete piers and carry the B8019 over the river at high level. The railway also passes beneath the far span adjacent to the abutment. The blasting took place on the slopes shown toward the skyline in the photograph. Plate 7.3 shows the site looking back down the hillside and shows the bridge deck centre left. This Plate also shows the cleared blasting area with the drifter rig in action.

PLATE 7.2 THE GARRY ROAD BRIDGE

PLATE 7.3 THE BLASTING AREA

7.3.3 The trial blasting sequence

The trial blasts were carried out in two series. Blasts designated 301 to 307 (Table 7.1) were carried out during the first Sunday rail possession and were pertinent to objectives a, b, c and d (*see* Section 7.1). Blasts 311 to 316 (Table 7.2) were carried out on the following Sunday and were pertinent to objectives e and f.

TABLE 7.1
First blasting sequence

Blast Ref.	Explosive type	Charge weight (kgf)	Hole size (mm)	Imposed condition
301/0	SG80	½	64	C
302/0	Trimobel	1	64	C
302/2	SG80	1	64	C
303/0	SG80	½	64	PC
303/2	Trimobel	½	75	D
304/0	SG80	1	64	PC
304/2	Trimobel	1	75	D
305/0	SG80	1.5	64	C
305/2	Trimobel	1.5	64	C
306/0	DC1	½	75	D
306/2	Trimobel	½	100	D
307/0	Trimobel	½	64	C
307/2	Trimobel	¾	100	D

TABLE 7.2

Second blasting sequence

Blast Ref.	Explosive type	Charge weight (kgf)	Hole size (mm)	Imposed condition
311/0	SG80	1	64	C
312/0	SG80	½	64	C
312/2	Trimobel	1	100	D
313/0	Trimobel	½	75	Water in hole
313/2	DC2	1	75	D
314/2	DC2	1	100	D
314/4	DC2	½	64	C
315/2	DC2	½	75	D
315/4	Cordtex	13 metres	64	D
315/6	Trimobel	½	100	D
316/4	SG80	2	75	C

The 'imposed condition' designations given in Tables 7.1 and 7.2 relate to the degree of confinement as discussed in Section 3.3 and are as follows:

C - confined by the rock with full stemming, well tamped no surface rock breakage.

PC - partially confined, well stemmed but some surface rock swelling.

D - decoupled. Small diameter explosive in larger diameter hole without stemming (after blast 306 these holes were stemmed in the top 1 m).

The first part of the blast reference number defines the particular trial blast round and the second part indicates the number of the ½ second delay detonator used for an individual charge. The zero delay gives instantaneous detonation, the number 2 gives 1 second delay, the number 4 gives 2 seconds, and so on. Thus each trial round comprised one, two or three charges fired at intervals of one second. This inter-

val was sufficient to prevent superposition of vibrations from successive delays.

The principal characteristics of the explosives used are given in Table 7.3. Special Gelatine 80 is a general purpose explosive used widely in rock excavation work. Trimobel and DC1 and 2 are trimming explosives commonly used for removing small volumes of excess rock on a face back to the design profile. These trimming explosives are ideal for the presplitting techniques which have been discussed earlier in this Chapter. Special Gelatine 80 and Trimobel are manufactured by ICI and DC1 and 2 by Explosive and Chemical Products Ltd.

TABLE 7.3
The Explosives

Explosive type	Weight strength (% BG)	Bulk strength (% BG)	Density (g/ml)
Special Gelatine 80	85	79	1.4
Trimobel	87	65	1.25
DC 1) DC 2)	88	85	1.45

The explosives were detonated by blasting cord initiated at the top of the drill hole by a standard No. 6 detonator. The strengths given for DC1 and DC2 relate to the basic Gelimex constituent explosive which is packaged in separate slugs within a plastic tube. DC1 tubes contain about 270 gms/m and DC2 about 540 gms/m. DC2 is similar in strength (per unit cartridge length) to Trimobel and DC1 is about half as strong.

Figure 7.5 shows the distribution of the drill-holes in the blast area shown in Figure 7.4. The diameter of the holes are shown and their

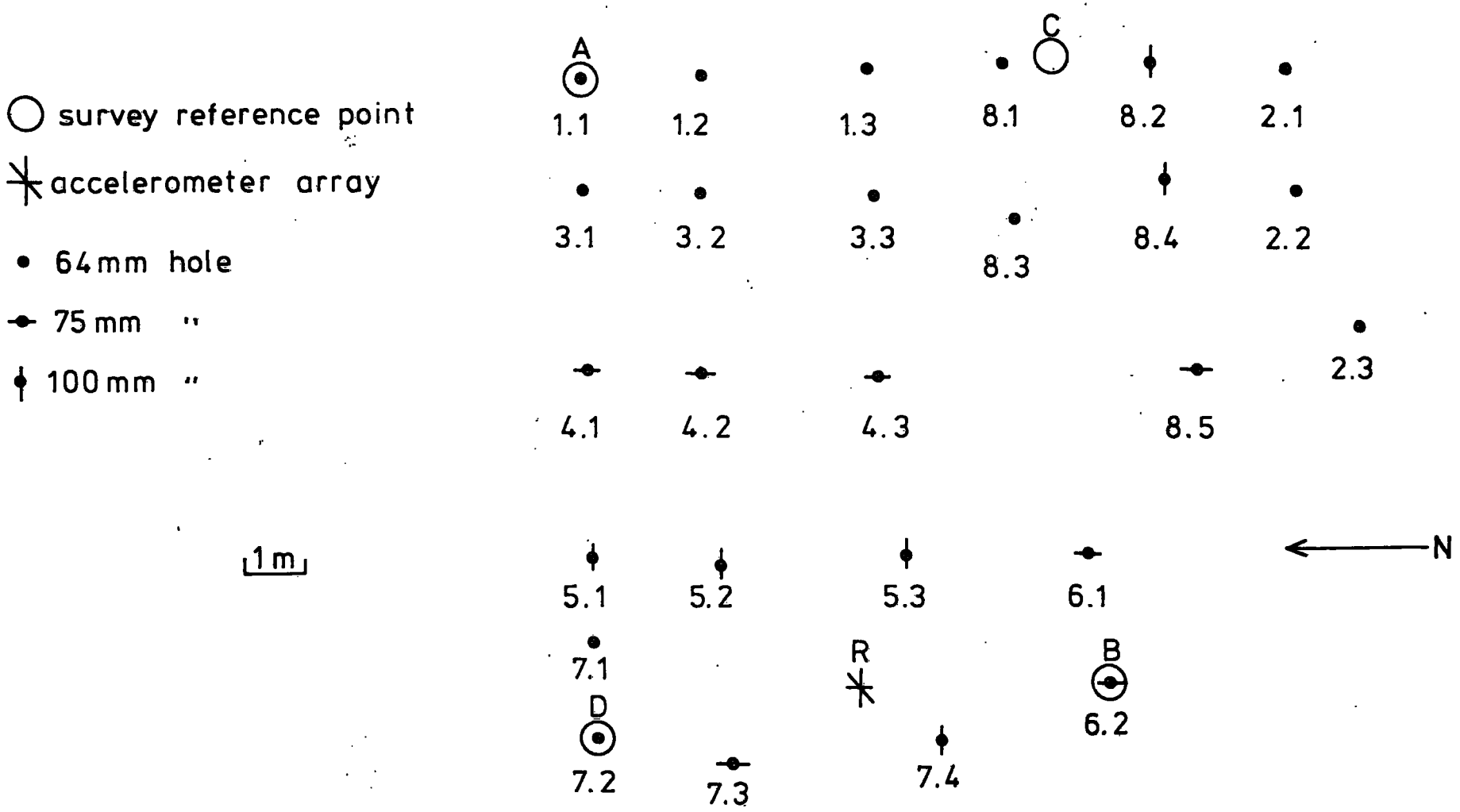

Fig. 7.5 BLAST AREA DRILL-HOLE PLAN

depths ranged between 1.6 m and 5.3 m. Three hole sizes were used, 64 mm for 'confined' and 75 mm and 100 mm for 'decoupled' conditions. The holes were drilled using an air flushed rotary percussion 'drifter' rig. The lengths, diameters and distribution of the drill-holes had been carefully planned so that the objectives outlined in Section 7.1 could be achieved with a few spare holes available to allow for any misfires or 'repeats' that were required. The holes were all located in competent rock and were generally dry. Water was present at the bottom of holes 2.3, 4.3, 6.1, 7.3 and 7.4, and care had to be taken that the specified blasting conditions were met, particularly in respect of the decoupled charges.

Initially, unstemmed holes were to be used for most decoupled explosions. However, this plan was revised after blast 306, when rock from the top of the drill-hole, was thrown considerable distances. It was therefore decided to stem the top 1 m of all decoupled explosions.

Prior to the blasting it had been agreed to limit the PPV to 5 mm/s at the bridge footings and in the brick arch culvert beneath the railway. Predictions based on results from other sites indicated that this limit would allow several kilograms of explosive to be detonated if required. The initial blast of ½ kgf confirmed that vibration levels were similar to those predicted and that charge weights could be increased to 2 kgf.

7.3.4 The transducers and their location

The vibration transducers were the same high performance geophones which were used at Penmaenbach (*see* Sections 5.3.1) but this time 6 triaxial arrays (18 geophones) were deployed.

Figure 7.4 shows the positions of the transducer arrays. The transducers were bolted to steel brackets which were rigidly screwed to the bedrock or structure as shown in Plate 5.2. For the first series (Table 7.1) triaxial arrays were placed at positions A, B, C (normal to the schistosity) and D, E and F (parallel to the schistosity). This configuration provided two lines of three transducers at approximately 20 m, 50m and 120 m from the blast area. The data gained from this series was used to establish the 'site laws' given in Section 7.4.2.

The second series (Table 7.2) was designed to assess the response of the culvert and bridge structures. Transducer arrays were placed in the following positions:

G Garry bridge pier foot

J On rock in culvert R1

K On brickwork in culvert R1

M On Garry bridge eastern abutment

N Garry bridge centre span

O Garry bridge pier top

In addition to the geophone arrays a triaxial accelerometer array was placed at position R within the blasting area. This allowed data at low 'scaled range' to be obtained which greatly improved the 'width' of the data base. In particular, confidence in the prediction of close-in vibration levels was greatly enhanced. This was of significance for the Killiecrankie scheme as the design required blasting excavation of rock very close to recently-cast concrete walls. These walls are to be advanced along the Pass in order to retain the up-slope drift deposits (which in places are of considerable depth) during the drift removal

prior to rock excavation.

Results from Penmaenbach had indicated that the geophones would not be suitable as their working range and frequency response was likely to be exceeded when placed close to the blasts. An array of Bell and Howell accelerometers with a flat response between DC and 2 kHz, and capable of measuring PPVs in excess of 200 mm/s, was therefore used. This array provided much valuable data and was used during both series of blasts.

The locations of the transducers were surveyed by the Engineers and provided as a series of grid references and levels, AOD. The locations of four reference points in the blast area were also given. The grid positions and levels are given in Table 7.4. This data allowed the specific distance between each drill hole and transducer position (r) to be readily calculated to an accuracy of better than 1%.

7.3.5 Instrumentation

The signal conditioning and recording equipment layout was similar to that shown in Figure 5.4, and is fully described in Chapter 5. However, experience from Penmaenbach had indicated that more data from each blast was desirable and therefore seven triaxial transducer arrays were deployed, requiring 21 channels of conditioning amplifiers and UV recording facilities. The two recorders shown in Plates 5.4 and 5.5 (*see* also Section 5.4 and 5.6) were run together during each blast and provided a combined chart width of 40 cm. The instrumentation provided excellent records with good resolution on all channels and examples are given in the following Sections.

TABLE 7.4

Transducer grid references and levels

Location (see Fig 7.4)	E - W (m)	N - S (m)	Level (m) AOD
A	21601.3	10996.1	158.23
B	21602.8	10967.4	155.63
C	21577.3	10917.6	134.15
D	21586.3	11015.0	157.06
E	21563.6	11016.6	150.26
F	21478.9	11006.1	108.97
G	21476.7	10990.3	111.45
H	21497.2	10923.2	120.30
J	21513.0	10904.4	118.17
K	21526.4	10906.0	121.54
L	21537.9	10988.7	135.30
M	21511.5	10987.4	134.03
R	21601.1	11011.5	162.00
A'	21611.14	11016.15	164.06
B'	21601.21	11007.30	161.38
C'	21611.60	11008.33	163.08
D'	21600.25	11015.79	162.23

A mobile laboratory was parked on the grass verge by the side of the existing A9 (*see* Figure 7.4) and was supplied with mains electric power from a disused house (purchased by SDD as it is on the new road line) some 100 m away.

On the Saturday before each blast series the transducers and recording equipment were set out and tested. This process took most of the day as over 2 km of cable had to be run over rather difficult terrain. A nightwatchman was employed to ensure the safety of the equipment left on site overnight, and a prompt start was made each Sunday morning as soon as the railway possession was obtained.

7.4 Results

7.4.1 Initial data processing

The data were treated in a similar manner to that described and illustrated in Section 6.1. Typical worked examples from each blast series (including data sheets and vibration recordings) are given below. Each of the 24 trial explosions were analysed in a similar manner.

Figure 7.6 shows the log sheet for blast 304/0, and gives details relevant to the first series of blasts. Similarly, log sheet 316/4 (Figure 7.7) gives basic information common to the second blast series.

The actual blast vibration records associated with blast 304/0 are given in Figure 7.8 (locations B, C, E and F) and Figure 7.9 (locations A, D and R). The records for 316/4 are given in Figure 7.10

(locations G, M, N and O) and 7.11 (locations J, E and R).

The tabular listings of the measurements taken from the UV records are given in Table 7.5 (blast 304/0) and Table 7.6 (blast 316/4). All the actual data listings are not presented here as the significant information is given in graphical format (Figures 7.12 - 7.17) and Appendices H, I, J, K and L.

7.4.2 The site laws

7.4.2.1 Coupled explosions

In order to determine any separate data groups within the results from all the coupled (fully-confined) explosions, the PPVs were plotted against scaled distance as shown in Figure 7.12a. A number of conclusions were drawn from this Figure:

(a) there was no observable difference in the attenuation of PPV attributable to the direction of the schistosity

(b) the three types of explosive (Trimobel, SG80 and DC2) all gave similar vibration levels and

(c) the 'partially-confined' detonations were, as observed on site, effectively similar to the fully confined detonations.

It was therefore decided to analyse all the coupled explosions as a group and Appendix H gives the full data listing input to the desk computer which performed the regression analysis (as in Appendix C). As listed the first number of each data pair (Y) is the measured PPV and

TABLE 7.5

Data listings for blast 304/0

Blast ref/ details	Transducer location/ orientation	Shot distance r (m)	Scaled distance $r/M^{\frac{1}{2}}$	Scaled distance $r/M^{\frac{1}{3}}$	PPV (mm/s)	Resultant (pseudo) PPV (mms)	Resultant (real time) PPV (mm/s)	Pulse duration (ms)	Wave packet duration (ms)	Remarks
304/0 Hole 2.2 64mm M = 1 kgf SG80	R/ V	11.0	11.0	11.0	22.0	62.2	57.0	2.0	8	Bench blast configuration but little rock 'lifted'.
	R				44.0					
	H				38.0					
	A/ V	11.8	11.8	11.8	24.0	41.3	35. o	1.0	20	
	R				27.0					
	H				20.0					
	B/ V	38.0	38.0	38.0	1.95	10.46	10.0	3.8	30	(Geophone resonance?)
	R				8.45					
	H				5.85					
	C/ V	95.5	95.5	95.5	0.46	1.02	1.0	3.7	50	
					0.75					
					0.52					
	D/ V	24.1	24.1	24.1	8.0	15.8	13.0	3.4	20	
	R				11.0					
	H				8.0					
	E/ V	47.9	47.8	47.8	1.63	3.80	3.6	5.4	55	
	R				1.79					
	H				2.93					
	F/ V	141.5	141.5	141.5	0.36	0.74	0.65	7.0	100	
	R				0.49					
	H				0.42					

TABLE 7.6

Data listings for blast 316/4

Blast ref/ details	Transducer location/ orientation	Shot distance r (m)	Scaled distance $r/M^{\frac{1}{2}}$	Scaled distance $r/M^{\frac{1}{3}}$	PPV (mm/s)	Resultant (pseudo) PPV (mms)	Resultant (real time) PPV (mm/s)	Pulse duration (ms)	Wave packet duration (ms)	Remarks
316/4	J/ V	148.7	105.2	118.0	0.30					
Hole 4.3 75mm	R				0.64	0.89	0.89	2.0	65	Confined, well tamped and stemmed in bottom of hole
M = 2 kgf SG80	H				0.54					
	E/ V	44.6	31.5	35.4	6.4					
	R				5.8	9.7	8.0	5.0	42	
	H				4.4					
	R/ V	7.14	5.05	5.67	125					
	R	(allows			220	269	240	1.6	5	
	H	for hole depth)			90					
	G/ V	140.9	99.6	111.8	0.55					
	R				0.71	0.99	0.8			
	H				0.42					
	M/ V	101.9	72.1	80.9	1.17					
	R				1.04	1.78	1.3			
	H				0.85					
	N/ V	) -	-	-	0.41					
	R	)			0.20	0.48	0.45			
	H	)			0.16					
	O/ V	) on bridge	-	-	1.24					
	R	)			0.46	1.81	1.70			
	H	)			1.24					

SEISMIC RECORD SHEET No 304/0

SITE Killiecrankie trial area

DATE 28/3/82 TIME 11.42

SOURCE 1 kgf SG80. Hole 2.2

	U.V. CHANNEL	GEOPHONE /CABLE IDENT.	GEOPHONE LOCATION/ ORIENTATION	AMP GAIN	U.V. mV/cm	SENS. mm/s/cm	TIMING MARK INTERVAL (s)	CASSETTE NA CODE/ CHANNEL	CASSETTE NA START/ FINISH	P.P.V mm/s	REMARKS
Micromovement Oscillograph	1,2,3		A/ V R H	÷10		40	0.01				Blast intended to be partially confined but little rock disturbance achieved
	4,5,6		D/	÷10		40	0.01				
	7,8,9		R/ (Acc)	x 1		40	0.01				
Bell + Howell Oscillograph	1,2,3		B/	x 2		3.25	100Hz Oscillator sine wave				
	4,5,6		C/	x 10		0.65					
	7,8,9		E/	x 2		3.25					
	10,11,12		F/	x 20		0.325					

Fig. 7.6 LOG SHEET 304/0

SEISMIC RECORD SHEET No 316/4

SITE Killucrankie trial area

DATE 4/4/82 TIME 12.00

SOURCE 2kgf SG80. Hole 4.3

	U.V. CHANNEL	GEOPHONE /CABLE IDENT.	GEOPHONE LOCATION/ ORIENTATION	AMP GAIN	U.V. mV/cm	SENS. mm/s/cm	TIMING MARK INTERVAL (s)	CASSETTE NA CODE/ CHANNEL	CASSETTE NA START/ FINISH	P.P.V mm/s	REMARKS
Micromemory	1,2,3		J/ V R H	×10		0·4	·01				Explosive well tamped and stemmed in 75mm hole.
	4,5,6		E/ moved from K after 314/4	× 1		4	·01				
	7,8,9		R/ (Acc)	÷ 10		400	·01				
Bell and Howell	1,2,3		G/	× 10		0·65	100 Hz sinewave				
	4,5,6		M/	× 5		1·30					
	7,8,9		N/	×20		0·325					
	10,11,12		O/	× 5		1·30					

Fig.7.7 LOG SHEET 316/4

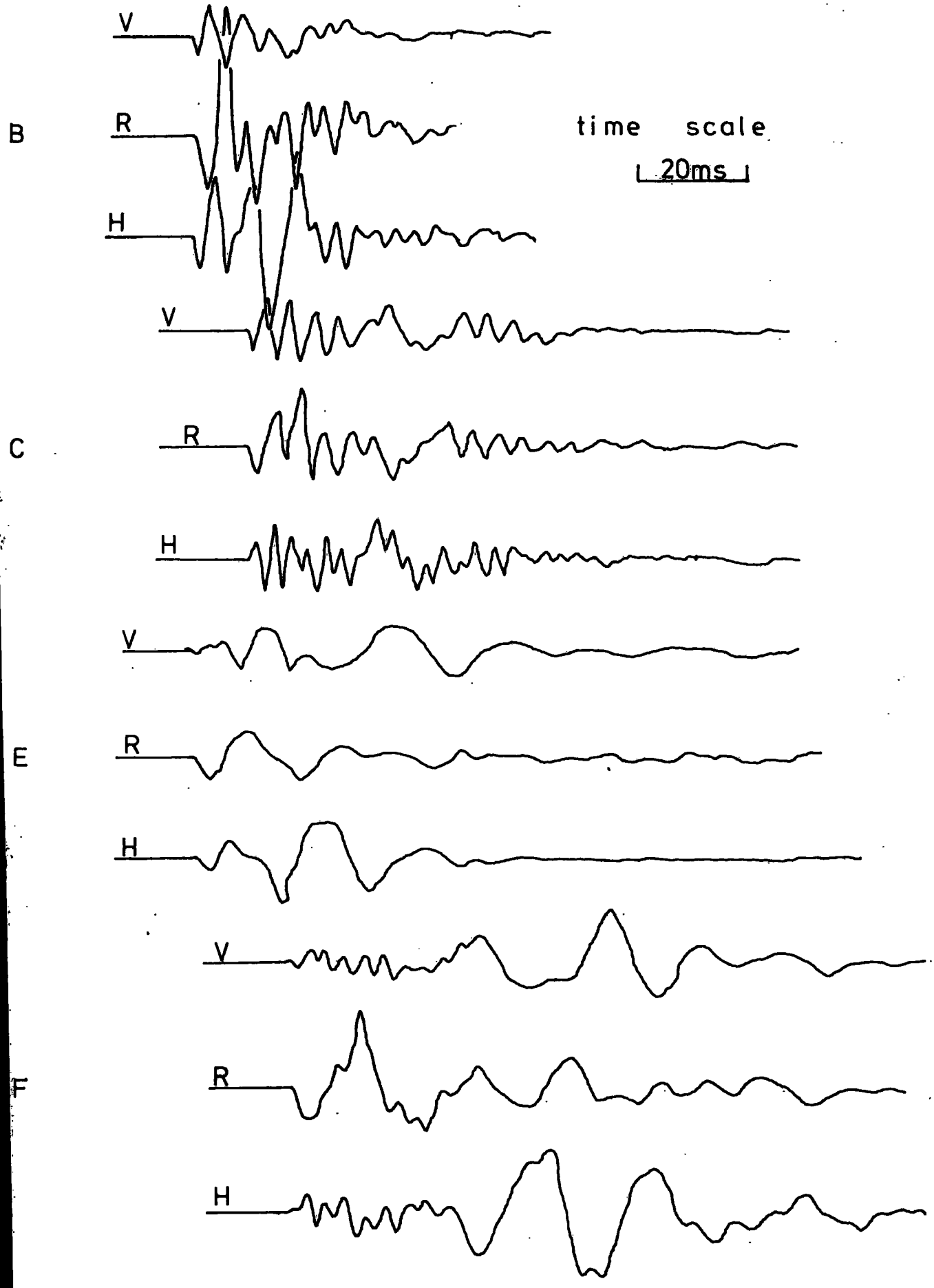

Fig. 7.8 BLAST 304/0 VIBRATIONS

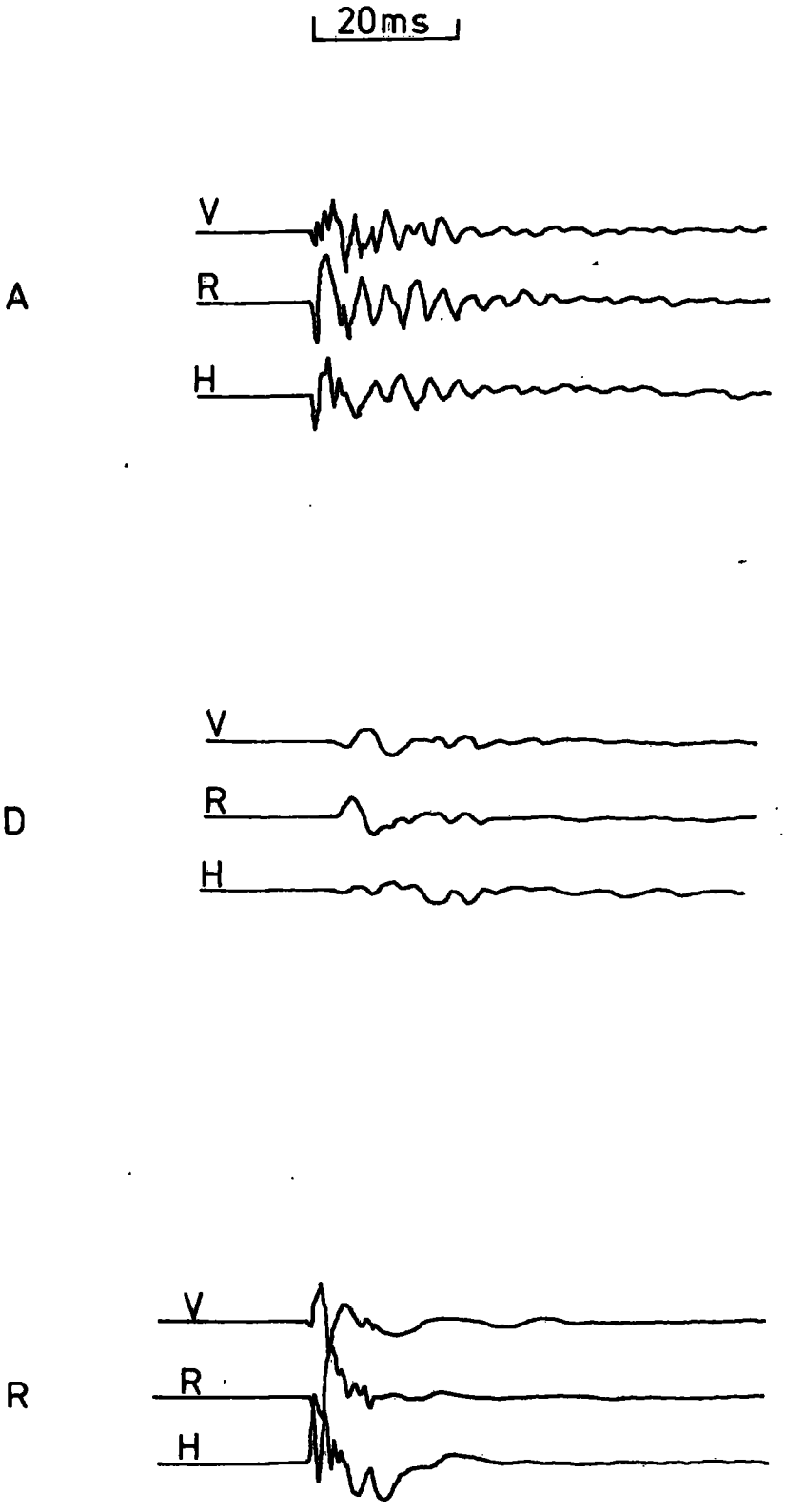

Fig.7.9 BLAST 304/0 VIBRATIONS (cont)

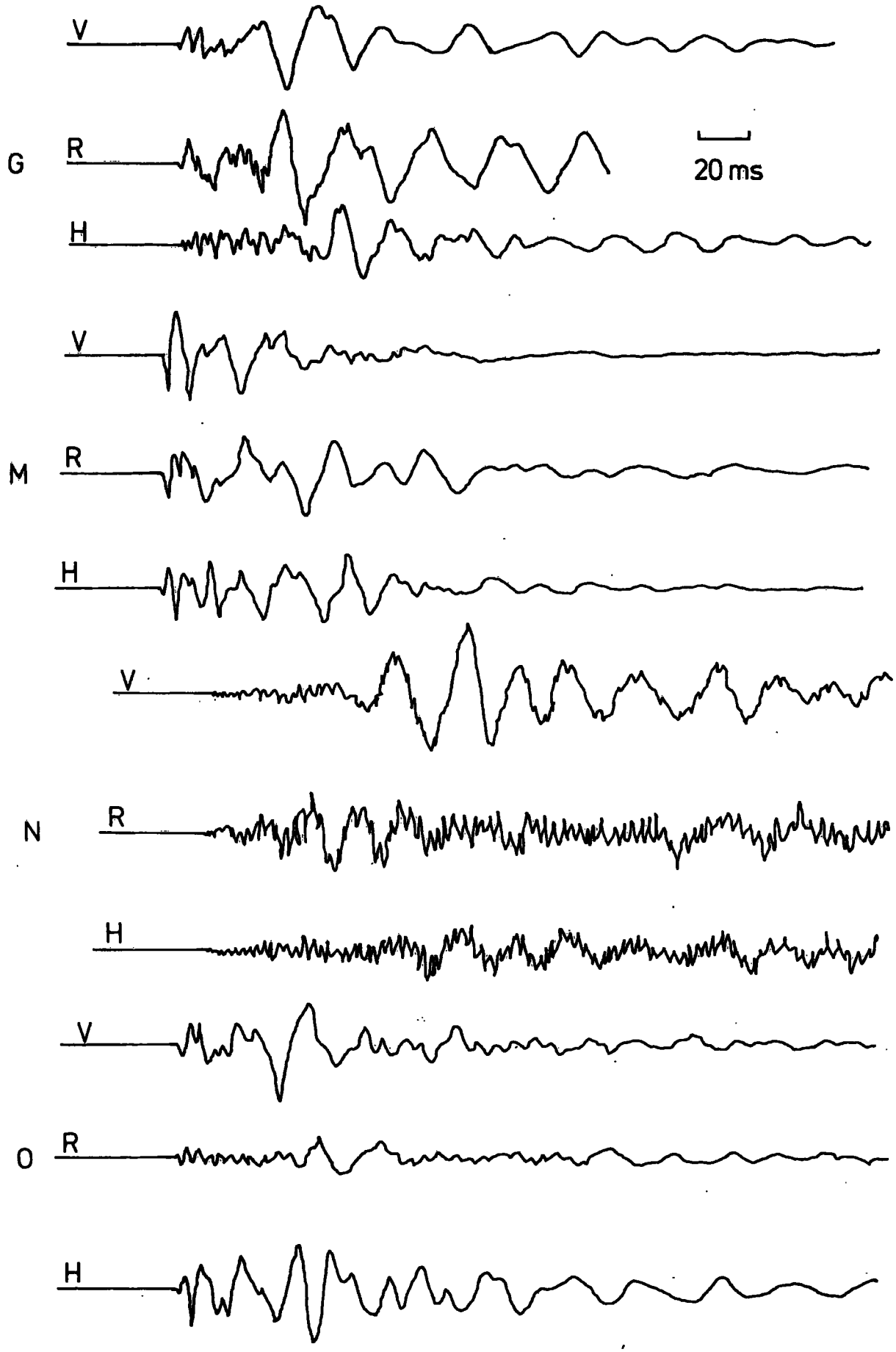

Fig 7.10 BLAST 316/4 VIBRATIONS

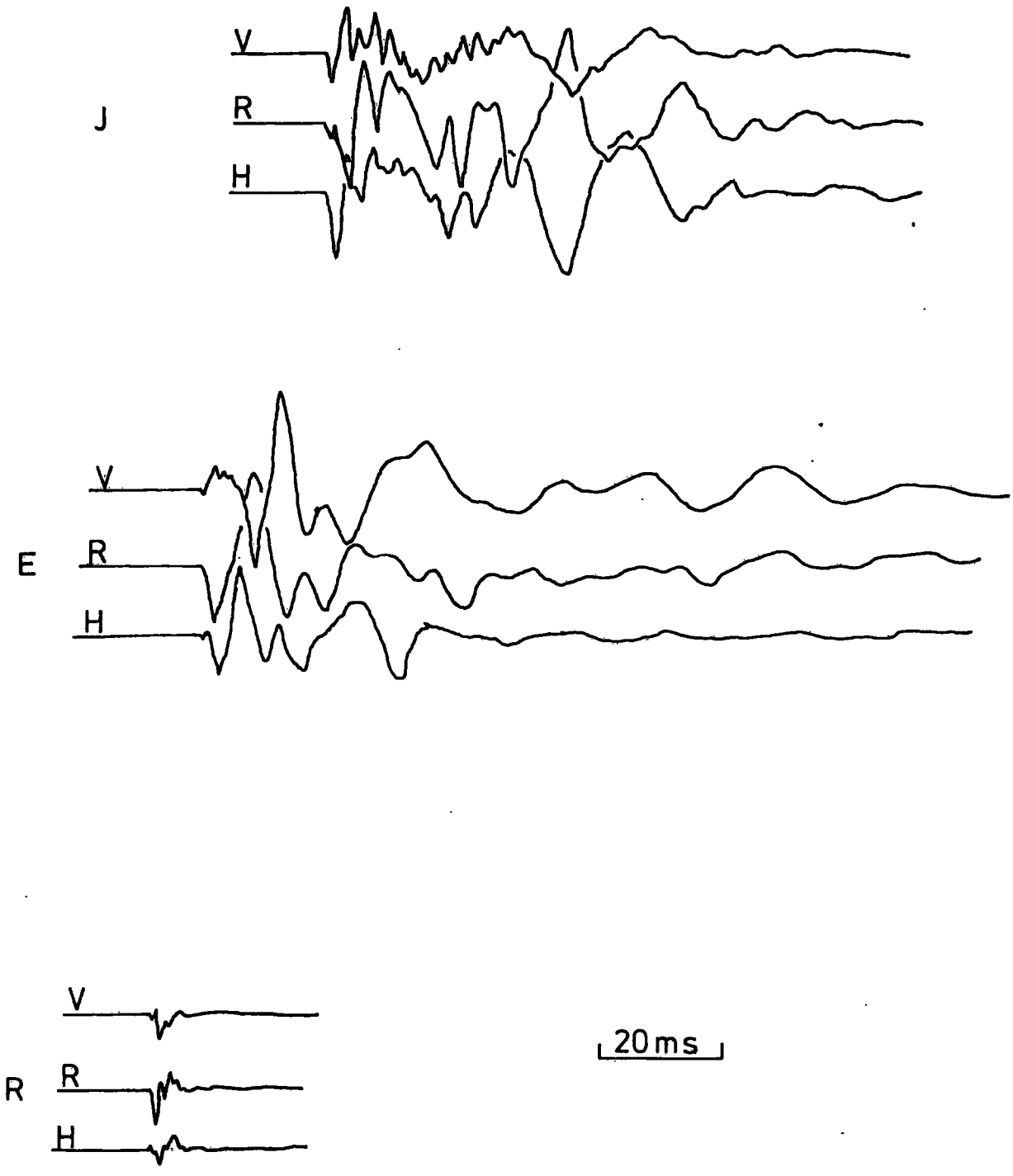

Fig. 7.11 BLAST 316/4 VIBRATIONS (cont)

the second (X) is the corresponding 'square root' scaled distance ($r/\sqrt{M}$).

The regression equation was found to be

$$PPV = 4857\ (r/M^{\frac{1}{2}})^{-1.84}$$

with a coefficient of determination of 0.96 indicating 'very significant' correlation when 'students t' tested.

A similar analysis was carried out using 'cube root' scaling but this resulted in poorer correlations and was therefore neglected. The same data were then analysed using the multiple correlation technique described in Section 3.2 and the data listing is given in Appendix I. As before, the first listed number of each data group (now Z) is the PPV, the second (Y) and the third the charge weight (M).

This analysis resulted in the following relation:

$$PPV = 4487\ M^{1.17}\ r^{-1.81}$$

with a multiple coefficient of determination of 0.97. This relation may be re-written as:

$$PPV = 4487\ \left(\frac{r}{M^{0.65}}\right)^{-1.81}$$

and in this form the data have been replotted and are given in 'site specific' scaling format in Figure 7.12b. Where comparison of various types of blasting are required, a common scaled distance must be adopted (*see* Section 7.4.2.4) and in this case it is convenient to use square root scaled data during comparisons.

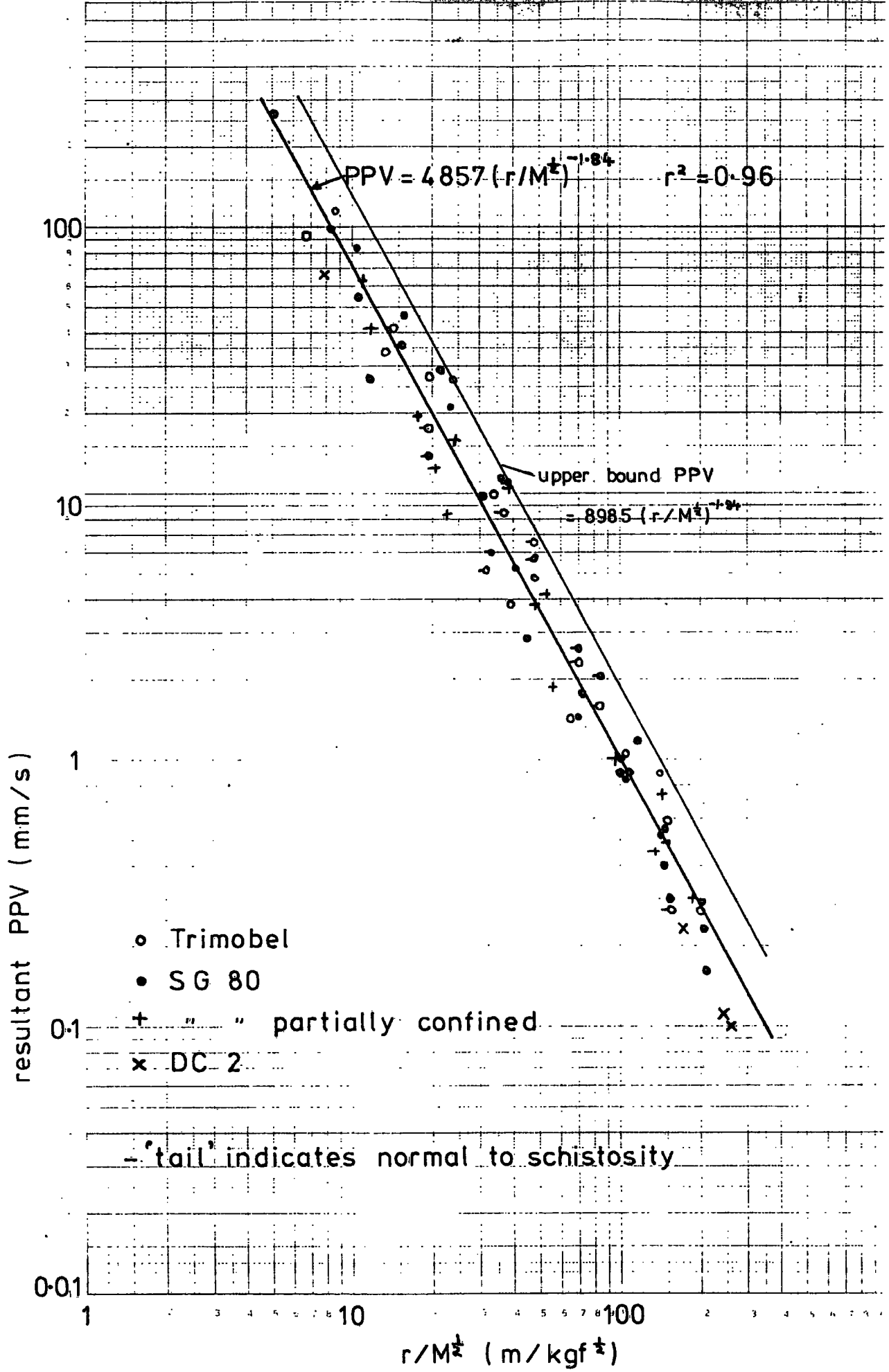

Fig 7.12a COUPLED EXPLOSIONS

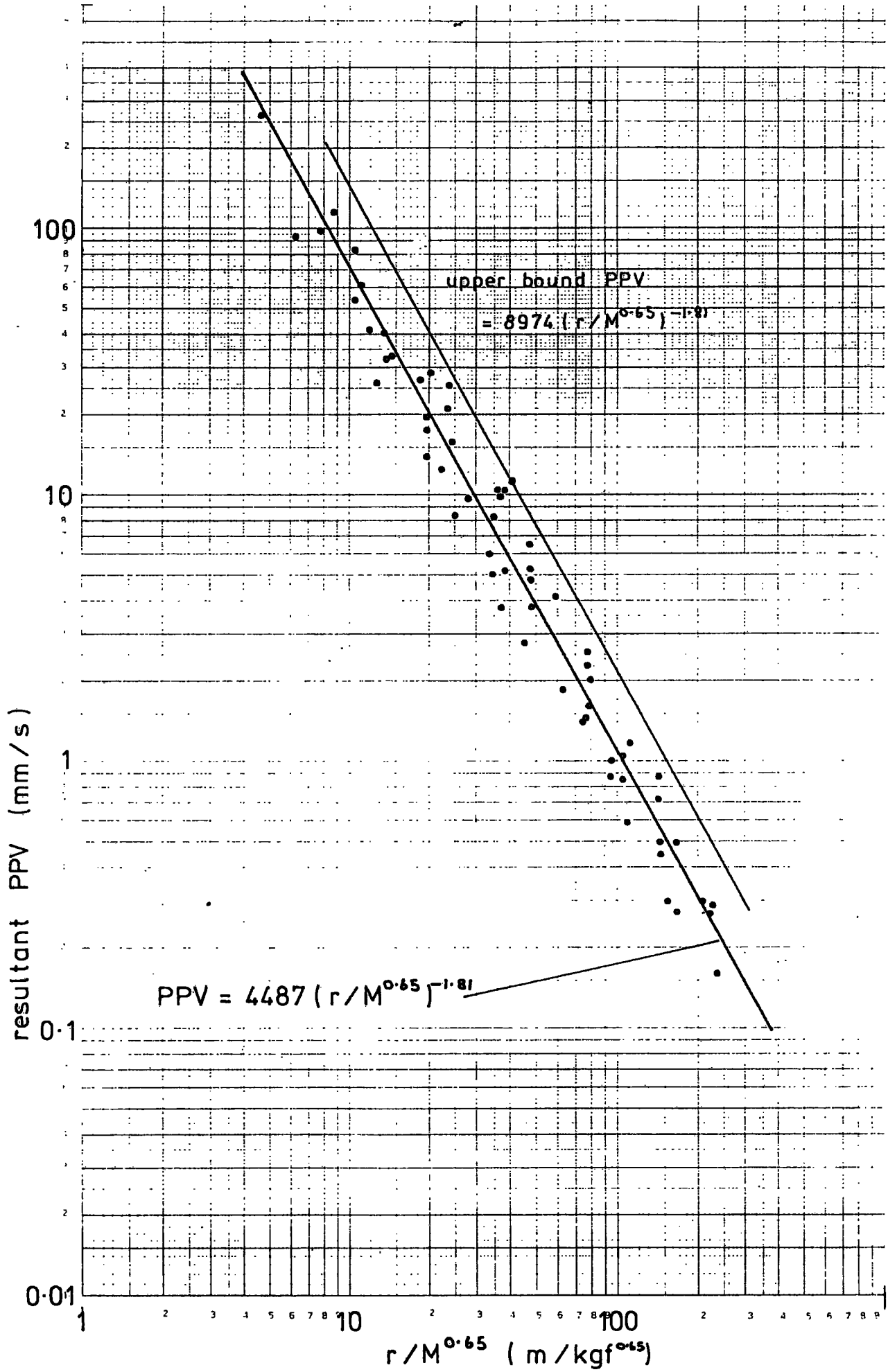

Fig. 7.12b COUPLED EXPLOSIONS (site specific scaling)

7.4.2.2 Decoupled explosions: 75 mm drill hole

The PPVs produced by the decoupled charges in a 75 mm diameter drill hole are shown in Figure 7.13. The results from the Trimobel and DC2 explosives were very similar, the decoupling ratio in each case being about 3:1. The packaging of the DC1 gives about half the weight of explosive per unit drill hole length and therefore results in an effective decoupling ratio of about 6:1.

The regression equations are

$$PPV = 3821\ (r/\sqrt{M})^{-1.89} \qquad (R^2 = 0.93)$$

for the Trimobel

and $$PPV = 239.4\ (r/\sqrt{M})^{-1.69} \qquad (R^2 = 0.96)$$

for the DC1

In each case the number of different charge weights fired was insufficient to justify multiple correlation analysis and the equations given above must be used cautiously when considering the effect of charge mass variation.

As with the coupled blasts the correlation of PPV with scaled distance was very good and no anisotropic attenuative properties associated with the direction of the schistosity were observed. The data listings and regression analysis printouts for the Trimobel and DC1 explosives are given in Appendix J.

A single blast 313/0 was fired to test the effect of water in the drill hole. The vibration level from this blast was, as expected, rather

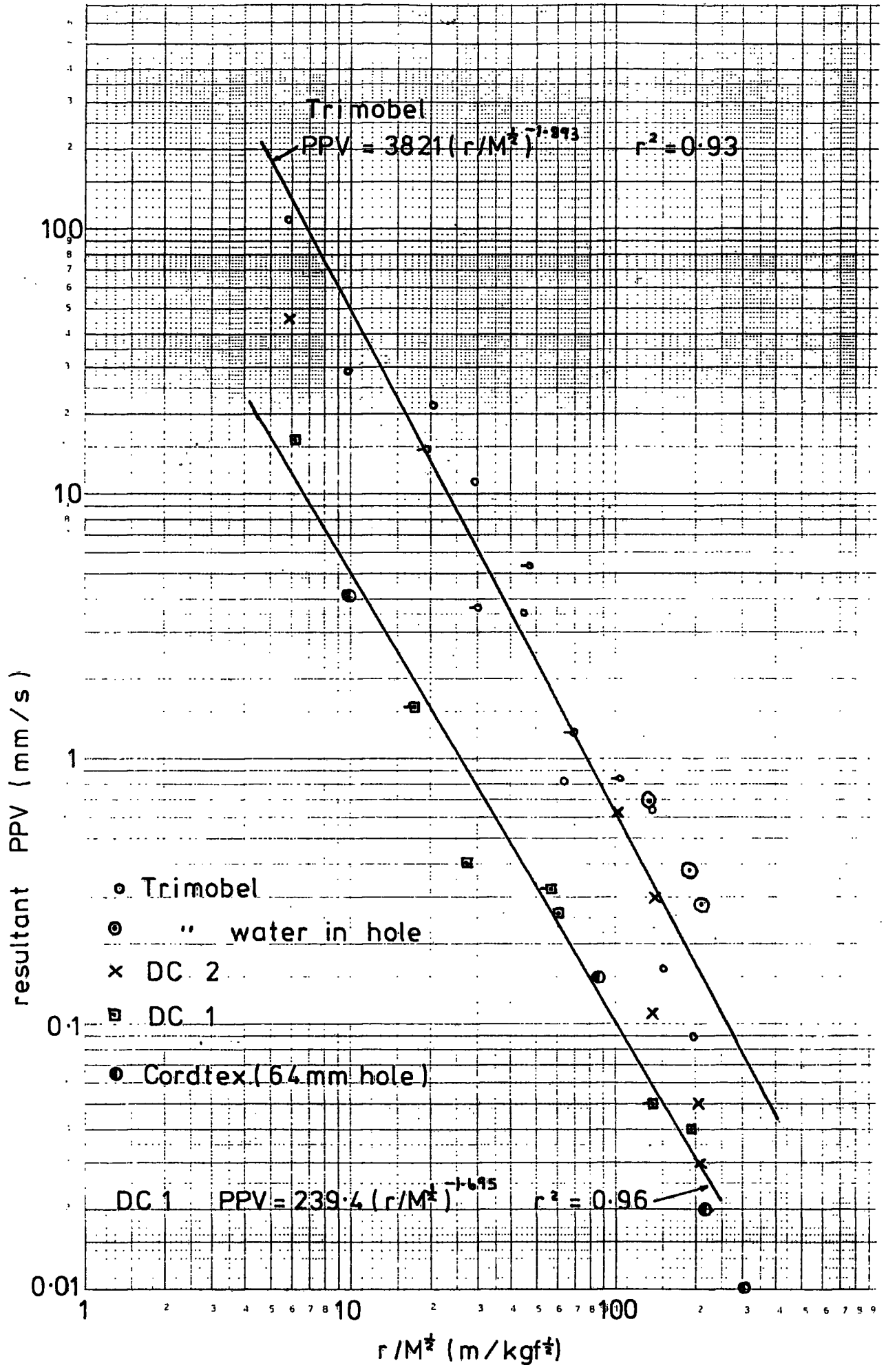

Fig.7.13 DECOUPLED ; 75 mm HOLE

higher than those where the charge was surrounded by an air void.

It has been suggested that detonating cord may be used for pre-splitting works and so blast 315/4 comprised four strands of Cordtex each 3 m long. This detonation produced a vibration level similar to that from the DC1.

7.4.2.3 Decoupled explosions: 100 mm drill hole

Figure 7.14 shows the PPVs induced by Trimobel detonated in a 100 mm drill hole. Also shown are the results from a single DC2 blast which again shows the similarity of these explosives.

As stated previously the top 1 m of the drill holes were stemmed (mainly to prevent fly rock) after blast 306. The results shown in Figure 7.14 do indicate that 'top stemmed' decoupled explosions give higher PPVs than unstemmed. This variation in blasting conditions may be responsible for the slightly less 'significance' indicated by the coefficient of determination for the regression on this data.

The regression equation is

$$PPV = 1763\ (r/\sqrt{M})^{-2.00} \qquad (R^2 = 0.90)$$

and the data listing is given in Appendix K.

The multiple regression equation is

$$PPV = 2529\ M^{1.15}\ r^{-1.96} \qquad (R^2 = 0.91)$$

and the data listing is given in Appendix L.

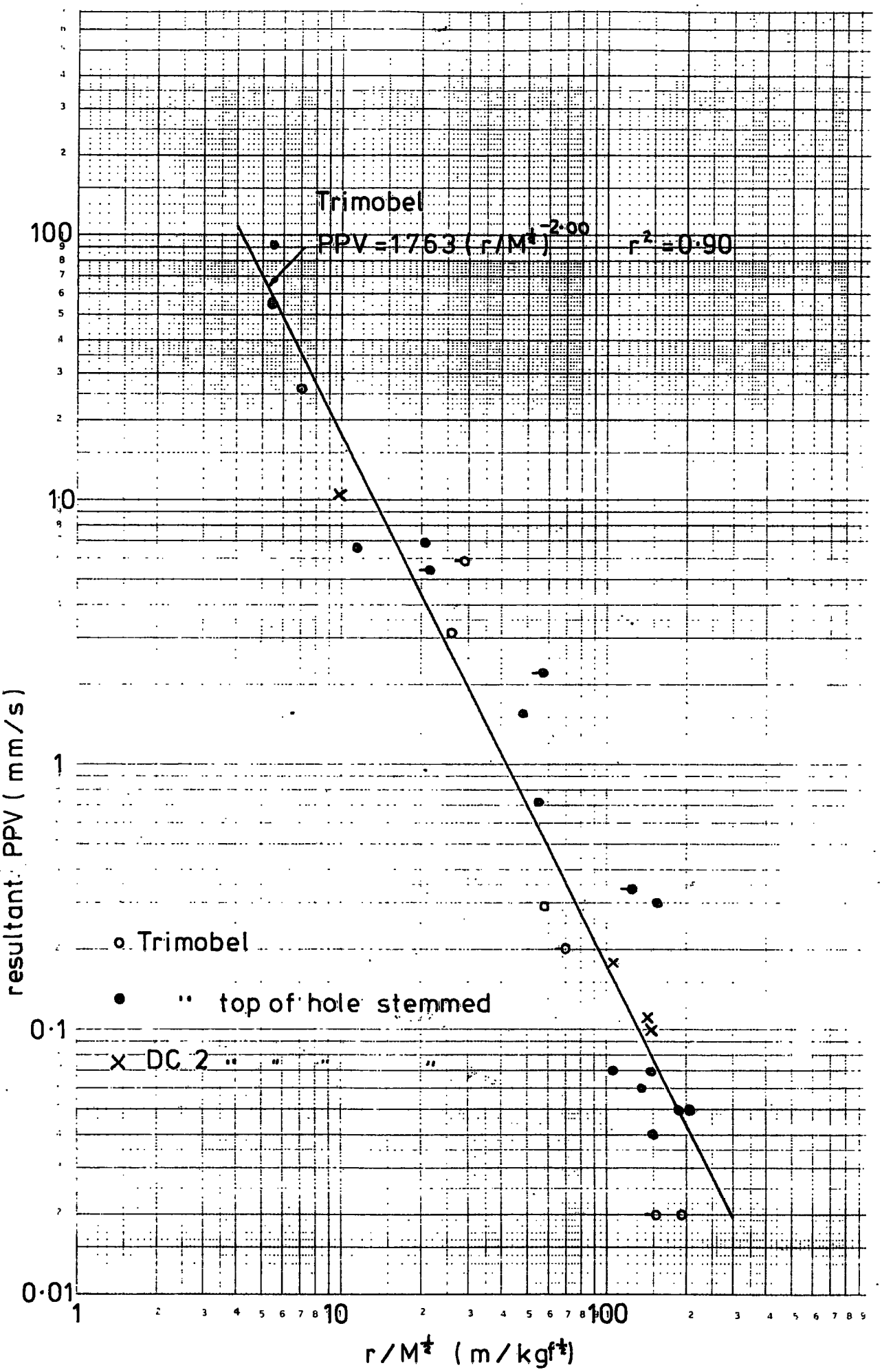

Fig.7.14 DECOUPLED ; 100 mm HOLE

7.4.2.4 Comparison of the site laws

The site law regression lines given above are plotted together in Figure 7.15 and provide considerable information concerning the relative effects of the various blasting techniques which may be used during the A9 reconstruction.

All coupled explosives gave closely similar results and the attenuation of PPV with distance was not significantly dependent on the direction of propagation in the rock mass. Decoupling the Trimobel in a 75 mm hole reduced the PPV, on average, by about 25%.

By effectively doubling the decoupling ratio (using DC1) the vibration levels were reduced by at least an order of magnitude from the coupled condition. This constitutes a dramatic reduction and may materially affect the design of the scheme.

Trimobel and DC2 again gave similar results when fired in 100 mm holes. The regression lines show that vibration levels are reduced (from the coupled condition) by a factor of between 3 and 6. The spread of these 100 mm hole decoupled results is noticeably greater than those from the confined blasts. This may be attributed to the fact that some detonations were completely unstemmed whilst others had the top 1 m of the drill hole tightly stemmed to prevent flyrock. Note that some of the decoupled (top of hole stemmed) results lie very close to the lower bound 'coupled' data.

The few results available from the water filled hole suggest that water is an effective energy coupling medium and if useful

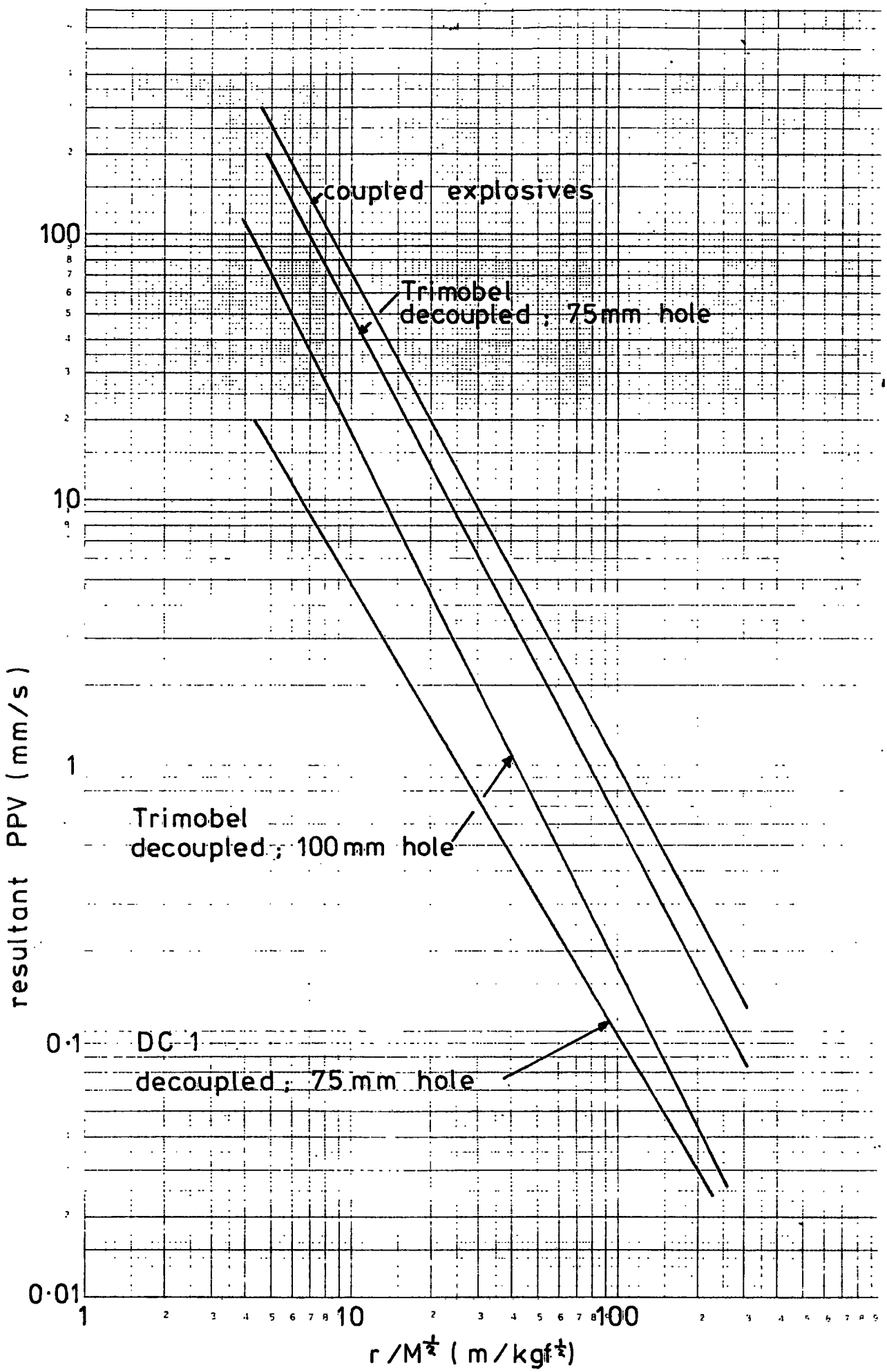

Fig.7.15. 'SITE LAW' REGRESSION LINES

reduction of PPV is to be achieved by decoupling the charged drill-holes must be dry.

The rate of decay of PPV as indicated by the slope of the regression lines (and the exponent of r in the multiple regression equations) is very similar for each blasting condition. This is to be expected as the design of each detonation was similar (single cylindrical hole) and the rock mass was a constant factor throughout.

7.4.3 Wave packet and pulse duration measurements

The Killiecrankie trials provided a considerable amount of data in confirmation of the discussion in Section 3.3.4 (and of the field results from Penmaenbach) which concerns the spreading of the wave packet and the initial pulse.

Figure 7.16 shows the increase in wave packet duration (as defined in Section 6.4.1) and again shows clearly the spreading of the vibrational energy into a longer wave packet. The assessment of the arbitarily-defined duration (see Section 6.4.1) is in practice rather difficult and results in considerable spread of data points. However, the trend is unmistakable. The data indicates that the increase in wave packet duration is rather greater in the direction of the schistosity.

Analysis of the wave packets in the frequency domain was undertaken and further examination of the directional propagation characteristics is given in Chapter 8.

The measured increase in the duration of the initial pulse is also very well defined (Figure 7.17) and again shows considerable spread.

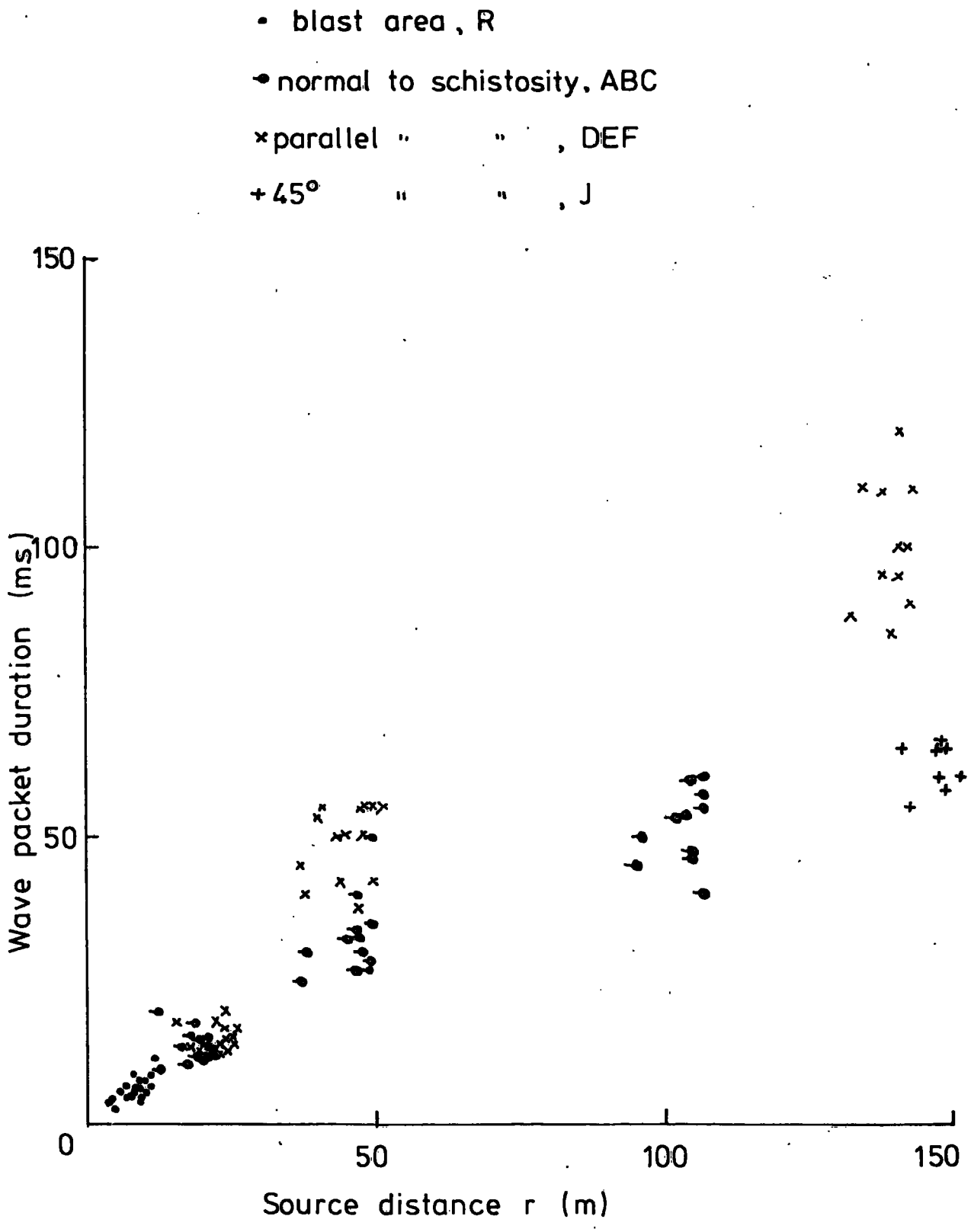

Fig. 7.16 WAVE PACKET DURATION v SOURCE DISTANCE

In this case there seems to be little, if any, dependence on the direction of wave propagation. Data for the initial 50 m of propagation distance is shown as beyond this distance the initial pulse becomes relatively small and its duration is more difficult to define.

The Killiecrankie results show the spreading in time (and therefore a third spatial dimension) of the wave energy even more clearly than those from Penmaenbach. In particular the accelerometer array close to the blasts has clearly shown the short wave packet with a high frequency (brief duration) pulse of dominant form. These observations offer good experimental confirmation of the diverging wave packet shell growing in thickness as well as radius with propagation distance.

7.4.4 The response of the Garry bridge and railway culvert

Table 7.7 lists the resultant peak particle velocities measured at various points on the principal nearby structures. Two transducer arrays were placed in the culvert, one on the brickwork (K) the other on rock (J). Four arrays were fixed to the Garry Bridge; these were at positions G (pier foot), M (abutment), N (centre span) and O (pier top). The accelerometer array was again placed close to the explosions to 'normalise' and allow direct comparison with the blasts listed in Table 7.1. The blast conditions are given in Table 7.2.

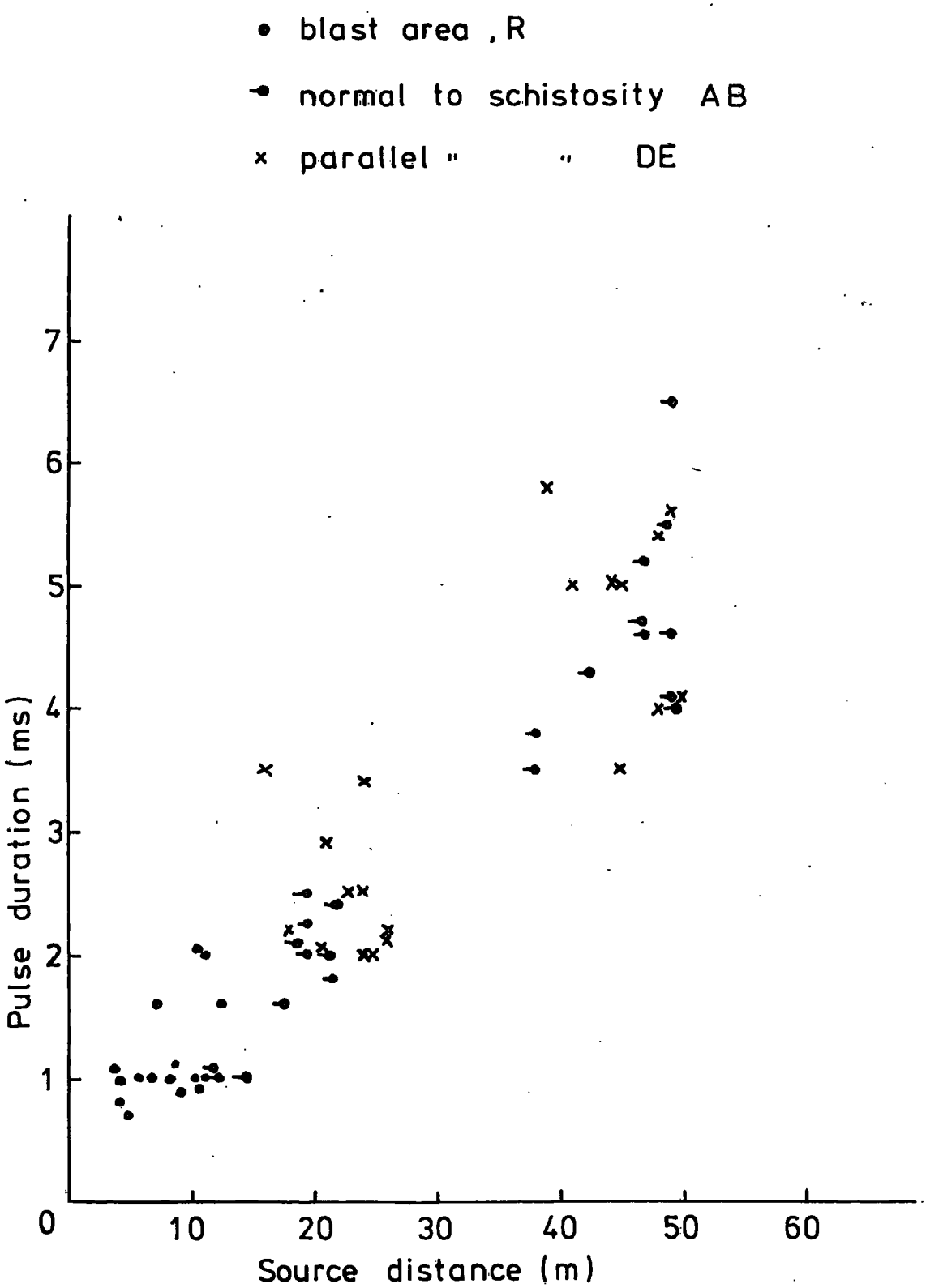

Fig.7.17 PULSE DURATION v SOURCE DISTANCE

TABLE 7.7

Structural PPVs

Blast Ref. (see Table 7.2)	Resultant peak particle velocity (mm/s)					
	G Pier foot	M Abut-ment	N Centre span	O Pier top	J Culvert (rock)	K Culvert (brickwork)
311/0	0.54	0.88	0.20	1.09	0.30	0.31
312/0	0.23	0.40	0.13	0.50	0.16	0.16
312/2	0.07	0.07	-	0.15	0.04	0.04
313/0	0.38	0.66	0.17	0.81	0.28	0.28
313/2	0.30	0.62	-	0.57	-	-
314/2	0.11	0.17	0.14	0.19	0.10	0.10
314/4	0.11	0.23	-	0.19	0.10	0.10
315/2	0.03	0.11	0.02	0.06	0.05	-
315/4	0.01	0.02	-	0.03	-	-
315/6	0.05	0.06	-	0.07	0.05	-
316/4	0.99	1./8	0.48	1.81	0.89	-

The culvert (rock and brickwork) and the Garry Bridge pier foot and abutment move with the rock mass and the particle velocities measured are therefore in accord with those predicted by the site laws given in Section 7.4.2.

The motions excited at the Garry Bridge pier top were consistently double those measured at the foot. Centre span vibrations are listed against the first explosion of any trial round as the motions were prolonged and the vibrations from later delays were superimposed upon earlier shocks. The relatively high frequencies excited by the blasting caused very small movements at the bridge centre span; clearly the mismatch between the response and input spectra to the bridge will be responsible. However if multiple millisecond delay rounds are to be fired, monitoring at the bridge centre will be necessary in case 'resonant'

excitation occurs. Any further measurements taken midspan on the bridge should use transducers (eg accelerometers) sensitive to frequencies down to ½ Hz as 1st mode bridge vibrations may be at or below the lower sensitivity limit for geophone type transducers.

7.4.5 Ambient vibration

When deciding vibration limits to be imposed at a site it is of interest to have information regarding the ambient levels at the site. This work is easily carried out during blasting trials and in this case was carried out during the two days immediately preceding each series of blasts.

7.4.5.1 The Garry bridge

The passing of trains produced the following range of vibrations (resultant PPV, mm/s) at the four positions indicated.

G/Pier	0.1-0.2
M/Abutment	0.3-0.8
N/Centre span	0.1-0.4
O/Pier top	0.1-0.3

The abutment M is within a few metres of the track and was therefore subjected to the highest vibration levels. The high frequencies put into the ground by the train do not appear to cause large resonant motions of the bridge deck.

The passage of road traffic across the bridge does excite fairly prolonged low frequency resonant motions at centre span. The range of

vibrations (resultant PPV, mm/s) were:-

G/Pier foot	0.05-0.25
M/Abutment	0.05-0.10
N/Centre span	0.25-1.20
O/Pier top	0.15-0.60

It seems likely that these values would be at least doubled if several heavy vehicles were crossing the bridge simultaneously. Higher levels may have been present at frequencies below 3 Hz at the centre span position although none were apparent to observers on the bridge either during the blasting or with the passing of road traffic.

7.4.5.2 The culvert R1

The passing of trains produced the following range of vibrations (resultant PPV, mm/s) at the two positions indicated in the culvert:-

J(on rock)	0.25-0.30
K(on brickwork)	0.05-0.1

Position J was about 10 m beneath the railway with position K a further 14 m to the east.

Lorries passing over the culvert along the A9 produced generally less than 0.05 mm/s at position K and less than 0.01 mm/s at J.

7.4.5.3 The rail tunnel and viaduct

At the northern end of the Pass (*see* Figure 7.3) two major railway structures, a tunnel and a viaduct, have recently caused considerable concern to their owners. Although blasting for the road scheme does not come within several hundred metres of these structures, the author was asked by British Rail to take vibration measurements at various positions on the viaduct and in the tunnel. The tunnel is partially unlined and has recently been subject to stability problems which have required support works. The stone-built viaduct has also been subject to considerable repair works and is a 'listed' structure.

Access to this part of the site was difficult and a portable measuring system based on the Micromovents UV recorder was put together and mounted in the rear of a Land Rover. Nine data channels from three triaxial geophone arrays were recorded at one time, and the range of measurement from several trains are given below.

	Resultant PPV (real time) mm/s
On rock in tunnel (eastern wall about 30 m from southern portal)	0.2-0.3
On brickwork in tunnel (eastern wall about 10 m from southern Portal)	0.4-0.5
Viaduct top (trackside wall, centre 3rd span from tunnel)	15-22
Viaduct pier foot	2-4

The range of PPV recorded within the rail tunnel was similar to that noted at other sites and gives no particular cause for concern. The PPV on the viaduct, however, often exceeded 20 mm/s and could easily

be contributing to the deterioration of the structure.

7.5 Application of the site laws

The site laws (given in Section 7.4.2) may be applied in the manner described and followed for Penmaenbach in Section 6.5. In this case the 'upper bound' site specific equation

$$PPV = 8974\ (r/M^{0.65})^{-1.81} \qquad (see\ Figure\ 7.12b)$$

will be used.

In order to establish acceptable individual charge weights it is necessary to speculate on the likely limiting PPVs that will be imposed on the Contractor in relation to the nearby structures. In the light of the discussion and review given in Chapter 2 it would seem unlikely that PPVs in excess of 100 mm/s would be acceptable to British Rail (railway and culvert) or Tayside Region (Garry bridge). Further, it would seem unreasonable to impose a limit below 25 mm/s for occasional blasting when trains regularly cause this level on a structure (the viaduct) which is likely to be less resistant than either the culvert or the relatively new road bridge.

Table 7.8 lists the charge weights for various ranges which may result in PPVs or 25 mm/s, 50 mm/s, 100 mm/s or 200 mm/s.

TABLE 7.8

Predicted allowable charge weights

Range r (m)	Charge weight M (kgf)			
	25 mm/s limit	50 mm/s limit	100 mm/s limit	200 mm/s limit
5	0.08	0.14	0.26	0.47
10	0.23	0.42	0.76	1.37
20	0.67	1.22	2.21	3.99
50	2.78	5.04	9.11	16.47
100	8.13	14.72	26.62	48.16

Table 7.9 gives the rock strain and stress associated with the four PPV limits given above. The calculations apply to the area close to the blast where compressional wave motions dominate the wave packet and assume a bulk density of 2.7 Mg/m^3 and an average compressional wave velocity of 4650 m/s. The method of calculation was as demonstrated in Section 6.5.

TABLE 7.9

Rock stress and strain

PPV (mm/s)	Strain (microstrain)	Stress (kN/m^2)
25	5	314
50	11	628
100	22	1255
200	43	2511

The predicted allowable charge weights given in Table 7.8 indicate that the great majority of the blasting required for the new A9 is not likely to be seriously inhibited by the imposition of a 25 mm/s or 50 mm/s limit at the Garry bridge footings or in the culvert R1. However, some blasting has been proposed well within 100 m of the bridge and culvert

and charge weights will need to be considerably reduced, from those required for optimum excavation or presplit blasting, if acceptable vibration levels are not to be exceeded.

An important feature of the proposed construction scheme was the early placement of cast *in situ* concrete walls to retain the often considerable depth of up-slope drift material. The placement of these walls was to be followed with excavation blasts which advanced the rock ledge along the hillside. This procedure is likely to be modified as the blasting trials have indicated that the nearby 'green' concrete may be subjected to unacceptably high levels of vibration.

It should be noted that Table 7.8 gives values of maximum charge weight based on the 'upper bound' coupled explosive site law equation. As shown in Figure 7.15 considerable reduction of induced particle velocity may be achieved by various degrees of decoupling and the site laws appropriate to the specific blasting conditions will be applied during the final design works.

A paper (New, 1982) has been presented to the Scottish Development Department and their Consultants, and forms the basis for aspects of the road design which are subject to vibration control problems.

CHAPTER 8

DATA ANALYSIS IN THE FREQUENCY DOMAIN

8.1 Introduction

Historically the prediction of vibration from construction blasting has been based on the acquisition and analysis of trials data in the time domain. That is, the variation of peak particle velocity (PPV) is considered a principal factor with respect to potential damage; this follows from the arguments presented in Chapter 2 which indicate that maximum dynamic strain is likely to be a major cause of damage. It must be noted however, that the calculation of ground strain from particle velocity measurements also requires a knowledge of the velocity of propagation of the wave motion. Further, a knowledge of the frequency of the disturbing ground motions will allow the calculation of wavelength and these factors may be of critical importance when considering effects to structures (*see* Section 2.2.2). It follows that frequency dependent damage criteria are increasingly being considered in the development of vibration standards relating to structural damage and human reactions.

Some care must be exercised in the use of data presented as distributions in the frequency domain. For instance, the actual distribution of energy in the frequency domain may be misleading as the peak strains imposed will not necessarily occur at the frequency shown to possess the maximum energy in the wave packet. This matter is discussed in the context of vibration prediction by Nicolls *et al.*(1971) of the US Bureau of Mines and they state that 'familiarity with seismic type records and their transforms leads one to conclude that there is little if anything contained in the transform that cannot be discerned from the original redord'. However, although the time domain analyses illustrated and

developed earlier in this thesis (PPV v scaled distance, site laws) will continue to be of prime importance in the prediction of ground vibration, analysis of the data in the frequency domain may yield useful insight as to the nature of the attenuative and source dependent mechanisms which influence the development and propagation of vibration in the rock mass.

8.2 The calculation of energy spectral density (ESD) and gain factor (GF)

Examination of the power or energy distribution (for 'continuous' and 'transient' processes respectively) with respect to frequency is an important and widely used technique in the analysis of many types of experimental data. In this Chapter the fast Fourier transform method (Cooley and Tukey, 1965) is used to obtain estimates of the energy spectra from digitised data sequences obtained from the vibration wave packets recorded at the test sites.

Detailed techniques and procedures for the calculation of Fourier spectra are given widely in the literature (eg Bendat and Piersol, 1971; Blackman and Tukey, 1958; Newland, 1975) and are dealt with here only where essential. An excellent review of techniques for spectral analysis with an extensive bibliography has recently been published by Kay and Marple (1981).

Using Fourier techniques a time varying waveform, x(t), may be analysed into an integral sum of harmonic oscillations over a continuous range of frequencies. Equally, the frequency spectrum may be converted back into the original waveform. The transformation from the time to frequency domain, or conversely from frequency to time, is expressed mathematically by the continous Fourier transform relations:

$$X(f) = \int_{-\infty}^{\infty} x(t) \exp(-j2\pi f t)dt \quad \text{(Transform)} \qquad \ldots\ldots \quad (8.1)$$

and $x(t) = \int_{-\infty}^{\infty} X(f) \exp(j\,2\,\pi\,f\,t)df$ (Inverse transform) ..... (8.2)

These relations constitute a Fourier transform pair. When the waveform has to be sampled for analysis by computer a discrete form of Fourier transform (DFT) must be used. For N data points a series of values will be required forming the sequence,

x_n, for n = 0, 1, 2, .., N-1

The Fourier components (DFT's) may be expressed in the form:

$$X_k = \frac{1}{N} \sum_{n=0}^{N-1} x_n \exp(-j\,2\,\pi\,kn/N); k = 0, 1, 2, .., N-1 \quad ..... \quad (8.3)$$

These complex quantities may be calculated using the Cooley-Tukey technique and the particular algorithm employed here is based on that given by Bice (1970).

Note that the complex DFT, X_k, = $A_k + jB_k$ where A and B represent the component real and imaginary amplitudes.

The magnitude $|X_k|$ is therefore given by

$$|X_k| = (A_k^2 + B_k^2)^{\frac{1}{2}} \quad ..... \quad (8.3a)$$

and the argument or phase Q_k, by

$$Q_k = \arctan B_k/A_k \quad ..... \quad (8.3b)$$

The A_k values include the DC term at the origin with N/2 real frequency points f apart (where f=1/N.DT and DT is the sample increment

period) and B_k the (N/2)-1 complex frequency points. Point zero is the DC or zero frequency, 1f the fundamental, and nf the n^{th} harmonic.

The sequence of quantities X_k provide a spectral description of the time series sequence x_n called its Fourier spectrum, $X_k(f)$, and it is usual to present this information in its power or energy spectrum form. Historically these Fourier techniques have been applied in the investigation of electrical signals (voltage) and the terms 'power' and 'energy' derived from electrical power (watts) and energy (joules). Thus power and energy spectra have taken the units watts per frequency and joules (watt-second) per frequency. In our case the power spectra take the units of particle velocity squared(per frequency). In fact the terms 'power' and 'energy' are also appropriate for our data as the power transmitted by a single harmonic component is proportional to its particle velocity squared for a wave motion in a material of constant density and wave propagation velocity (Jaeger and Cook, 1976). For a full discussion on the 'unit' aspect of power spectra *see* Magrab and Blomquist (1971) and Newland (1971). Bendat and Piersol (1971, Ch 10) provide detailed information with examples related to transient processes which result in energy spectra.

The energy spectrum G(f) is given by

$$G(f) = 2|X_k(f)|^2 \qquad \ldots\ldots \quad (8.4)$$

where the factor 2 occurs to fold over the energies at negative frequencies to yield a quantity defined for positive frequencies only. This function is referred to as the energy spectral density (ESD) of the transient process described by the series x(n). The principal difference between this expression and that for the power spectral density (applied to a continuous rather than transient process) is that the 'power' expression is divided by

the record duration. This results in an expression giving energy per unit time, that is, power. Thus the procedures appropriate for the determination of power spectra may be applied directly to the determination of energy spectra although the estimation of errors is different for the transient case. It must be remembered that validity of power spectra measurements is dependent on the stationarity of the 'continuous' signal whereas a transient signal is by definition non-stationary in character and the validity of spectra can only be assessed by operation on repeats of the transient phenomena.

A particular requirement of frequency domain analysis is to calculate the gain factor between two sample records, x(t) and y(t). In our case it will be of interest to observe how the particle velocity is affected by charge variations, and attenuated with propagation distance throughout the range of frequencies present.

The gain factor related to particle velocity, H(f), may be calculated from the energy spectra in the traditional manner (*see* Bendat and Piersol, 1971) as,

$$H(f) = [G_x(f)/G_y(f)]^{\frac{1}{2}} \qquad \ldots\ldots \quad (8.5)$$

where $G_x(f)$ and $G_y(f)$ are the energy spectra associated with the real transients x(t) and y(t). However, an interesting and useful property of the complex fast Fourier transform allows the gain factor to be computed directly from a single fast Fourier transformation.

If we input one series of data points x(n) as the real part and the other series y(n) as the imaginary part of a complex record z(n) into the FFT algorithm, we may obtain both the Fourier transforms X(k) and Y(k) as follows:

let $z(n) = x(n) + jy(n); n = 0, 1, - -, N-1$ ..... (8.6)

The discrete Fourier transforms of z(n) are

$$Z(k) = \frac{1}{N}\sum_{n=0}^{N-1} [x(n)+jy(n)] \exp [-j2 \pi kn/N]; k = 0,1,--,N-1 \quad ..... \quad (8.7)$$

and Z(k) is calculated using the complex FFT algorithm.

It can be shown that (Bendat and Piersol, Ch 9, 1971) the two real valued records x(n) and y(n) have Fourier transforms X(k) and Y(k) which are given by

$$X(k) = [Z(k) + Z^*(N-k)]/2 \quad ..... \quad (8.8)$$

$$\text{and} \quad Y(k) = [Z(k) - Z^*(N-k)]/2j \quad ..... \quad (8.9)$$

$k = 0,1,--,N-1$

where * indicates the complex conjugate.

Now the individual gain factors H(k) are given by

$$H(k) = X(k)/Y(k) \qquad k = 0,1,--,N-1 \quad ..... \quad (8.10)$$

since X(k) and Y(k) are proportional to $(G_x(k))^{\frac{1}{2}}$ and $(G_y(k))^{\frac{1}{2}}$ respectively.

In practice this provides the gain factor spectra in a single operation on two related records and the software requirements are further discussed below.

8.3 Software requirements and implementation

The frequency domain processing of the field data was carried out on a CBM microcomputer equipped with printer, twin floppy disc drives and a

Hewlett-Packard digitising/plotting table. The software was written by the author incorporating the BASIC FFT algorithm by Bice (1970) and routines for plotting output.

8.3.1 Data preparation

The field data were in the form of U.V. chart recordings and the initial requirement was the preparation of digital data files from the analogue geophone traces. For the Penmaenbach site there were 8 wave packets per explosion and from Killiecrankie site 21 wave packets per explosion. In total some 200 wave packets were digitised and data files were titled as shown by the following example:

File title 302/4CR

Here 302 refers to the blast number at Killiecrankie, 4 to the particular delay, C to the triaxial geophone array location and R to the direction (R, V or H) of sensitivity of the geophone. The 2XX series blasts are those carried out at Penmaenbach.

A programme titled DIGIT (Appendix M) was written to create data files which contained the data in a form readable, from the floppy disc storage, by the main processing programme.

Each data file contains the following information:

(a) the file title,

(b) the time increment between data points (DT),

(c) the digitised sequence of data points from the chart record.

The variable frequency content of geophone traces at differing ranges required that three sampling rates (0.25, 0.5 and 1ms) should be used. The raw data were already of a 'band limited' form in that the electronic conditioning removed very high frequencies (possibly present in noise) and

therefore prevented any aliasing effects from this source. A sample size of 128 points was sufficient to cover all the wave packets, and sampling sequences were initiated at a zero point preceding the first arrival. The sequences were 'zero filled' to complete the 128 samples, where necessary, and there was no significant truncation of any wave packet. These procedures follow those given by Bendat and Piersol (1971).

In order to rationalise plotting routines the input data sequences were normalised with respect to the maximum particle velocity; where amplitude (as well as distribution) of the spectra was relevant this factor was corrected subsequently by rescaling the computed spectrum. The quality of the geophone traces was generally good and the magnifying sight on the digitiser allowed the accurate and speedy placement of the cursor at each automatically incremented position on the chart records.

To reduce the possibility of operator error DIGIT also provided the facility of immediately plotting the digitised data for comparison with the original chart records.

8.3.2 Computation of the Energy Spectral Density (ESD)

The programme 'FFT' (Appendix N) was written to compute and plot the energy spectra from the data files prepared by DIGIT. The output format gave graphical presentation of the energy spectra (Eq 8.4), this calculation taking place in line 820 where the individual Fourier components are square and doubled as required. The phase spectrum was also calculated (line 950) and output in graphical format although this was not found useful during the subsequent interpretation of the data. Generally, the phase spectra took an erratic form which reflected the considerable complexity of the wave packet structure and no helpful pattern of phase distribution was apparent.

Although the programme appears rather lengthy the actual fast Fourier transform is carried out in the compact algorithm provided by Bice (1970) in lines 320 to 790. The programme is lengthened by the plotting routines and other subroutines included to assist programme development. These routines are included to allow modifications if required for other purposes.

The graphical output of ESD is normalised with respect to the maximum value (in array P(I)). This value is designated PM and is printed to allow comparison of amplitude between various spectra. A value (PT = Σ P(I)) is also printed to give the sum of the 'energies' at all harmonic frequencies. Comparison of spectra will also require correction for the original data normalisation factor, as noted above.

The frequency scale is given in Hertz and comprises the sixty four harmonics given by the 128 sample point analysis (*see* Section 8.2). The programme is easily adapted to deal with a greater or lesser number of samples by changing the exponent G in line 200 (subject to adequate computer memory).

The accuracy of the programme was tested using various trial functions. In particular validation using various sine and cosine generated wave packets is a stringent test of any fast Fourier transformation. In all cases the programme yielded the expected form of spectral distribution with correct peak spectral amplitude (PM) and total 'energy'(PT). The FFT algorithm was further tested by performing the inverse transform (from the Fourier spectrum) operation which returned the original data sequence, as required.

8.3.3 Computation of the gain factor (GF)

The programme FFT was then developed to produce a spectral description of the gain factor between the Fourier spectra of two data

files. This programme is referred to as GF-FFT and is given in Appendix 0.

As discussed in Section 8.2 the respective data files are input to the real and imaginary array locations and the complex output transform is used to calculate (lines 880 to 910) the individual transforms of the real data sequences by way of equations 8.8 and 8.9. The ratio of the Fourier components is calculated giving a spectrum comprising the ratio of the particle velocities at each harmonic. The gain factor spectra may be scaled with reference to the input particle velocities and the value of PM for each spectra. This programme was validated by sample calculation of gain factor based on data from individual power spectra using equation 8.5.

In order to assist interpretation of the gain factor distribution the spectra were smoothed by taking a 'rolling average' comprising the average of five harmonics. Thus the spectral value for the i^{th} harmonic was calculated from

$$H(i) = (H(i-2) + H(i-1) + H(i) + H(i+1) + H(i+2))/5 \quad \ldots\ldots \quad (8.11)$$

8.4 The effect of charge weight and coupling

8.4.1 Charge weight

An important influence on the rate of decay of vibration with propagation away from an explosive source will be the frequency of the motions generated at the source. Although the primary mechanism causing PPV decay (radial spreading) will not be influenced by input frequency, other causes such as scattering and absorption losses will be dependent on frequency. A full discussion of the complex factors which may influence the source characteristics of construction blasts is given in Section 3.3 and analysis of all the field data in the time domain is given in Chapters 6 and 7. As

well as the possibility of influencing the decay rate of the vibration, the frequency content will also be of importance where the stimulated ground motions are to be interpreted with regard to the excitation of structures.

To investigate the frequency domain characteristics of the vibration source we will consider the energy spectral density of the particle velocity as close to the explosions as possible. At Killiecrankie the accelerometer array located at position R was just a few metres from each explosion and provided a range of data for charge weights between 0.5 kgf and 2 kgf.

Direct observations of the field seismograms, obtained close to the source, showed that the peak particle velocity occurred during the initial radial motion and that the subsequent oscillations were heavily damped. Initial pulse durations were between 1 and 2½ milliseconds and the significant motions in the wave packet lasted less than ten milliseconds (*see* Figs 6.14, 6.15, 7.16, 7.17).

Figure 8.1 shows the ESD of the time domain record (also shown) for blast 304/ORR. This record was obtained at a distance of 11 m from a 1 kgf Special Gelatine 80 charge and is typical of many records taken close to the source, that is, it comprises a dominant initial pulse followed by a rapidly decaying oscillation. It is of interest to note that a simple synthetic waveform may replicate that observed in the field. Figure 8.2 shows the ESD for a heavily damped sinusoidal waveform at 200 Hz where

$$\text{particle velocity} = \exp\left[-\alpha t\right] \sin \omega t$$

Although the waveform and spectral distribution shown in Fig 8.1 is naturally more complex than that in 8.2, the distribution of energy is

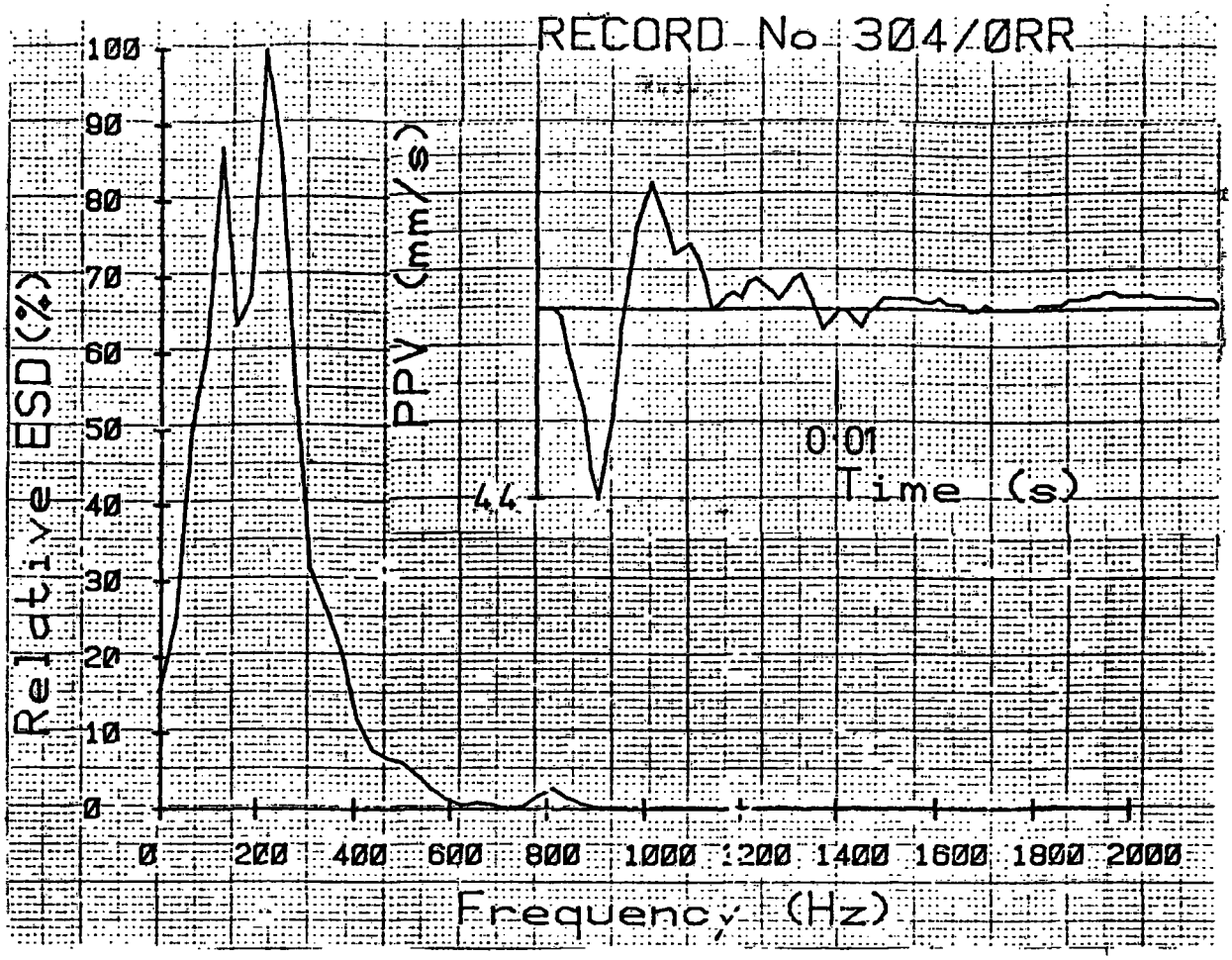

Fig.8.1 TYPICAL NEAR SOURCE SPECTRUM

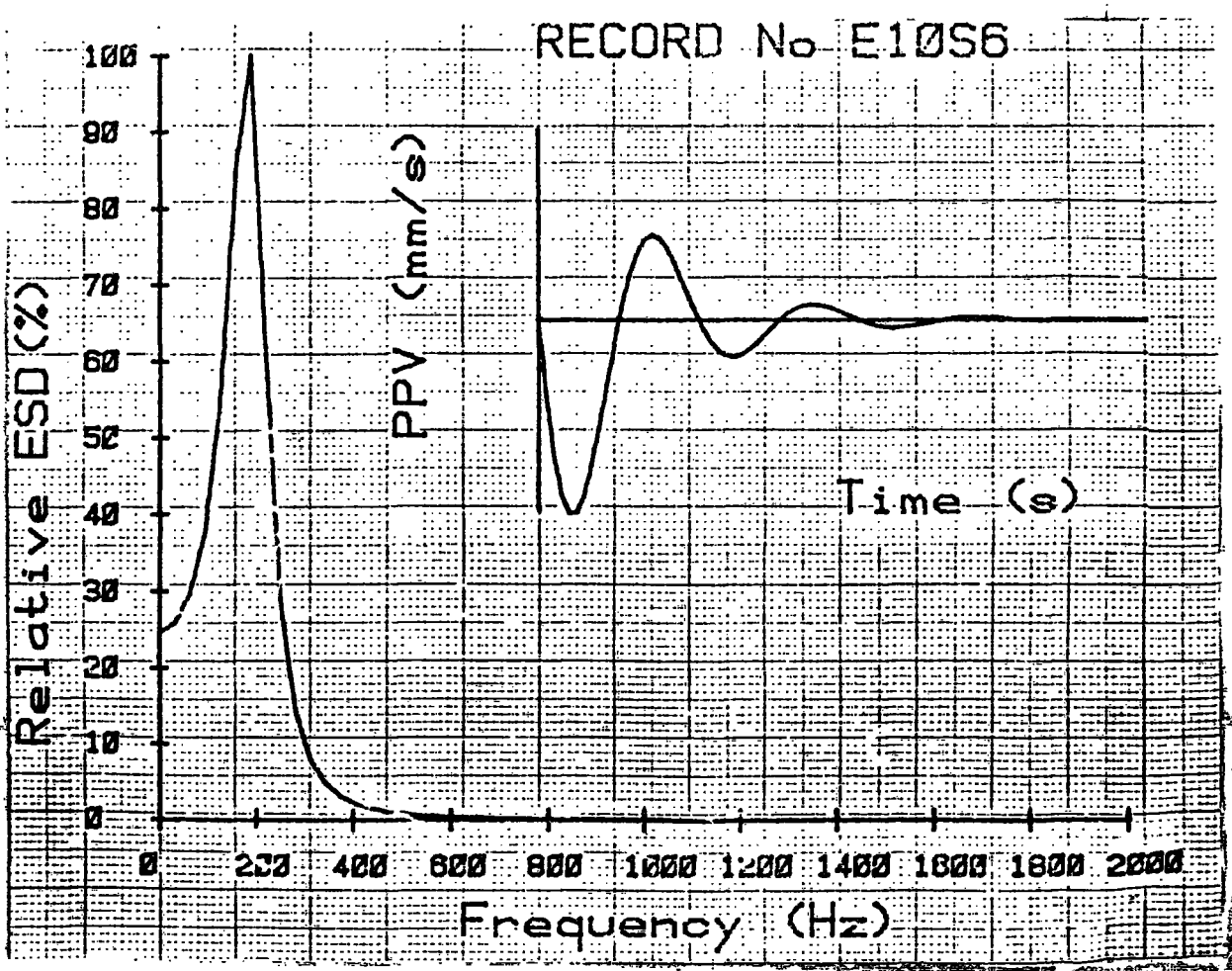

Fig.8.2 SYNTHESISED SPECTRUM

essentially the same.

It will be noted that the shape of this observed wave packet is very similar to that calculated by Sharpe (1942), and many others (*see* Section 3.3) for a pulse due to an exponential rise and fall of pressure on the wall of a sperical cavity within an elastic continuum. This theoretical approach predicts the amplitude of the motions to comprise a sinusoidal oscillation of frequency ω, which is heavily damped by an exponential factor α. The PPV of the motion is proportional to the peak applied pressure and the 'cavity' radius, a, and is inversely proportional to the material acoustic impedance, ρC, and the range, r. The geomechanical rock properties which define the amplitude, frequency and duration of the motions are simply described in terms of wave velocity and Poissons' ratio, the combination providing a full description of the dynamic elastic properties of the material. It is of considerable interest to test the quantitative accuracy of this theory with particular regard to the frequency of the observed motions which is given by:

$$\omega = C(1-2\nu)^{\frac{1}{2}}/a(1-\nu) \qquad \ldots\ldots \quad (8.12)$$

$$\text{or} \quad a = C(1-2\nu)^{\frac{1}{2}}/\omega(1-\nu) \qquad \ldots\ldots \quad (8.13)$$

In practice the charge takes cylindrical rather than spherical form and 'a' must be considered as a measure of an 'equivalent cavity' rather than a precise measure of the radius of the spherical source.

Figure 8.3 shows the spectral distribution of energy for several charge weights and indicates that most of the energy in the wave packet is carried at or around 200 Hz. (The apparent lack of variation with charge weight will be discussed later.) Taking the velocity C to be

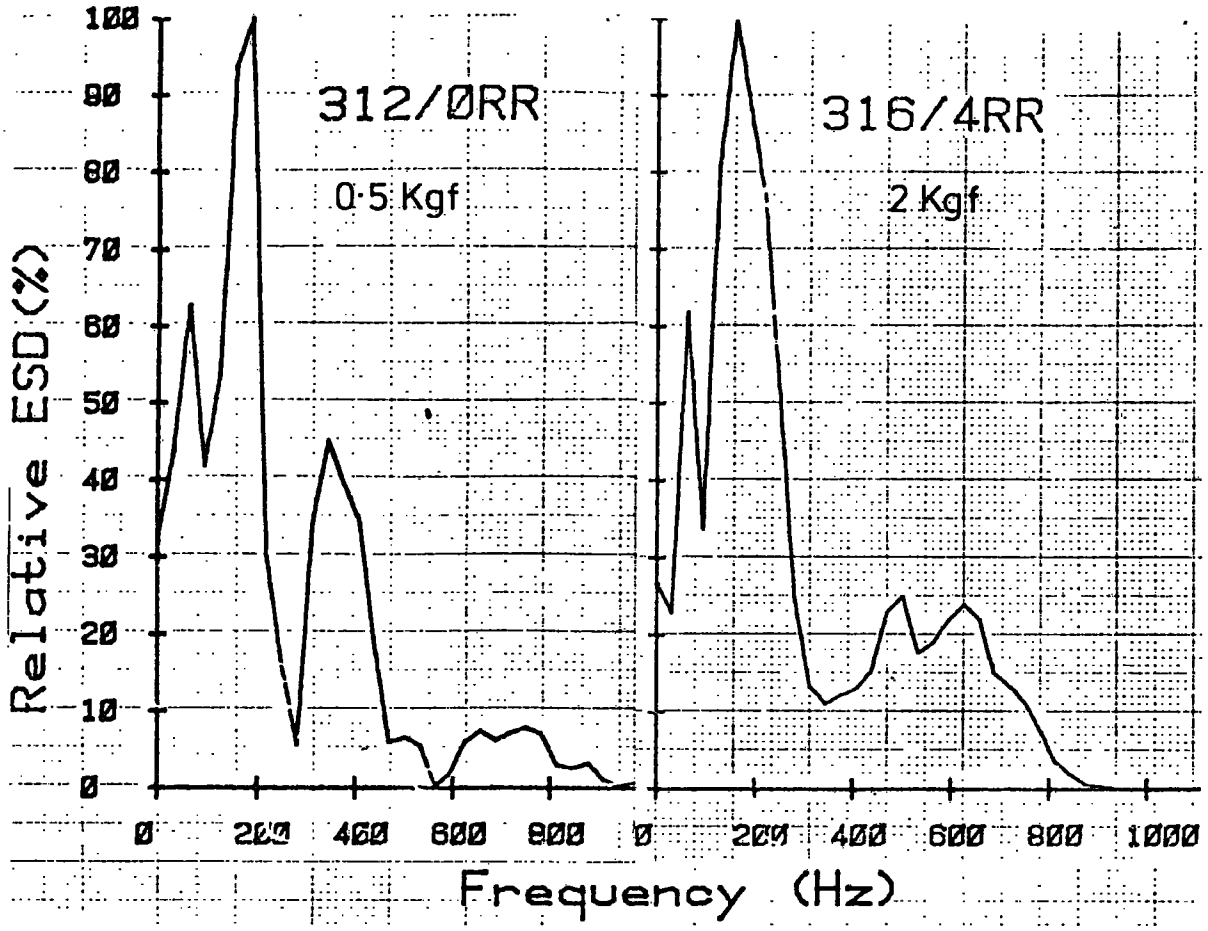

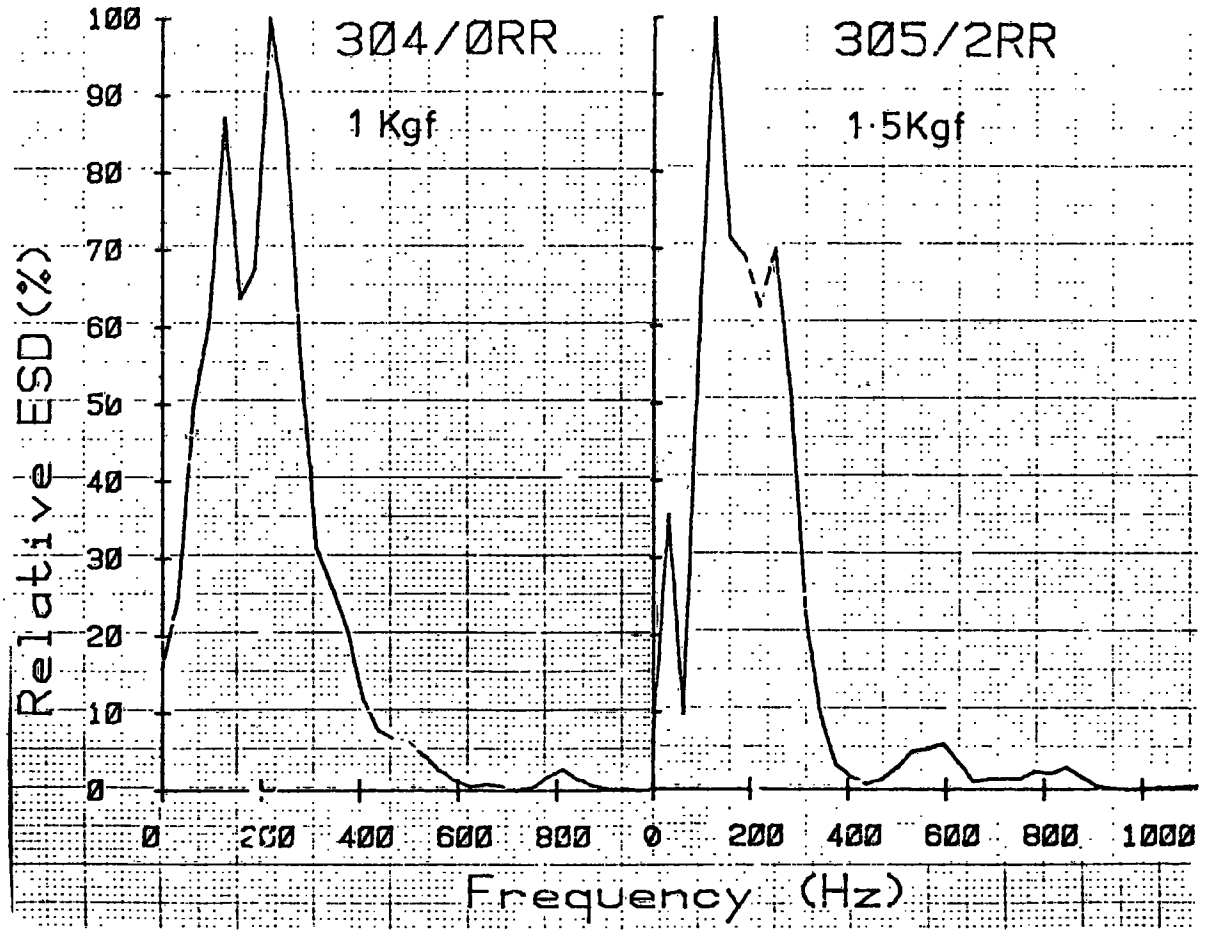

Fig. 8.3 EFFECT OF CHARGE WEIGHT VARIATION AT KILLIECRANKIE

5000 m/s and Poissons ratio as 0.25, then the 'equivalent cavity' dimension, a, is given using equation 8.13 as 3.75 m.

A similar calculation may be made using the initial pulse width (*see* Fig 7.17, average pulse duration at 10 m taken as 1.25 ms) rather than the spectral peak to fix ω. This yields an equivalent cavity size of 1.9 m. The difference is due to the slightly higher frequency of the initial pulse compared to the following motions. Clearly this equivalent cavity radius cannot be considered as being directly related to a spherical explosive volume which would, of course, be very much smaller. We require that the equivalent cavity represents the dimensions of a radiator which, for the given elastic properties, will resonate at the observed frequency. This matter is discussed at some length in a most useful paper by O'Brien (1969) in relation to the equivalent cavity dimensions due to seismic exploration pulses in Bunter sandstone. O'Brien discusses the 'equivalent radiator hypothesis' and uses it to describe and explain his field observations which are similar to those reported here in that the size of the equivalent radiator was larger than predicted by theory. (His results gave a value for 'a' of 3.9 m for a charge of 8.5 kgf, based on initial pulse duration.) He rightly argues that 8.5 kgf of explosive could not blow a cavity of this size "but since the boundary conditions within a solid are more complex than those at a cavity wall, there is no immediate reason to seek quantitative agreement between the forcing function at an equivalent radiating surface and the actual stress-time relation in the rock". In seeking an explanation O'Brien suggests that this equivalent radiator radius may represent a tensile failure envelope inside which the rock behaves in a similar manner to a fluid. This serves to explain the observed motions and is consistent with his field conditions.

O'Brien's results lead to the calculation of an equivalent cavity 2.4 m in radius for a 2 kgf explosion in the Bunter sandstone. That is a radius about 25% larger than that observed in the stronger rocks investigated in this thesis. Thus, as might be expected, the stronger material has a smaller tensile failure envelope, which results in a smaller equivalent cavity and higher frequency motions. The equivalent radiator hypothesis proposed by O'Brien may therefore provide an apparently satisfactory explanation which relates the observed source frequencies to the geometric, strength and elastic parameters of the trial blasts described.

However, there appears to be a significant difference between the observed source characteristics of geophysical exploration and construction related explosions. The spectral distribution of energy would be expected to be dependent on the size of the equivalent radiator and this should vary with charge size. In fact, in exploration seismology it is well known that the distribution of energy with respect to frequency is dependent on the charge weight. The expected predominant frequency has been shown to be inversely proportional to the cube root of the charge weight (Ziolkowski and Lerwill, 1979) and this has also been noted in the field. In particular, O'Brien has given seismic energy spectra which conform closely to this condition. For construction blasts this frequency dependence on charge weight has not been generally observed and Duvall and Atchison (1950) have undertaken studies to investigate why the frequency content of the initial motions close to a construction blast are "apparently independent of the charge or cavity size". Their work did little to suggest an explanation of this effect which had been noted previously by their colleagues at the US Bureau of Mines. Indeed, even the recent Bureau of Mines publication (Stagg and Engler, 1980) which

reports data related to a wide variety of charge sizes shows a very narrow and consistent bandwidth for the frequencies induced by construction blasts.

The spectra shown in Fig 8.3 show remarkably similar energy distributions with a spectral peak at just below 200 Hz for various charge weights. Note that for a charge weight decrease from 2 kgf to 0.5 kgf we would expect the frequency at the spectral peak to increase by a factor of 1.6, that is, $\left[\frac{2}{0.5}\right]^{\frac{1}{3}}$. Comparison of spectra is more sensitively undertaken using the relative gain factor spectrum between explosions of different weights. Figure 8.4 (upper and lower) shows an almost totally consistent gain factor for all frequencies below 300 Hz, the part of the spectrum where the majority of the energy lies. (Above 300 Hz there is relatively little energy and variation of gain factor is greatly exaggerated where Fourier components of one of the records, tend to zero.) It is of interest to note that the time domain records, normalised with respect to their PPV, and superimposed on the Figure, show great similarity despite the variations in charge weight. The trials at Penmaenbach showed the same lack of frequency dependence on charge weight although little data were available closer than 40 m to the source. Figure 8.5 shows spectra for a range of charge weights from 0.68 kgf to 3 kgf. Note that all the spectral peaks occur at about 45 Hz when we may have expected a frequency difference factor of $(3/0.68)^{\frac{1}{3}}$, that is, 1.65. The lower frequency of the spectral peak at Penmaenbach compared to that at Killiecrankie is directly related to the increased range at which the measurements were made. This is discussed in the following section. Again, the gain factors between the spectral distributions for different charge weights (Fig 8.6) show no significant variation at all at frequencies below 200 Hz (where the energy levels are significant).

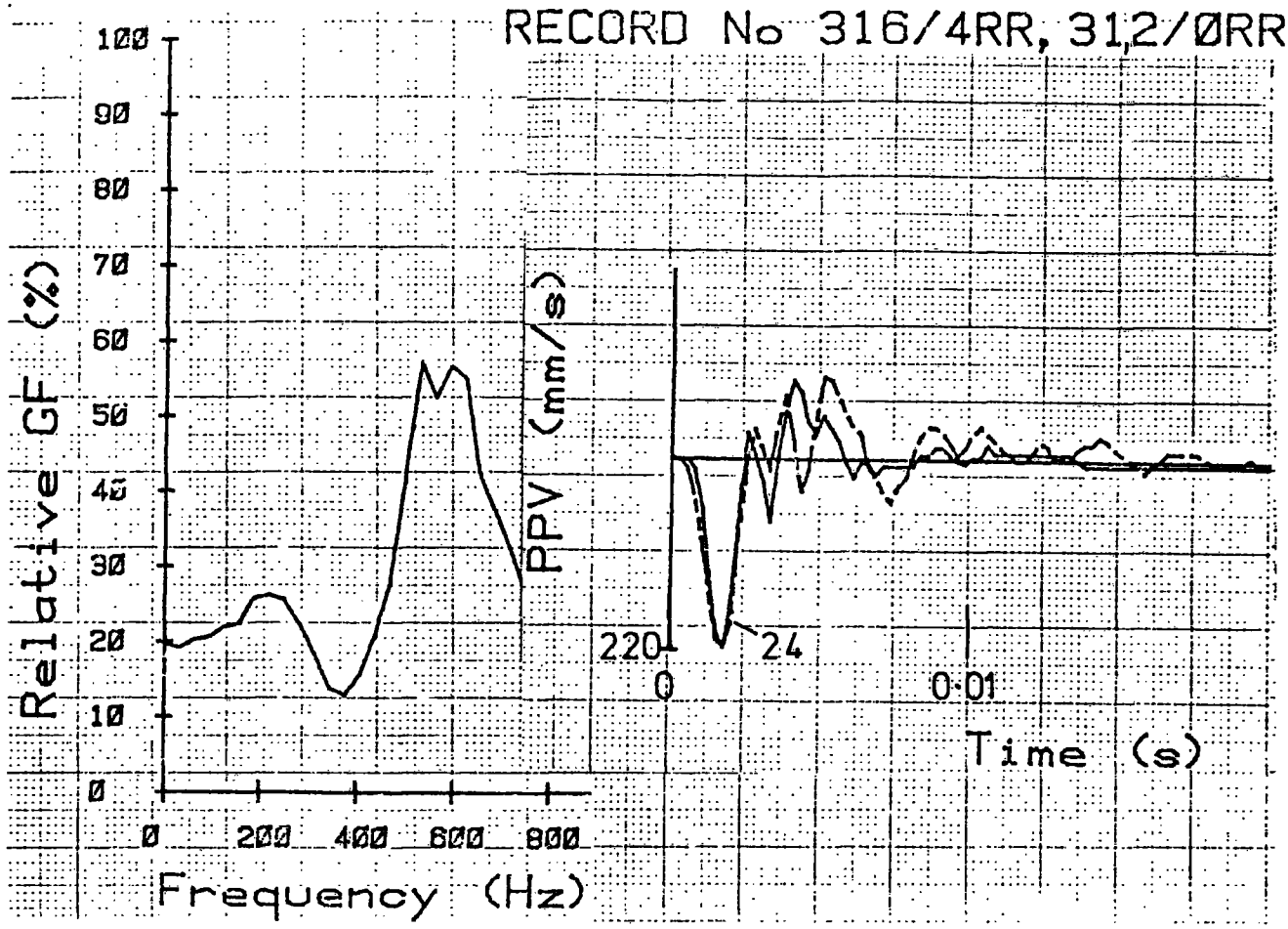

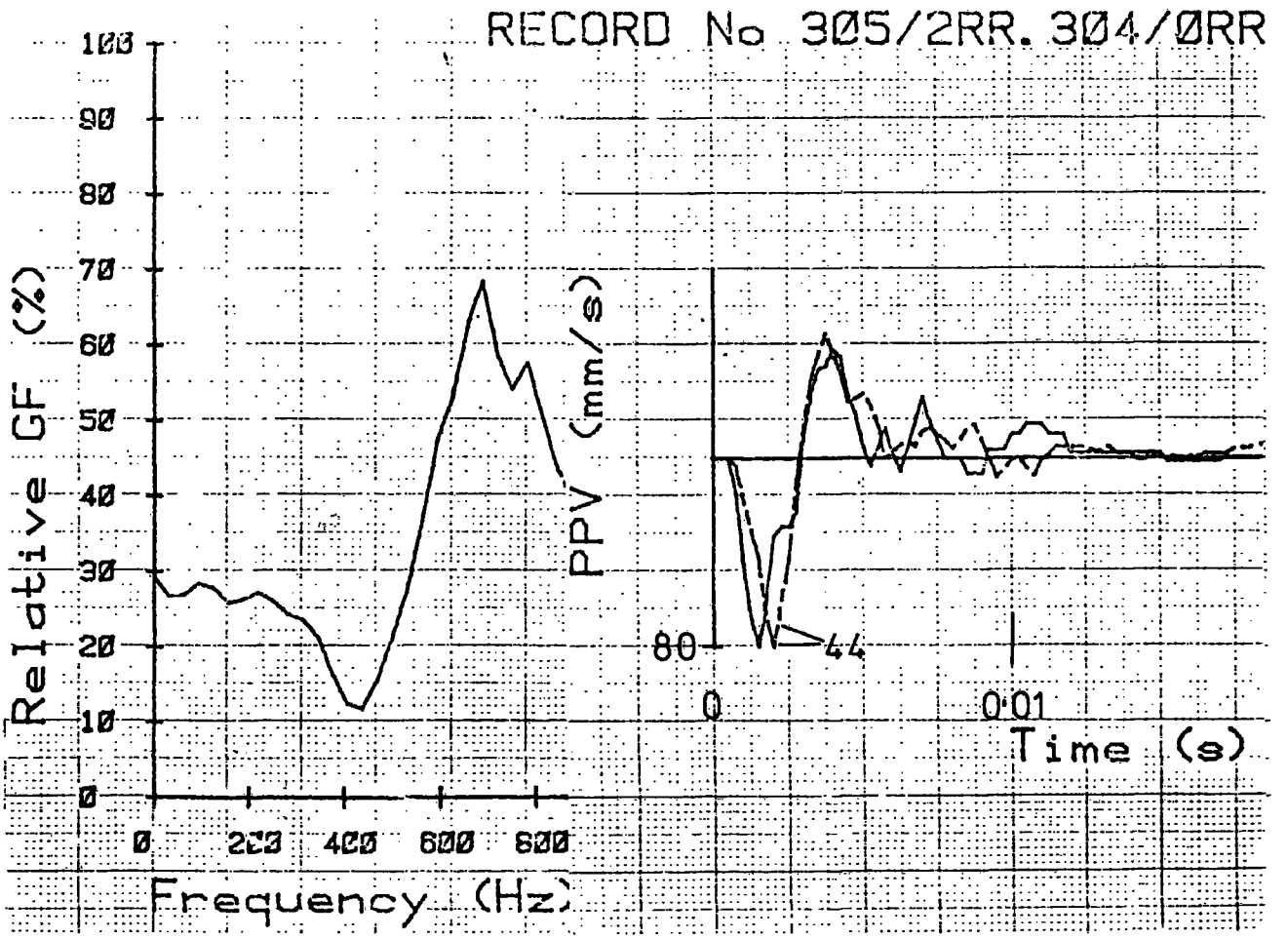

Fig. 8.4 GAIN FACTORS BETWEEN CHARGE WEIGHTS

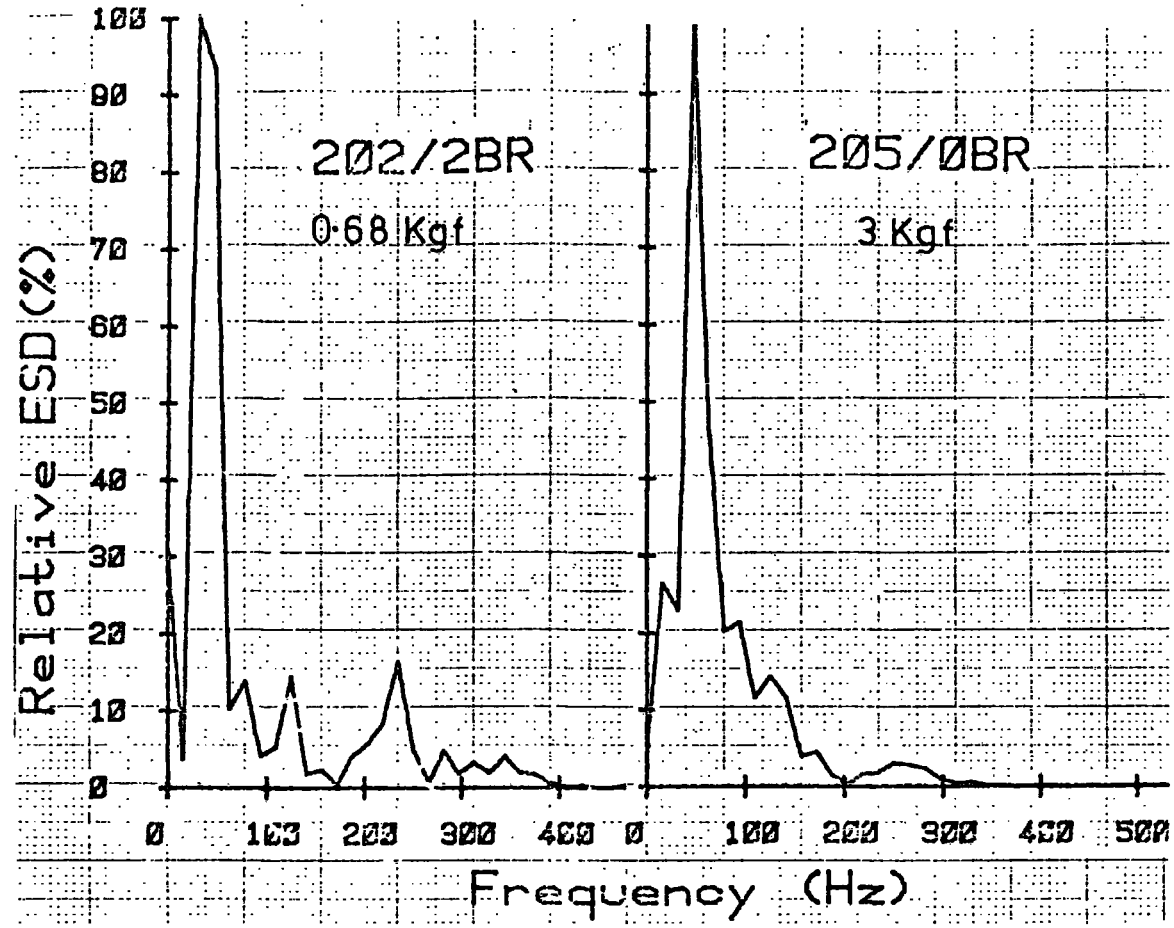

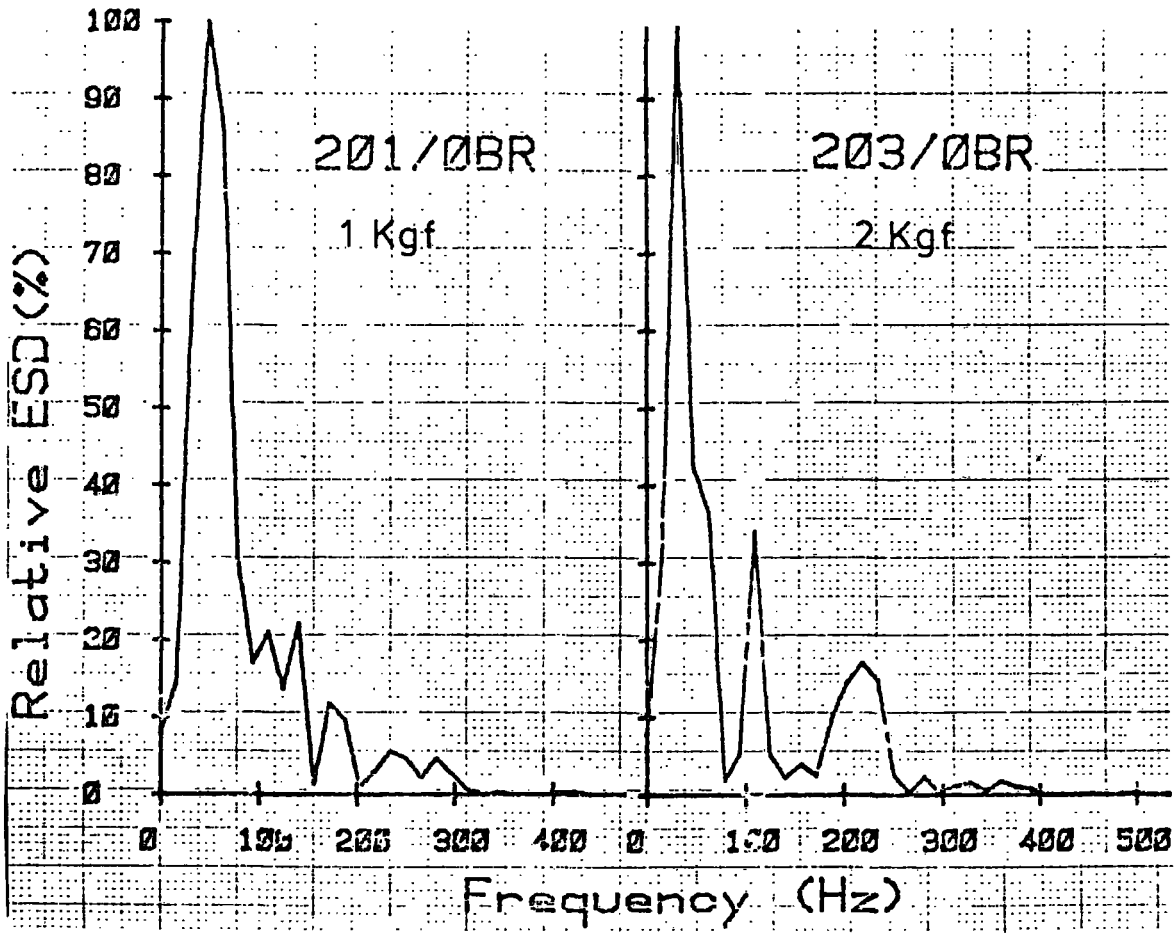

Fig. 8.5 EFFECT OF CHARGE WEIGHT VARIATION AT PENMAENBACH

We may conclude that although the range of field charge weights was not large it was sufficient to produce a distinct variation in the ESD of particle velocity if the size of the equivalent radiator had in fact varied in the manner described by O'Brien and others. Such a variation was not observed and it is of interest to speculate as to why this was so.

All the trial 'construction' blasts took place within 5½ m of the surface whereas 'exploration' charges are generally placed at greater depth to remove the modifying effect of the weathered upper layers. O'Brien's trials were carried out with charges at an average depth of 60 m (with a range between about 15 m and 80 m). Indeed, it is well known that in order to preserve the spectral breadth of frequencies generated for reflection seismic work it is desirable to place the source below the 'weathered' layers. By working with charges close to the surface we would therefore expect to lose spectral breadth (in particular, the high frequencies) associated with the source. It may be that at depth O'Brien's concept of a tensile zone of failure dominates the size of the equivalent cavity; near the surface, however, it may be reasonable to suppose that the natural discontinuities, which are not tightly closed by substantial overburden induced stresses, may have an important effect in determining equivalent cavity size. For instance, a borehole 5 m in length will have intercepted many discontinuities (at Killiecrankie, Penmaenbach and most sites) and if the explosive pressures are considered to act from within these discontinuities as well as from the borehole then it is clear that the size of the equivalent radiator will be more dependent on the discontinuity form and distribution than the weight of the charge in the borehole. Thus the size of the equivalent radiator (hence the input vibration frequencies) may be dependent on the geometrical conditions imposed by the site rather than on the weight of the charge. Most of

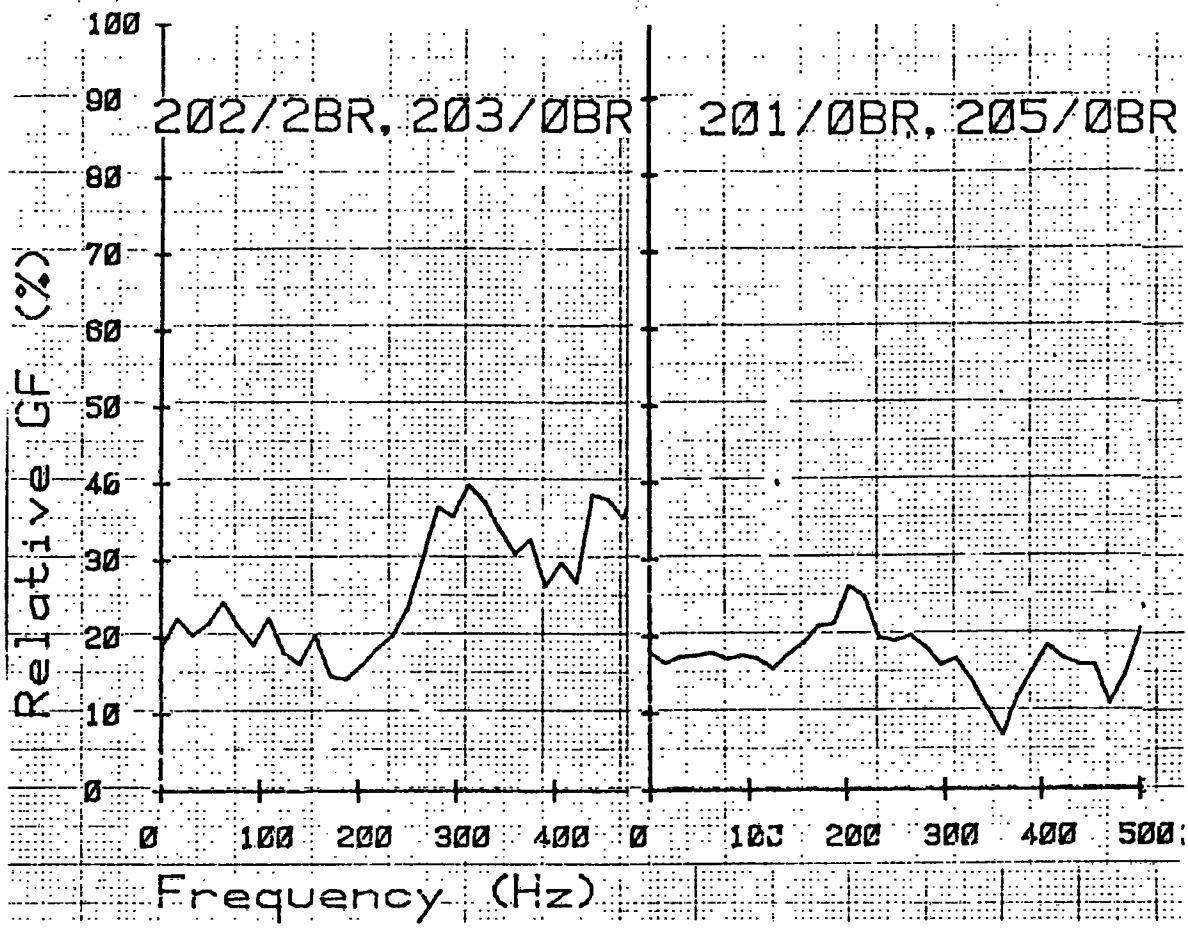

Fig.8.6 GAIN FACTORS BETWEEN CHARGE WEIGHTS

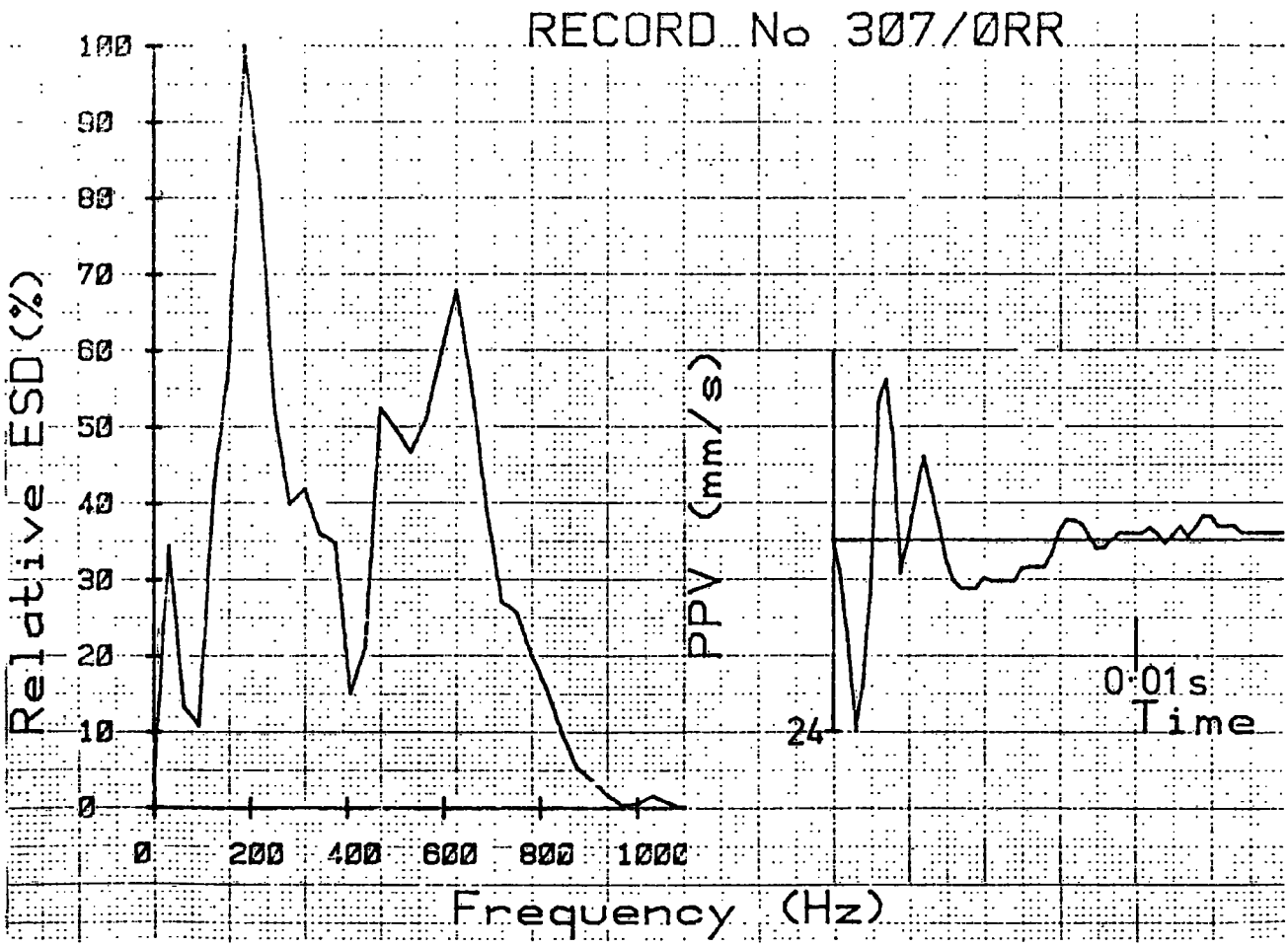

Fig.8.7 WIDE BAND INPUT (SMALL CHARGE WEIGHT)

measurements of construction induced blasts have been taken with sources within 10 m of the surface and it is to be expected that rock in this strata will generally be well-jointed. Observations of seismic exploration pulses have deliberately excluded this zone because of its objectionable filtration characteristics and it is suggested that this difference in rock weathering and *in situ* stress condition may explain the observed difference in source characteristics.

There is another consideration relative to the equivalent radiator hypothesis which again relates to the observed lack of variation of spectral distribution with respect of charge weight from construction explosions. For effective excavation purposes the total charge is distributed in the rock mass such that many boreholes containing a similar charge weight may be fired at one time. The total charge weight detonated is generally increased by increasing the number of charged holes, <u>not</u> by increasing the charge weight in the same number of holes. If we consider each charged borehole to act individually as an equivalent radiator of fixed dimension, then superposition of the motions could occur without changing the spectral distribution of the energy. Therefore, as charge weights are increased by firing more boreholes at one time, the amplitude of the motions will increase, but the spectral distribution of the energy could remain similar to that for an individual equivalent radiator.

As a footnote to this discussion it is necessary to mention the spectra from two of the eight ½ kgf charges at Killiecrankie. Six of the charges gave similar spectral distributions to those in Fig 8.3 with a clearly dominant peak at just below 200 Hz. However, two charges, one of which is illustrated in Fig 8.7, revealed spectra with a more complex structure having significant amounts of energy shifted to higher

frequencies. This would in principle be consistent with a small charge length intercepting fewer (and therefore probably less expansive) discontinuities, thereby producing a smaller equivalent cavity. In order to investigate this isolated effect further detailed observations of discontinuity frequency and aperture within the blastholes would be required prior to the blasting.

8.4.2 Charge decoupling

The effects of decoupling the explosive charge from the rock by leaving a substantial air space around the charge is discussed in Section 3.3.2.3. The major effect that this decoupling has on the PPV is shown in Section 7.4.2, and Fig 7.15 quantifies the substantial and important reduction in PPV that may be obtained by decoupling in this way. Having quantified PPV reduction it is also of interest to determine the spectral distribution of energy close to the source, since any change in frequency content might be expected to alter the rate of attenuation with propagation.

Figure 8.8 shows the time domain and spectral records for 25 mm diameter decoupled charges in 75 mm and 100 mm drillholes. Note that the spectral distribution of energy is similar in both cases to that shown for normally stemmed charges in Fig 8.3. Further, the time domain records show the familar heavily damped sinusoidal oscillation at about 200 Hz. From these observations we may conclude that although decoupling substantially reduces the level of particle velocity it does not materially change its spectral distribution. We may therefore assume that the decay with propagation characteristics of the motions may be considered as similar to those of normally coupled charges. The field results confirm this conclusion and are consistent with the discussions regarding equivalent radiator dimensions given in the previous section.

It is worth mentioning here that in an empty cylindrical hole a kind

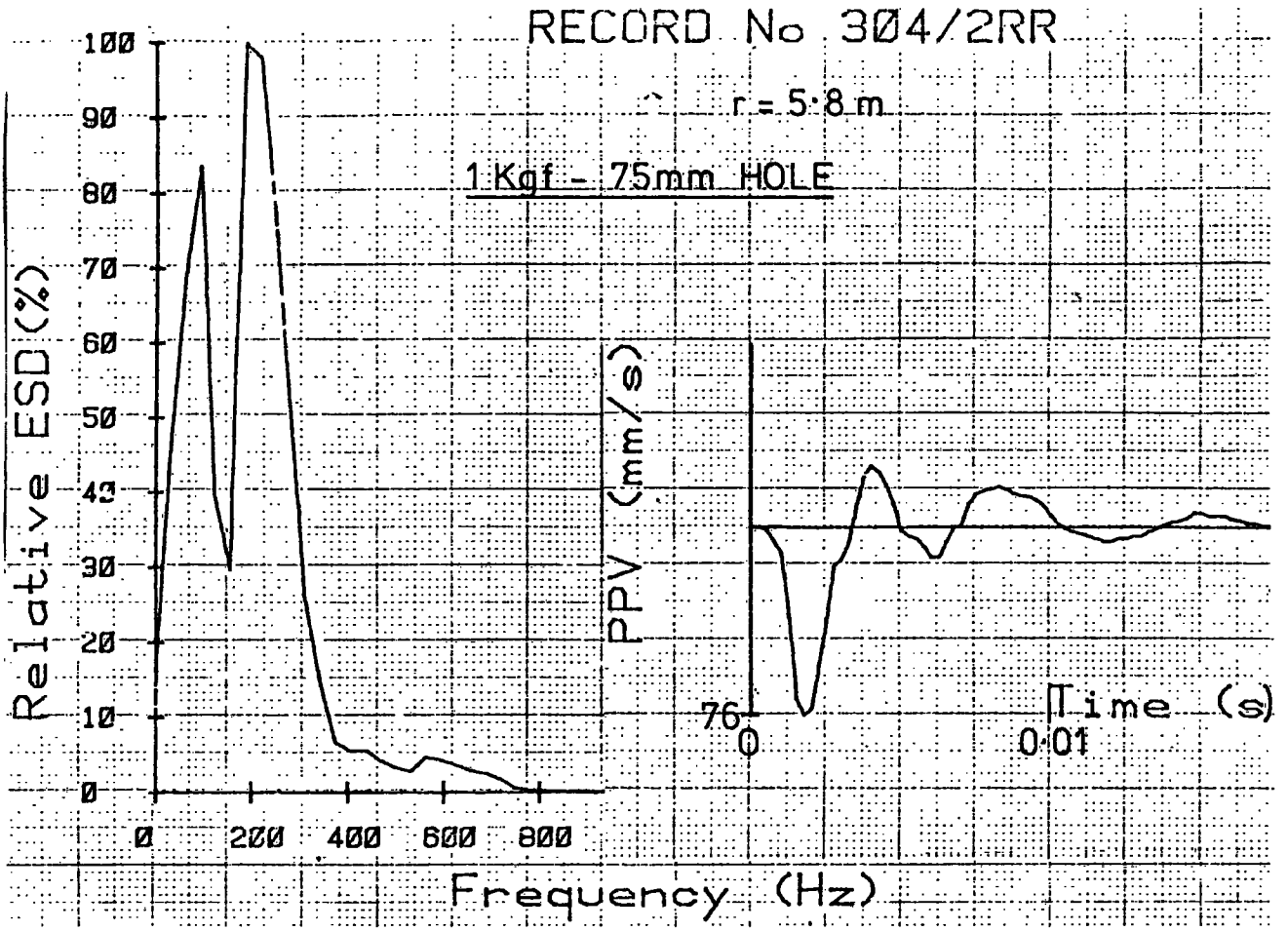

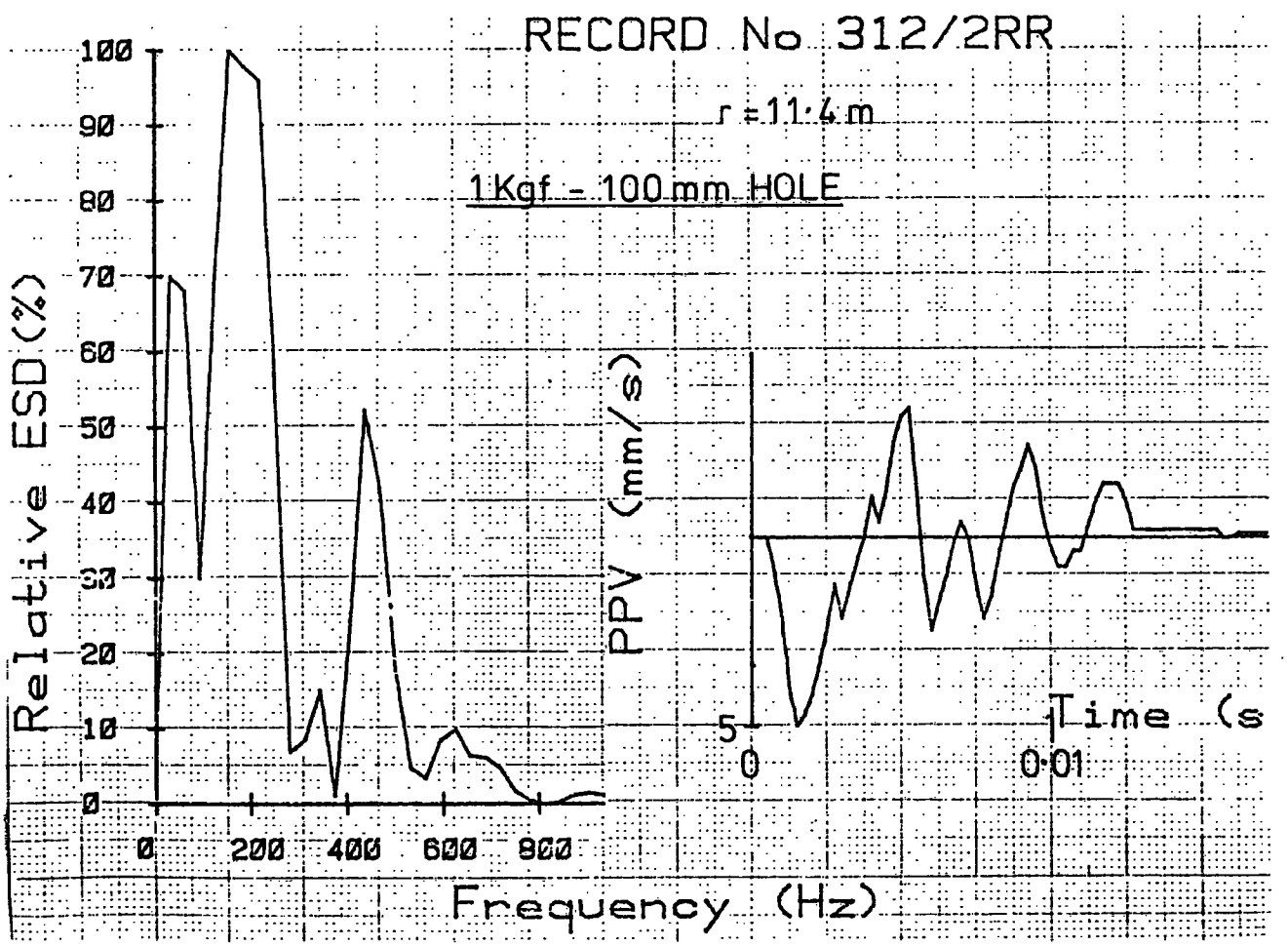

Fig. 8.8 EFFECT OF DECOUPLING THE EXPLOSIVE

of surface wave, known as a tube wave, can propagate along the axis of the hole with its energy confined to the vicinity of the hole. At wavelengths beyond about three times the borehole radius (as in our case) they are swiftly attenuated, their energy being radiated into the rock mass as shear waves. If significant this mechanism would cause greater motions in the horizontal and vertical directions (as opposed to radial) for decoupled explosions. However, no such variation was noted and it would therefore appear that the effect is negligible for our explosive configuration.

8.4.3 Explosive energy input

Although it is the distribution of energy in the frequency domain which is of primary interest we may for completeness calculate the energies radiated by the diverging wave packet. This is most usefully expressed as a percentage of the chemical energy of the explosive which is taken as 4×10^6 j/kgf for the 80% strength blasting gelatine (personal communication with Nobel Explosives Co).

It can be shown that (Jaeger and Cook, Ch 13, 1976), for a single harmonic component, the energy passing through a spherical envelope of radius, r, during a period of time, t, is given by:

$$P = 2\pi\rho C r^2 V^2 t \qquad \ldots\ldots \quad (8.14)$$

This equation may be readily evaluated for the wave packets processed in the frequency domain using the computed value PT (*see* Section 8.3.2) which is the sum of the individual energies at each harmonic component over the total spectral range. The time, t, must be taken as the total sampling period (N.DT) and ρ the density of the material. There is a major source of uncertainty inherent in this calculation, this being

associated with the fact that the recorded motions will comprise waves with more than one characteristic velocity. Close to the source, say within 15 m, where the motions are reasonably well defined it may be acceptable to assume that the majority of the particle motion can be attributed to compressional wave motion propagating radially away from the source. At greater distances however, the character of the motions is changed considerably by mode conversion effects dependent on the many discontinuities present in the near surface strata. This change in character of the motions is discussed in Section 3.3.4 and is further considered with respect to frequency content in the following section. Unless the distribution of energy between wave types can be identified total energy calculations of this kind are likely to be most unreliable. This is particularly true at distances where the wave packet is a complex summation of direct, scattered, reflected, refracted and diffracted arrivals with shear, surface and compressional wave velocities. Table 8.1 shows the vibrational energy transmitted through a hemisphere of radius 10 m at Killiecrankie for various coupling conditions. It is of interest to note the effect of decoupling which greatly reduces the seismic energy input to the rock mass. This is to be expected as a result of the significantly reduced particle velocity with retention of similar spectral and wave packet duration characteristics.

TABLE 8.1

Seismic energy 10 m from explosion as percentage of available chemical energy

	Total Radiated Energy %		
Charge weight (kgf)	0.5	1	2
coupled explosions	2.39	3.02	3.91
Decoupled 75 mm hole	1.05	1.32	-
Decoupled 100 mm hole	0.31	0.44	-

An annular void around a centrally located explosive charge causes not only a significant drop in the stress applied to the borehole wall/'equivalent cavity' but also greatly reduces the efficiency of energy transmission into the rock. This may be due to the greatly increased impedance mismatch caused by the air gap and further detailed study of this effect would seem desirable particularly as this type of detonation will be increasingly used for presplitting work. Lack of significant change in energy spectral distribution has been reported (Atchison *et al*, 1964) for sand decoupled charges but no data regarding the spectra, PPV or energy propagation from air spaced charges have previously been available. The energies are calculated on the basis of spectral summation in the radial direction only, however sample calculations of energy content at this range in the 'vertical' and 'horizontal' directions showed that, for the majority of blasts, less than 20% of the energy was transmitted in what may be taken as source generated shear wave motions. The energy values given are similar to those found by other workers (eg O'Brien, 1969) for shots at shallow depth and indicate that larger charges tend to be more efficient sources of seismic energy. This is consistent with the exponent associated with charge weight determined from the site law regression equations (*see* Section 7.4.2.1) which indicated that PPV was proportional to $M^{1.17}$. As energy is proportional to PPV squared, this equation suggests that the seismic energy output will vary as $M^{1.37}$ (ie, $(M^{1.17})^2$).

Similar calculations were carried out for 1 kgf detonations at Penmaenbach where it was found that approximately 2.7% of the explosive chemical energy was transmitted to the rock mass. At this site the particle velocity was observed at some 30 to 50 m from the source however, and the motions were clearly of a complex nature, comprising both P & S

waves in indistinguishable proportions. The total seismic energy was computed by summation of radial, horizontal and vertical component energies. It was assumed that compressional wave velocity was appropriate to all radial motions and shear wave velocity appropriate to all horizontal and vertical motions.

8.5 The effect of range

Although the decay of PPV with range has been observed to be remarkably consistent over a wide variety of sites, the redistribution of energy within the wave packet is not well understood (*see* Section 3.3.4). The mechanisms which change the form of wave packets as they propagate in inhomogenous anisotropic materials are extremely complex and, although there is a body of information emerging related to certain geophysical problems, the 'weathered' surface strata have generally been avoided as being either of little interest or because of difficulties with their variety and unpredictable nature. Unfortunately, for construction blasting it is usually this strata which is of greatest importance. Further, much of the geophysical research effort has concerned wave propagation at distances considerably in excess of those associated with damage or intrusion from construction works.

Seismic prospecting has stimulated considerable effort towards a better understanding of source and transmission functions for small explosions. The work of O'Brien (1969) and Ziolkowsi and Lerwill (1979) has been mentioned previously and Aki and Richards (1980) deal with wave propagation theory in considerable detail. In particular Aki and Richards deal with scattering processes which are classified using two dimensionless parameters dependent on wavelength, inhomogeneity scale length and wave travel distance. For the media with which we are concerned it is extremely

difficult to determine, and especially to predict, the effects of the wide range of discontinuity scale present in the near surface strata. For use in the study of earthquake induced motions observed at relatively long ranges the distribution of inhomogeneities may be satisfactorily described by both statistical and deterministic methods. These techniques are being continuously refined. In particular Crampin (1981) has published a wide ranging review of wave motion in anisotropic and cracked elastic media, although it is at present difficult to anticipate any useful exploitation of these advances in the field of civil engineering construction.

For typical construction sites the scale of the inhomogeneities may vary from less than 1 mm (crystal structure) to tens or even hundreds of metres (faulting, lithological changes). We may therefore expect to observe effects ranging from totally isotropic scattering due to discontinuities much smaller than the wavelength to strongly forward scattered motions from larger discontinuities. The presence of discontinuities will elongate the wave packet and these changes will be heavily dependent on frequency and are therefore usefully observed in the frequency domain. The prediction of this energy redistribution is hampered by the lack of effective knowledge of the size and distribution of the discontinuities although the other relevant field parameters, wavelength and propagation distance, may usually be determined. Reflections and refracted waves from surface and sub-surface formations will also contribute to the extended duration and complexity of the motions, particularly in the tail of the wave packet.

Where motions with different characteristic propagation velocities are superimposed this will again cause the wave packet to increase in duration. This added difficulty will occur where various types of wave are created by non-spherical symmetry at the source and by mode conversions at discontinuities. Sato (1977) has analysed the redistribution

of energy during isotropic scattering, including mode conversion effects, to qualitatively describe the temporal development of seismic energy density close to small earthquakes. For our purposes an extension of this work to deal with forward scattering processes would seem potentially of interest.

Although the fields of earthquake and exploration seismology have heavily influenced geophysical wave propagation research, recent interest in the exploitation of the potential energy resources of hot rocks at depth has also provoked some interesting investigations. In particular, Fehler (1979) has used the seismological properties of the rock mass between a piezoelectric transmitter and receiver on a 'geothermal' borehole to investigate the nature and geometry of the hydraulically fractured rock structure. His work provides a theoretical backgroumd and useful bibliography with some experimental confirmation of scattering processes from relatively high frequency wave motions. In the United Kingdom Batchelor *et al.* (1983) have used the microseismic emissions given out during hydraulic well stimulation to monitor the location and growth of the geothermal reservoir. Again, these studies relate to rock at depth and the receiving transducers were positioned in boreholes 200 m deep to avoid difficulties associated with the near surface region.

This section provides spectral analysis of the field data to determine how the distribution of energy in the wave packet varies with range. Changes in wave packet form can be qualitatively described in terms of the general mechanisms which redistribute or absorb the vibrational energy, but because the actual geometrical and absorption properties of the rock mass are not accurately known quantitative solutions or predictions of wave packet form are found difficult to achieve.

Similar difficulties have been encountered by Young and Hill (1981)

who have attempted to characterise rock masses for opencast mining applications in terms of their frequency selective transmission properties. They conclude that although near surface strata do act as a severe low pass filter the mechanism is non-linear and cannot therefore be accurately explained in terms of a specific dissipation constant (Q). Their absorption spectroscopy techniques show that 'a linear relationship is seldom obtained due to the broken state of the rock and that certain frequencies are attenuated dependent upon the ratio of the seismic wavelength to the size of the characteristic rock fractures'. The fact that these complex site-specific filter characteristics can probably be used to evaluate the quality of near surface rocks indicates that the waveform from a complex construction blast is unlikely to be reliably predictable, except for its general loss of high frequency components.

A recent meeting on 'the geophysical aspects of cracks in rocks' (Joint Association for Geophysics, Burlington House, London, 16 November 1983) indicated that although theoretical models are becoming available there is often little field evidence to support them. Indeed, during the informal discussions at this meeting it became clear that researchers from various eminent establishments found it hard to agree on some of the mechanisms involved, and the interpretation of the sparse field data (S Crampin, IGS Edinburgh; S A F Murrell, University College, London; G Simmons, MIT, Massachusetts; and others).

8.5.1 Penmaenbach

Figures 8.9 and 8.10 show the effect of propagation distance on spectral energy distribution for two different charges at Penmaenbach. It must be noted that the distances from the source are not in quite the same direction (*see* Fig 4.2) and therefore comparison is difficult as each

wave packet will have travelled through different volumes of rock. However, the trends shown by all the data are clear and consistent:

(a) the energy spectral peaks occur at a frequency of about 40 Hz at all distances observed.

(b) at distances between 30 and 50 m energy at frequencies up to 400 Hz is present.

(c) at distances in excess of 80 m there is no significant energy present at frequencies above 200 Hz.

Figure 8.11 gives the variation of gain factor with range and shows how the higher frequencies are progressively attenuated to a greater and greater extent. There is a steady general trend of decreasing gain factor which is locally disturbed at harmonics where the Fourier components of the shorter range record happen to approach a near zero value. Also there is an apparently high attenuation of the lowest frequencies present at the zero, and lower order harmonics. This initially unexpected effect is also present in the processed records from Killiecrankie. At both sites there is relatively little energy present at these very low frequencies but it is nevertheless relevant to explain this apparent anomaly when comparing spectral distributions at different ranges. Note that it does not occur when comparing differing charge weights (Figs 8.4 and 8.6) at similar ranges.

The wave packet close to the source is generally of a simpler form than that observed at distance (*see* Fig 8.1). That is, it comprises a large initial disturbance which is rapidly attenuated whereas at distance the longer duration wave packet comprises many oscillations about the zero level and which are of more similar amplitude. A short wave packet is necessarily richer in low frequencies than a longer one comprising motions with similar period. Thus the wave packet observed close to the source

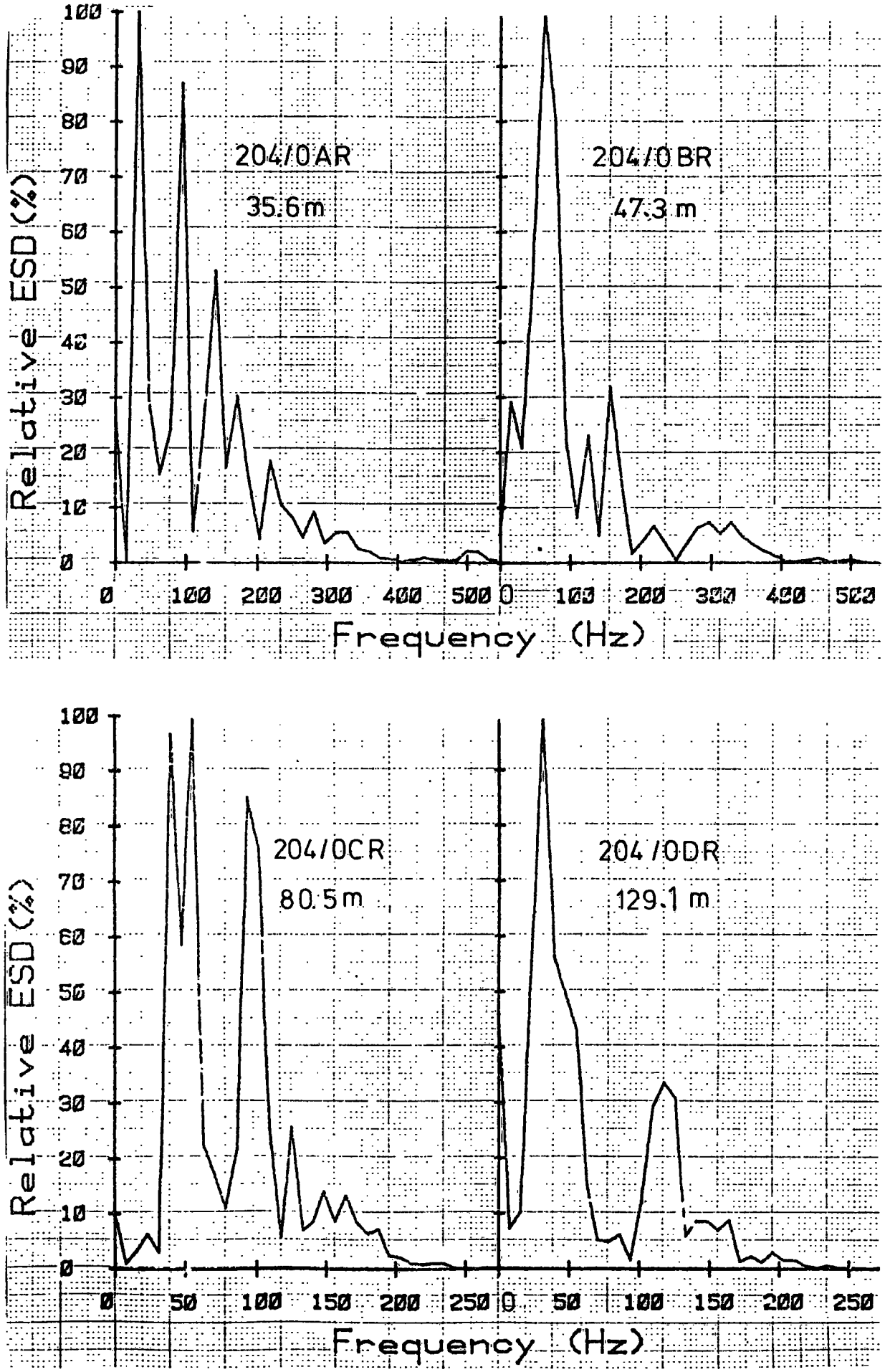

Fig. 8.9 EFFECT OF SOURCE DISTANCE (3Kgf , PENMAENBACH)

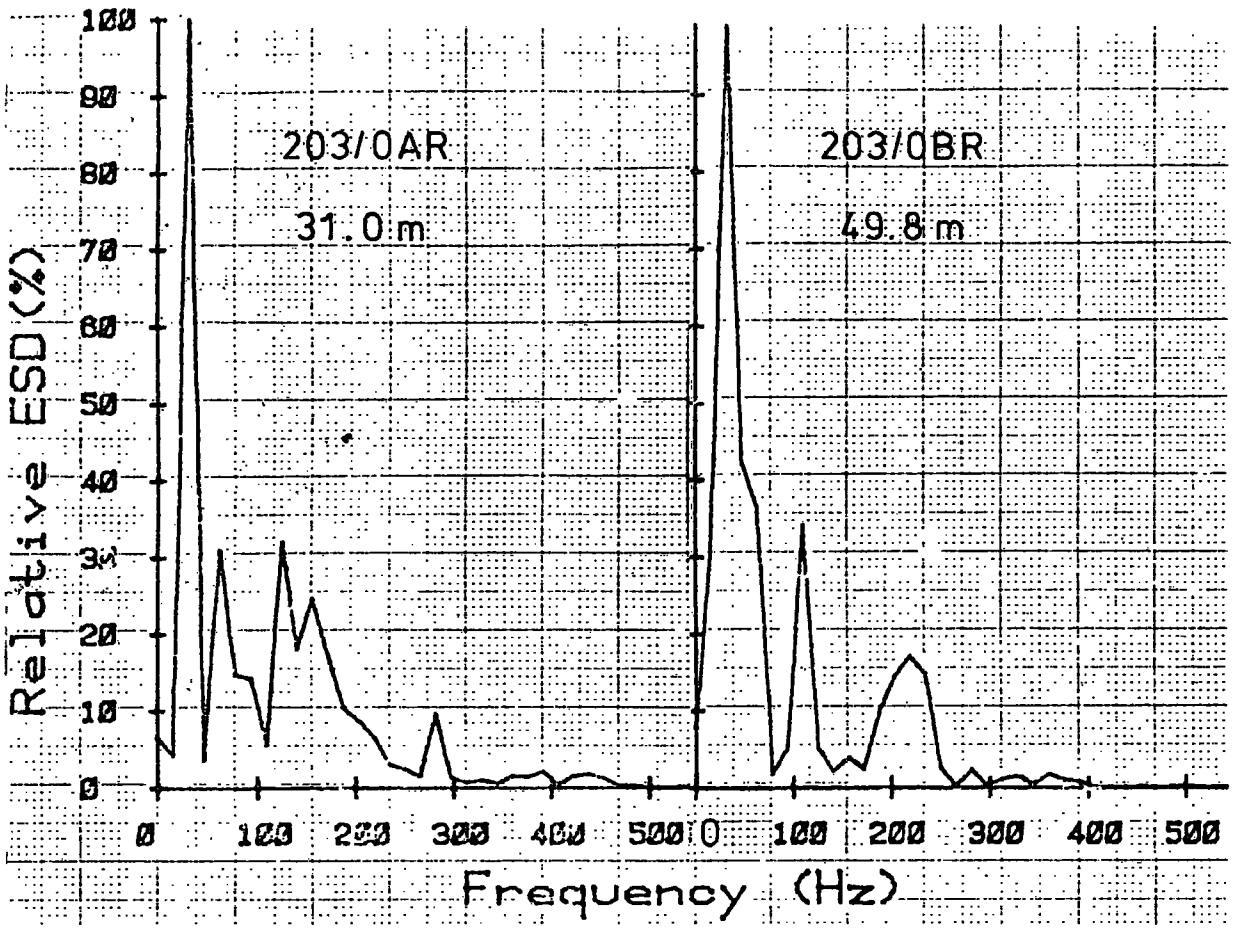

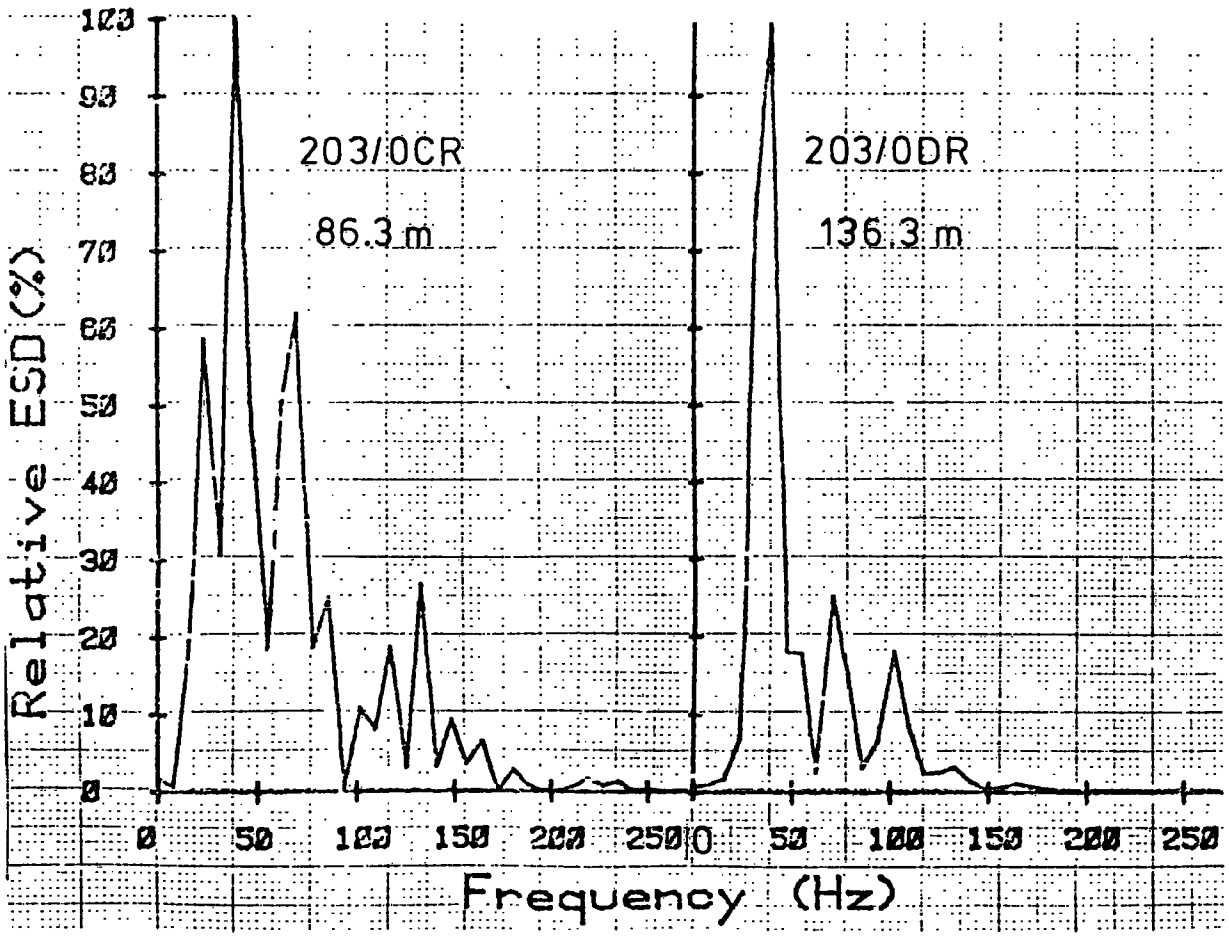

Fig.8.10 EFFECT OF SOURCE DISTANCE (2Kgf, PENMAENBACH)

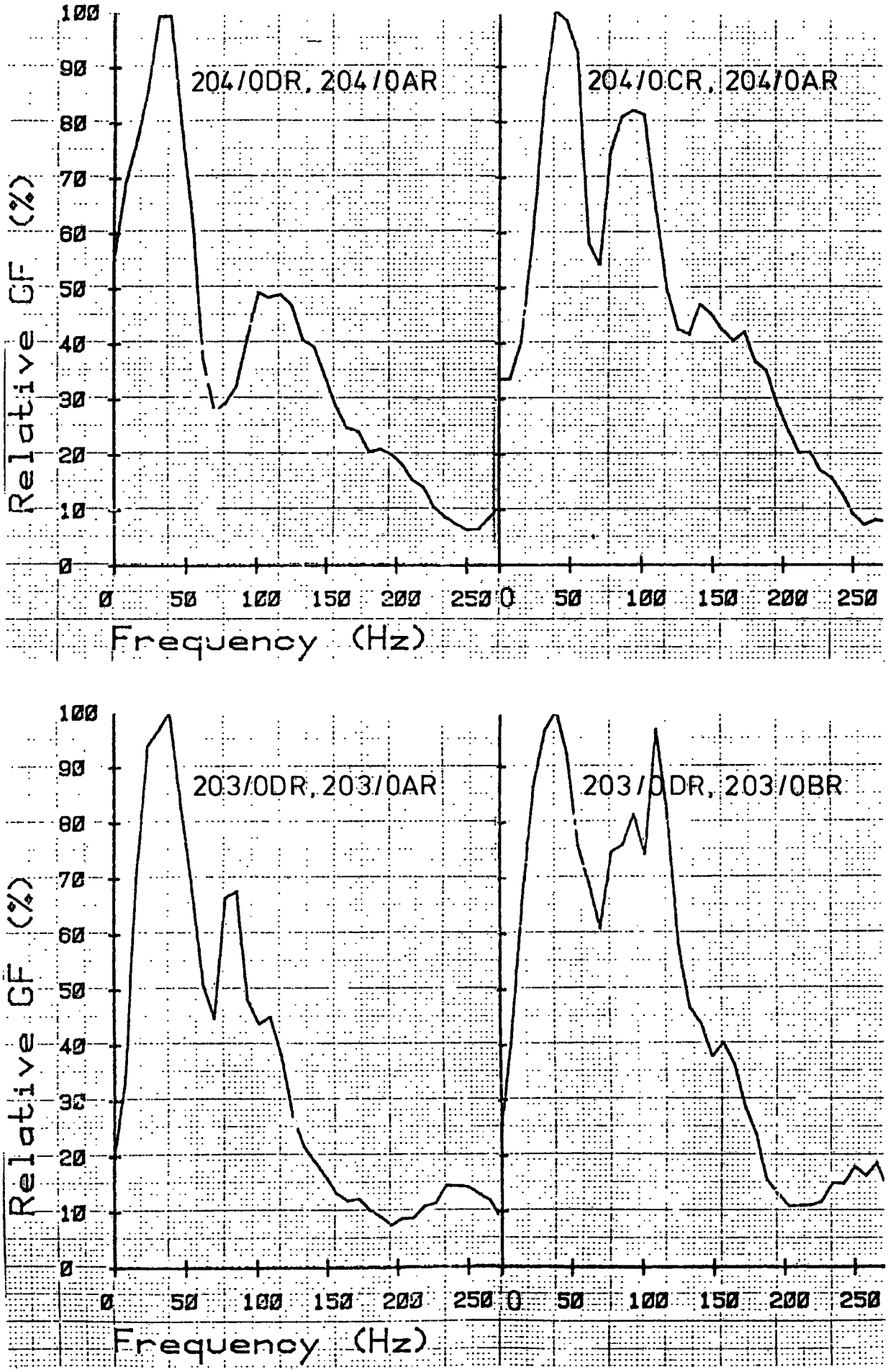

Fig.8.11 EFFECT OF RANGE ON GAIN FACTOR (PENMAENBACH)

is relatively rich in low frequencies as a result of its brief duration.

The presence of energy at the zero order harmonic may be indicative of some experimental error (most likely due to the transducer response characteristics) as the integral of particle velocity over the whole wave packet (that is, the total particle displacement) should be zero unless permanent rock deformation was actually caused at the transducer location.

8.5.2 Killiecrankie

Time domain analyses have shown that the decay of PPV with distance was essentially the same in directions parallel and normal to the schistosity. However, it has been observed (*see* Fig 7.16) that, although there was little variation in the duration of the initially received pulse, the duration of the wave packet at distance was noticeably greater for vibration propagating parallel to the schistosity. The spectra of the motions also show rather differemt characteristics in relation to the schistosity which are reflected in observations of spectral variation with source distance as follows:

(a) As discussed in Sections 8.4 the energy spectral peak of the motions close to the source occurred at about 200 Hz with significant energy content to at least 400 Hz (Figs 8.12 - 8.16)

(b) Parallel to the schistosity the change in spectral energy distribution was rather similar to that noted at Penmaenbach. At all ranges greater than about 20 m the spectral peak occurred between 40 and 60 Hz and beyond 30 m there was very little energy at frequencies greater than 150 Hz (Figs 8.13 and 8.16)

(c) Normal to the schistosity the attenuation of non-radial,

low frequency motions was more severe than it was parallel to the schistosity. This is a direct consequence of the more persistent propagation of shear wave motions in the long 'tail' of the wave packet parallel to the schistosity. This is discussed below with spectral analysis of partial wave packets. Although at distances of greater than 40 m the spectral peak had again shifted to lower frequencies (40 - 60 Hz) some energy at higher frequencies persisted at distances of over 100 m (Figs 8.12 and 8.15). This characteristic is shown clearly by comparison of the gain factors, over similar range variation, for blast 302/2. The gain factors are given in Figs 8.14 (upper and lower left) and show how, parallel to the schistosity, the ESD falls to less than 10% of its peak by a frequency of 160 Hz. Normal to the schistosity however, a similar decay has not occurred until a frequency of about 300 Hz. A further example of this difference in frequency selective attenuation is given in Fig 8.17 (upper left and right) for blast 304/0.

(d) For ranges greater than 40 m, even in a direction normal to the schistosity, there was little or no energy present at frequencies above 300 Hz.

Further spectral analyses were also carried out to determine whether the distribution of energy in the frequency domain was uniform throughout the individual wave packets. After careful inspection of the time domain records it was decided to analyse each wave packet in two sections, the first relating to the primary arrivals (which were in general the dominant compressional wave motions) and the second to the generally lower particle

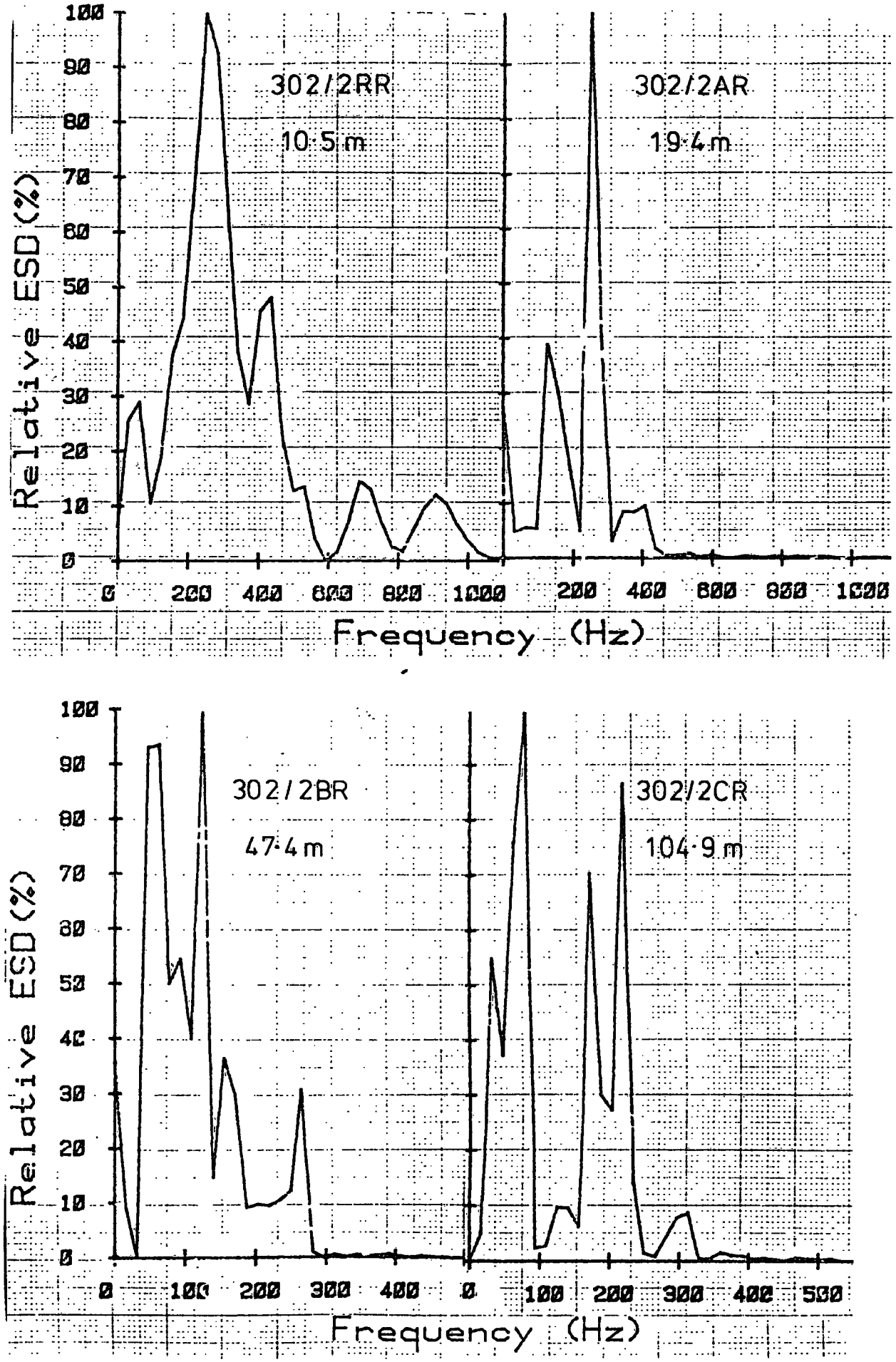

Fig.8.12. EFFECT OF SOURCE DISTANCE – NORMAL TO SCHISTOSITY (1·0Kgf , KILLIECRANKIE)

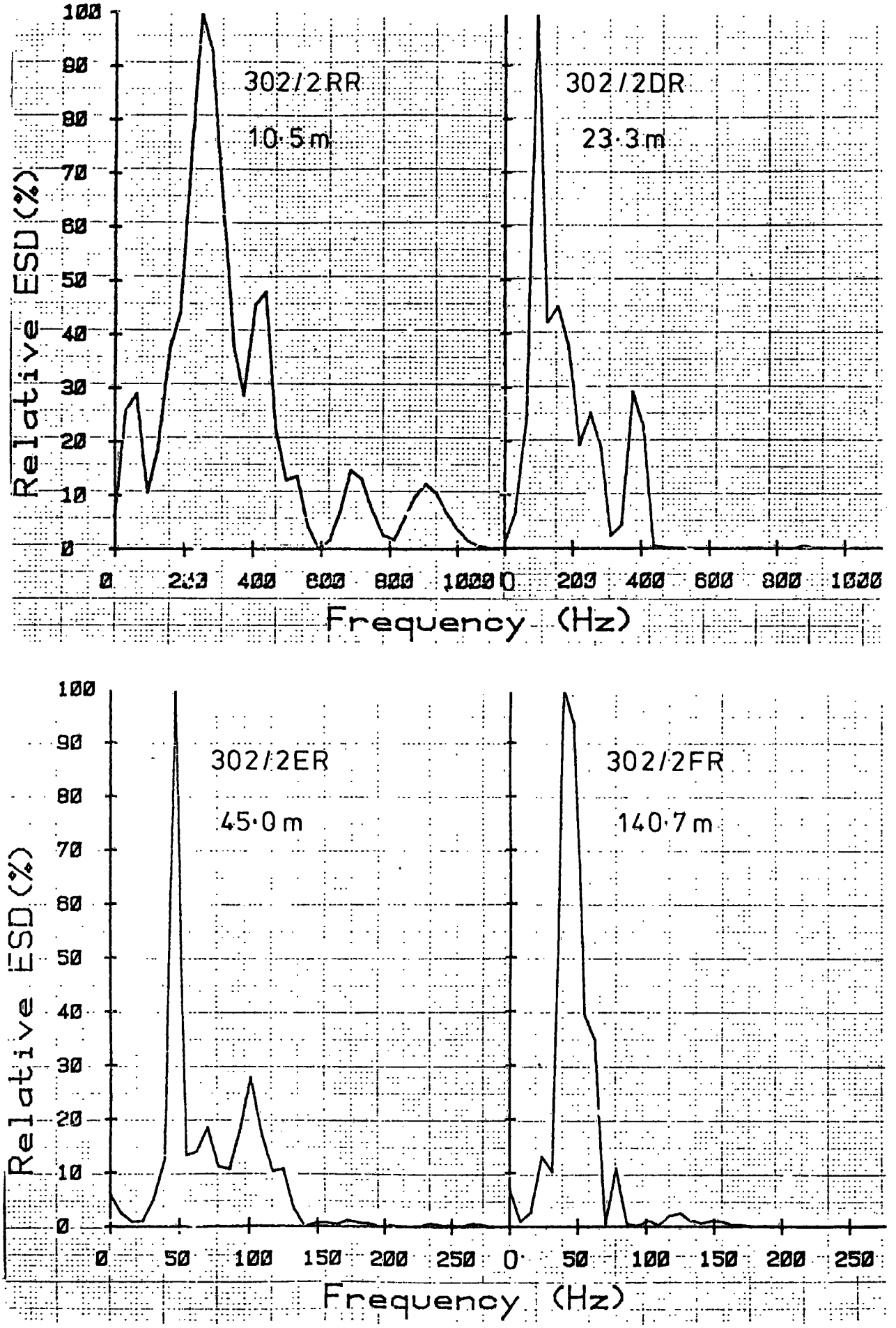

Fig. 8.13 EFFECT OF SOURCE DISTANCE – PARALLEL TO SCHISTOSITY (1·0Kgf, KILLIECRANKIE)

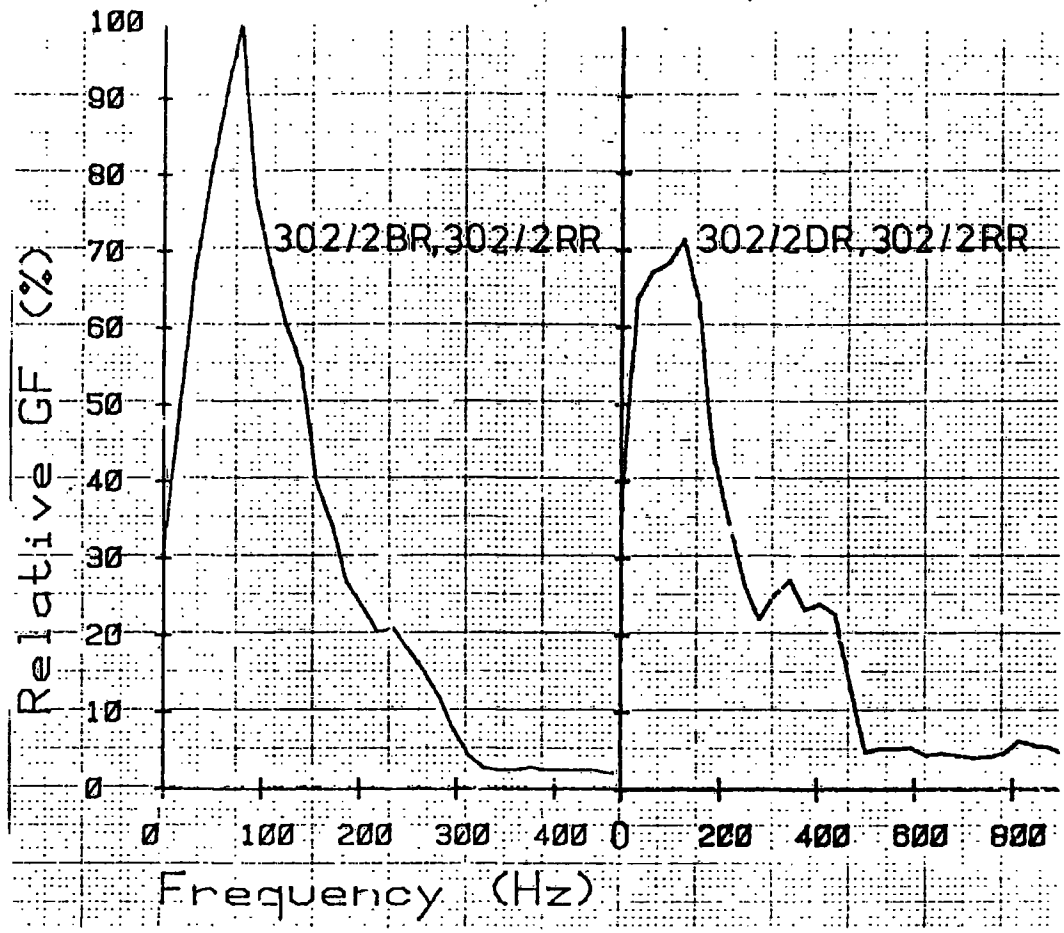

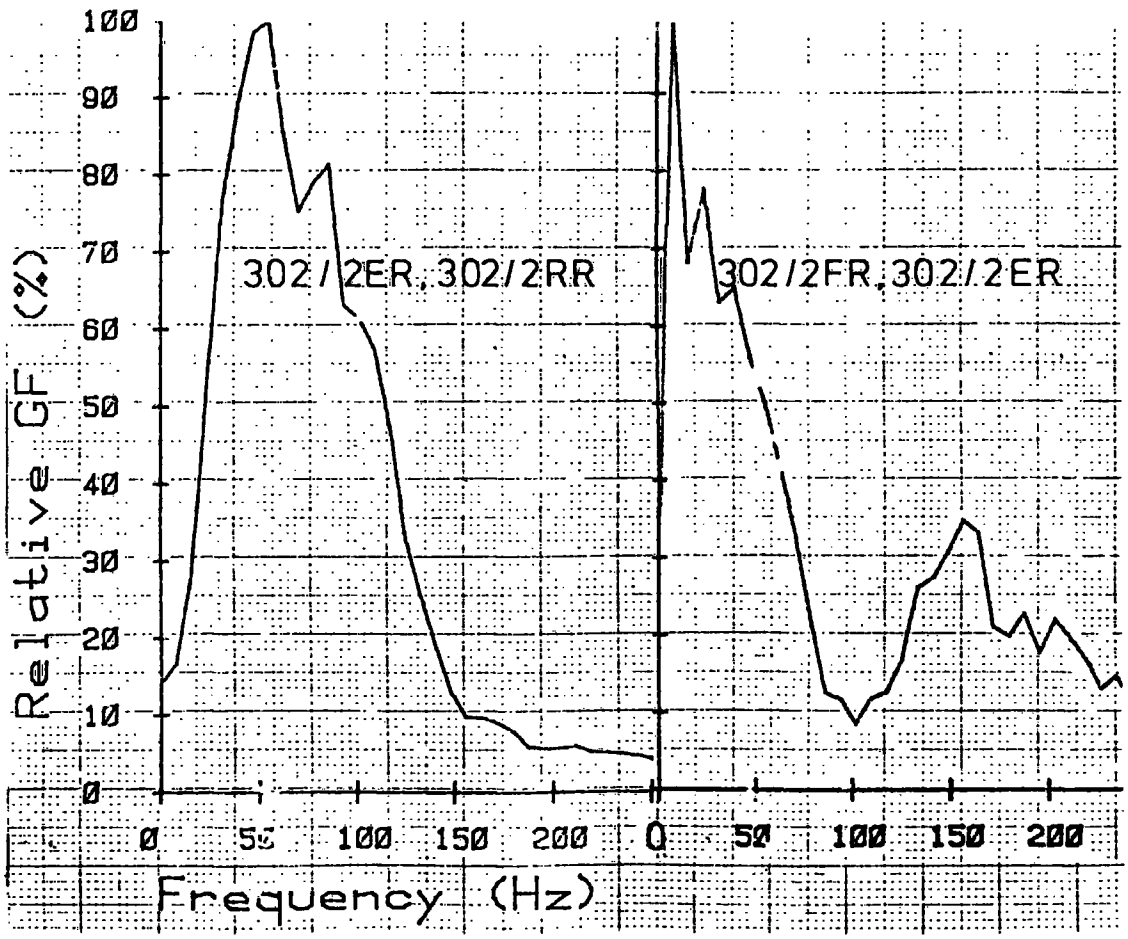

Fig. 8.14 EFFECT OF RANGE ON GAIN FACTOR
(1·0 Kgf, KILLIECRANKIE)

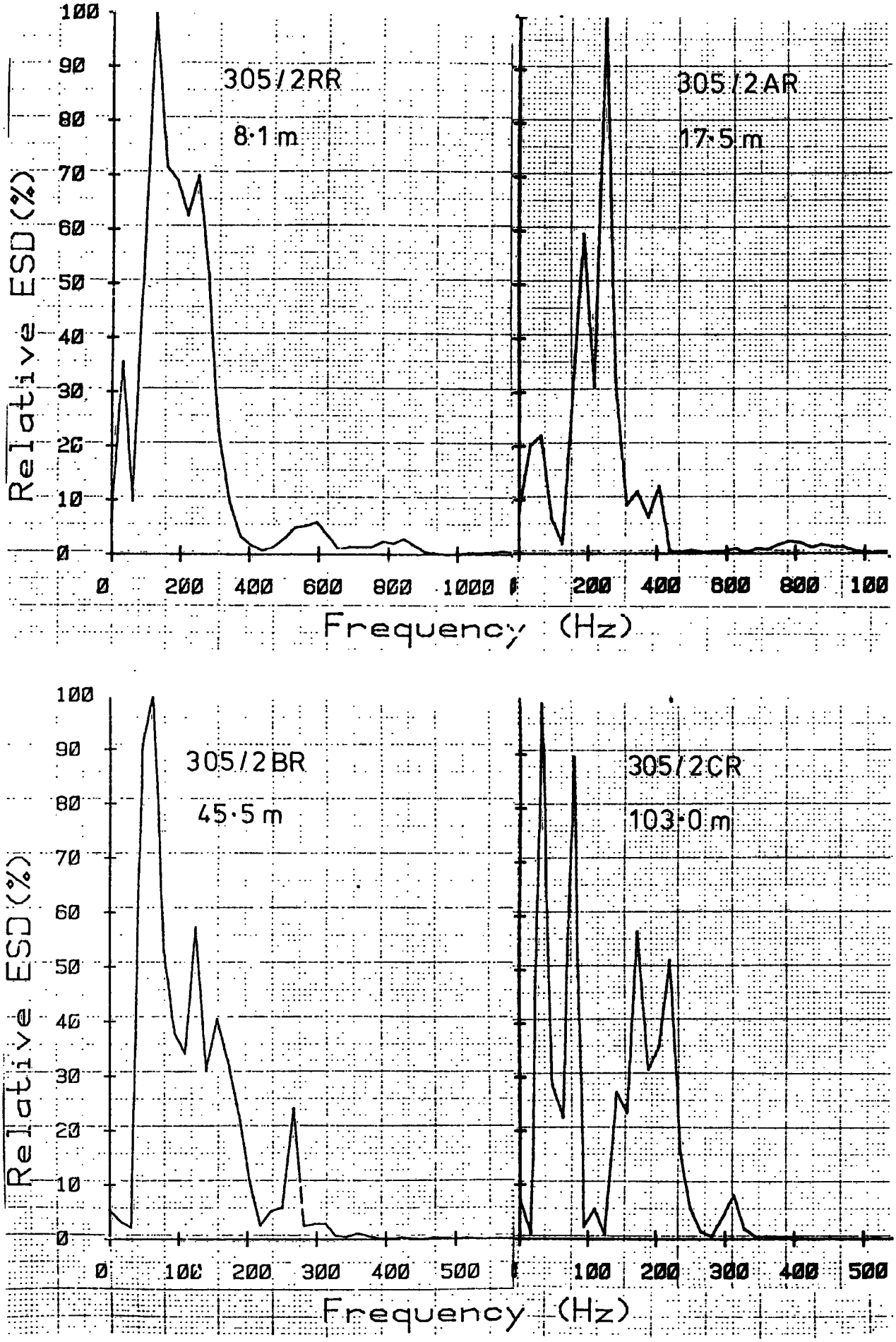

Fig. 8.15 EFFECT OF SOURCE DISTANCE – NORMAL TO SCHISTOSITY (1·5 Kgf, KILLIECRANKIE)

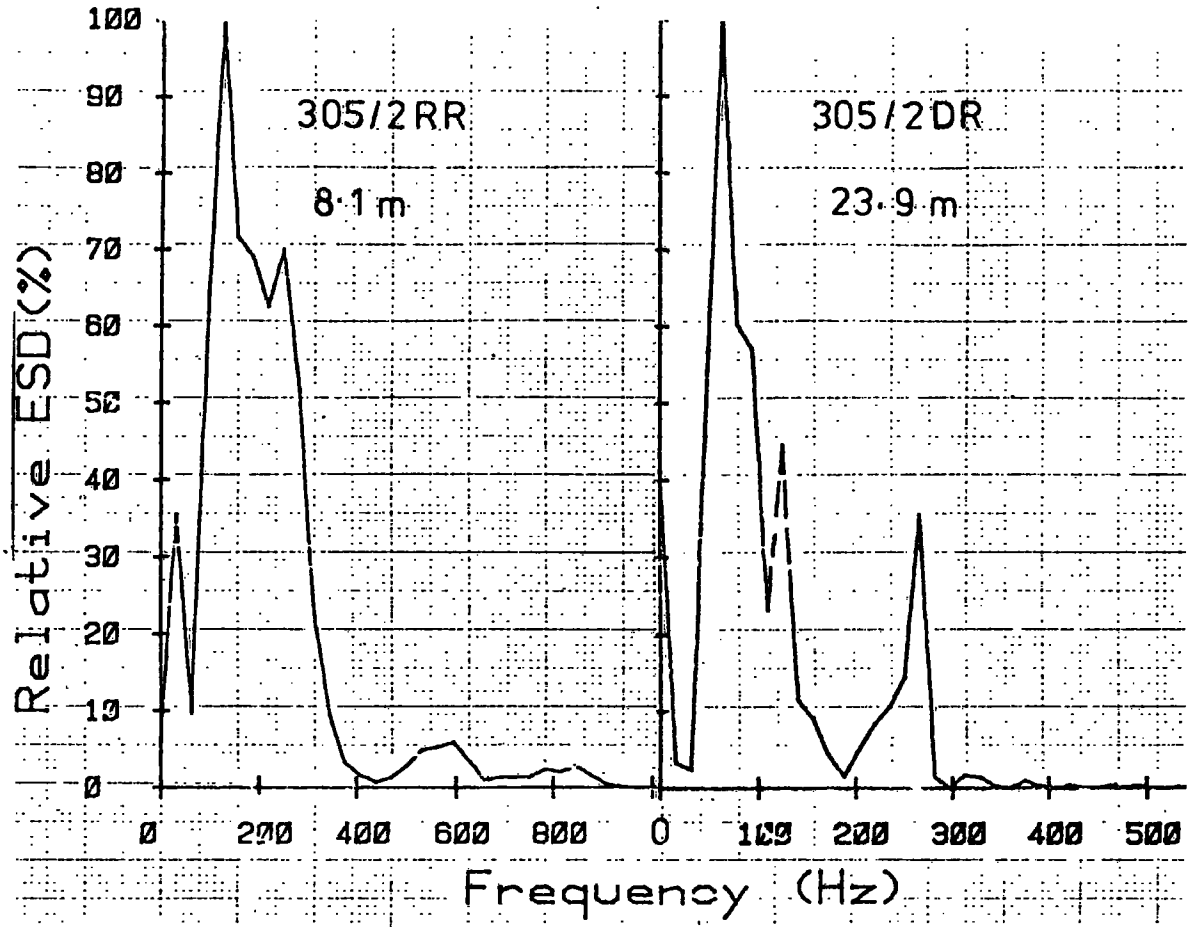

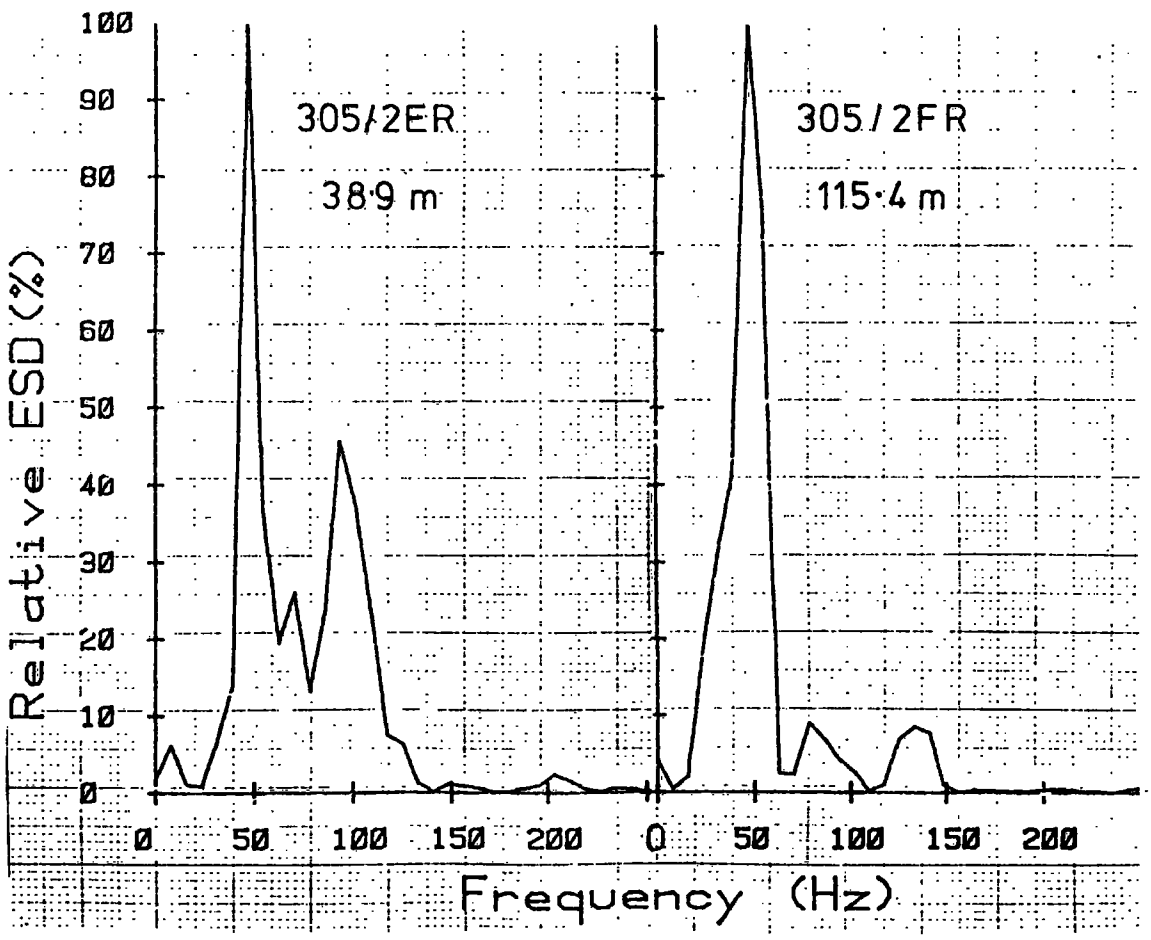

Fig. 8.16 EFFECT OF SOURCE DISTANCE - PARALLEL TO SCHISTOSITY (1·5 Kgf, KILLIECRANKIE)

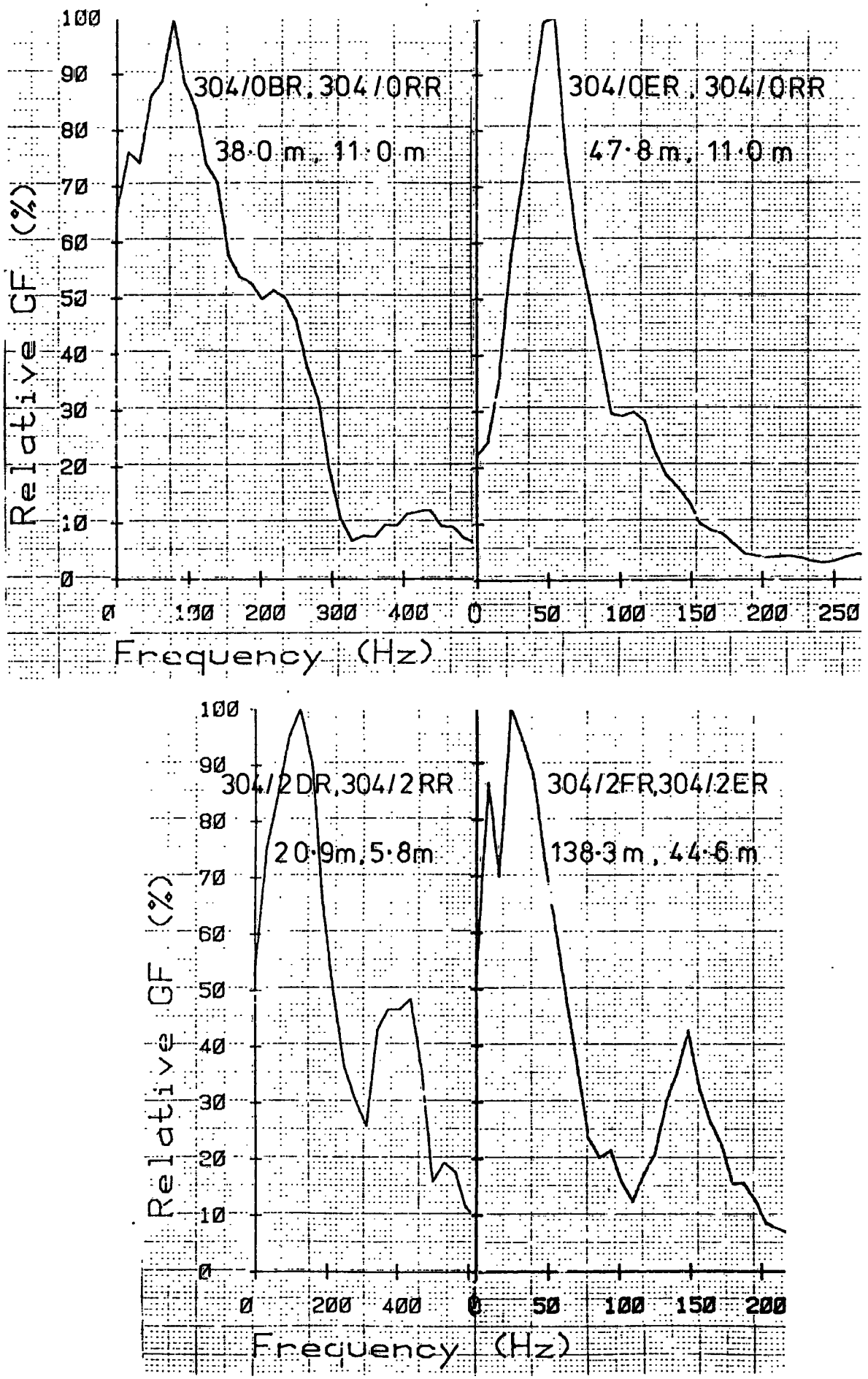

Fig.8.17 EFFECT OF RANGE ON GAIN FACTOR – FURTHER EXAMPLES

velocities in the 'tail' motions. Analysis of many spectra from all locations, except E and F, showed no significant variation of frequency content between the two parts of the wave packet. However, spectra from position F consistently indicated that the motions in the long tail were of lower frequency than those of the earlier arrivals. This was particularly noticeable in the horizontal and vertical directions rather than the radial. A similar although less marked effect was noted in spectra from position E.

Figure 8.18 shows a typical radial particle motion induced by blast 304/0 at position F. Spectrum (a) shows the ESD for the complete wave packet whilst (b) and (c) show ESD for the 'initial' and 'tail' arrivals respectively. Note that the distribution of energy is similar in both sections of the wave packet: also the computed value for PT showed that the first 30 ms of the wave packet contained nearly twice as much energy as the remaining 100 ms.

Figures 8.19 and 8.20 show similarly analysed spectra for the vertical and horizontal directions. Note how the PPV now occurs during the later arrivals (although the maximum value still occurs in the radial direction). Further, the spectral distribution of energy is different in each part of the wave packet. The initial arrivals, which are of low amplitude, are at much higher frequencies than those in the tail motions. Note how because of their low energy content the early arrival frequencies are not noticeable in the spectrum for the complete wave packet.

For both the horizontal and vertical directions the initial 30 ms of the wave packet contained less the 5% of the total wave packet energy, the remainder occurring during the passage of the later lower frequency arrivals. Again, this is reflected in the relatively small high

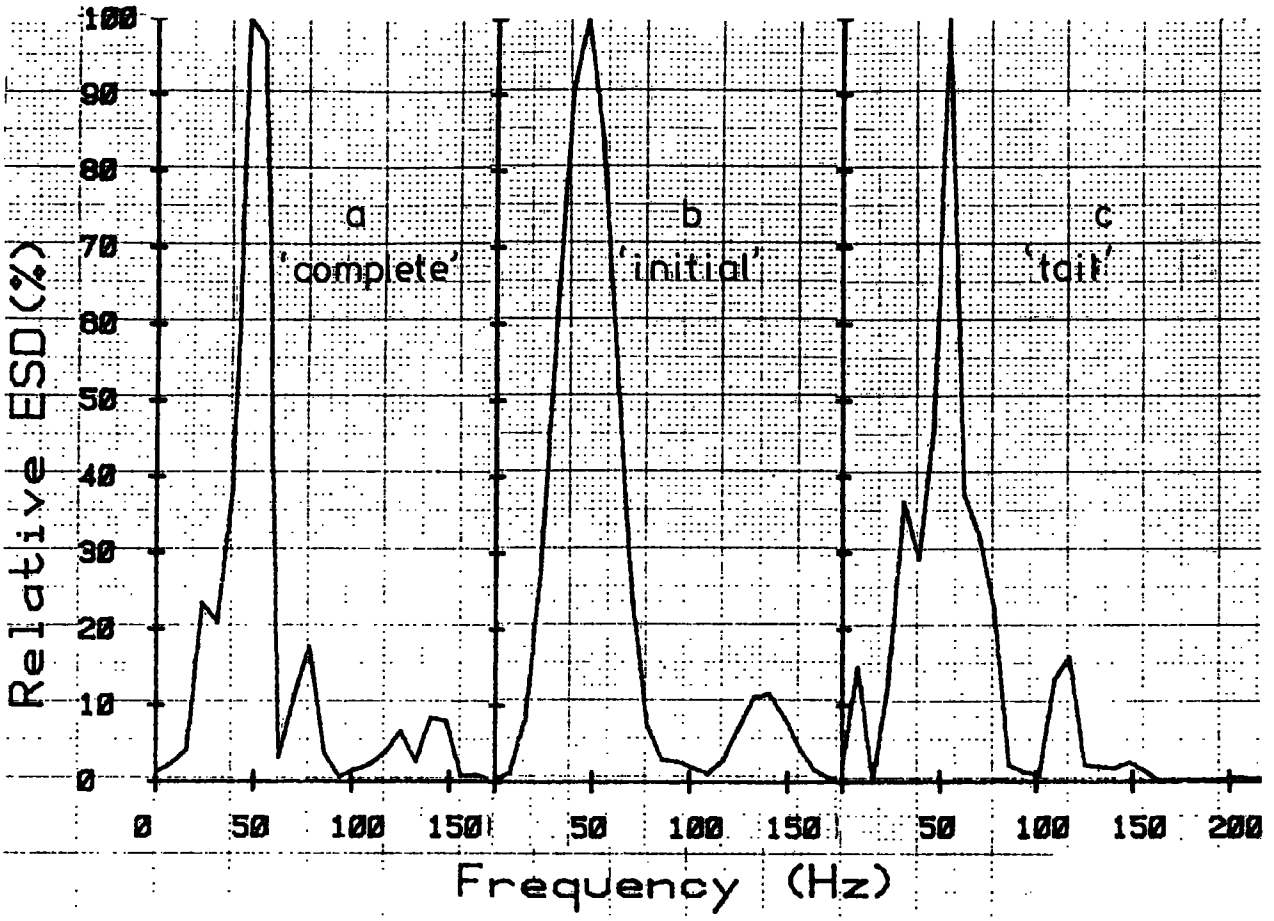

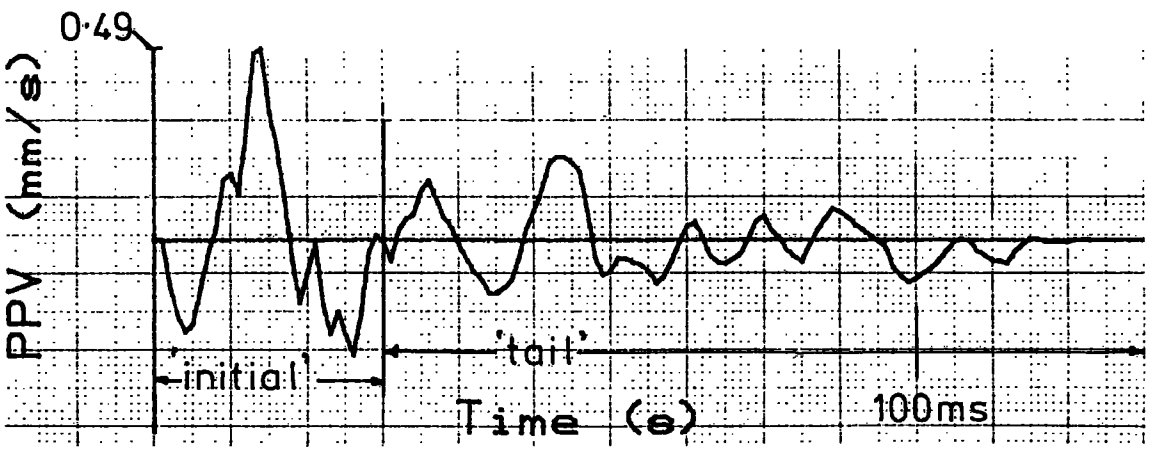

Fig.8.18 COMPLETE AND PARTIAL WAVE PACKET SPECTRA FOR BLAST 304/0FR

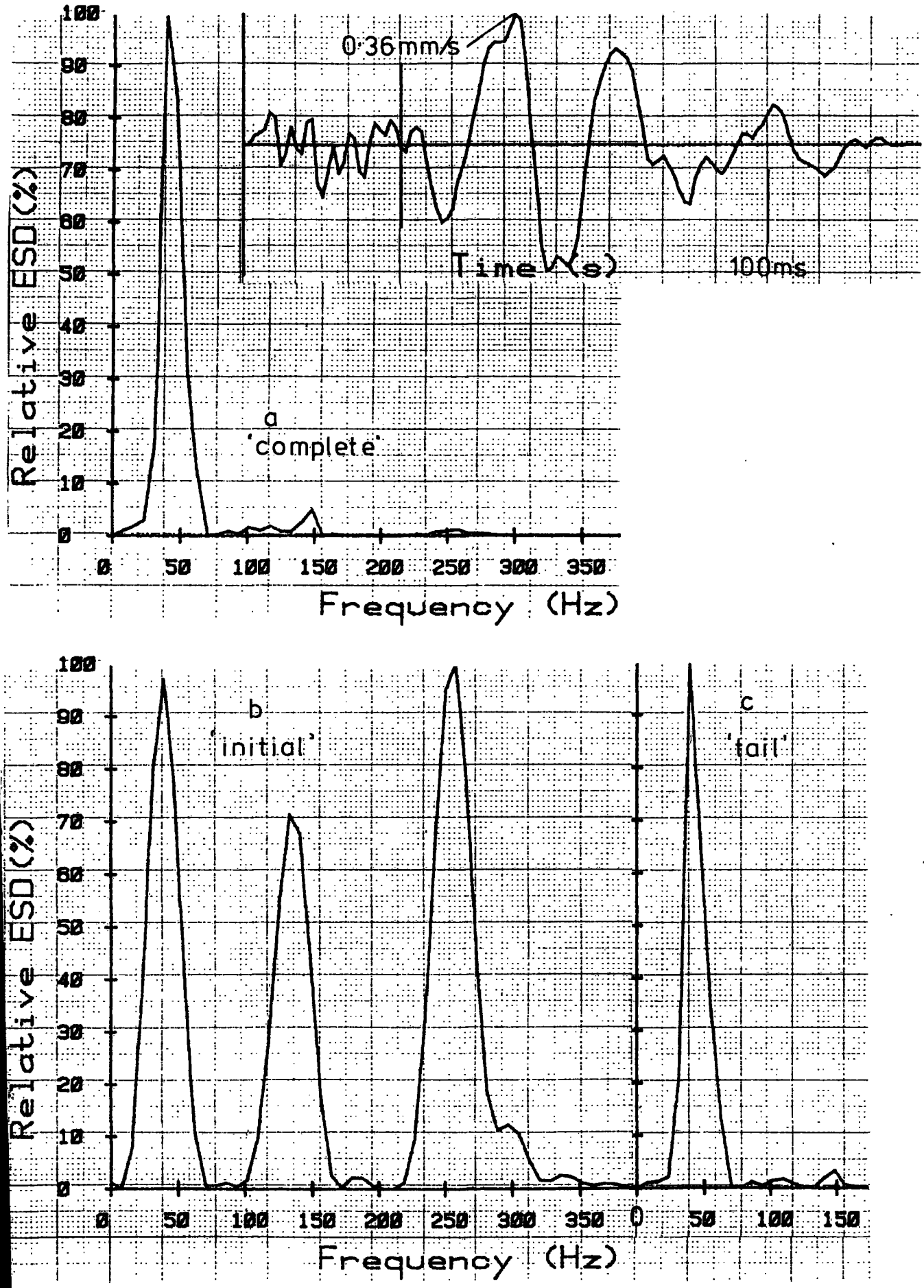

Fig. 8.19 COMPLETE AND PARTIAL WAVE PACKET SPECTRA
BLAST 304/0FV (VERTICAL MOTIONS)

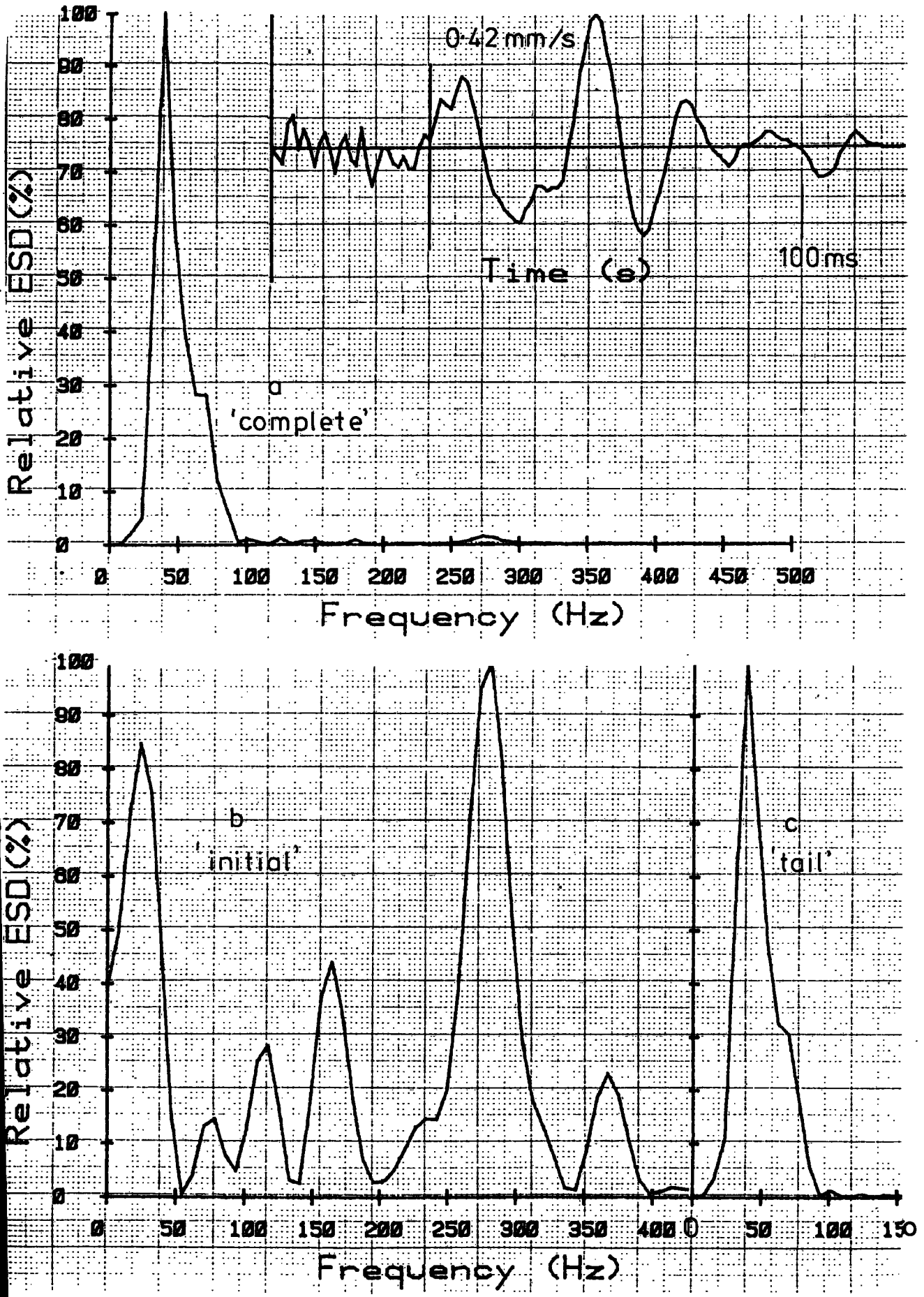

Fig. 8.20 COMPLETE AND PARTIAL WAVE PACKET SPECTRA
BLAST 304/0FH (HORIZONTAL MOTIONS)

frequency content apparent in the whole wave packet spectra.

Although the wave packets observed are generally complex the analysis of the more distant motions in both time and frequency domains shows, as described above, distinctly different characteristics parallel to and normal to the schistosity. This had been considered a possibility during the design of the trial blasts and arose from observations contained in the site investigation report prepared by Soil Mechanics Ltd which had stated that the great majority of the rock mass discontinuities were directly associated with the well-defined direction of the schistosity. The analysis of the data does lead to a possible explanation of the differences observed in the distant wave motions parallel to and normal to the schistosity. The motions observed parallel to the schistosity (positions E and F) show strong shear wave motions in the long tail of the wave packet. These motions travel more slowly and are of lower frequency content than the initially dominant compressional waves and are, therefore, to be observed later in the wave packet. The motions normal to the schistosity, however, do not possess such a long 'tail' and no significant low frequency shear wave motions are apparent. These observations are consistent with a foliated structure which is substantially weaker with regard to the transmission of shearing motions occurring in the direction of the majority of the discontinuities. As observed at position C these shearing motions are greatly attenuated whilst at position F they are becoming important constituents of the wave packet.

As previously discussed the site laws are dominated by the major early compressional wave arrivals and the attenuation of *these* motions is similar in both directions. However, we may speculate that at distances greater than 150 m the later shear wave motions parallel to the schistosity could become dominant and the decay of PPV with distance may become rather

less in this direction.

8.5.3 Loss of energy and PPV with range

Despite the uncertainties present in the calculation of wave packet energy discussed above (Section 8.4) average values for wave packet energy were calculated for distances 40 m and 100 m from the source. Table 8.2 gives the percentage of input chemical energy passing various distances from the source.

TABLE 8.2
Seismic energy at various ranges for a 1 kgf explosion

	Total radiated energy (as percentage of initial explosive energy)		
Source distance (m)	10	40	100
Killiecrankie (parallel to schistosity)	3.02	2.1	1.8
Killiecrankie (normal to schistosity)	3.02	1.8	1.4
Penmaenbach	NA	1.9	1.6

Although these average values represent a progressive loss of energy with propagation distance, it must be noted that sample calculations based on individual blasts occasionally yielded rather erratic results. The calculations were again based on the summation of energies at each harmonic, divergence with hemispherical symmetry and that motions normal to the direction of propagation had the characteristic velocity of shear waves. All radial motions were assumed to be attributable to compressional waves.

Note that the energy loss is rather higher for waves travelling normal to the schistosity than for those travelling parallel to the

schistosity. This is consistent with other observations given above that although the early radial motions which produce the PPV are similar for both directions the wave packet duration was greater, parallel to the schistosity. For both directions of propagation the loss of energy is most severe near the source. That is during propagation between 10 and 40 m about one-third of the energy is lost whereas from 40 m to 100 m, twice as far, the loss is less than one-quarter. Examination of the spectra and gain factors given in Figures 8.12 to 8.17 indicate clearly why this is so. At 10 m the majority of the energy is carried at frequencies around 200 Hz whereas at distances in excess of 30 m the bulk of the energy is carried at frequencies between 40 and 60 Hz. The losses at the higher frequencies are higher than those at lower frequencies and this accounts for the more rapid loss of energy close to the source. It is of interest to note that no similar effect is apparent in the decay of PPV near to the source. This reflects the fact that PPV is the result of the complex summation of energies at each harmonic and this 'resultant' in the time domain, that is, the critical value of PPV which determines ground stress, is not necessarily dependent on the total energy carried by the wave packet. This point underlines the idea that where the criteria of damage are considered purely in terms of PPV the distribution of energy as observed in the frequency domain is of little practical value. It is the peak instantaneous power which is important and this is given in terms of PPV in the time domain. However, where the dynamic response characteristics of the particular structures at risk have been established, a knowledge of the spectral distribution of the energy and its frequency selective attenuation with distance as described by the gain factor spectra may prove most helpful.

It is of interest to note that for both sites at distances of greater

than about 30 m the majority of the energy is carried beween 30 and 60 Hz; this confirms very closely a wide variety of observations given by Lucole and Dowding (1979).

Where the peak energy at various distances is carried at similar frequencies it is of interest to estimate a value for the specific dissipation constant Q; taking the frequency of the dominant spectral peak (say 50 Hz) and the compressional wave velocity (5000 m/s) to calculate the wavelength of the major motions (100 m).

For both sites at ranges between 40 m and 100 m the loss was between 1 and 2 dB per wavelength which corresponds to a value for Q between 13 and 27. Parallel to the schistosity at Killiecrankie the loss was slightly less. This value for Q is rather lower (indicating higher attenuation) than some other field observations which have generally been obtained at depth (eg O'Brien, 1969) or from intact samples in the laboratory. The weathered nature of the near surface strata and low *in situ* stress would both give rise to relatively high energy attenuation and this value falls well within the range of values for attenuation given by Attewell and Ramana (1966). It is important that this energy loss is considered in the context of the overall loss of particle velocity which is mainly attributable to geometrical spreading amd the general lengthening of the wave packet by scattering and other mechanisms.

Note that the loss of particle velocity given for coupled explosions (Fig 7.12b) for an equivalent distance of one wavelength, say between 30 and 130 m, is approximately 24 dBs. The permanent loss of vibrational energy described by Q is therefore small (even where Q takes its highest observed field values) compared to the reduction in energy passing unit wavefront area due to the geometrical redistribution of energy with propagation.

Although frictional losses close to the source are clearly considerably higher, as would be expected from the high ground strains induced, there is a corresponding increase in the effect of geometrical spreading and geometrical losses still dominate. (The loss expressed as dBs/unit distance are of course higher for small values of r).

The dominance of geometrical factors over frictional losses explains to a large extent why the wide range of field data shows a remarkably consistent decay of PPV with range, that is,site geometries are usually similar. Coupled with the discussion given in the section on the frequencies generated by the majority of construction explosions (in near surface strata) we are left with a reasonable explanation of the remarkable stability of the site law exponents which describe the decay of the particle motions. Factors regarding the *level* rather than slope of the site law regression line are clearly dependent on how well the explosive energy is coupled to the rock and these matters are discussed elsewhere in this thesis.

CHAPTER 9

CONCLUSIONS

9.1 The prediction of ground vibration hazard

All present methods used to predict vibration levels from construction sites are empirical and are based on a wide variety of case history data. Prediction equations are usually shown in graphical form relating PPV to distance from the source (scale distance for explosive sources). Because of the extremely complex nature of the problem the prediction will inevitably be imprecise and a wide spread of possible vibration levels must be allowed for when considering environmental impact. Predictions of PPV from various construction plant are given in Figure 2.1 and from explosives in Figure 3.2. Explosive sources are by far the most serious with regard to causing damage as even small charges induce vibration levels considerably in excess of those from plant and machinery.

The 'site law' method of data presentation described in Section 3.1, provides a convenient and useful working tool for engineers, and the application of 'square' or 'cube root' scaling is widespread throughout the mining and civil engineering industries. The investigations presented in Chapter 3 have shown that the scaling relationship between range (r) and charge weight (M) should not be arbitarily fixed as both 'square' and 'cube root' methods demand. There is no defensible theoretical justification for either fixed scaling relationship when applied to working sites and field blasting conditions. The data will be best presented using the 'site specific' scaling method described in Section 3.2 and demonstrated in Chapters 6 and 7. The use of multiple regression analysis to determine the 'site specific' constants is now easily carried

out on desk computers and this method of analysis inevitably improves the fit of the prediction equation to the field data.

It is therefore recommended that the equation

$$PPV = K\, r^{-\beta}\, M^{\alpha}$$

should be used in the prediction of vibration and that the site specific scaling equation (as developed in Section 3.2 and used in Ch 6 and 7)

$$PPV = K \left(r/M^{\alpha/\beta} \right)^{-\beta}$$

should be used for graphical data presentation. This 'site specific' graphical presentation provides the field engineer with a familiar form of working document which now incorporates the advantages of the enhanced correlation provided by the multiple regression analysis without the need for repeated calculations using the multiparameter equation.

Theoretical analyses indicate that the size of the charge should materially affect the frequencies generated at the source and therefore frequency selective attenuation mechanisms would be expected to change the rate of attenuation of PPV with propagation distance for different size charges. Research in the field of exploration seismology has confirmed this variation of spectral energy distribution with charge weight but extensive review of the literature shows that this important effect is not generally observed during construction blasts. Further, the spectral analysis of data obtained during the field trials reported by this thesis shows that the spectral distribution of energy was almost completely independent of charge weight. The near-surface weathered strata are necessarily subject to low *in situ* stresses and these conditions impose severe low pass filter characteristics on the stress waves propagated

into the rock mass. Indeed, for the typical sites investigated here the ESD peak occurred at frequencies below 60 Hz after propagation through less than 30 m of rock, although close to the source much of the energy was at higher frequencies (100-400 Hz). The detailed observations of spectral distribution given are in good agreement with other observations from many sites (eg Lucole and Dowding, 1979).

The dimensions of the 'equivalent radiator' cavity (which determines input frequency) are effectively controlled by factors which may depend on the effective tensile strength and the distribution of explosive pressures, both of which will be influenced by rock mass discontinuities and the physical shape of the charge. The relatively narrow bandwidth of low frequency vibration observed from a wide range of construction sites is consistent with the known filter characteristics of near surface strata. Indeed, in exploration seismology this region is avoided when possible precisely because the high frequency motions required for high resolutions are not transmitted 'in the weathering'.

As the fractured, low stress rock conditions which are present at most construction sites are broadly similar in character, it seems reasonable to infer that the severely band limited nature of construction induced vibrations may be considered general except at locations close to the source.

It is also of interest to consider why the exponent of PPV decay with distance is so similar for a wide range of site conditions.

It has been established that the filter characteristics of the near surface strata are likely to create a similarly low frequency input for most construction works. It has also been shown that for the ranges of interest (Section 8.5) the losses due to the frictional properties of the rock are likely to be small compared to those associated with site geometry. As the site geometry is broadly similar (a halfspace) for most construction works it therefore follows that the attenuation of PPV with distance is likely to be similar.

The predicted range of PPV from various types of explosion given by Oriard (1971) has been closely confirmed by the trials reported in this thesis, and may be used in initial desk studies to determine whether vibration problems are likely to arise during blasting operations. Further, the trials have shown that the major factor which significantly influenced the PPV (for a given charge weight) is the degree to which the explosive energy is coupled to the rock mass. The Penmaenbach trials showed that PPV was noticeably reduced where the explosive was not tightly confined and rock was broken out allowing the early venting of explosive pressures to the atmosphere. The experiments at Killiecrankie showed that, although the spectral distribution of energy and the rate of decay of PPV with propagation was not influenced by decoupling the charges, the reduction in PPV was most severe. This effect has not previously been quantified and has significant implications with regard to the future use of decoupled presplit blasting during road construction works.

9.2 Damage and intrusion criteria

Criteria are given in Chapter 2 which provide a sound basis for the assessment of risk to structures subjected to blasting vibrations. These criteria should not be regarded as rigid rules and should be expertly interpreted with regard to specific site conditions. In general, most residential structures will not be damaged by occasional blast vibrations of 25 mm/s (below 40 Hz) or 50 mm/s (above 40 Hz). It is the rôle of the engineering geologist to predict, measure and describe the ground vibrations and the effects should be determined in collaboration with the structural engineer. At the present time there is a lack of detailed information on the effects of both dynamic and quasi-static deformations on structures, and more field-based research is required. It is important to remember that damage is a distortion-related phenoma, and although PPV is a good measure of dynamic distortion, it is not the only factor involved (*see* Section 2.2.1).

Fatigue associated vibration damage may be caused at considerably lower levels of PPV (than that due to transient sources) from 'continuous' sources such as road traffic. This problem provides another area where research is required and is being undertaken.

It is important that observed damage is attributed to the correct cause if appropriate remedies are to be promulgated. For instance, it is possible wrongly to blame damage caused by construction-induced quasi-static ground deformations to vibration. The presence of vibration may be easily detected by the human senses whereas slow ground movements may not. Where excavations are taking place close to buildings it will often be prudent to measure both ground deformation and and vibration.

The review undertaken in Chapter 2, also indicates that underground structures are far more resistant to damage by vibration than surface structures. A value of 300 mm/s is generally accepted as a threshold for 'the fall of rock in unlined tunnels' although there are cases where PPVs in excess of this value have not damaged rock structures. This threshold may be applied to both lined and unlined tunnels in good condition but clearly cannot account for the dislodging of rock fragments or blocks which have become loosened by weathering processes. It would therefore seem prudent to adopt a lower value, say 100 mm/s, as a general working limit. This threshold is unlikely to inhibit blasting operations in most situations and may be relaxed under close supervision if, exceptionally, the site conditions require high charge masses per delay at close proximity.

Rock mass stability analyses indicate that for blasting vibrations both the inertial effects on block stability and the increase of shear stress on weakened shear zones caused by the imposed dynamic stresses must be considered. Similar considerations apply to slopes around underground constructions, and slope stability analyses must also include a factor allowing for dynamic effects imposed by blasting vibrations.

Care should be taken when comparing the effects of earthquake and near blast-induced damage as the damage mechanisms may be of a different nature due to the wide disparity in the frequency of the motions. In the UK little or no consideration need be given to earthquake damage to underground structures except within about 10 km of an active geological fault.

Human perception and intrusion criteria are given and discussed in

Section 2.1.2. Experience has shown that where vibration from an unusual source exceeds the threshold of human perception complaints may occur, and good public relations involving the provision of information to affected persons are most important.

9.3 Vibration related constraints on the Penmaenbach and Killiecrankie road schemes

The trials carried out at Penmaenbach showed that the imposition of any reasonable vibration limit for the adjacent rail tunnel (say, 50 mm/s, PPV) would not unreasonably inhibit the road tunnel construction method. Besides the determination of the specific site laws by trial blasting, the review of acceptable levels of vibration in subsurface structures played an important part in the submission to British Rail by the Department of Transport. Specific vibration monitoring procedures and PPV limits are currently being written into the detailed design for the tunnel which will be commenced early in 1984.

The results from the Killiecrankie site were not as favourable with regard to the proposed design and construction methods for the A9 rock cuts. Although the trials showed that much of the blasting will not be hazardous to the nearby structures, some severe restrictions or redesign will be necessary. The charge weight per delay may be severely restricted close to certain structures. This may preclude the use of presplitting in certain areas despite the fact that the trials showed that the decoupling of the explosive, inherent in the method proposed, did considerably reduce the vibration levels. At greater ranges, however, the site laws obtained for the decoupled charges will allow for pre-splitting where it may otherwise not have been permitted.

The data obtained from the Killiecrankie trials show that decoupled presplit explosive charges produce less vibrations than that indicated by Oriard (1971) for (non-decoupled) presplit charges. Resultant PPVs may be reduced by up to an order of magnitude and Figure 7.15 provides a quantitative indication as to the degree of PPV reduction with increased decoupling.

Aspects of the design which involved the firing of bulk excavation blasts close to 'green' concrete retaining structures, which form part of the new road construction, will require modification. At both sites the measurement of ambient vibration levels provided useful background data. In particular, at Killiecrankie the high level of train-induced vibrations on the old stone viaduct would make it difficult for unreasonably low limits to be imposed upon the Contractor.

The A9 improvement scheme for the Pass of Killiecrankie is now under urgent revision, taking into account the trial blasting results. Invitations to tender will be issued as soon as possible.

Both trials indicated that useful research could be carried out in parallel to the acquisition of data specifically relevant to the road design. The road and rail closures necessary for such works would not have been possible for research purposes alone, and so the combined objectives were mutually supportive and cost effective.

9.4 Rock mass classification by seismic methods

Seismic methods show promise as supplementary techniques in the acquisition of site investigation data for underground excavations. They

offer exploration of large volumes of rock without direct access and will often be relatively inexpensive to carry out. Besides its well-known use in the delineation of lithologies the analysis and interpretation of seismic data may provide information on rock mass structure which is of direct interest in an engineering context. Given a knowledge of intact material properties (from core samples), the detailed analysis of vibrations from geophysical sources (explosive, hammer etc) can provide information related directly to the frequency and the nature of the jointing, the discontinuous rock properties being of dominant importance in the design and construction of underground openings.

The principal methods of analysis are based on the measurement of body-wave velocities and the frequency of the wave motions. Both these parameters are linked through their dependence on rock mass moduli to rock classification and support requirements. The relationships are of an empirical nature with some theoretical support and the discussions given in Chapters 3 and 6 help to explain the strengths and weaknesses of the seismic methods. The two most promising techniques have been carried out at Penmaenbach and the results are summarised below. The site constitutes an almost ideal environment for comparisons of seismic and conventional geotechnical techniques in a relatively uniform and well-known (in an engineering context) rock mass.

Blasting trials to establish the site laws provide excellent records from which most of the geophysical data may be recovered and the 'combined' trial concept is therefore particularly cost effective. Similarly hammer seismic tests may be used to produce a wide range of information concerning specific site rock mass properties.

9.4.1 Seismic velocity and RQD

As shown in Section 3.5 seismic velocity measurements may be used indirectly to assess the Rock Quality Designation which in turn has been used to design underground support systems. There are a number of potential difficulties with this 'velocity ratio' approach the most serious of which is the acoustic closure of joints under stress. This may render the joints 'seismically transparent', so concealing their presence. In practice this seemingly significant deficiency may not always invalidate the method as joints which are unaltered and tight are frequently not critical in engineering design. The power of velocity measurements to reveal the presence of altered and open jointing has been demonstrated (New and West, 1980) and the method should be considered for use during site investigations.

In the area of the blasting trials at Penmaenbach the measurements of P-wave velocity, translated into RQD by way of velocity ratio, give a mean RQD of 75 per cent with a range from 65 per cent to 85 per cent. RQD measurements based on mutually-perpendicular scanlines in the same vicinity indicate a mean RQD of 72 per cent with a range from 61 per cent to 89 per cent. Therefore, at this site, and despite the predominance of tight unaltered jointing, this seismic method provides an excellent estimate of RQD.

Other measurements indicate volumes of rock with significantly lower P-wave velocity. In particular, a section of the rail tunnel, supported by brickwork, showed a velocity of only 3333 m/s indicating an RQD of only 38 per cent.

9.4.2 S-wave frequency and Rock Mass Classification

Schneiders' correlation between S-wave frequency and *in situ* static modulus has been developed in Chapter 3 to provide a direct value for RMR (Geomechanics Rock Mass Rating). The RMR classification has been correlated with other well-known systems and is used in the design of support systems. The simplified equation given below combines Schneiders' concept with Bieniawski's (1978) correlation of RMR and *in situ* static modulus; it provides a value of RMR directly from S-wave frequency (f)

$$RMR = 0.031f + 43$$

At Penmaenbach the average S-wave frequency was 975 Hz giving a 'seismic' RMR of 73. The value of RMR calculated in the traditional manner lay in the range 48-70. Thus the seismic value indicates a better 'class' of rock requiring less support, a situation verified, at this site, by the rail tunnel which for much of its length has remained virtually unsupported for 130 years.

Techniques based on S-wave frequency have been little used (outside France) but do seem to offer an extremely useful method of investigating rock mass properties. The concept that 'stiffer' rock masses (having relatively few open joints) have high characteristic S-wave frequencies is not difficult to understand and is certainly worthy of further exploitation. Further field trials supplemented by theoretical developments based on appropriate rheological models (such as that proposed by Roussel, 1968) are recommended. In particular field trials must determine the effect of source variation and investigate the spreading of the wave packet with distance. A worthy research objective may be to devise a rock support system based directly on S-wave frequency rather than through its correlation with RMR.

9.5 Contractual specification and vibration control

Figure 9.1 provides a flow diagram of questions which should be asked at the planning stage of major construction projects. These procedures were followed for both the road construction projects described by this thesis and found to provide an excellent basis for the investigation of vibration associated difficulties. The trial blasting schemes are described and form the basis for the development of a system of trials, described in Section 3.4, which has not been previously published.

Trial blasting will sometimes be necessary to determine the vibration propagation characteristics at a potentially sensitive site. Carried out as part of the site investigation, trial blasts usually provide valuable information for the preparation of contracts and tenders. Trial blast charges should, as far as possible, simulate expected excavation conditions. In particular, the effect of the degree of confinement of the charge should be investigated.

For given site conditions it is the weight of the composite charge per delay and the confinement imposed on the charge that are the principal factors controlling the level of vibration produced. The greater the number of delays (the smaller the weight/delay) and the lower the degree of confinement the lower will be the level of induced vibration.

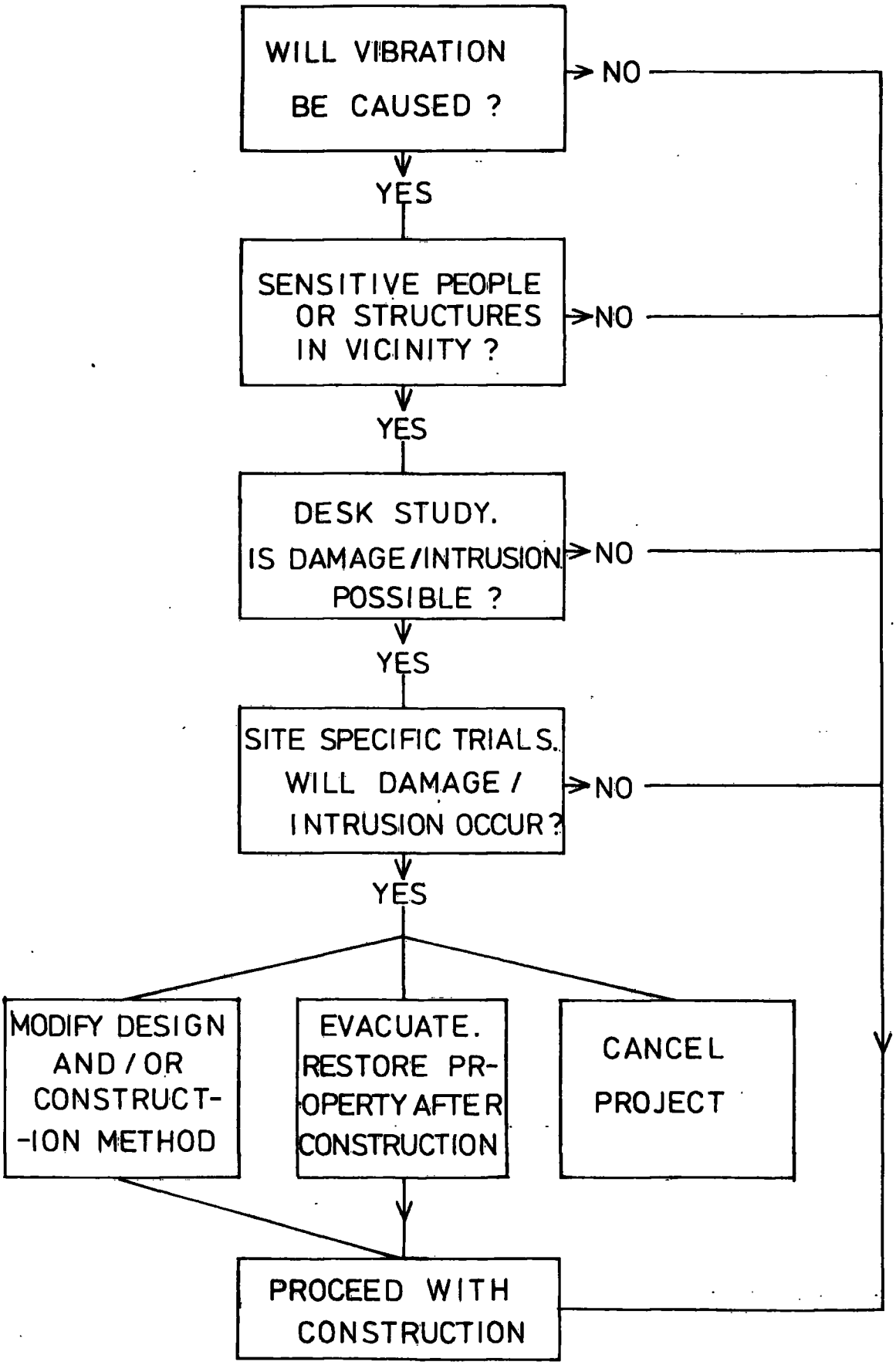

Fig. 9.1 VIBRATION HAZARD–PLANNING FLOW DIAGRAM

Where millisecond delay detonators are used (instead of ½ sec) the minimum delay period should be sufficient to allow the vibrations from a given delay to die away before the arrivals from the next. Where blasting or other vibrations are to be produced close to unstable geological strata analyses of stability should include allowances for dynamically induced stresses.

The design of the trial blasting scheme should use preliminary site investigation data (when specifying the distribution of the transducer arrays) to allow for possible directional variations in the propagating characteristics of the rock mass. Where possible it is particularly cost-effective to carry out research at sites where trial blasting is an essential element in the design of an actual excavation programme.

Much of the data on blast vibration has come from the mining and quarrying industries, and great care must be exercised if this information is to be used in a civil engineering context. Mineral extraction blasts generally comprise large rounds which are detonated at sites fairly remote from habitation. Construction blasts often involve much smaller rounds but may be very close indeed to vulnerable environments. Because of important differences in the character of the significant wave motions, measuring systems with a more demanding specification may be required for civil engineering applications. For instance, triaxial transducer arrays should be used and the frequency response of the system must often be able to cope with at least 500 Hz.

At present there are three basic approaches used with regard to the contractual specification of vibration control. They are as follows:

(a) Complete neglect of the problem with no mention of vibration in the contract,

(b) The inclusion of a 'no damage, no intrusion' clause intended to absolve the Client of any responsibility, and

(c) The imposition of a limiting value for vibration usually defined in terms of resultant PPV at some distance or structure.

Method (a) may be adopted when it is the considered opinion of the Client and his Engineer that there are no possible vibration problems. It is also used widely by default and can often lead to serious problems. Notably these problems will result in claims made under clause 12 of the Institution of Civil Engineers Conditions of Contract (5th Edition), and will be based on additional costs necessarily incurred by the Contractor due to circumstances unforeseen at the time of tender.

Method (b) is often used where the Client is not inclined to incur the additional expense of extending his site investigation to cover vibration. The inclusion of the 'no damage/no intrusion' clause may seem to be of great assistance to the Client by throwing vibration linked risks upon the Contractor.

This approach has two main drawbacks. Firstly, the Contractor may

may still feel that he can recover his additional costs through the Clause 12 claims procedure. Secondly, bidders for the Contract may feel obliged to increase their prices to allow for the vibration associated losses for which he feels liable. Neither circumstance is conducive to obtaining the best job at the lowest final cost.

Method (c) should involve an initial desk study perhaps followed by blasting trials as found necessary. Where trial blasting is carried out as suggested in Section 3.4, and an appraisal of environmental hazard is made, a considerable element of risk may be removed from many blasting contracts. Where full disclosure of trial blasting results is made to bidders an otherwise unquantified element of contractural risk is removed and bids may therefore be made with less allowance for vibration damage contingencies.

It must be recognised that the specification of vibration criteria by the Client does result in some extent of risk-sharing with his Contractor. This circumstance follows recent trends within the construction industry which suggest that such risk sharing may be mutually beneficial to Employer and Employee (*see* CIRIA, 1978).

It will be the Engineer's role to act as the supervising authority in relation to vibration control and measurement. If suitable expertise and equipment are not available 'in house' he should employ a sub-contractor with the appropriate experience. In most situations the monitoring and retention of vibration records from all construction blasts will be found useful. The difficulties in acceptance or rejection of damage claims will be greatly eased where such records are available.

Some Clients and Engineers are attracted by the idea of imposing unjustifiably low limits of vibration on their Contractors. These limits are a form of regressive conservatism which is to be deplored. An example is the use of the 'method of halves' whereby a specifying engineer halves the limit set by his predecessor on a similar job, thereby appearing 'cautious' to his peers. These methods inevitably impose unreasonable restraints on the Contractor, thereby increasing costs to the Client.

The majority of major civil engineering works are sponsored by the public sector and, although safe limits must be imposed to protect the local people, overconservative limits and unnecessary restrictions will be a charge on the community as a whole. It is therefore vital that authorities responsible for setting vibration limits do so on an informed rather than on an arbitrary basis.

REFERENCES

AKI, K and RICHARDS, P G. 1980. Quantitative seismology - Theory and Methods. Vols 1 and 2. W H Freeman and Co., San Francisco.

AMBRASEYS, N N and HENDRON Jr, A J. 1968. Dynamic behaviour of rock masses. Ch. 7, Rock mechanics in engineering practice, Ed. Stagg and Zeinkiewicz. John Wiley and Sons, London.

ANON. 1974. Suppression of noise and vibration on LT underground link with Heathrow Airport. Rail Engineering International, 4, No 6, 285-287.

ASHLEY, C and PARKES, D B. 1976. Blasting in urban areas. Tunnels and Tunnelling Sept, 8, No 6, 60-67.

A.S.T.M. 1970. Determination of the in-situ modulus of deformation of rock, ASTM STP 477. American Society for Testing and Materials.

ATCHISON, T C, DUVALL, W I and PUGLIESE, J M. 1964. Effect of decoupling on explosion generated strain pulses in rock. U.S. Bureau of Mines, Report of Investigations, 6333.

ATCHISON, T C and PUGLIESE, J M. 1964. Comparative studies of explosives in granite. Second series of tests. U.S. Bureau of Mines, Report of Investigations, 6434.

ATTEWELL, P B. 1978. Ground movements caused by tunnelling in soil. Proc. Large ground movements and structures. Cardiff, July, 1977. (Plymouth, London: Pentech Press).

ATTEWELL, P B and FARMER, I W. 1976. Principles of engineering geology. Chapman and Hall Ltd, London.

ATTEWELL, P B and RAMANA, Y V. 1966. Wave attenuation and internal friction as functions of frequency in rocks. Geophysics. 31, No 6, 1049-1056.

BARTON, N, LIEN, R and LUNDE, J. 1974. Engineering classification of rock masses for the design of tunnel support. Rock Mechanics 6, 4, 183-236.

BATCHELOR, A S, BARIA, R and HEARN, K. 1983. Monitoring the effects of hydraulic stimulation by microseismic event location: A case study. Presented at 58th Annual Conference of Society of Petroleum Engineers, AIME, San Francisco, Oct 5-8.

BAUGHAN, P E. 1972. The Chester and Holyhead Railway. Vol 1. David and Charles : Newton Abbot.

BEAN, R and PAGE, J. 1976. Traffic induced ground vibration in the vicinity of road tunnels. Dept of Environment, TRRL Report SR 218 UC. Crowthorne, (Transport and Road Research Laboratory).

BENDAT, J S and PIERSOL, A G. 1971. Random data: analysis and measurement procedures, Wiley-Interscience, New York.

BICE, P K. 1970. Speed up the fast Fourier Transform. Electronic Design, 9, April 26.

BIENIAWSKI, Z T. 1974. Geomechanics classification of rock masses and its application in tunnelling. Proc. 3rd Internat. Cong. Rock Mech. ISRM, Denver Colo. Vol IIA, 27-32.

BIENIAWSKI, Z T. 1976. Rock mass classifications in rock engineering. Proc. Symp. on exploration for rock engineering. Balkema Press, Rotterdam, 97-106.

BIENIAWSKI, Z T. 1978. Determining rock mass deformability : Experience from case histories. Int. J. Rock Mech. Min. Sci. and Geomech. Abstr. 15, 237-247.

BIENIAWSKI, Z T. 1979. Tunnel design by rock mass classifications. Pennsylvania State University. Tech. Report GL-79-19 U.S. Army Engineer Waterways Experiment Station Geotechnical Laboratory, Box 631, Vicksburg, Miss.

BLACKMAN, R B and TUKEY, J W. 1958. The measurement of power spectra. Dover, New York.

BLAKE, F G. 1952. Spherical wave propagation in solid media. J, Acoust. Soc. Am. 24, 211-215.

BOLLINGER, G A. 1971. Blast vibration analysis. Southern Illinois University Press. Feffer and Simons Inc. London and Amsterdam.

BRADLEY, J J and FORT Jr, A N. 1966. Internal friction in rocks. Handbook of physical constants. Editor S P Clark Jr. The Geological Society of America, New York.

BRENNAN, B J and SMYLIE, D E. 1981. Linear viscoelasticity and dispersion in seismic wave propagation. Rev. Geophys. Space Phys. 19, 223-246.

BURTON, P W. 1978. Assessment of seismic hazard in the UK. Proc. Conf. Instrumentation for ground vibration and earthquakes, Keele University. 1977. The Institution of Civil Engineers.

CARTER, P G and SNEDDON, M. 1977. Comparison of Schmidt hammer, point load and unconfined compression tests in carboniferous strata. Proc. Rock Engineering 4-7 April, Newcastle-upon-Tyne.

CECIL, O S. 1971. Correlation of seismic refraction velocities and rock support requirements in Swedish tunnels. Reprints and preliminary report, No 40, Swedish Geotechnical Institute, Stockholm.

CIRIA. 1978. Tunnelling-improved contract practices. Report 79. Construction Industry Research and Information Association, London.

CLARK, G B. 1966. Blasting and dynamic rock mechanics. Ch. 19, Failure and breakage of rock. Proc. 8th Symp. Rock Mech. Minnesota. Am. Inst. Min. Met. and Petr. Engrs. (1967) New York.

CLARK Jr, S P. 1966. Handbook of physical constants. The Geological Society of America.

COOLEY, J W and TUKEY, J W. 1965. An algorithm for the machine calculation of complex Fourier series. Math. of Comput.; 19, April, 297-301.

COON, R. 1968. Correlation of engineering behaviour with the classification of in-situ rock. Ph.D Thesis, Univ. Illinois.

CORDING, E J et al. 1975. Methods for geotechnical observations and instrumentation in tunnelling. Volume 2 Appendices. Dept. Civil Eng. Univ. of Illinois, Urbana.

CRAMPIN, S. 1981. A review of wave motion in anisotropic and cracked elastic media. Wave Motion 3, 343-391. North Holland Publishing Co.

CRATCHLEY, C R, GRAINGER, P and McCANN, D M. 1972. Some applications of geophysical techniques in engineering geology with special reference to the Foyers hydro-electric scheme. Proc. Internat. Geol. Cong., 24th, 13 : 163-175.

DADSON, J. 1981. Blast! Its curtains for Stratford New Civil Engineer. 19th Nov.

DAVIES, J V. 1970. Ground vibrations from tunnel blasting : Experience from blasting 12 ft dia Mersey pilot tunnel. Tunnels and Tunnelling, 2, May, 141-144.

DEERE, D U. 1964. Technical description of rock cores for engineering purposes. Rock Mechanics and Engineering Geology Vol 1, No 1, 17-22.

DEERE, D U. 1968a. In : Rock Mechanics in Engineering Practice, Stagg, K G and Zienkiewicz, O C. (Editors) Wiley, NY.

DEERE, D U. 1968b. Indexing rock for machine tunnelling. Proc. Conf. Rapid Excavations : Problems, Progress. 32-38.

DEERE, D U, HENDRON Jr, A J, PATTON, F D, CORDING, E J. 1966. Design of surface and near surface construction in rock. Proc. Symp. Rock Mech. 8th Minn.

DEVINE, J F. 1966. Avoiding damage to residences from blasting vibrations. Highway Res. Record No 135. Highway Res. Board, Natl. Res. Council - Natl. Acad. Sci.

DEVINE, J F, BECK, R J, MEYER, A V C and DUVALL, W I. 1965. Vibration levels transmitted across a presplit fracture plane. U.S. Bureau of Mines, Report of Investigations, 6695.

DEVINE, J F and DUVALL, W I. 1963. Effect of charge weight on vibration levels for millisecond delayed quarry blasts. Earthquake Notes, Eastern Section, Bull. Seismol. Soc. Am., 34, No 2, 17.

DICK, R A. 1968. Factors in selecting and applying commercial explosives and blasting agents. U.S. Bureau of Mines Information Circular 8405.

DOWDING, C H. 1977. Seismic stability of underground openings. Proc. Storage in excavated rock caverns - Rockstore 77. Stockholm, Sweden. Vol 2, 231-32. Pergamon Press.

DOWDING, C H. 1979. Earthquake stability of rock tunnels. Tunnels and Tunnelling, 11, 5, June. 15-20.

DOWDING, C H and ROZEN, A. 1978. Damage to rock tunnels from earthquake shaking. Journal of the Geotech. Eng. Div., ASCE, 104, GT2, Feb, 175-191.

DUVALL, W I and ATCHISON, T C. 1950. Vibrations associated with a spherical cavity in an elastic medium. RI 4692. U.S. Bureau of Mines.

DUVALL, W I, ATCHISON, T C and FOGELSON, D E. 1966. Empirical approach to problems in blasting research. Ch. 20, Failure and breakage of rock. Proc. 8th Symp. Rock Mech. Minnesota. Am. Inst. Min. Met and Petr. Engrs. (1967) New York.

EDWARDS, A T and NORTHWOOD, T D. 1960. Experimental studies of the effects of blasting on structures. The Engineer, 210, Sept 30, 538-546.

EGGER, P. 1980. Deformations at the face of the heading and determination of the cohesion of the rock mass. Underground Space, 4, No 5, 313-318.

EINSTEIN, H H and SCHWARTZ, C W. 1979. Simplified analysis for Tunnel Supports. Journal of the Geotechnical Engineering Division, ASCE. 105, April, 499-518.

ELVERY, R H and VALE, D W. 1973. Developments in the measurement of ultrasonic pulse velocity in concrete. Proc. 7th Internat. Conf. on Non Destructive Testing. Warsaw.

ESTEVES, J M. 1978. Control of vibrations caused by blasting. Laboratorio National De Engenharia Civil, Lisboa, Portugal, Memoria 498.

EWING, W M, JARDETZKY, W S and PRESS, F. 1957. Elastic waves in layered media. McGraw-Hill, New York.

FAIRHURST, C and DAEMEN, J J K. 1980. Practical inferences from research on the design of tunnel supports. Underground Space, 4, No 5, 297-311.

FARR, J B. 1978. Seismic wave attenuation and rock properties. Proc. of Speciality Workshop on Site characterisation and exploration (Ed C H Dowding) Northwestern Universisty, Illinois. ASCE.

FEHLER, M. 1979. Seismological investigations of the mechanical properties of a hot dry rock geothermal system. Ph.D. Thesis. Massachusetts Institute of Technology.

FOGELSON, D E, D'ANDREA, D V, FISCHER, R L. 1965. Effects of decoupling and type of stemming on explosion generated pulses in mortar : A laboratory study, U.S. Bureau of Mines, Report of Investigations, 6679.

FOGELSON, D E and DOWDING, C H. 1977. Bureau of Mines research on response to ground vibrations from blasting. Proc. 18th Symp. Rock Mech. Colorado June 22-24. Colorado School of Mines Press.

GLADWIN, M T and STACEY, F D. 1974. Anelastic degradation of acoustic pulses in rock. Phys. Earth planet. Interiors, 8, 332-336.

GOLDSMITH, W. 1966. Pulse propagation in rocks. Ch. 22, Failure and breakage of rock. Proc. 8th Symp. Rock Mech. Minnesota. Am. Inst. Min. Met. and Petr. Engrs. (1967). New York.

GOLDSMITH, W and ALLEN, W A. 1955. Graphical representation of the spherical propagation of explosive pulses in elastic media. J. Acoustical Soc. Am. 27, 47-55.

GRAFF, K F. 1975. Wave motion in elastic solids. Clarendon Press, Oxford.

GUIGNARD, J C and GUIGNARD, E. 1970. Human response to vibration - a critical survey of published work. Univ. Southampton, Inst. Sound and Vibn. Res. Memo 373.

GUTENBERG, B and RICHTER, C F. 1942. Earthquake magnitude, intensity, energy and acceleration. Bull. Seism. Soc. Am. 32, 163.

HARDING, H J B. 1945. Emergency repair to the Tower Subway, London, after air-raid damage. The Institution of Civil Engineers Journal, November.

HATCH, F H, WELLS, A K and WELLS, M K. 1972. Petrology of Igneous Rocks. Allen and Unwin.

HENDRON Jr, A J. 1977. Engineering of rock blasting on civil projects. In Structural and Geotechnical Mechanics. Ed. W J Hall. Prentice-Hall, New Jersey, U.S.A, 242-277.

Herepaths Journal and Railway Magazine Nov. 21, 1846. 1479.

HOEK, E and BRAY, J W. 1977. Rock slope engineering, 2nd Edition. The Institution of Mining and Metallurgy, London.

HOEK, E and BROWN, E T. 1980. Underground excavations in rock. The Institution of Mining and Metallurgy, London.

HOLMBERG, R and PERSSON, P A. 1979. Design of tunnel perimeter blasthole patterns to prevent rock damage. Proc. Tunnelling '79. The Institution of Mining and Metallurgy, London.

HUDSON, J A, JONES, E J W and NEW, B M. 1980. P-wave velocity measurements in a machine-bored, chalk tunnel. Q.J. Eng. Geol. 13, 33-43.

HUDSON, J A and PRIEST, S D. 1979. Discontinuities and rock mass geometry. Int. J. Rock Mech. Min. Sci. and Geomech. Abstr. Vol 16. 339-362.

HUMPHREYS, C L H. 1937. The reconstruction of the Chester-Holyhead Road near Penmaenmawr, North Wales. Journal of the Institution of Civil Engineers. Volume 6, Paper 5085.

JACKSON, M W. 1967. Thresholds of damage due to ground motion. Proc. Internat. Symp. Wave Prop. Dyn. Props. Earth Mats., New Mexico 961-969.

JAEGER, J C and COOK, N G W. 1976. Fundamentals of rock mechanics, 2nd Edition. Chapman and Hall Ltd, London.

KAY, S M and MARPLE, S L. 1981. Spectrum analysis - A modern perspective.Proc. IEEE, 69, 11, Nov., 1380-1419.

KEIL, L D, BURGESS, A S and NIELSEN, N M. 1977. Blast vibration monitoring of rock excavations. Can. Geotech. Jour. 14, 603-619.

KJARTANSSON, E. 1979. Constant Q wave propagation and attenuation. J. Geophys. Res. 84 (B9), 4737-4748.

KNOPOFF, L. 1956. The seismic pulse in materials possessing solid friction, I : Plane waves. Bull. Seismological Soc. Am. 46, 175-183.

KOLSKY, H. 1963. Stress waves in solids. Dover Publications Inc. New York.

LAMA, R D and VUTUKURI, V S. 1978. Handbook on Mechanical Properties of Rocks, Vol II, Trans. Tech. S.A. CH 4711 Aedermannsdorf, Switzerland.

LANGEFORS, U and KIHLSTROM, B. 1978. The modern technique of rock blasting, 3rd Edition, John Wiley and Sons, New York.

LARSON, D B. 1982. Explosive energy coupling in geologic materials. Int. J. Rock Mech. Min. Sci. and Geomech. Abstra., Vol 19, 157-166.

LUCOLE, S W and DOWDING, C H. 1979. Statistical analysis of blast emission records from quarrying, mining and construction operations in the State of Illinois. Report to Illinois Institute of Natural Resources. No. 79/02 Jan.

LUNDBORG, N, HOLMBERG, R and PERSSON, P A. 1978. Relation between vibration, distance and charge weight. Rep. Swedish Council for Building Res. R11:1978. Cited by Holmberg and Persson, 1979.

McKENZIE, C K, STACEY, G P and GLADWIN, M T. 1982. Ultrasonic characteristics of a rock mass. Int. J. Rock Mech. Min. Sci. and Geomech. Abstra., 19, 25-30.

MAGRAB, E B and BLOMQUIST, D S. 1971. The measurement of time-varying phenomena, Wiley-Interscience, New York.

MEDEARIS, K. 1978. Rational damage criteria for low-rise structures subjected to blasting vibrations. Proc. Instn. Civ. Engrs. Part 2, 65, Sept. 611-621.

MERRITT, A H. 1972. Geologic prediction for underground excavations. Proc. Rapid Excav. and Tun. Conf. AIME, New York, 115-132.

MORONEY, M J. 1971. Facts from figures. Penguin Books.

NEUMANN, F. 1954. Earthquake intensity and related ground motion. University of Washington Press, Seattle, WA.

NEW, B M. 1974. Versatile electo-optic alignment system for field applications. Applied Optics. 13 (April), 937-941.

NEW, B M. 1976. Ultrasonic wave propagation in discontinuous rock. Dept. of Environment, TRRL Report LR 720, Crowthorne.

NEW, B M. 1978. The effects of ground vibration during bentonite shield tunnelling at Warrington. Dept. of Environment, TRRL Report LR 860, Crowthorne.

NEW, B M. 1979. Train and blast induced vibration in the Penmaenbach rail tunnel. Tunnels and Underground Pipes Division Working Paper No 31. TRRL Crowthorne.

NEW, B M. 1982a. Ambient and blasting induced vibrations at the Pass of Killiecrankie. Transport and Road Research Laboratory Working Paper 5/82. TRRL Crowthorne.

NEW, B M. 1982b. Vibration caused by underground construction. Proc. Tunelling 82, (London : IMM), 217-229.

NEW, B M and WEST, G. 1980. The transmission of compressional waves in jointed rock. Engineering Geology, 15, 151-161.

NEW, B M, WILD, P T and BISHOP, C J. 1980. Bentonite tunnelling beneath major services in loose ground. Tunnels and Tunnelling 12, 5, June.

NEWLAND, D E. 1975. Random vibrations and spectral analysis. Longman, London.

NEWMARK, N M. 1968. Problems in wave propagation in soil and rock. Proc. Int. Soc. Wave Propagation and Dynamic Properties of Earth Materials, Univ. of New Mexico Press, Albaquerque, 7-26.

NEWMARK, N M and HALTIWANGER, J D. 1962. Principles and practices for design of hardened structures. Tech. Rep. No AFSWC-TDR-62-138 Air Force Special Weapons Center, Kirtland Air Force Base, New Mexico.

NICHOLLS, H R and HOOKER, V E. 1965. Comparative study of explosives in granite. Third series of tests. U.S. Bureau of Mines, Report of Investigations, 6693.

NICHOLLS, H R, JOHNSON, C F and DUVALL, W I. 1971. Blasting vibrations and their effects on structures. U.S. Bureau of Mines Bulletin 656, Washington.

O'BRIEN, P N S. 1969. Some experiments concerning the primary seismic pulse. Geoghysical Prospecting, 17, 511-547.

O'BRIEN, P N S and LUCAS, A L. 1971. Velocity dispersion of seismic waves. Geophysical prospecting, 19, 1-26.

OKAZAWA, H et al. 1975. The effect of vibration in nearby tunnels caused by blasting and its preventive measures. - The case of Koi-Tunnel on Sanyo-Shinkansen. Tunnels and Underground, 6, 11, 789-797.

ONODERA, T F. 1963. Dynamic investigation of foundation rocks in-situ. Proc. Symp. Rock Mech. 5th, Minn.

O'REILLY, M P and NEW, B M. 1982. Settlements above tunnels in the United Kingdom - their magnitude and prediction. Proc. Tunnelling 82, (London, IMM), 173-181.

ORIARD, L J. 1971. Blasting operations in the urban environment. Bulletin of the Association of Engineering Geologists, Winter.

ORIARD, L J. 1979. Modern blasting in an urban setting. Report No UMTA-GA-06-0007-79-1. The Atlanta Research Chamber Applied Research Monographs, June, Interim report. NTIS Springfield, Virginia.

PAKES, G. 1976. Edinburgh sewage disposal scheme; Tunnelling works. Proc. Symp. Tunnelling 76. IMM. London.

PAO, Y H and MOW, C C. 1971. Diffraction of elastic waves and dynamic stress concentrations. Adam Hilger, London.

PERSSON, P A, HOLMBERG, R, LANDE, G and LARSSON, B. 1980. Underground blasting in a city. Proc. Rockstore 80.

PRATT, H R, HUSTRULID, W A and STEPHENSEN, D E. 1978. Earthquake damage to underground facilities. Du Pont, Savannah River Laboratory, South Carolina. For U.S. Dept. Energy Contract AT (07-2)-1.

PRIEST, S D and HUDSON, J A. 1976. Discontinuity spacings in rock. Int. J. Rock Mech. Min. Sci. and Geomech. Abstr. Vol 13, 135-148.

READ, H H. 1948. The Grampian Highlands, British Regional Geology Series. HMSO, Edinburgh.

REIHER, H and MEISTER, F J. 1931. Human sensitivity to vibrations (in German) Forsch. auf dem Geb. des Ingen., 2(11), 381-6.

RICKER, N. 1953. The form and laws of propagation of seismic wavelets. Geophysics, 18, 10-39.

RICKER, N. 1977. Transient waves in visco-elastic media. Elsevier, (Amsterdam).

ROBERTS, A. 1969. Vibrations produced by engineering processes. Construction Industry Research and Information Association (CIRIA) Technical Note 6, London.

ROUSSEL, J M. 1968. Theoretical and experimental considerations of the dynamic modulus of rock masses. Revue de l'Industrie Minerale, 80, August, No 8, 573-600. (In French translated by TRRL).

ROZEN, A. 1976. Response of rock tunnels to earthquake shaking. M.Sc. Thesis in Civil Engineering. Massachusetts Institute of Technology.

RUTLEDGE, T C. 1978. Engineering classifications of rock for the determination of tunnel support. Proc. Internat. Tunnelling Symp. Tokyo.

SAKURAI, S and KITAMURA, Y. 1977. Vibration of tunnel due to adjacent blasting operation. Internat. Symp. on Field Measurement in Rock Mechanics. Zurich, April, 4-6.

SARMA, S K. 1975. Seismic stability of earth dams and embankments. Geotechnique, 25, 4, 743-761.

SARMA, S K. 1981. Seismic displacement analysis of earth dams. Journal of the Geotech. Eng. Div., ASCE, 107, GT12, Dec. 1735-1739.

SATO, H. 1977. Single isotropic scattering model including wave conversions simple theoretical model of the short period body wave propagation. J. Phys. Earth, 25, 163-176.

SAUER, F M, CLARK, G B and ANDERSON, D C. 1964. Nuclear geoplosics - Part IV - Empirical analysis of ground motion and cratering. Stanford Res. Inst. for the Defence Atomic Support Agency, Report DASA-1285(IV).

SCHNEIDER, B. 1967. Contribution a l'etude des massifs de fondation de barrages. Trans. du labor de geol. de la fac. des sci. de Grenoble. Monsoir No 7, 235p Grenoble.

SCOTT, J H, CARROLL, R D, ROBINSON, C S and LEE, F T. 1974. Engineering geologic, geophysical, hydrologic and rock mechanics investigations of the Straight Creek tunnel site pilot bore, Colorado, U.S. Geol. Surv. Profess. Papers 815.

SEED, H B and GOODMAN, R E. 1964. Earthquake stability of slopes of cohesionless soils. Journal of Soil Mech. and Found. Div. ASCE. 90, Nov, 43-73.

SHARPE, J A. 1942. The production of elastic waves by explosion pressures. Theory and empirical field observations, Geophysics 7, 144-154.

SISKIND, D E, STACHURA, V J, STAGG, M S and KOPP, J W. 1980. Structure response and damage produced by airblast from surface mining. U.S. Bureau of Mines, Report of Investigations, 8485.

SISKIND, D E, STAGG, M S, KOPP, J W and DOWDING, C H. 1980. Structure response and damage produced by ground vibration from surface mine blasting. U.S. Bureau of Mines, Report of Investigations, 8507.

SJOGREN, B, OFSTHUS, A and SANDBERG, J. 1979. Seismic classification of rock mass qualities. Geophysical Prospecting, 27, 409-442.

SNODGRASS, J J and SISKIND, D E. 1974. Vibrations from underground blasting. RI 7937. U.S. Bureau of Mines, Washington, USA.

SOIL MECHANICS. 1974. A55 North Wales coast road - Site investigations/Contract B. Parts I and II.

SOLIMAN, J T. 1968. A scale for the degrees of vibration perceptibility and annoyance. Ergonomics, 2, 101-122.

STAGG, M S and ENGLER, A J. 1980. Measurement of blast-induced ground vibrations and seismograph calibration. U.S. Bureau of Mines, Report of Investigations, 8506.

STARFIELD, A M. 1966. Strain wave theory in rock blasting. Ch. 23, Failure and breakage of rock. Proc. 8th Symp. Rock Mech. Minnesota. Am. Inst. Min. Met. and Petr. Engrs. (1967) New York.

STEFFENS, R J. 1974. Structural vibration and damage. Building Research Establishment Report. HMSO, London.

SWISS ASSOCIATION OF STANDARDISATION. Effects of vibration on construction. Seefeldstrasse 9, CH 8008, Zurich, Switzerland.

TIMOSHENKO, S P and GOODIER, J N. 1970. Theory of elasticity, 3rd Edition. McGraw-Hill Book Co., New York.

VOROB'EV, I T et al. 1972. Features of the development and propagation of the Rayleigh surface wave in the Dzhezkazgan deposit. Fiz-Tekh. Probl. Raz. Polez, Isk. 8, No 6, 36-43. Soviet Min. Sci. 8, (1972), 634-9. Cited by Holmberg and Persson, 1979.

WALKER, S, YOUNG, P A and DAVEY, P M. 1982. Development of response spectra techniques for prediction of structural damage from open-pit blasting vibrations. Trans. Instn. Min. Metall. (Sect. A; Min. industry), 91, A55-62.

WALLIS, P F and KING, M S. 1980. Discontinuity spacings in a crystalline rock. Int. J. Rock. Mech. Min. Sci. and Geomech. Abstr. 17, 63-66.

WARD, W H. 1978. Ground supports for tunnels in weak rocks, Geotechnique, 28, No 2, 133-171.

WHIFFIN, A C and LEONARD, D R. 1971. A survey of traffic induced vibrations. Department of the Environment, RRL Report LR 418, Crowthorne.

WICKHAM, G E, TIEDEMANN, H R and SKINNER, E H. 1974. Support determination based on geologic predictions. Proc. Rapid Exc. Tun. Conf. AIME 43-64.

WINKLER, K, NUR, A and GLADWIN, M T. 1979. Friction and seismic attenuation in rocks. Nature, 277, 528-531.

WISS, J F. 1981. Construction vibrations : State of the art. Journal of the Geotechnical Engineering Division, ASCE. 107, February, 167-181.

WISS, J F and PARMALEE, R A. 1974. Human perception of transient vibrations. J Structural Div., ASCE, 100, ST4, Proc. Paper 10495, April, 773-787.

YOSHIMI, Y, RICHART Jr, F E, PRAKASH, S, BARKAN, D D and ILYICHEV, V A. 1977. Soil dynamics and its application to foundation engineering. State of the Art Report. Proc. 9th Conf. Soil Mech. and Found. Eng. Vol 2. Tokyo.

YOUNG, R P and HILL, J J. 1981. Seismic remote sensing of rock masses for the optimisation of excavation efficiency. Proc. Internat. Geoscience and Remote Sensing Symp. San Francisco Aug. 31-Sept. 2. IEEE 83CH1837-4.

ZIOLKOWSKI, A and LERWILL, W E. 1979. A simple approach to high resolution seismic profiling for coal. Geophysical Prospecting, 27 No 2, 360-393.

Vibration caused by underground construction

B. M. New
Transport and Road Research Laboratory, Crowthorne, England

Synopsis
Environmental considerations play an important and often critical part in the acceptance of a construction project. Although tunnelling may have a number of obvious advantages, there are, nevertheless, situations in which underground construction may endanger nearby structures and services and intrude upon the community. This is true, particularly, in urban areas, where conditions may inhibit or even preclude the use of certain methods, e.g. drill and blast. In recent years mechanization of tunnelling methods has resulted in the use of plant that may introduce significant vibrational energy into the ground. In particular, the use of full-face tunnel-boring machines at shallow depths may give rise to environmental problems.

Damage criteria from various sources are critically reviewed and vibration data obtained from a number of tunnelling sites within the United Kingdom are presented. The vibration measurements are correlated with various modes of environmental impact, including structural damage, human tolerance and ground settlement by compaction.

The viability of civil engineering construction techniques will often depend on their effects on existing structures and their disturbance of the local population. Tunnelling frequently takes place beneath sensitive urban environments and although subsurface works have many advantages, some difficulties may arise. Ground movements of a quasi-static nature have been extensively investigated, but the effects of vibrations due to tunnelling operations have received considerably less attention. Vibration and noise from construction sources will generally be of a temporary nature, but the disturbance caused may result in permanent damage to property and substantial nuisance to the surrounding population. Either factor may lead to restraints on the working method that result in additional costs or even, in extreme circumstances, curtailment of activity.

Blasting and piling operations have in the past been the cause of greatest concern, but in recent years construction works have utilized larger plant as economic pressures have forced greater emphasis on mechanized rather than labour-intensive techniques. These developments have resulted in the use of machines that dissipate large amounts of energy, in the form of ground vibrations and noise, into the environment. Tunnelling works have followed this trend and, in particular, the use of full-face tunnelling machines in shallow urban works is now commonplace.

In many countries statutory environmental authorities must be satisfied that proposed construction work will conform to acceptable standards; in the United Kingdom these powers are vested in Local Authorites through the Control of Pollution Act, 1974.

This paper considers the effects of machine (continuous) and blasting (transient) induced vibrations in the context of tunnelling in urban areas. Measurements of vibration from a number of sites are given with a discussion of current 'damage' and 'intrusion' criteria.

Vibration measurement

It is necessary to briefly consider what measurements are necessary to define construction-induced vibrations. Harmonic vibrations may be described by any two of the following parameters: frequency, peak particle displacement, peak particle velocity or peak particle acceleration. The 'peak particle' preface indicates that it is the maximum value associated with the motion of a particle at a point in the ground (or on a structure) that is considered.

In the context of structural damage it is usual to express vibration in terms of peak particle velocity (PPV) and frequency. It is of interest to note that the stress induced in a solid by a travelling wave is proportional to the particle velocity of the wave motion. With regard to human perception of vibration, the relevant parameter is related to the frequency range involved. At frequencies below 10 Hz acceleration seems to be the dominant consideration, whereas at higher frequencies velocity or displacement criteria may be appropriate.

Transducers are readily available with output voltages proportional to particle velocity and geophone types are self-generating (need no power supply) and are ruggedly designed for field use. Measurement of particle velocity allows single-process derivation of acceleration, by differentiation, and of displacement by integration if required.

Measurement of particle velocity should be made in three mutually perpendicular directions. This allows the calculation of the resultant particle velocity, V_R, by the vector summation of the component velocities (V_1, V_2 and V_3):

$$V_R = (V_1^2 + V_2^2 + V_3^2)^{1/2}$$

Fig. 1 shows a triaxial geophone array being rigidly secured to a tunnel side wall.

Fig. 1 Mounting triaxial geophone array on tunnel wall

Vibration measuring instruments that display the resultant peak particle velocity directly on a chart record are available. If such an instrument is not used, the three

vectors must be summed by 'hand' or computer processing. The true resultant is obtained by summing the three component values at simultaneous times. The 'pseudo resultant', sometimes referred to, is obtained by summing the maximum value obtained for each component during the period of the vibrations.

It is vital for the specification of the instrument chosen to be appropriate to the vibrations that it is to record, particularly in terms of frequency response and sensitivity. For instance, some instruments are limited to an upper frequency bound of 200 Hz. This type of equipment may generally be quite satisfactory but will, of course, be insensitive to vibrations above 200 Hz that could be present. High frequencies (200–500 Hz) will sometimes be encountered in the region very close to tunnelling works. Where doubt exists expert opinion should be sought and trial measurements made with systems sensitive to high frequencies.

Instruments that record peak particle velocity only may be left for many days without attention and are particularly useful for routine monitoring during construction. Systems that provide high-speed recordings that show the full vibration waveform will, however, often prove useful for diagnostic purposes during initial works. Periodic checking and recalibration of site measuring equipment is essential for reference purposes. Bollinger[5] and Stagg and Engler[27] have dealt fully with the theory and choice of vibration measuring equipment, and Jaeger and Cook[11] and Kolsky[12] have provided an appropriate background on strain wave propagation in rock and other solids.

Construction-induced vibration in urban areas

'Continuous' types of vibration source

A 'state of the art' review of construction-induced vibration has recently been published by Wiss[32] and usefully presents measurements of vibration caused by various construction operations. These data have been converted to metric scales and combined with other information and are presented in Fig. 2. This graph represents approximate values and provides general guidance only, as conditions that affect the input and transmission of vibration will vary considerably from site to site. This form of presentation shows the likely relative intensities from various sources and highlights the fact that even a small charge of dynamite (0.45 kg) will produce larger vibrations than those from most 'continuous' types of source. Fatigue effects that result from repeatedly taking a structure through a stress cycle will, however, be more likely to occur under conditions of 'continuous' vibration. Acceptable levels will therefore be related to the nature and duration as well as the maximum level of the vibration.

Little, if any, information has been published on vibrations of a 'continuous' nature caused by tunnel construction, although some data are available from tunnels that are operational. Bean and Page[4] gave details of vibration in and around road tunnels and the suppression of noise and vibration from underground trains has also been reported.[2] The writer has measured vibrations due to various types of train passing through an unlined hard rock tunnel. The maximum peak particle velocity recorded on the tunnel side wall was 1.2 mm/sec and the predominant frequencies of the motion lay in the surprisingly high bandwidth 200–800 Hz. It should be noted that the track was long-welded and rather higher vibration levels would be expected where jointed track occurs.

Steffens[28] has published a general review of vibration measurements and effects from many sources and this work also provides an extensive bibliography.

Vibrations from full-face tunnelling machines

As part of a broad research programme to determine the effects of tunnelling in urban areas vibration measurements have been made at a number of working sites in the United Kingdom. Three sites – at Warrington, Cardiff and Sutton – that were using full-face tunnelling machines are described below. The work at Warrington was part of an extensive series of measurements reported elsewhere[15,16,21] and only a summary of the vibration measurements is given here. Table 1 gives details of the tunnelling conditions and of the resulting ground vibrations at various distances ahead of the tunnel faces. Fig. 3 presents the resultant peak particle velocities and illustrates their decay with increasing distance from the tunnel face. Comparison of Figs. 2 and 3 shows that the machine excavating moderately strong rock at Cardiff produced a level of vibration rather lower than that attributed to a large bulldozer by Wiss.[32] Similarly, the vibration from the very small machine driving through London Clay at Sutton was less than that expected from a

Table 1

Tunnel	Machine type	Ground conditions	Tunnel diameter, m	Tunnel cover, m	Tunnel face, geophone separation, m	Resultant PPV, mm/sec
Acton Grange trunk outfall sewer (Warrington New Town Development Corporation)	Bentonite shield; full-face machine fitted with disc cutters	Very loose to dense cohesionless drift deposits with very strong glacial erratic cobbles and boulders and some sandstone	2.44	4.5	2 18 (Many other measurements taken between 1 and 20 m)	3.9 0.15
Cardiff cable tunnel (General Post Office)	McAlpine full-face machine with Big A picks in compressed air	Moderately strong (12.5–50 MN/m^2) red-brown mudstone (Keuper Marl) overlain with gravel drift	2.44	11	11 19	1.3 0.42
Sutton–Worcester Park sewer (Thames Water Authority)	Full-face mini-tunnel machine fitted with picks	Brown stiff clay weathered and silty at top becoming fissured at depth (London Clay)	1.2	4	4.5 13	0.12 0.04

small bulldozer. At Sutton the very low level of vibration was not perceptible at the surface and no complaints relating to vibration or noise caused by excavation during this part of the drive were received. The vibrations were at a reasonably constant level during each mucking and clearly attributable to the action of the picks at the tunnel face. At Cardiff the vibrations produced by the rock cutting process were clearly perceptible to an observer on the ground surface directly above the machine, although their level was well below that associated with even the most conservative damage criteria. Some concern had been expressed about the possible effects of vibration at this site, but in the event no such complaints were received. The vibrations were of a more fluctuating nature than those observed at Sutton, maximum peak particle velocities occurring in random wave packets, which lasted for about ½ sec, set in a lower general level. It should be noted that although the vibrations produced by the Cardiff machine were larger than those from the Warrington machine (at a similar distance), their surface effects were less noticeable owing to the greater tunnel cover.

The relative position of the Warrington tunnel and adjacent houses is shown in Fig. 4 and Fig. 5 shows the signal processing and recording equipment used in the mobile laboratory on site. This tunnel was driven through cohesionless Drift deposits with a cover of less than 6 m. The environmental effects of the ground vibration caused by the excavation process were investigated with particular regard to ground settlement by compaction.

Vibration data were recorded from transducers located in boreholes, on the ground surface, on the tunnelling machine and on the concrete tunnel lining. These records were processed to characterize the vibrations in terms of peak particle velocities and frequency spectra. The maximum measured ground vibration (expressed in terms of resultant peak particle velocity) was 3.9 mm/sec. The

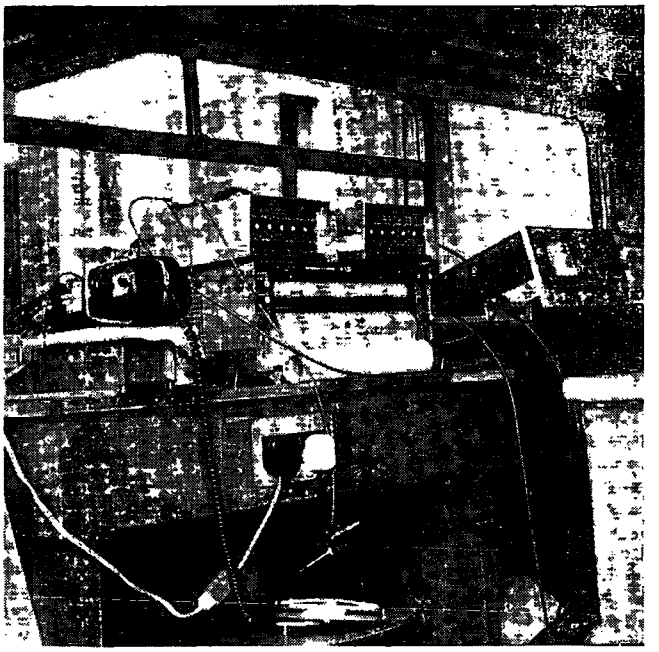

Fig. 5 Vibration processing and recording equipment in mobile laboratory

vibration was characterized by random high velocity particle motions that resulted from impacts between the machine's disc cutters and glacial boulders in the tunnel face.

Spectral analysis of the vibrations within a few metres of the tunnel face showed that much of the energy was being transmitted at frequencies between 200 and 400 Hz.

Surface and subsurface settlement measurements were made along the tunnel line. Laboratory tests and other field data showed that the ground in this area was likely to settle at levels of vibration lower than those measured from

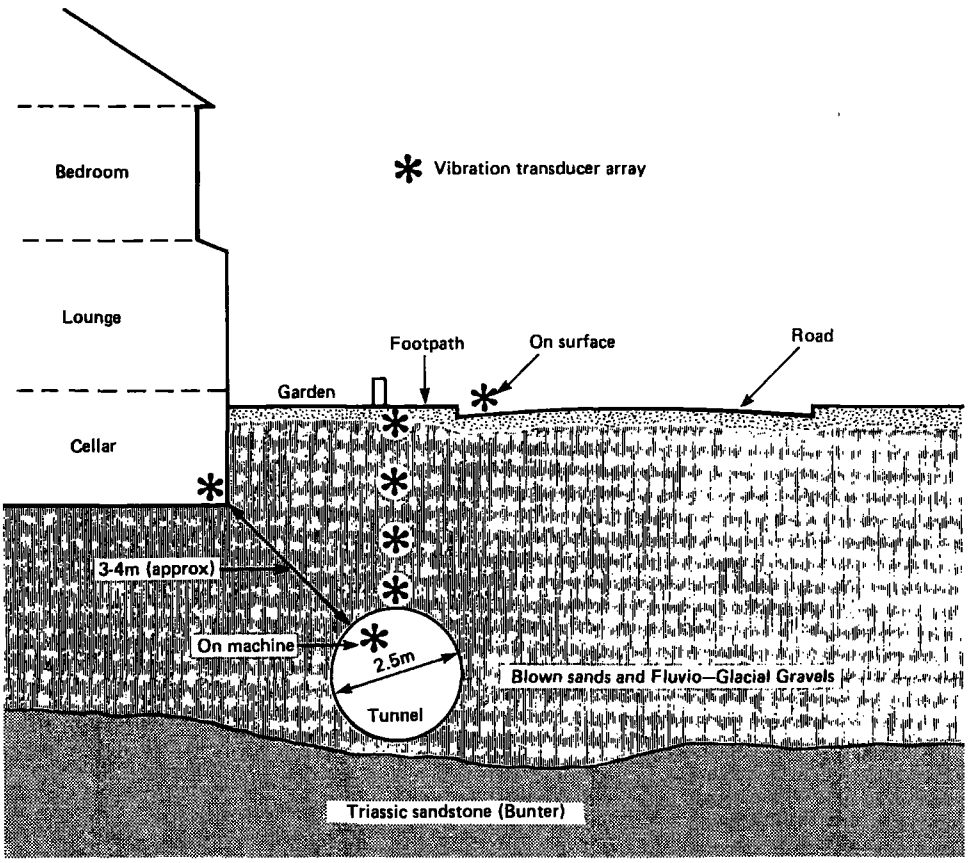

Fig. 4 Vibration measurements during tunnel construction at Warrington (other measurements include surface and subsurface deformations)

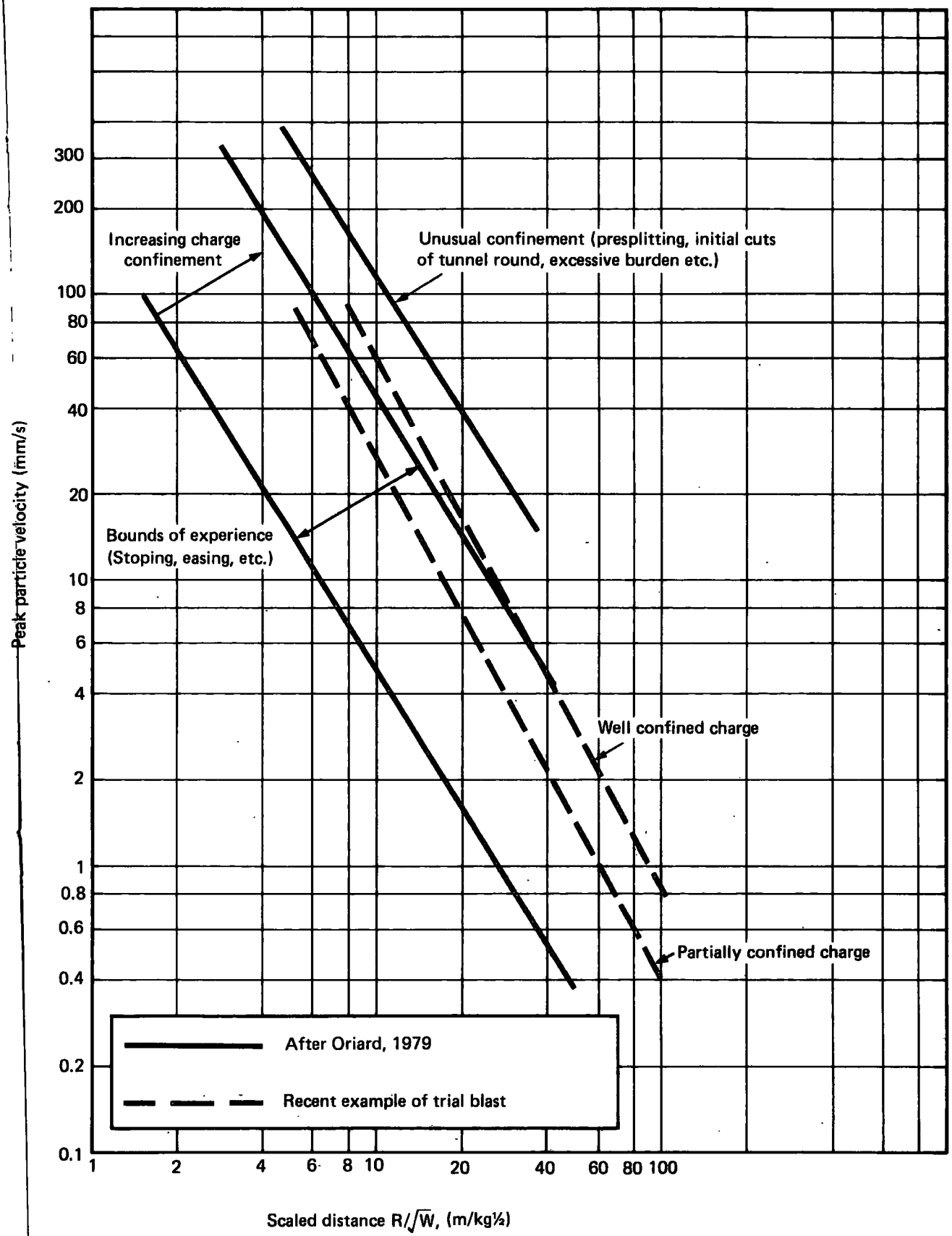

Fig. 6 Prediction curves for blasting vibrations

PPV, based on Fig. 6, may be separated by an order of magnitude, it does, nevertheless, provide a useful starting point for predictive investigations.

If trial blast data are available to contractors at the tender stage, it will provide valuable guidance as to the maximum charge weight per delay that may be used in the tunnel round. Where no such information is provided the usual course of action is for the contractor to use the initial construction blasts to determine his own 'safe' charge weights with sometimes unexpected consequences. Clearly, the pre-knowledge provided by a trial blast is invaluable to all parties concerned.

There are a few points regarding trial blasts that are worthy of specific mention.

Trial blast charges are often relatively small in comparison with working charge weights per delay and the

Table 4 Risk of damage in ordinary dwelling houses with varying ground conditions. After Langefors and Kihlström[13]

	Sand, shingle, clay under groundwater level	Moraine, slate, soft limestone	Hard limestone, quartzy sandstone gneiss, granite, diabase	Type of damage
Wave velocity, m/sec	300–1500	2000–3000	4500–6000	
Vibration velocity, mm/sec	4–18	35	70	No noticeable cracks
	6–30	55	110	Insignificant cracking (threshold value)
	8–40	80	160	Cracking
	12–60	115	230	Major cracks

Table 5 Typical specifications for limiting blasting PPV levels. After Ashley and Parkes[3]

Type of structure	PPV, mm/sec
Welded steel gas mains, sound sewers and engineering structures	50
Good residential/commercial and industrial property	25
Housing in poor repair	12
Ancient and historic monuments	7.5

damage to structures, although such a document is in the course of preparation.

Attempts to establish safe levels of vibration have, not unnaturally, tended to be of a conservative nature and the German Standard DIN4150 is an example that is generally held to be overcautious and unworkable. The recently published Swiss standards (Table 2) again seem rather cautious. They provide a guide to acceptable levels from blasting or traffic/machinery forms of excitation for various types of structure. Persson *et al.*[19] reported vibration limits enforced in Swedish cities (Table 3). Langefors and Kihlström[13] provided a risk assessment for ordinary dwelling houses with varying ground conditions (Table 4). In the United Kingdom Ashley and Parkes[3] have quoted typical specifications for limiting PPV, again related to various types of structure (Table 5). Other workers[6,7] have also given 'safe vibration values' and it is of interest to note the overall trend that the more recent the publication the lower the acceptable values have become. This trend does not appear to be supported by much new field evidence of damage at lower particle velocities and indicates a shifting social climate rather than a change in engineering values.

Siskind *et al.*[24] have produced a comprehensive account of structure response and damage produced by ground vibration from surface mine blasting. This work provides damage probability analyses for various conditions and Fig. 7 is, in part, based on their 'alternative safe blasting level criteria' for residential structures. The 'safe' levels indicated fit the case history information well and it is suggested that these levels provide a useful basis for risk assessment. It must be emphasized that there are many recorded instances of particle velocities well in excess of those indicated not having damaged structures. Conversely, if a structure is in very poor condition, even the slightest vibration may cause inherent weaknesses to become apparent.

Research is being carried out on response spectra techniques intended to improve prediction of vibration damage to structures.[14,24,30] These techniques use measurements of the mass, stiffness and damping characteristics of the subject structures to assess their likely response to vibration. This approach shows promise, particularly where specific structures are at risk and the additional investigations are financially acceptable.

In some respects the conventional form of damage criteria already incorporate an important element of response spectra techniques. For instance, the safe level of PPV (Fig. 7) reduces considerably at frequencies less than 40 Hz. This coincides with the predominant frequencies (10–30 Hz) associated with the response of residential structures. Further, the variation in safe level shown in Table 4 may also be attributed partly to the fact that footing materials characterized by low compressional wave velocities will tend to propagate low-frequency wave motions. Again, the recommended safe PPV is reduced, albeit indirectly, for the lower-frequency vibrations. In each of these cases the known response characteristics of residential structures are matched empirically with an appropriate safe vibration level, taking into account the frequency of the forcing motions.

Geological structures

Besides damage to man-made structures, consideration must sometimes be given to potentially unstable soil or rock conditions in the vicinity of construction works. Cohesive soils are unlikely to be adversely affected by vibration, whereas loose sands may be caused to settle. In certain circumstances liquefaction may take place and result in large ground settlements. A recent 'state of the art' report on soil dynamics (and its application to foundation engineering) has been published by Yoshimi *et al.*[34] and it provides a useful background to the subject with an extensive bibliography. Seed and Goodman[23] and Sarma[22] have provided analyses concerned with the earthquake stability of soil slopes.

Blasting vibrations may also impose substantial dynamic loading on nearby rock slopes, which may result in rock fall or total slope failure. This problem will generally be greatest in portal areas where slopes are often at their steepest and the blasting is close to the surface. By the nature of their formation such slopes may have static factors of safety approaching unity and any additional dynamic loads may result in failure. An example of this type of failure is shown in Fig. 8. During the initial blasting work for this tunnel some 3000 ton of rock was dislodged from the daylighting discontinuity (a rock joint or flow banding plane), which is clearly seen just above the portal stonework. Incidents of this kind can prove hazardous to the workforce and may require costly additional works.

Fig. 8 Tunnel portal with rock slope failure

The analysis of rock slope stability has received considerable attention,[9] but most texts tend to consider only the 'static' (gravitational, hydrostatic, etc.) loadings that affect stability. Although it is reasonably straightforward to calculate the imposed dynamic loads (elastic and inertial) due to a given vibration, it is in practice difficult to assess their effects on the overall stability of the slope. Allowance for even quite moderate values of PPV will result in major destabilizing dynamic stresses in the stability equations. Calculations of this kind often give very pessimistic values for the slope's 'factor of safety' that are not evidenced in the field. This may be explained, at least in part, by considering the oscillating character of the imposed vibrations in relation to the frictional properties of the discontinuity plane taken as the failure surface. The displacements that result from blast vibrations will almost invariably be very much smaller than the persistence (or 'wavelength') of the major interlocking asperities that contribute to the effective friction along the assumed failure surface. Thus, in practice, the vibrations may not produce sufficient relative movement, on either side of the discontinuity, for the asperities to 'ride over' each other and result in slope failure. Further research into this problem would seem to be desirable.

Air overpressure

Blasting-induced air overpressures may cause problems, usually by breaking windows or dislodging loose plaster, but structures close enough to a blast to suffer such damage will usually be subjected to potentially damaging ground vibration as well. That is, where overpressures in excess of 0.7 kN/m^2 occur ground vibrations are likely to exceed 50 mm/sec PPV. High overpressures are associated with near-surface blasting with low degrees of confinement and are therefore not usually a cause of complaint during underground construction. When blasting in portal areas, however, it is clearly advisable to ensure good stemming of the blastholes. Table 6 relates sound pressure level to human and structural response. Damage due to air overpressure is most unlikely during careful construction operations, but the noise may cause complaints by the local population. Siskind *et al.*[25] have reviewed structure response and damage produced by surface mining air overpressure.

Table 6 Response to sound pressure level

Sound pressure level dB	N/m^2	lb/in^2	Example source	Response
180	20 000	3		Structural damage
170				Most windows break
160	2 000	0.3	Jet aircraft (close to)	
150				Some windows break
140	200	0.03		Damage threshold
130			Large siren at 100 ft	Hearing pain
120	20	3×10^{-3}	Thunder	Hearing discomfort
110			Riveting machine	Windows rattle (blasting complaint threshold)
100	2	3×10^{-4}	Very busy street	
90			Shouting voice	
80	0.2	3×10^{-5}	Pneumatic drill at 20 m	Risk of hearing damage
70			Vacuum cleaner at 2 m	
			Normal speech	
60	0.02	3×10^{-6}		
50			Office, light road traffic	
40	2×10^{-3}	3×10^{-7}		
30			Whisper	
20	2×10^{-4}	3×10^{-8}	Sound recording studio	
10				
0	2×10^{-5}	3×10^{-9}		Threshold of hearing

Machinery (continuous) vibration damage criteria

Where ground vibration is of a continuous nature potential damage thresholds should be set at rather lower levels than those discussed above for transient vibrations. How much lower is a matter for some speculation, as little research has been carried out to determine the effects of continuous vibration on urban structures. Some guidance may be provided, however, by analogy with damage criteria associated with road traffic induced vibration. Whiffin and Leonard[31] reviewed traffic induced vibration and concluded that 'architectural' damage may occur at PPV in excess of 5 mm/sec and that structural damage may take place at PPV in excess of 10 mm/sec. These levels may be regarded as conservative when applied to tunnelling works, as frequencies due to tunnelling machinery will often be rich in the less damaging (for a given PPV) higher frequencies. It should also be noted that much of the vibration induced in structures from road traffic is transmitted as sound through the air rather than vibration through the ground.

Criteria recommended by the Swiss Association of Standardisation for sources of a continuous nature are given in Table 2. Here too 'traffic' and 'machine' sources are grouped together.

Measurements of vibrations induced by full-face tunnelling machines reported in this paper indicate that such machines are most unlikely to damage urban structures in reasonable condition. Evidence from the Warrington site, in particular, showed that the vibration induced by the excavation of sand and sandstone with hard granite cobbles and boulders was less than 1 mm/sec at the footings of houses less than 5 m from the face. It would require a large machine excavating within a few metres of a

Damage due to air overpressures is unlikely during most tunnelling works. In blasting in portal areas, however, precautions may be necessary to avoid causing alarm to the local inhabitants.

In tunnelling it is important to provide full information through good public relations procedures. Moreover, the works must be carried out as quickly as possible with the minimization of vibration through good excavation techniques.

Most tunnelling is sponsored by the public sector and, although safe limits must be imposed to protect the local people, overconservative limits and unnecessary restrictions will be a charge on the community as a whole. It is therefore vital that authorities responsible for setting vibration limits do so on an informed rather than on an arbitrary basis.

Acknowledgment

The work described in this paper forms part of the programme of the Transport and Road Research Laboratory and the paper is published by permission of the Director. The author gratefully acknowledges the valuable contributions made by the employers, consulting engineers and contractors without whose permission and cooperation the site measurements presented in this paper could not have been obtained. He also wishes to thank Professor P. B. Attewell (Durham University) for his help and advice.

References

1. Ambraseys N. N. and Hendron A. J. Jr. Dynamic behaviour of rock masses. In *Rock mechanics in engineering practice* Stagg K. G. and Zienkiewicz O. C. eds (London, etc.: Wiley, 1968), 203–36.
2. Suppression of noise and vibration on LT underground link with Heathrow Airport. *Rail Engng Int.*, 4, no. 6 1974, 285–7.
3. Ashley C. and Parkes D. B. Blasting in urban areas. *Tunnels Tunnell.*, 8, no. 6, Sept. 1976, 60–7.
4. Bean R. and Page J. Traffic induced ground vibration in the vicinity of road tunnels. *Transport Road Res. Lab. Supplem. Rep.* 218, 1976.
5. Bollinger G. A. *Blast vibration analysis* (Carbondale, Ill.: Southern Illinois University Press, 1971), 147 p.
6. Edwards A. T. and Northwood T. D. Experimental studies of the effects of blasting on structures. *Engineer, Lond.*, 210, Sept. 30 1960, 538–46.
7. Esteves J. M. Control of vibration caused by blasting. *Memoria Laboratorio National de Engenharia Civil, Lisbon*, no. 498, 1978, 11 p.
8. Guignard J. C. and Guignard E. Human response to vibration – a critical survey of published work. University of Southampton, Institute of Sound and Vibration Research Memo 373, 1970.
9. Hoek E. and Bray J. W. *Rock slope engineering, revised 2nd edn* (London: IMM, 1977), 402 p.
10. Jackson M. W. Thresholds of damage due to ground motion. *Proceedings international symposium on wave propagation and dynamic properties of earth materials, University of New Mexico*, 1967, 961–9.
11. Jaeger J. C. and Cook N. G. W. *Fundamentals of rock mechanics, 2nd edn* (London: Chapman and Hall; New York: Wiley, a Halsted Press Book, 1976), 585 p.
12. Kolsky H. *Stress waves in solids* (New York, etc.: Dover Publications, 1963), 223 p.
13. Langefors U. and Kihlström B. *The modern technique of rock blasting, 3rd edn* (New York, etc.: Wiley, Halsted Press, 1978), 438 p.
14. Medearis K. Rational damage criteria for low-rise structures subjected to blasting vibrations. *Proc. Instn civ. Engrs*, 65, pt 2, 1978, 611–21.
15. New B. M. The effects of ground vibration during bentonite shield tunnelling at Warrington. *Transport Road Res. Lab. Rep.* 860, 1978.
16. New B. M. Wild P. T. and Bishop C. J. Bentonite tunnelling beneath major services in loose ground. *Tunnels Tunnell.*, 12, no. 5, June 1980, 14–6.
17. Oriard L. J. Modern blasting in an urban setting. Atlanta Research Chamber Applied Research Monographs, interim report. Rep. no. UMTA-GA-06-0007-79-1, June 1979.
18. Pakes G. Edinburgh sewage disposal scheme: tunnelling work. In *Tunnelling '76* Jones M. J. ed. (London: IMM, 1976), 3–15.
19. Persson P. A. *et al.* Underground blasting in a city. In *Subsurface space: proceedings of the international symposium (Rockstore '80), Stockholm, 1980* Bergman M. ed. (Oxford, etc.: Pergamon, 1980), vol. 1, 199–206.
20. Reiher H. and Meister F. J. Human sensitivity to vibrations. *Forschung auf dem Gebiete des Ingenieurwesen*, 2, no. 11 1931, 381–6. (German text)
21. Ryley M. D. *et al.* Measurements of ground movements around three tunnels in loose cohesionless soil. *Transport Road Res. Lab. Rep.* 938, 1980.
22. Sarma S. K. Seismic stability of earth dams and embankments. *Géotechnique*, 25, no. 4 1975, 743–61.
23. Seed H. B. and Goodman R. E. Earthquake stability of slopes of cohesionless soils. *J. Soil Mech. Found Div. ASCE*, 90, Nov. 1964, 43–73.
24. Siskind D. E. *et al.* Structure response and damage produced by ground vibration from surface mine blasting. *Rep. Invest. U.S. Bur. Mines* 8507, 1980, 74 p.
25. Siskind D. E. *et al.* Structure response and damage produced by airblast from surface mining. *Rep. Invest. U.S. Bur. Mines* 8485, 1980, 111 p.
26. Soliman J. T. A scale for the degrees of vibration perceptibility and annoyance. *Ergonomics*, 2, 1968, 101–22.
27. Stagg M. S. and Engler A. J. Measurement of blast-induced ground vibrations and seismograph calibration. *Rep. Invest. U.S. Bur. Mines* 8506, 1980, 62 p.
28. Steffens R. J. *Structural vibration and damage* (London: HMSO for Building Research Establishment, 1974).
29. Swiss Association of Standardisation. *Effects of vibration on construction* (Zurich: The Association).
30. Walker S. Young P. A. and Davey P. M. Development of response spectra techniques for prediction of structural damage from open-pit blasting vibrations. *Trans. Instn Min. Metall. (Sect. A: Min. industry)*, 91, 1982, A55–62.
31. Whiffin A. C. and Leonard D. R. A survey of traffic induced vibrations. *Transport Road Res. Lab. Rep.* 418, 1971.
32. Wiss J. F. Construction vibrations: state of the art. *J. geotech. Engng Div. ASCE*, 107, Feb. 1981, 167–81.
33. Wiss J. F. and Parmelee R. A. Human perception of transient vibrations. *J. struct. Div. ASCE*, 100, ST4, April 1974, 773–87.
34. Yoshimi Y. *et al.* Soil dynamics and its application to foundation engineering: state of the art report. In *Proceedings 9th conference on soil mechanics and foundation engineering, Tokyo, 1977*, vol. 2, 605–50.

APPENDIX B

"RIGID BODY" BLOCK STABILITY

Consider a cubic block of rock (side length, D) formed by vertical intersecting joints in the roof of an underground opening which is subjected to shaking. Let the wavelength λ of the disturbing wave motion be large compared to the size of the block. (This will be the case in almost all practical situations.) Any cohesion across the joint is neglected.

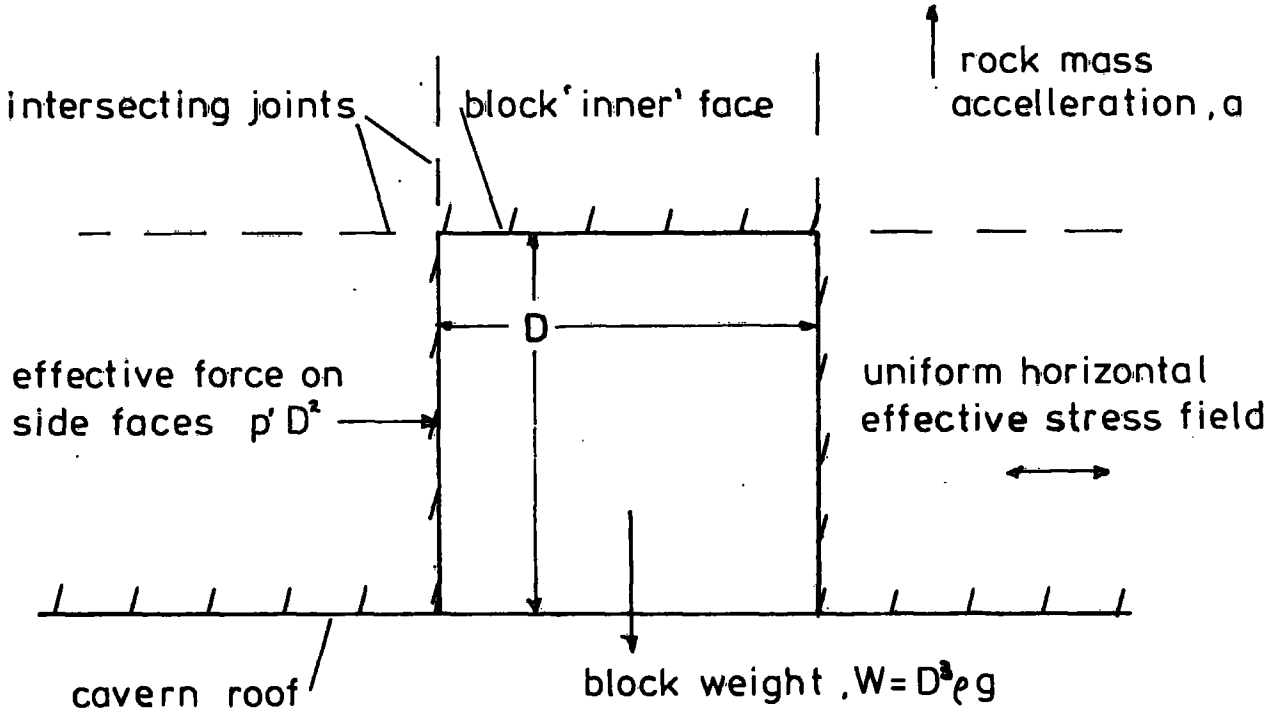

The block will start to fall when the retaining force, applied by a uniform horizontal effective stress field, (p') and effective joint friction (μ'_r), is less than the dislodging force which comprises the block weight plus the force required to accelerate the block with the vibrating rock

mass.

The block retaining force = Stress x Joint contact area x coeff of friction

$$= p'.4D^2\mu'_r \qquad \ldots (B.2.1)$$

(this assumes stress on 'inner' block face is zero due to radial stress relief.)

Without shaking, the dislodging force = $D^3\rho g$, (the block weight)

$$\ldots (B.2.2)$$

where ρ is the density of the rock and g the acceleration due to gravity.

Let the acceleration (a) of the rock mass be upward. The force required to accelerate the block upwards with the rock mass = $D^3\rho$ a (= mass x acceleration). The total force required to retain and accelerate the block upward and therefore maintain its integrity with the rock mass

= block weight + accelerating force

$$= D^3\rho g + D^3\rho a = D^3\rho\ (g + a) \qquad \ldots (B.2.3)$$

In the albeit oversimplified circumstances defined above this is the dislodging force due to block inertia. The condition, $\lambda >> D$, neglects the effect of shear wave induced forces (*see* Section 2.3.2) and considers only the effect of block inertia. Now if the total dislodging force, $D^3\rho\ (g + a)$, is greater than the retaining force, $p'.4D^2\mu'_r$, the block will slip downward relative to the rock mass.

That is, if $D^3\rho(g + a) > p'4D^2\mu'_r$,

$$(\ D\ \rho(g + a) > 4p'\mu'_r\ ) \qquad \ldots (B.2.4)$$

movement of the block relative to the rock mass will occur.

APPENDIX C

THE DETERMINATION OF THE SITE CONSTANTS

Consider the equation $V = K\,(r/\sqrt{M})^n$ from Eq 3.2

Site data will provide values for V for a variety of $r/\sqrt{M}$ conditions.

Let $r/\sqrt{M} = x$

then $V = Kx^n$

$$\ln V = n \ln x + \ln K$$

This equation may be solved as a problem of linear regression and the constants K and n computed to establish a power curve fitted to the data such that the sum of the squares of the deviations shall be a minimum. The values for V may be applied for both $x = r/\sqrt{M}$ and $x = r/\sqrt[3]{M}$

The regression coefficients may be computed from a set of data points $(x_i, V_i;\ i = 1,2,3....N)$ using the equations

$$n = \frac{\Sigma(\ln x_i)(\ln V_i) - [(\Sigma \ln x_i)(\Sigma \ln V_i)/N]}{\Sigma(\ln x_i)^2 \quad -[(\Sigma \ln x_i)^2/N]}$$

$$\text{and } K = \exp\left[\frac{\Sigma \ln V_i}{N} - \frac{n \Sigma \ln x_i}{N}\right], x_i > 0,\ V_i > 0$$

The coefficient of determination

$$R^2 = \frac{\left[\Sigma(\ln x_i)(\ln V_i) - \frac{(\Sigma \ln x_i)(\Sigma \ln V_i)}{N}\right]^2}{\left[\Sigma(\ln x_i)^2 - \frac{(\Sigma \ln x_i)^2}{N}\right]\left[\Sigma(\ln V_i)^2 - \frac{(\Sigma \ln V_i)^2}{N}\right]}$$

These equations may be readily evaluated using a programmable calculator and a suitable program is given in below. This program is reproduced from a Hewlett-Packard Applications book and is suitable for use with a

model HP25 calculator. (Note that the designations n, K and V_i are replaced by b, a and y_i in the program.)

H-P 25 POWER CURVE FIT PROGRAM (after HANDBOOK)

DISPLAY LINE	DISPLAY CODE	KEY ENTRY
00		
01	14 07	f LN
02	31	f
03	15 02	g x^3
04	23 51 02	STO + 2
05	22	R↓
06	21	$x \rightleftarrows y$
07	14 07	f LN
08	25	Σ+
09	13 00	GTO 00
10	24 05	RCL 5
11	24 07	RCL 7
12	24 04	RCL 4
13	61	x
14	24 03	RCL 3
15	71	÷
16	41	−
17	24 06	RCL 6
18	24 07	RCL 7
19	15 02	g x^2
20	24 03	RCL 3
21	71	÷
22	41	−
23	71	÷
24	23 01	STO 1

DISPLAY LINE	DISPLAY CODE	KEY ENTRY
25	24 07	RCL 7
26	61	x
27	32	CHS
28	24 04	RCL 4
29	51	+
30	24 03	RCL 3
31	71	÷
32	15 07	g e^x
33	23 00	STO 0
34	74	R/S
35	24 01	RCL 1
36	74	R/S
37	21	$x \rightleftarrows y$
38	22	R↓
39	61	x
40	24 02	RCL 2
41	24 04	RCL 4
42	15 02	g x^2
43	24 03	RCL 3
44	71	÷
45	41	−
46	71	÷
47	13 00	GTO 00
48		
49		

REGISTERS
R_0 a
R_1 b
R_2 $\Sigma (\ln y)^2$
R_3 n
R_4 $\Sigma \ln y$
R_5 $\Sigma (\ln x)(\ln y)$
R_6 $\Sigma (\ln x)^2$
R_7 $\Sigma \ln x$

STEP	INSTRUCTIONS	INPUT DATA/UNITS	KEYS				OUTPUT DATA/UNITS
1	Key in program						
2	Initialize		f	REG	f	PRGM	
3	Perform for i = 1,..., n:						
	Input x-value and y-value	x_i	f				
		y_i	R/S				i
4	Compute constants		GTO	10	R/S		a*
			R/S				b*
5	Compute coefficient of determination						
			R/S				r^2
6	Input x-value and compute $\hat{y}$	x	RCL	1	f	y^x	
			RCL	0	x		$\hat{y}$
7	Perform step 6 as many times as desired						
8	For new case, go to step 2.						
	* The stack must be maintained at these points.						

The correlation may be tested for significance using the Students t test where

$$t = R\sqrt{(N-2)/(1-R^2)}$$

Reference to tables giving the distribution of t will indicate the significance of the correlation. Some authors show confidence limits, usually displaced by plus and minus two standard errors about the regression lines, where the standard error is given by

$$S = \sigma\sqrt{1-R^2}$$

where σ is the standard deviation. These are usually described as the 95% 'confidence limits'. It must be noted that these tests are dependent on the normal distribution of the data and the user must be satisfied that this condition is appropriate. Moroney (1971) gives useful practical guidance with regard to correlation statistics.

APPENDIX D

TUNNEL SUPPORT REQUIREMENTS BASED ON RQD

Deere (1968b) gives the following description of ground classification and support requirements correlated with RQD values:

> An RQD, that is a modified core recovery, of 0 to 25 per cent, indicates a very poor quality rock. This would only be found in weathered rock near the surface, in shear zones, and in fault zones. An RQD at 25 to 50 per cent has been categorized as poor rock, 50 to 75 per cent as fair rock, and 75 to 90 per cent as excellent rock. Obviously the orientation of the fractures with respect to direction of driving also has to be taken into account in the system. For an RQD of 0 to 25 per cent, in a tunnel, one would have to anticipate that squeezing conditions could apply, that there would be raveling ground, perhaps flowing ground, and support requirements would be heavy steel sets, perhaps even skintight and perhaps invert struts would be necessary. For an RQD of 25 to 50 per cent, that is poor rock, steel sets would also be required in normal practice. It is in the range of 50 to 75 per cent, the so-called fair rock, that quite often problems are encountered in understanding the type of support needed. The contractor would often prefer to place steel sets, even though they might be spaced at 5 or 6 ft centers because in rock of this fair quality there are enough joints and often weathering or alteration on the joints so that the blocks can slip out - it is truly blocky ground with some seaminess. The design engineers would often like to see rock bolts put into this quality of ground. When rock is in the 75 to 90 per cent category, so-called good rock such as normal good granite, there is very little necessity for anything other than a random rock bolt.

Figure D.1 gives Merritts' (1972) 'comparison of rock quality criteria from various sources'. This Figure correlates RQD with tunnel support and span.

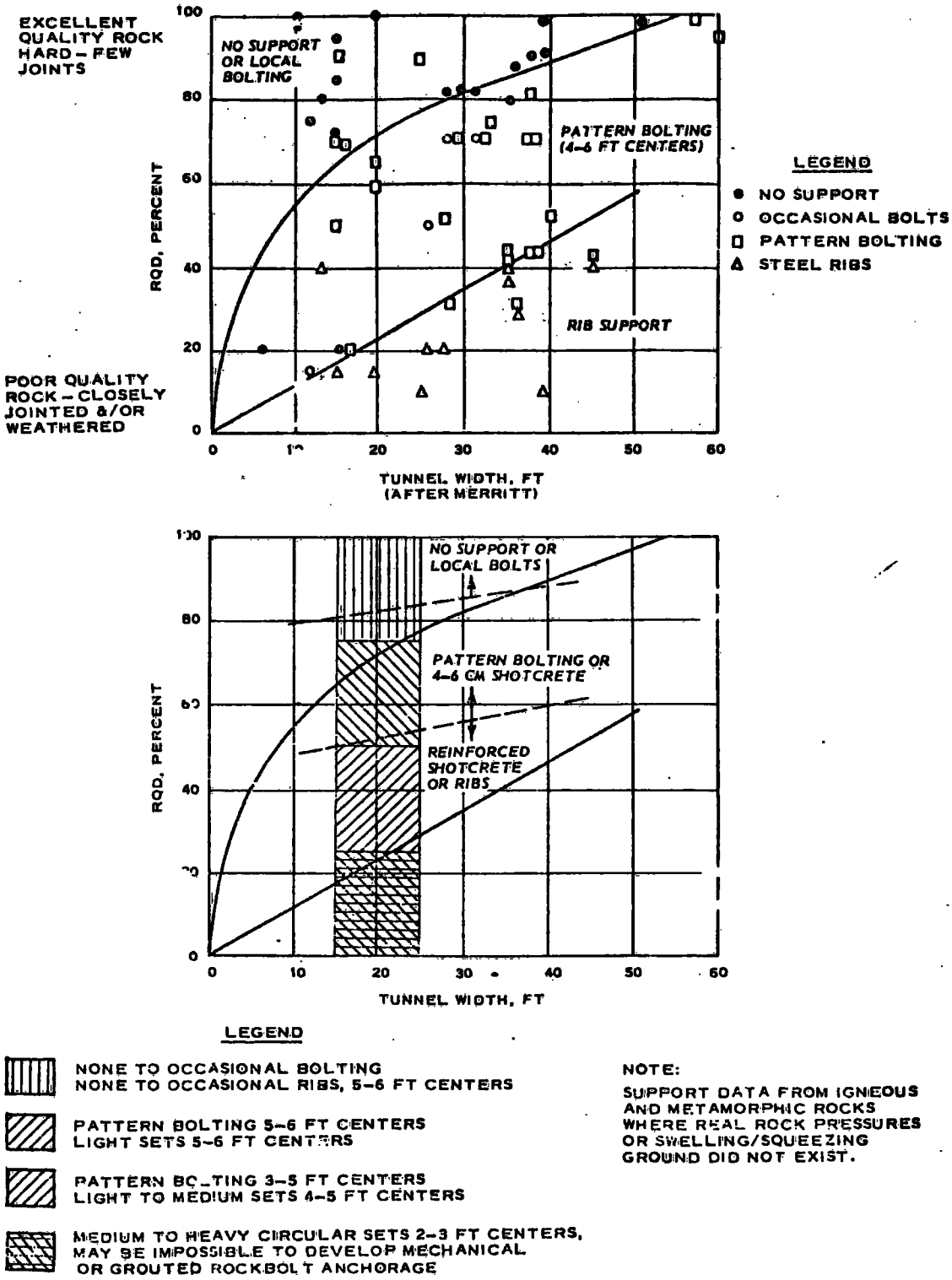

Fig.D1 COMPARISON OF ROCK QUALITY SUPPORT CRITERIA FROM VARIOUS SOURCES (after MERRITT, 1972)

APPENDIX E

RESULTANT PEAK PARTICLE VELOCITY

CONFINED BLASTS (*see* Figures 6.6a, b and 6.9)

Blast No.	PPV (mm/s)	r (m)	M (kgf)	$rM/^{\frac{1}{2}}$	$r/M^{\frac{1}{3}}$	$r/M^{\alpha/\beta}$
1	2.95	43.1	1	43.1	43.1	43.1
2	6.54	34.1	1	34.1	34.1	34.1
2	2.42	54.7	1	54.7	54.7	54.7
2	4.04	33.4	2/3	40.9	38.2	39.3
2	1.74	53.7	2/3	65.8	61.5	63.1
2	2.81	32.1	1/3	55.6	46.3	49.8
2	1.17	51.9	1/3	89.9	74.8	80.5
3	16.0	31.0	2	21.9	24.6	23.5
3	4.84	49.8	2	35.2	39.5	37.8

Regression equations for:

square root scaling $PPV = 3665\ (r/M^{\frac{1}{2}})^{-1.820}$ $R^2 = 0.961$

cube root scaling $PPV = 19692\ (r/M^{\frac{1}{3}})^{-2.278}$ $R^2 = 0.965$

'site specific' scaling $PPV = 10{,}000\ M^{0.835}\ r^{-2.093}$

$= 10{,}000\ (r/M^{0.399})^{-2.093}$ $R^2 = 0.972$

PARTIALLY CONFINED BLASTS

Blast No.	PPV (mm/s)	r (m)	M (kgf)	$r/M^{\frac{1}{2}}$	$r/M^{\frac{1}{3}}$	$r/M^{\alpha/\beta}$
3	2.42	35.1	1	35.1	35.1	35.1
3	1.15	49.3	1	49.3	49.3	49.3
4	4.51	35.6	2	25.2	28.3	16.2
4	4.54	47.3	2	33.5	37.5	21.6
4	2.81	35.6	1	35.6	35.6	35.6
4	2.15	47.3	1	47.3	47.3	47.3
5	4.78	40.0	3	23.1	27.7	11.5
5	7.69	44.0	3	25.4	30.5	12.7
5	1.91	37.4	1	37.4	37.4	37.4
5	1.77	46.5	1	46.5	46.5	46.5

Regression equations for:

square root scaling $PPV = 2126\ (r/M^{\frac{1}{2}})^{-1.860}$ $R^2 = 0.783$

cube root scaling $PPV = 10{,}475\ (r/M^{\frac{1}{3}})^{-2.272}$ $R^2 = 0.676$

'site specific' scaling $PPV = 67.45\ M^{1.072}\ r^{-0.947}$

$= 67.45\ (r/M^{1.132})^{-0.947}$ $R^2 = 0.846$

APPENDIX F

RESULTANT ('REAL TIME') PEAK PARTICLE VELOCITY

CONFINED BLASTS (*see* Figures 6.7a, b and 6.10)

Blast No.	PPV (mm/s)	r (m)	M (kgf)	$r/M^{\frac{1}{2}}$	$r/M^{\frac{1}{3}}$	$r/M^{\alpha/\beta}$
1	2.95	43.1	1	43.1	43.1	43.1
2	1.95	54.7	1	54.7	54.7	54.7
2	3.3	33.4	2/3	40.9	38.2	40.1
2	1.3	53.7	2/3	65.8	61.5	64.5
3	12.3	31.0	2	21.9	24.6	22.7
3	3.9	49.8	2	35.2	39.5	36.4

Regression equations for:

square root scaling $PPV = 5424\ (r/M^{\frac{1}{2}})^{-1.995}$ $R^2 = 0.991$

cube root scaling $PPV = 21{,}343\ (r/M^{\frac{1}{3}})^{-2.354}$ $R^2 = 0.978$

'site specific' scaling $PPV = 8138\ M^{0.948}\ r^{-2.102}$

$= 8138\ (r/M^{0.451})^{-2.102}$ $R^2 = 0.993$

APPENDIX G

RADIAL PEAK PARTICLE VELOCITY

CONFINED BLASTS (*see* Figures 6.8a, b and 6.11)

Blast No.	PPV (mm/s)	r (m)	M (kgf)	$r/M^{\frac{1}{2}}$	$r/M^{\frac{1}{3}}$	$r/M^{\alpha/\beta}$
1	0.2	117.5	1	117.5	117.5	117.5
1	0.6	70.9	1	70.9	70.9	70.9
1	1.2	41.9	1	41.9	41.9	41.9
1	2.4	43.1	1	43.1	43.1	43.1
2	0.24	141.1	1	141.1	141.1	141.1
2	0.38	91.3	1	91.3	91.3	91.3
2	4.75	34.1	1	34.1	34.1	34.1
2	1.64	54.7	1	54.7	54.7	54.7
2	0.16	140.1	2/3	171.6	160.4	163.0
2	0.18	90.2	2/3	110.5	103.3	104.9
2	2.5	33.4	2/3	40.9	38.2	38.9
2	1.04	53.7	2/3	65.8	61.5	62.5
2	0.1	138.5	1/3	240.0	199.7	208.7
2	0.14	88.5	1/3	153.4	127.6	133.4
2	1.7	32.1	1/3	55.6	46.3	48.4
2	0.6	51.9	1/3	89.9	74.8	78.2
3	0.32	136.3	2	96.4	108.2	105.2
3	0.56	86.3	2	61.0	68.5	66.6
3	12.0	31.0	2	21.9	24.6	23.9
3	2.8	49.8	2	35.2	39.6	38.4

Regression equations for:

square root scaling $PPV = 4587\ (r/M^{\frac{1}{2}})^{-2.044}$ $R^2 = 0.935$

cube root scaling $PPV = 8876\ (r/M^{\frac{1}{3}})^{-2.212}$ $R^2 = 0.945$

'site specific' scaling $PPV = 7727\ M^{0.813}\ r^{-2.177}$

$= 7727\ (r/M^{0.373})^{-2.177}$ $R^2 = 0.947$

PARTIALLY CONFINED BLASTS

Blast No.	PPV (mm/s)	r (m)	M (kgf)	$r/M^{\frac{1}{2}}$	$r/M^{\frac{1}{3}}$	$r/M^{\alpha/\beta}$
3	0.14	132.3	1	132.3	132.3	132.3
3	0.32	83.4	1	83.4	83.4	83.4
3	1.28	35.1	1	35.1	35.1	35.1
3	0.88	49.3	1	49.3	49.3	49.3
4	0.36	129.1	2	91.3	102.5	88.1
4	0.72	80.5	2	56.9	63.9	54.9
4	2.4	35.6	2	25.2	28.3	24.3
4	4.0	47.3	2	33.5	37.5	32.3
4	0.2	129.1	1	129.1	129.1	129.1
4	0.32	80.5	1	80.5	80.5	80.5
4	1.6	35.6	1	35.6	35.6	35.6
4	1.6	47.3	1	47.3	47.3	47.3
5	0.38	120.6	3	69.6	83.6	65.8
5	1.16	73.4	3	42.4	50.9	40.0
5	2.4	40.0	3	23.1	27.7	21.8
5	6.64	44.0	3	25.4	30.5	24.0
5	0.14	126.5	1	126.5	126.5	126.5
5	0.32	78.4	1	78.4	78.4	78.4
5	0.96	37.4	1	37.4	37.4	37.4
5	1.44	46.5	1	46.5	46.5	46.5

Regression equations for:

square root scaling $PPV = 1434\ (r/M^{\frac{1}{2}})^{-1.881}$ $R^2 = 0.899$

cube root scaling $PPV = 2217\ (r/M^{\frac{1}{3}})^{-1.961}$ $R^2 = 0.874$

'site specific' scaling $PPV = 1197\ M^{1.018}\ r^{-1.845}$

$= 1197\ (r/M^{0.552})^{-1.845}$ $R^2 = 0.900$

APPENDIX H COUPLED EXPLOSIONS (simple regression)

```
ENTER DATA
  Y → Y
  X → X

 4.610000000 01
 1.580000000 01

 6.000000000 00
 3.030000000 01

 2.560000000 00
 6.990000000 01

 4.900000000-01
 1.512000000 02

 1.124000000 01
 3.660000000 01

 1.430000000 00
 7.010000000 01

 2.900000000-01
 2.027000000 02

 1.148000000 02
 8.600000000 00

 1.729000000 01
 1.950000000 01

 6.500000000 00
 4.750000000 01

 1.050000000 00
 1.050000000 02

 2.613000000 01
 2.390000000 01

 4.750000000 00
 4.760000000 01

 8.800000000-01
 1.413000000 02

 8.286000000 01
 1.050000000 01

 1.390000000 01
 1.940000000 01

 5.320000000 00
 4.740000000 01

 8.400000000-01
 1.049000000 02

 2.095000000 01
 2.330000000 01

 2.820000000 00
 4.500000000 01

 5.100000000-01
 1.407000000 02

 1.940000000 01
 1.770000000 01

 1.220000000 01
 2.050000000 01

 4.150000000 00
 5.330000000 01

 4.500000000-01
 1.346000000 02

 8.210000000 00
 2.220000000 01

 1.850000000 00
 5.570000000 01

 3.000000000-01
 1.882000000 02

 6.220000000 01
 1.100000000 01

 4.130000000 01
 1.180000000 01

 1.046000000 01
 3.800000000 01

 1.020000000 00
 9.550000000 01

 1.580000000 01
 2.410000000 01

 3.800000000 00
 4.780000000 01

 7.400000000-01
 1.415000000 02
```

```
 9.800000000 01
 8.410000000 00

 3.600000000 01
 1.530000000 01

 1.050000000 01
 3.840000000 01

 2.030000000 00
 8.530000000 01

 2.900000000 01
 2.130000000 01

 5.210000000 00
 4.070000000 01

 1.170000000 00
 1.172000000 02

 9.230000000 01
 6.610000000 00

 4.050000000 01
 1.430000000 01

 8.270000000 00
 3.720000000 01

 1.600000000 00
 8.410000000 01

 2.700000000 01
 1.950000000 01

 3.770000000 00
 3.890000000 01

 5.900000000-01
 1.154000000 02

 3.370000000 01
 1.330000000 01

 5.050000000 00
 3.130000000 01

 2.270000000 00
 7.000000000 01

 2.700000000-01
 1.513000000 02
```

```
 9.870000000 00
 3.390000000 01

 1.430000000 00
 6.750000000 01

 2.700000000-01
 2.000000000 02

 3.000000000-01
 1.520000000 02

 5.400000000 01
 1.060000000 01

 1.600000000-01
 2.107000000 02

 2.660000000 01
 1.160000000 01

 8.900000000-01
 1.052000000 02

 9.600000000 00
 3.150000000 01

 2.686000000 02
 5.050000000 00
```

```
 B
 A
 N

-1.840140588 00
 4.857056432 03
 6.300000000 01

CORRELATIONS
POWER
LINEAR

 9.641368125-01
 1.969315959-01
```

APPENDIX I COUPLED EXPLOSIONS (multiple regression)

```
ENTER DATA
Z →Z                    8.286000000 01          4.130000000 01
Y →Y                    1.050000000 01          1.180000000 01
X →X                    1.000000000 00          1.000000000 00

 4.610000000 01         1.390000000 01          1.046000000 01
 1.120000000 01         1.940000000 01          3.800000000 01
 5.000000000-01         1.000000000 00          1.000000000 00

 6.000000000 00         5.320000000 00          1.020000000 00
 2.140000000 01         4.740000000 01          9.550000000 01
 5.000000000-01         1.000000000 00          1.000000000 00

 2.560000000 00         8.400000000-01          1.580000000 01
 4.940000000 01         1.049000000 02          2.410000000 01
 5.000000000-01         1.000000000 00          1.000000000 00

 4.900000000-01         2.095000000 01          3.800000000 00
 1.069000000 02         2.330000000 01          4.780000000 01
 5.000000000-01         1.000000000 00          1.000000000 00

 1.124000000 01         2.820000000 00          7.400000000-01
 2.590000000 01         4.500000000 01          1.415000000 02
 5.000000000-01         1.000000000 00          1.000000000 00

 1.430000000 00         5.100000000-01          9.000000000 01
 4.960000000 01         1.407000000 02          1.030000000 01
 5.000000000-01         1.000000000 00          1.500000000 00

 2.900000000-01         1.240000000 01          3.600000000 01
 1.433000000 02         1.250000000 01          1.870000000 01
 5.000000000-01         5.000000000-01          1.500000000 00

 1.148000000 02         1.220000000 01          1.650000000 01
 8.600000000 00         1.450000000 01          4.700000000 01
 1.000000000 00         5.000000000-01          1.500000000 00

 1.729000000 01         4.150000000 00          2.030000000 00
 1.950000000 01         3.770000000 01          1.045000000 02
 1.000000000 00         5.000000000-01          1.500000000 00

 6.500000000 00         4.500000000-01          2.900000000 01
 4.750000000 01         9.520000000 01          2.610000000 01
 1.000000000 00         5.000000000-01          1.500000000 00

 1.050000000 00         8.210000000 00          5.210000000 00
 1.050000000 02         1.570000000 01          4.980000000 01
 1.000000000 00         5.000000000-01          1.500000000 00

 2.613000000 01         1.850000000 00          1.170000000 00
 2.390000000 01         3.940000000 01          1.435000000 02
 1.000000000 00         5.000000000-01          1.500000000 00

 4.750000000 00         3.000000000-01          9.230000000 01
 4.760000000 01         1.331000000 02          8.100000000 00
 1.000000000 00         5.000000000-01          1.500000000 00

 3.800000000-01         6.220000000 01          4.050000000 01
 1.413000000 02         1.100000000 01          1.750000000 01
 1.000000000 00         1.000000000 00          1.500000000 00
```

```
 8.270000000 00
 4.550000000 01
 1.500000000 00

 1.600000000 00
 1.030000000 02
 1.500000000 00

 2.700000000 01
 2.390000000 01
 1.500000000 00

 3.770000000 00
 4.760000000 01
 1.500000000 00

 5.900000000-01
 1.413000000 02
 1.500000000 00

 3.370000000 01
 9.400000U000 00
 5.000000000-01

 5.050000000 00
 2.210000000 01
 5.000000000-01

 2.270000U000 00
 4.950000000 01
 5.000000000-01

 2.700000U000-01
 1.070000000 02
 5.000000000-01

 9.670000000 00
 2.400000000 01
 5.000000000-01

 1.430000000 00
 4.770000000 01
 5.000000000-01

 2.700000000-01
 1.414000000 02
 5.000000000-01

 3.000000000-01
 1.520000000 02
 1.000000000 00

 5.400000000 01
 1.060000000 01
 1.000000000 00

 1.600000000-01
 1.490000000 02
 5.000000000-01

 2.660000000 01
 8.200000000 00
 5.000000000-01

 8.900000000-01
 1.487000000 02
 2.000000000 00

 9.690000000 00
 4.460000000 01
 2.000000000 00

 2.686000000 02
 7.140000000 00
 2.000000000 00

COEFFICIENTS
  A0
  A1
  A2
 2.651991372 00
 1.167001839 00
-1.009667409 00

XMAX
XMIN

 3.010299957-01
-3.010299957-01

YMAX
YMIN

 2.181843588 00
 8.536982118-01

ZMAX
ZMIN

 2.429106008 00
-7.958800173-01

SIMPLE
  CORRELATIONS
  RYZ
  RXZ
  RXY

-9.374701017-01
 3.003807599-01
-1.314773328-03

 2
R
 9.683399913-01
```

log 2487

APPENDIX J DECOUPLED EXPLOSIONS : 75mm HOLE

Trimobel

```
 2.890000000 01
 9.800000000 00

 3.710000000 00
 3.010000000 01

 1.240000000 00
 6.970000000 01

 1.600000000-01
 1.510000000 02

 1.107000000 01
 2.960000000 01

 8.200000000-01
 6.310000000 01

 9.000000000-02
 1.956000000 02

 1.085000000 02
 5.800000000 00

 1.460000000 01
 1.940000000 01

 5.250000000 00
 4.740000000 01

 8.400000000-01
 1.049000000 02

 1.170000000 01
 2.090000000 01

 3.510000000 00
 4.460000000 01

 6.400000000-01
 1.383000000 02

 B
 A
 N

-1.893170761 00
 3.820692283 03
 1.400000000 01

CORRELATIONS
POWER
LINEAR

 9.344245365-01
 2.307976037-01
```

DC 1

```
 1.673000000 01
 6.200000000 00

 1.560000000 00
 1.750000000 01

 3.200000000-01
 5.730000000 01

 5.000000000-02
 1.386000000 02

 4.100000000-01
 2.740000000 01

 2.600000000-01
 6.100000000 01

 4.000000400-02
 1.935000000 02

 B
 A
 N

-1.695295702 00
 2.393632057 02
 7.000000000 00

CORRELATIONS
POWER
LINEAR

 9.633702654-01
 2.168645491-01
```

APPENDIX K DECOUPLED TRIMOBEL : 100 mm HOLE
(simple regression)

```
 3.580000000 01
 7.100000000 00

 5.800000000-01
 2.900000000 01

 2.000000000-01
 7.000000000 01

 2.000000000-02
 1.513000000 02

 3.210000000 00
 2.520000000 01

 2.900000000-01
 5.870000000 01

 2.000000000-02
 1.912000000 02

 9.260000000 01
 5.540000000 00

 5.330000000 00
 2.110000000 01

 2.180000000 00
 5.680000000 01

 3.400000000-01
 1.232000000 02

 6.940000000 00
 2.060000000 01

 1.540000000 00
 4.790000000 01

 3.000000000-01
 1.561000000 02

 4.000000000-02
 1.499000000 02

 6.560000000 00
 1.140000000 01

 5.000000000-02
 2.029000000 02

 7.200000000-01
 5.460000000 01

 5.440000000 01
 5.440000000 00
```

```
B
A
N

-2.001461839 00
 1.762815683 03
 1.900000000 01

CORRELATIONS
POWER
LINEAR

 8.948963710-01
 2.029434330-01
```

APPENDIX L DECOUPLED TRIMOBEL: 100mm HOLE
(multiple regression)

```
 2.580000000 01
 5.000000000 00
 5.000000000-01

 5.800000000-01
 2.050000000 01
 5.000000000-01

 2.000000000-01
 4.950000000 01
 5.000000000-01

 2.000000000-02
 1.070000000 02
 5.000000000-01

 3.210000u000 00
 1.780000000 01
 5.000000000-01

 2.900000000-01
 4.150000000 01
 5.000000000-01

 2.000000000-02
 1.352000000 02
 5.000000000-01

 0.240000000 01
 3.920000000 00
 7.500000000-01

 5.330000000 00
 1.830000000 01
 7.500000000-01

 2.180000000 00
 4.920000000 01
 7.500000000-01

 3.400000000-01
 1.067000000 02
 7.500000000-01

 6.940000000 00
 1.780000000 01
 7.500000000-01

 1.540000000 00
 4.150000000 01
 7.500000000-01

 3.000000000-01
 1.352000000 02
 7.500000000-01

 4.000000000-02
 1.499000000 02
 1.000000000 00

 6.560000000 00
 1.140000000 01
 1.000000000 00

 5.000000000-02
 1.435000000 02
 5.000000000-01

 7.200000000-01
 3.860000000 01
 5.000000000-01

 5.440000000 01
 3.850000000 00
 5.000000000-01

COEFFICIENTS
  A0
  A1
  A2
 3.402935270 00
 2.148359795 00
-1.956401908 00

XMAX
XMIN

 0.000000000 00
-3.010299957-01

YMAX
YMIN

 2.175801633 00
 5.854607295-01

ZMAX
ZMIN

 1.965671971 00
-1.698970004 00

SIMPLE
  CORRELATIONS
  RYZ
  RXZ
  RXY

-9.297271487-01
 1.734943923-01
 4.488964915-02

 2
R
 9.108098508-01
```

```
100 REM    GF-FFT (BMN 9/83)
110 OPEN1,8,15
120 PRINT#1,"I0"
130 INPUT"ENTER 2 DATA FILE";A$,A1$
140 V$="0:"+A$+",DAT,USR,READ"
150 V1$="0:"+A1$+".DAT,USR,READ"
160 OPEN 2,8,2,V$
170 OPEN 3,8,3,V1$
180 INPUT#2,DT : PRINT"DT =";DT
190 INPUT#3,DI : PRINT"DT =";DI
200 NN=130
210 DIM X(NN),Y(NN),P(NN),Q(NN),D(NN),DI(NN),F(NN),G(NN),H(NN),J(NN)
220 REM INDEX G VERIFYS SIZE OF TRFM.
230 G=7:N=2↑G:P=8*ATN(1)/N
240 S0=SQR(N/(DT/1000))
250 FORI=1TO128
260 INPUT#2,X(I)
270 INPUT#3,Y(I)
280 D1(I)=INT(Y(I)*500)
290 D(I)=INT(X(I)*500)
300 Y(I)=Y(I)/S0
310 X(I)=X(I)/S0
320 PRINT X(I),Y(I)
330 NEXTI
340 CLOSE2:CLOSE1
350 PRINT"□":PRINT:PRINT:PRINT:PRINT
360 PRINT"    WAIT !"
370 REM PLOT TO VERIFY INPUT DATA
380 GOSUB 2320 : REM PLOT TO VERIFY INPUT DATA
390 REM FFT ROUTINE
400 REM T=-1 FOR TRANSFORM :T=1 FOR INVERSE TRANSFORM
410 T=-1
420 FOR L=0 TO G-1
430 G1=2↑(G-L-1)
440 M=0
450 FOR I=1 TO 2↑L
460 K1=INT(M/G1)
470 GOSUB790
480 Y1=COS(P*K2):Y2=T*SIN(P*K2)
490 FOR J=1 TO G1
500 MG=M+G1+1:M1=M+1
510 Y3=X(MG)*Y1-Y(MG)*Y2
520 Y4=X(MG)*Y2+Y(MG)*Y1
530 X(MG)=X(M1)-Y3
540 Y(MG)=Y(M1)-Y4
550 X(M1)=X(M1)+Y3
560 Y(M1)=Y(M1)+Y4
570 M=M+1
580 NEXT J
590 M=M+G1
600 NEXT I
610 NEXT L
620 FOR I=0 TO N-1
630 K1=I
640 GOSUB790
650 IF K2>=I THEN720
660 K3=X(I+1)
670 X(I+1)=X(K2+1)
680 X(K2+1)=K3
690 K3=Y(I+1)
700 Y(I+1)=Y(K2+1)
710 Y(K2+1)=K3
720 NEXTI
730 GOTO780
740 FOR I=0 TO N-1
750 PRINTI;SPC(4-LEN(STR$(I)));X(I+1);SPC(20-LEN(STR$(X(I+1))));
760 PRINT"+I";SPC(3);Y(I+1)
770 NEXTI
780 GOTO870
790 K2=0
800 FOR K=1 TO G
810 K3=K1-2*INT(K1/2)
820 K1=INT(K1/2)
830 IF K3=0 THEN850
840 K2=K2+2↑(G-K)
850 NEXT K
860 RETURN
870 PMAX=0:  REM CALC GAIN FACTOR
880 FORI=0TON-1
890 F(I+1)=SQR(((X(I+1)+X(N-(I-1)))↑2+(Y(I+1)-Y(N-(I-1)))↑2)/4)
900 G(I+1)=SQR(((Y(I+1)+Y(N-(I-1)))↑2+(X(I+1)-X(N-(I-1)))↑2)/4)
910 NEXT I
920 PRINTX(5),X(125)
930 PRINTY(5),Y(125)
940 PRINTF(5),F(125)
950 PRINTG(5),G(125)
960 PRINTH(4),H(124)
970 PRINTHMAX
980 PRINTHT
990 H(0)=(F(1)+F(2)+F(3))/3
1000 J(0)=(G(1)+G(2)+G(3))/3
1010 H(1)=(F(1)+F(2)+F(3)+F(4))/4
1020 J(1)=(G(1)+G(2)+G(3)+G(4))/4
1030 FORI=2TON/2
1040 H(I)=(F(I-1)+F(I)+F(I+1)+F(I+2)+F(I+3))/5
1050 J(I)=(G(I-1)+G(I)+G(I+1)+G(I+2)+G(I+3))/5
1060 NEXTI
1070 FORI=0TON/2
1080 P(I)=H(I)/J(I)
1090 IFP(I)>PMAXTHENPMAX=P(I)
1100 NEXTI
1110 FOR I=0TON/2
1120 P(I)=P(I)*100/PMAX
1130 NEXTI
1140 GOTO 1250 : REM  SKIP PRINT STATEMENTS
1150 OPEN4,4
1160 CMD4
1170 L$="RECORD NUMBER = "+A$+" , "+A1$
1180 PRINT L$ :PRINT:PRINT:PRINT
1190 FORI=0TON
1200 PRINTI;SPC(5);X(I+1);SPC(16);Y(I+1);SPC(16);P(I);SPC(16);Q(I)
1210 NEXTI
1220 PRINT#4
1230 CLOSE4
1240 REM PLOTTING
1250 REM
1260 PRINT#5,"IN"
1270 M=500/DT
1280 PRINT#5,"IP 915,228,10915,7410"
1290 PRINT#5,"SC -1500,1000,-1500,300"
1300 PRINT#5,"SI 0.171,0.243"
1310 PRINT#5,"PU;PA 0,0"
1320 FOR I=0 TO 1000 STEP 100
1330 PRINT#5,"PD;PA",I,",0;XT;PU"
1340 PRINT#5,"DI 0,-1"
1350 PRINT#5,"CP -5,0,-0.25;LB";I/10;CHR$(3)
1360 PRINT#5,"DI 1,0"
1370 PRINT#5,"PA",I,",",0,";PD"
1380 NEXT I
1390 A=0
1400 PRINT#5,"DI 0,-1"
1410 PRINT#5,"PU;PA0,0"
1420 FOR I=0 TO -1280 STEP -128
1430 PRINT#5,"PD;PA",0,",",I";YT;PU"
1440 PRINT#5,"CP -2,0,-1.5;LB";(MHA)/10;CHR$(3)
1450 PRINT#5,"PA0,",(I),";PD"
1460 A=A+1
1470 NEXT I
1480 PRINT#5,"DI 1,0"
1490 PRINT#5,"PU"
1500 X=INT((P(0)*10)+0.5)
1510 PRINT#5,"PA",(X),",",0,";PD"
1520 FOR I=1 TO N/2
1530 X=INT((P(I)*10)+0.5)
1540 PRINT#5,"PA",(X),",",(-I*20),";PD"
1550 NEXT I
1560 PRINT#5,"PU;PA 1050,350;DI0,-1"
1570 PH$="PH="+STR$(PH)+" , PT="+STR$(PT)
1580 PRINT#5,"LB";PM$;CHR$(3)
1590 CLOSE5,5
1600 OPEN5,5
1610 PRINT#5,"IN"
1620 PRINT#5,"IP 915,228,10915,7410"
1630 PRINT#5,"SC -700,1800,-1500,300"
1640 PRINT#5,"SI 0.171,0.243"
1650 PRINT#5,"PU;PA 0,0"
1660 GOTO1940
1670 FOR I=0 TO 600 STEP 100
1680 PRINT#5,"PD;PA",I,",0;XT;PU"
1690 PRINT#5,"DI 0,-1"
1700 PRINT#5,"CP -5,0,-0.25;LB";6*I/10;CHR$(3)
1710 PRINT#5,"DI 1,0"
1720 PRINT#5,"PA",I,",",0,";PD"
1730 NEXT I
1740 PRINT#5,"DI 0,-1"
1750 PRINT#5,"PU;PA0,0"
1760 PRINT#5,"IP 915,228,10915,7410"
1770 A=0
1780 FOR I=0 TO -1280 STEP -128
1790 PRINT#5,"PD;PA",0,",",I";YT;PU"
1800 PRINT#5,"CP -2,0,-1.5;LB";(M*A)/10;CHR$(3)
1810 PRINT#5,"PA0,",I,";PD"
1820 A=A+1
1830 NEXT I
1840 PRINT#5,"DI 1,0"
1850 PRINT#5,"PU"
1860 X=INT((Q(0)*10)/6)+0.5)
1870 PRINT#5,"PA",(X),",",0,";PD"
1880 FOR I=1 TO N/2
1890 IF P(I)<5  THEN PRINT#5,"PU"
1900 X=INT((Q(I)*10)/6)+0.5)
1910 PRINT#5,"PA",(X),",",(-I*20)";PD"
1920 IF P(I)<5 THEN PRINT#5,"PU"
1930 NEXT I
1940 PRINT#5,"SI 0.285,.405"
1950 R$="R~L◆|↖X~  GF (X)"
1960 Z$=R$ : GOSUB 2580
1970 R$=E$
1980 S$="P №φ~  (D~I_~~φ)"
1990 Z$=S$ : GOSUB 2580
2000 S$=E$
2010 U$="RECORD NΓ "+A$+","+A1$
2020 Z$=U$ : GOSUB 2580
2030 U$=E$
2040 W$="F_~φ↗~/~| (Hφ)"
2050 Z$=W$ : GOSUB 2580
2060 W$=E$
2070 O$="                "
2080 Z$=O$ : GOSUB 2580 : O$=E$
2090 P$="T.\_ (φ)" :Z$=P$
2100 GOSUB 2580: P$=E$
2110 I$="PPV (\.φ)" : Z$=I$
2120 GOSUB 2580 : I$=E$
2130 PRINT#5,"PU;PA 900,150"
2140 PRINT#5,"LB";R$;CHR$(3)
2150 PRINT#5,"PA -600,150"
2160 PRINT#5,"LB";I$;CHR$(3)
2170 PRINT#5,"DI 0,-1"
2180 PRINT#5,"PA 1800,-450"
2190 PRINT#5,"LB";U$;CHR$(3)
2200 PRINT#5,"PA 650,0"
2210 PRINT#5,"LB";W$;CHR$(3)
2220 PRINT#5,"PA -850,100"
2230 PRINT#5,"LB";O$;CHR$(3)
2240 PRINT#5,"PA -850,-400"
2250 PRINT#5,"LB";P$;CHR$(3)
2260 PRINT#5,"DI 1,0"
2270 CLOSE2 :CLOSE1 :  CLOSE5,5
2280 PRINT"□" :PRINT:PRINT:PRINT:PRINT
2290 PRINT"    PMAX =";PMAX
2300 PRINT"    PT=";PT
2310 END
2320 REM PLOT TO VERIFY INPUT DATA
2330 OPEN5,5
2340 PRINT#5,"IN"
2350 PRINT#5,"IP 915,228,10915,7410"
2360 PRINT#5,"SC -250,2250,-1500,300"
2370 PRINT#5,"PU;PA 0,0;PD"
2380 PRINT#5,"PA 0,-1300;PU"
2390 PRINT#5,"PA -250,0;PD"
2400 PRINT#5,"PA 250,0;PD"
2410 PRINT#5,"PU;PA",(INT(D(1)/2)),",",0,";PD"
2420 X=0
2430 FOR I=2 TO N
2440 X=(X+(10*1))
2450 PRINT#5,"PA",INT(D(I)/2),",",-X,";PD"
2460 NEXT I
2470 PRINT#5,"LT6"
2480 PRINT#5,"PU"
2490 PRINT#5,"PU;PA",(INT(D1(1)/2)),",",0,";PD"
2500 X=0
2510 FOR I=2 TO N
2520 X=(X+(10*1))
2530 PRINT#5,"PA",INT(D1(I)/2),",",-X,";PD"
2540 NEXT I
2550 PRINT#5,"PU"
2560 PRINT#5,"LT "
2570 RETURN
2580 REM LOWER CASE CHARACTERS
2590 E$=""
2600 A=LEN(Z$)
2610 FOR I=1 TO A
2620 V$=LEFT$(Z$,I)
2630 V$=RIGHT$(V$,1)
2640 A=ASC(V$)
2650 IF A>192 THEN A=A-96
2660 E$=E$+CHR$(A)
2670 NEXT I
2680 RETURN
READY.
```

APPENDIX N

```
100 REM THE GENERAL FAST FOURIER TRANSFORM PROGRAM (BMN 9/83)
110 OPEN1,8,15
120 PRINT#1,"I0"
130 INPUT"ENTER TITLE OF DATA FILE";A$
140 V$="0:"+A$+",DAT,USR,READ"
150 OPEN 2,8,2,V$
160 INPUT#2,DT : PRINT"DT =";DT
170 NN=130
180 DIM X(NN),Y(NN),P(NN),O(NN),D(NN)
190 REM INDEX 0 SETS SIZE OF TRFM.
200 G=7:N=2↑G:P=8*ATN(1)/N
210 S0=SQR(N/(DT/1000))
220 FORI=1TO128
230 INPUT#2,X(I)
240 D(I)=INT(X(I)*500)
250 X(I)=X(I)/S0
260 PRINT X(1)
270 NEXTI
280 PRINT"□":PRINT:PRINT:PRINT:PRINT
290 PRINT"      WAIT !"
300 REM PLOT TO VERIFY INPUT DATA
310 GOSUB 2210 : REM PLOT TO VERIFY INPUT DATA
320 REM FFT ROUTINE BY BICE (1970) ENDS LINE 790
330 REM T=-1 FOR TRANSFORM :T=1 FOR INVERSE TRANSFORM
340 T=-1
350 FOR L=0 TO G-1
360 G1=2↑(G-L-1)
370 M=0
380 FOR I=1 TO 2↑L
390 K1=INT(M/G1)
400 GOSUB720
410 Y1=COS(P*K2):Y2=T*SIN(P*K2)
420 FOR J=1 TO G1
430 M5=(M+G1+1):M1=M+1
440 Y3=X(M5)*Y1-Y(M5)*Y2
450 Y4=X(M5)*Y2+Y(M5)*Y1
460 X(M5)=X(M1)-Y3
470 Y(M5)=Y(M1)-Y4
480 X(M1)=X(M1)+Y3
490 Y(M1)=Y(M1)+Y4
500 M=M+1
510 NEXT J
520 M=M+G1
530 NEXT I
540 NEXT L
550 FOR I=0 TO N-1
560 K1=I
570 GOSUB720
580 IF K2>=I THEN650
590 K3=X(I+1)
600 X(I+1)=X(K2+1)
610 X(K2+1)=K3
620 K3=Y(I+1)
630 Y(I+1)=Y(K2+1)
640 Y(K2+1)=K3
650 NEXTI
660 GOTO710
670 FOR I=0 TO N-1
680 PRINTI;SPC(4-LEN(STR$(I)));X(I+1);SPC(20-LEN(STR$(X(I+1))));
690 PRINT"+I";SPC(3);Y(I+1)
700 NEXTI
710 GOTO800
720 K2=0
730 FOR K=1 TO G
740 K3=K1-2*INT(K1/2)
750 K1=INT(K1/2)
760 IF K3=0 THEN780
770 K2=K2+2↑(G-K)
780 NEXT K
790 RETURN
800 PMAX=0
810 FORI=0TO(N/2)-1
820 P(I)=2*((X(I+1)↑2)+(Y(I+1)↑2))
830 IF P(I)>PMAX THEN PMAX=P(I)
840 PT=PT+P(I)
850 NEXT I
860 PRINTPMAX
870 PRINTPT
880 REM CONVERT TO PERCENTAGE
890 FOR I=0 TO N
900 P(I)=P(I)*100/PMAX
910 NEXT I
920 FORI=0TON-1
930 IF P(I)<0.0001 GOTO990
940 IFX(I+1)=0THENX(I+1)=Y(I+1)/1000
950 O(I)=57.2957*ATN(Y(I+1)/X(I+1))
960 IFV(I+1)>0ANDX(I+1)<0THENO(I)=O(I)+180
970 IFV(I+1)<0ANDX(I+1)<0THENO(I)=O(I)+180
980 IFV(I+1)<0ANDX(I+1)>0THENO(I)=O(I)+360
990 NEXTI
1000 GOTO 1110 : REM  SKIP PRINT STATEMENTS
1010 OPEN4,4
1020 CMD4
1030 L#="RECORD NUMBER = "+A$
1040 PRINT L# :PRINT:PRINT:PRINT
1050 FORI=0TON
1060 PRINTI;SPC(5);X(I+1);SPC(16);Y(I+1);SPC(16);P(I);SPC(16);O(I)
1070 NEXTI
1080 PRINT#4
1090 CLOSE4
1100 REM PLOTTING
1110 REM
1120 PRINT#5,"IN"
1130 M=500/DT
1140 PRINT#5,"IP 915,228,10915,7410"
1150 PRINT#5,"SC -1500,1000,-1500,300"
1160 PRINT#5,"SI 0.171,0.243"
1170 PRINT#5,"PU;PA 0,0"
1180 FOR I=0 TO 1000 STEP 100
1190 PRINT#5,"PD;PA",I,",0;XT;PU"
1200 PRINT#5,"DI 0,-1"
1210 PRINT#5,"CP -5.0,-0.25;LB";I/10;CHR$(3)
1220 PRINT#5,"DI 1,0"
1230 PRINT#5,"PA",I,",",0,";PD"
1240 NEXT I
1250 A=0
1260 PRINT#5,"DI 0,-1"
1270 PRINT#5,"PU;PA0,0"
1280 FOR I=0 TO -1280 STEP -128
1290 PRINT#5,"PD;PA",0,",",I";YT;PU"
1300 PRINT#5,"CP -2.0,-1.5;LB";(M*A)/10;CHR$(3)
1310 PRINT#5,"PA0,"(I),";PD"
1320 A=A+1
1330 NEXT I
1340 PRINT#5,"DI 1.0"
1350 PRINT#5,"PU"
1360 X=INT((P(0)*10)+0.5)
1370 PRINT#5,"PA"(X),",",0,";PD"
1380 FOR I=1 TO N/2
1390 X=INT((P(I)*10)+0.5)
1400 PRINT#5,"PA"(X),",",(-I*20),";PD"
1410 NEXT I
1420 PRINT#5,"DI0,-1"
1430 PRINT#5,"PU;PA 1050,350"
1440 P0$="PM="+STR$(PMAX)+" PT="+STR$(PT)
1450 PRINT#5,"LB";P0$;CHR$(3)
1460 CLOSE5,5
1470 OPEN5,5
1480 PRINT#5,"IN"
1490 PRINT#5,"IP 915,228,10915,7410"
1500 PRINT#5,"SC -700,1800,-1500,300"
1510 PRINT#5,"SI 0.171,0.243"
1520 PRINT#5,"PU;PA 0,0"
1530 FOR I=0 TO 600 STEP 100
1540 PRINT#5,"PD;PA",I,",0;XT;PU"
1550 PRINT#5,"DI 0,-1"
1560 PRINT#5,"CP -5.0,-0.25;LB";6*I/10;CHR$(3)
1570 PRINT#5,"DI 1,0"
1580 PRINT#5,"PA",I,",",0,";PD"
1590 NEXT I
1600 PRINT#5,"DI 0,-1"
1610 PRINT#5,"PU;PA0,0"
1620 PRINT#5,"IP 915,228,10915,7410"
1630 A=0
1640 FOR I=0 TO -1280 STEP -128
1650 PRINT#5,"PD;PA",0,",",I";YT;PU"
1660 PRINT#5,"CP -2.0,-1.5;LB";(M*A)/10;CHR$(3)
1670 PRINT#5,"PA0,"I",";PD"
1680 A=A+1
1690 NEXT I
1700 PRINT#5,"DI 1.0"
1710 PRINT#5,"PU"
1720 X=INT((((0↑(0)*10)/6)+0.5)
1730 PRINT#5,"PA"(X),",",0,";PD"
1740 FOR I=1 TO N/2
1750 X=INT((((0↑(I)*10)/6)+0.5)
1760 PRINT#5,"PA"(X),",",(-I*20)";PD"
1770 NEXT I
1780 PRINT#5,"PU"
1790 PRINT#5,"SI 0.285,.405"
1800 R#="R~L◆|◆X~  ESD(%)"
1810 Z#=R# : GOSUB 2380
1820 R#=E#
1830 S#="P !◆▼~  (D~!_~~◆)"
1840 Z#=S# : GOSUB 2380
1850 S#=E#
1860 U#="RECORD N" "+A#
1870 Z#=U# : GOSUB 2380
1880 U#=E#
1890 W#="F_~◆_~~!(W◆)"
1900 Z#=W# : GOSUB 2380
1910 W#=E#
1920 O#="                "
1930 Z#=O# : GOSUB 2380 : O#=E#
1940 P#="T\\~`(◆)" :Z#=P#
1950 GOSUB 2380: P#=E#
1960 I#="PPY (\\/◆)" : Z#=I#
1970 GOSUB 2380 : I#=E#
1980 PRINT#5,"RU;PA 900,150"
1990 PRINT#5,"LB";R#;CHR$(3)
2000 PRINT#5,"PA 0,150"
2010 PRINT#5,"LB";S#;CHR$(3)
2020 PRINT#5,"PA -600,150"
2030 PRINT#5,"LB";I#;CHR$(3)
2040 PRINT#5,"DI 0,-1"
2050 PRINT#5,"PA 1800,-500"
2060 PRINT#5,"LB";U#;CHR$(3)
2070 PRINT#5,"PA -150,-400"
2080 PRINT#5,"LB";W#;CHR$(3)
2090 PRINT#5,"PA 650,-400"
2100 PRINT#5,"LB";W#;CHR$(3)
2110 PRINT#5,"PA -850,100"
2120 PRINT#5,"LB";O#;CHR$(3)
2130 PRINT#5,"PA -700,-400"
2140 PRINT#5,"LB";P#;CHR$(3)
2150 PRINT#5,"DI 1,0"
2160 CLOSE2 :CLOSE1 : CLOSE5,5
2170 PRINT"□" :PRINT PRINT:PRINT:PRINT
2180 PRINT"    PMAX =";PMAX
2190 PRINT"    PT=";PT
2200 END
2210 REM PLOT TO VERIFY INPUT DATA
2220 OPEN5,5
2230 PRINT#5,"IN"
2240 PRINT#5,"IP 915,228,10915,7410"
2250 PRINT#5,"SC -250,2250,-1500,300"
2260 PRINT#5,"PU;PA 0,0;PD"
2270 PRINT#5,"PA 0,-1300;PU"
2280 PRINT#5,"PA -250,0;PD"
2290 PRINT#5,"PA 250,0;PD"
2300 PRINT#5,"PU;PA",(INT(D(1)/2)),",",0,";PD"
2310 X=0
2320 FOR I=2 TO N
2330 X=(X+(10*1))
2340 PRINT#5,"PA",INT(D(I)/2),",",-X,";PD"
2350 NEXT I
2360 PRINT#5,"PU"
2370 RETURN
2380 REM LOWER CASE CHARACTERS
2390 E#=""
2400 A=LEN(Z#)
2410 FOR I=1 TO A
2420 V#=LEFT#(Z#,1)
2430 V$=RIGHT$(V$,1)
2440 A=ASC(V$)
2450 IF A>192 THEN A=A-96
2460 E#=E#+CHR$(A)
2470 NEXT I
2480 RETURN
READY.
```

APPENDIX M

```
100 REM ######## DIGIT #########
110 OPEN 5,5
120 DIM X(150),Y(150),D(150)
130 INPUT"INPUT TITLE OF DATA FILE";A$
140 PRINT"□":PRINT:PRINT
150 INPUT"INPUT TIME INCREMENT, DT";DT
160 LET DA=DT*100
170 PRINT"DT=";DT
180 T1=T*100
190 N=128
200 PRINTN
210 REM        INITIALISE PLOTTER AND SET                UP SCALE
220 PRINT#5,"IN"
230 PRINT#5,"IP 400,305,10400,7505"
240 PRINT#5,"SC 0,25000,0,18000"
250 GOSUB 520   : REM DIGITISING SUB
260 X=25000-A
270 Y=18000-B
280 REM       RESCALE RELATIVE TO ORIGIN
290 PRINT#5,"IP 400,305,10400,7505"
300 PRINT#5,"SC",-A,",",X,",",-B,",",Y,";PU"
310 PRINT#5,"PU;PA 0,0"
320 X(0)=0 : Y(0)=0
330 FOR I=1 TO (N-1)
340 PRINT#5,"PA"(I*DA),",",Y(I-1),";PD"
350 GOSUB 520   : REM DIGITISING SUB
360 X(I)=A : Y(I)=B
370 IF I=(N-1) THEN Y(I)=0
380 NEXT I
390 FOR I= 0 TO (N-1)
400 PRINT
410 NEXT I
420 REM FIND YMAX
430 GOSUB 710   : REM FIND YMAX
440 REM SEND DATA TO DISK
450 GOSUB 610    : REM SEND DATA TO DISK
460 GOTO 510
470 REM VERIFY INPUT PLOT
480 GET Z$
490 IF Z$="" THEN 480
500 GOSUB 790 : REM VERIFY INPUT PLOT
510 CLOSE2 :CLOSE 1 : END
520 REM
530 PRINT"□" : PRINT:PRINT
540 PRINT"############  ENTER COORDINATE #######"
550 PRINT:PRINT:PRINT "X(";I;")=";(I*DT)
560 GET Z$
570 IF Z$="" THEN 560
580 PRINT#5,"OC;"
590 INPUT#5,A,B,C
600 RETURN
610 REM SUB TO SEND DATA TO DISK
620 OPEN 1,8,15
630 PRINT#1,"I0"
640 V$="@0:"+A$+",DAT,USR,WRITE"
650 OPEN 2,8,2,V$
660 PRINT#2,DT;CHR$(13);
670 FOR I=0 TO N-1
680 PRINT#2,Y(I);CHR$(13);:NEXT I
690 CLOSE2 :CLOSE1
700 RETURN
710 YMAX=0
720 FOR I= 0 TO N-1
730 IF ABS(Y(I))>YMAX THEN YMAX=ABS(Y(I))
740 NEXTI
750 FOR I =0 TO N-1
760 Y(I)=Y(I)/YMAX
770 NEXT I
780 RETURN
790 REM VERIFY INPUT PLOT
800 OPEN 1,8,15
810 PRINT#1,"I0"
820 V$="0:"+A$+",DAT,USR,READ"
830 OPEN 2,8,2,V$
840 FOR I=0 TO (N-1)
850 INPUT#2,D(I)
860 D(I)=INT(D(I)*500)
870 NEXT I
880 REM VERIFY INPUT PLOT
890 PRINT#5,"IN"
900 PRINT#5,"IP 915,228,10915,7410"
910 PRINT#5,"SC -3000,22000,-900,900"
920 PRINT#5,"PU;PA 0,0;PD"
930 PRINT#5,"PA 22000,0 ; PU"
940 PRINT#5,"PA 0,500;PD"
950 PRINT#5,"PA 0,-500;PU"
960 PRINT#5,"PU;PA" ,0,",",D(I),";PD"
970 X=0
980 FOR I=1 TO (N-1)
990 X=X+DA
1000 PRINT#5,"PA",X,",",D(I),";PD"
1010 NEXT I
1020 PRINT#5,"PU"
1030 CLOSE2: CLOSE1 : RETURN
READY.
```